LIFE ON THE EDGE: MORPHOLOGICAL AND BEHAVIORAL ADAPTATIONS FOR SURVIVAL ON WAVE-SWEPT SHORES

A DISSERTATION

SUBMITTED TO THE DEPARTMENT OF BIOLOGY

AND THE COMMITTEE ON GRADUATE STUDIES OF

STANFORD UNIVERSITY

IN PARTIAL FULFILLMENT OF THE

REQUIREMENTS FOR THE DEGREE OF DOCTOR OF

PHILOSOPHY

Luke Paul Miller

May 2008

I certify that I have read this dissertation and that, in my opinion, it is fully adequate in scope and quality as a dissertation for the degree of Doctor of Philosophy.

_____

Mark W. Denny (Principal Adviser)

I certify that I have read this dissertation and that, in my opinion, it is fully adequate in scope and quality as a dissertation for the degree of Doctor of Philosophy.

_____

George N. Somero

I certify that I have read this dissertation and that, in my opinion, it is fully adequate in scope and quality as a dissertation for the degree of Doctor of Philosophy.

_____

Fiorenza Micheli

I certify that I have read this dissertation and that, in my opinion, it is fully adequate in scope and quality as a dissertation for the degree of Doctor of Philosophy.

_____

Judith L. Connor

Approved for the University Committee on Graduate Studies

Abstract

Wave-swept rocky shores serve as a home to a great diversity of organisms and are some of the most biologically productive habitats on earth. This burgeoning community exists in spite of the fact that the zone between the high and low tide marks can be one of the most physically harsh environments on earth. Large forces imposed by breaking waves and wide swings in temperature require the organisms living on rocky shores to adapt to a constantly changing environment or risk extirpation by physical forces. I have explored a number of hypothesized adaptations for survival on rocky shores and discuss how the results influence the evolutionary and ecological processes shaping shoreline communities. I developed a biophysical model to predict body temperatures for high shore littorine snails in order to address the role of evolved morphological and behavioral traits for controlling body temperature during extreme temperature exposures. The results demonstrate that while the behaviors of these snails allow them to reduce body temperatures by several degrees, the hypothesized roles of shell shape and color contribute relatively little to controlling body temperature. A similar biophysical model for predicting organismal body temperature was combined with a physiological study to examine the role of temperature stress in setting the distributional limits of an important mid-intertidal limpet, *Lottia gigantea*. With a temperature exposure protocol based on realistic field conditions, I measured sub-lethal and lethal temperature limits for this species, and found that the vertical distribution of *L. gigantea* may be set directly by high temperatures within certain microhabitats on the shore. The final section describes the role of behavior in barnacles in compensating for limits in the phenotypic plasticity of their feeding appendages. By directly monitoring the feeding activity of barnacles under breaking waves, I show that fast reaction times allow barnacles to avoid damaging water flows while still exploiting much of the available time for feeding. The studies in this thesis provide a number of new insights into the role of the abiotic environment in the evolution and ecology of organisms living on wave-swept rocky shores.

Acknowledgements

While there is only one author's name on the front of this dissertation, the document and the studies described within would not have come to be without the assistance of a large number of people. I am indebted to many people for their scientific, technical, philosophical, and emotional support through the course of my studies. What follows are my all-too-brief acknowledgements for everyone's help.

Primacy of place must of course go to my thesis advisor, Mark Denny. Perusing the acknowledgement sections of theses from Mark's previous students, terms such as "endless knowledge", "boundless enthusiasm", "diplomacy", "patience", and "the right answers" keep coming up, for good reason. Mark was always willing to provide as much or as little guidance as each person desired, and could always be counted on for a fruitful discussion of any new idea, no matter how outlandish it might have seemed at first. His office door was always open, and he was amazingly adept at dropping whatever project was at hand and immediately coming up to speed on your current topic to lend any bit of advice or knowledge he had. Mark provided me with a constant stream of new ideas and new ways to visualize the bigger picture, and his influence is evident throughout this dissertation.

Perhaps Mark's greatest strength was his ability to attract a lab full of dynamic and motivated people. I had the chance to overlap with a number of wonderful Denny Lab members during my time here. In my early days as a lab technician, Ben, Loretta, and Elizabeth introduced me to the diversity of experiences waiting to be had in the lab. Joanna Nelson put up with me as an office mate with constant good cheer and the ability to look past the constantly growing pile of "work" on the desks, shelves, drawers, walls and floor of our office. After Joanna, it wasn't until Kevin Miklasz arrived to start graduate school that someone else deigned to share an office with me. I benefitted from the help and advice of a number of laboratory technicians in my time: Lisa Walling, Tad Finkler, Anton Staaf, and Katie Mach. Katie went on to join the lab as a graduate student as well, and has been the source of many discussions over the

years about science, society, politics and food. I thank Luke John Hoot Hunt, a.k.a. Luke 1, for his many insightful conversations, his helpful programming, and his numerous cockamamie ideas.

Patrick and Rebecca Martone have been my closest compatriots through the graduate school journey. We spent a year in Palo Alto, commiserating and reminding each other that it would all get better when we moved down to Pacific Grove to start the real work of the PhD. Patrick was a great help with suggestions while writing, preparing presentations, and trudging through statistical methods. Rebecca served as a sounding board for all manner of topics on science and life, and she supplied me with just enough Spanish vocabulary to keep me out of trouble in Baja.

The later years of my research were helped immeasurably by Michael Boller, who lent help and equipment whenever he could. Mike was another inveterate tinkerer, and we built a number of successful and occasionally not-so-successful pieces of equipment that provided hours of entertainment and a bit of data as well. Together we managed to leave a number of permanent marks on the landscape at Hopkins Marine Station.

Rounding out the long list of lab-mates, I have to acknowledge Michael “Moose” O’Donnell and Chris Harley. Moose was there from the beginning of my stay in the Denny lab, and was more responsible for my occasional delinquency than anyone else. My method of experimentation has always tended towards the idea that there was only one way to find out if a plan was going to work, and that was to stop worrying and just try it. Moose shared the same sensibility, and together we made the most of the laboratory environment. Chris Harley showed up during those critical early years of my degree, and served as a superb role model for a young scientist. Chris mixed an infectious sense of humor with a vast knowledge of ecology, and provided a great deal of wisdom on how to go about doing science. These were the people that made research the enjoyable endeavor that I always hoped it would be.

I owe a debt of gratitude to the other members of my committee as well. Fiorenza Micheli, Judith Connor, and George Somero all lent advice and encouragement. George in particular opened up his lab to a naïve biomechanics student and provided

the tools and guidance to delve into the world of physiology. The members of his lab, including Jon Sanders, Tyler Evans, Cheryl Logan, Brent Lockwood, along with Melissa Pespeni, Maria-Inês Seabra, Yunwei Dong, and Lars Tomanek were all extremely helpful in troubleshooting techniques and explaining the intricacies of bench work.

The rest of the faculty at Hopkins was helpful and supportive over the years as well. I owe particular thanks to Stuart Thompson for giving over a portion of his coffee maker space to the equipment I used for the data collection in the fourth chapter of this dissertation. Jim Watanabe provided a substantial amount of statistical help, and served as a great teacher for several courses I took or assisted with at Hopkins.

The staff at Hopkins Marine Station was a great help throughout my studies. Judy Thompson made things magically happen on the administrative side and was my 'landlord' while I lived in the caretaker's cottage. Joe Wible, along with Susan Harris and Vicki Pearse, always succeeded in finding whatever obscure references I could come up with, and they allowed me to photocopy a substantial portion of the library for my own personal files. John Lee assisted me in the machine shop and helped with designing and building electronic equipment that I subsequently used to produce much of the data in this dissertation. Bob Doudna provided a wealth of practical advice when building equipment and was always willing to stop and explain how stuff worked. Chris Patton played many roles, the most important of which was that of the safety officer that blessed my sometimes-questionable equipment designs. Barbara Compton just laughed at me when I managed to melt things in her autoclave, while Sharon Pagni, Doreen Zelles, and Tim Knight helped keep things running smoothly. Freya Sommer was most helpful with all things diving-related, and always enjoyed spending a day on the water working on underwater projects.

The graduate students, post-docs, and lab technicians at Hopkins Marine Station formed a wonderful community that I was happy to be a part of for many years. Christian Reilly and Andre Boustany spun an oral tradition of the Marine Station that helped us connect to the long line of graduate students that preceded us. Carrie Kappel

made sure we got the complete graduate school experience by organizing educational and recreational activities. Heather Galindo reminded me that even serious scientists can have crafty hobbies and horrible taste in music. Kim Heiman convinced me to stand waist-deep in an estuary measuring water speeds while an armed robbery suspect was being chased by police helicopters somewhere up the channel, because the data come first. Some of these folks were my housemates: Kevin Weng, Jason Blank, Ole Shelton, Mat Brock, while some of them were sports teammates: Alison Haupt, Rebecca Vega Thurber, Michelle Roux, Chris Perle, Pedro Castilho, Sal Jorgensen. One constant through all of these years was the promise of Friday afternoon beer hour and the people that could be counted on for good conversation, such as Steve Litvin, Ryan Kelley, Emily Jacobs-Palmer, Doug McCauley, Tom Oliver, and many others. Amro Hamdoun made sure I knew just how good I had it. I also have to acknowledge Suzanne Cowden, Kimi Kato, and Ernest Daghir for their encouragement and shared good food through the years.

While much of my graduate school career was spent at Hopkins Marine Station, I need to also acknowledge the people that encouraged me before I arrived here. For many years I have been lucky to know Michael Jelenic, Travis Brooks, and Kara Czap, all of whom help remind me of where I came from. My path to graduate school was forged by my experiences at UC Santa Barbara, where Steven Gaines took in this gangly sophomore and let him run around the intertidal zone of southern and central California for four years. Christopher Krenz, Ben Miner, Tiffany Jenkins, Clara Svedlund, and particularly Carol Blanchette and Brian Gaylord were all important mentors early on during my time in Santa Barbara. When I arrived at Stanford to start graduate school, I was lucky to be surrounded by a bright group of new ecology and evolution graduate students with a diverse array of backgrounds and interests. Nadia Singh, Will Cornwell, Megan Frederickson, Lauren Buckley, Jai Ranganathan and Greg Petersen helped me settle in to life in graduate school. Most of all, I thank Paula Spaeth and her little dog named after General George Washington's horse for all of their support and help over the years.

Finally, I would not have followed this path were it not for my family. As the son of two intertidal ecologists, it might have seemed inevitable that I would be drawn to the ocean. I study the critters living on the coast not because of any overt suggestion from my parents, but rather because of the experiences I had growing up. The ocean was always just down the street, the dinner conversation often revolved around the happenings at the aquarium or the university, and every trip to the desert, mountains, or seashore was an opportunity to teach me just a bit more about nature. My brother David and I were encouraged to try anything and everything, provided it didn't burn down the house. The pile of projects on my office desk today harkens back to the toy projects on the floor of my room as a child, or the endless string of projects I had in the garage as a teenager. My family is responsible for me being the person I am today, and I thank them for it.

TABLE OF CONTENTS

List of Figures

List of Tables

Introduction

Perhaps the most consistently intriguing facet of nature is the ability of organisms to adapt and survive in seemingly inhospitable habitats. Our personal biases may color our concept of what constitutes an inhospitable habitat, but we can certainly agree that there are characteristics of certain habitats that should make them difficult to live in, even for creatures much tougher than ourselves. A cursory examination of conditions in the intertidal zone, that strip of land between the low and high tide marks on shores around the world, makes it readily apparent that life in the intertidal zone consists of a variety of physical and physiological insults constantly being dealt out to the inhabitants of this habitat.

The inundation of the intertidal zone by the ocean once or more a day at high tide requires the organisms living on the shore to be capable of surviving in the ocean waters for hours on end. Not surprisingly, the inhabitants of the intertidal zone, save for a few species, are primarily of marine origin, and therefore are equipped to deal with submersion in seawater. Thus, the environmental conditions that might make the intertidal zone inhospitable are related more to the changes that occur as the tide drops and exposes the shore to the air. The transition to aerial emersion forces behavioral and physiological changes in the organisms on the shore in order to cope with the more variable conditions present between high tides, including wide swings in temperature and the action of waves breaking on the shore.

Aerial exposure brings with it rapid swings in environmental temperatures. While the high specific heat of water and the huge volume of the ocean tend to damp short-term fluctuations in ocean temperature, much wider changes in temperature are possible in the aerially-exposed intertidal zone, similar to those on dry land. At times, body temperatures in the intertidal zone go from ocean temperature (~10 – 14°C during the year at Hopkins Marine Station in Pacific Grove, CA) to highs of over 40°C during the

course of just a few hours, with potentially disastrous physiological consequences. In colder climes, environmental temperatures during low tide may take equally wide excursions to temperatures below freezing.

The other primary stress on intertidal shores, at least for those exposed to the open ocean, is the arrival of waves on the shore. Below the ocean's surface, ocean swells may sweep over the benthos and create fast flows of several meters per second. However, the truly destructive water flows occur when waves reach the shoreline and dissipate their energy by breaking on the shore. Organisms that were already dealing with aerial exposure must suddenly contend with water flowing over the rocks at speeds that may reach beyond 30 m s^{-1}. This rushing water creates lift and drag forces that may pry organisms from the rocks or simply break them into pieces.

Despite the physical harshness of the intertidal zone, this narrow strip of land is home to at least seventeen phyla of organisms, including three phyla of algae and a group of flowering plants. The central coast of California is home to more than 3,500 species of invertebrate animals. The wave-exposed rocky intertidal zone may seem dangerous to humans, but the rich array of organisms occupying this habitat demonstrates that there is a broad range of adaptations that can mitigate the stresses of this environment.

The goal of the studies detailed in this dissertation was to explore some of those behavioral and physiological adaptations that allow intertidal organisms to flourish in this habitat. The work aims to examine these adaptations in both an evolutionary and ecological context to create a better understanding of the physical and physiological characteristics of organisms that interact with the environment to shape these communities.

The first two chapters are concerned with the adaptive nature of evolved morphologies and behaviors present in a group of gastropod snails occupying the mid- and high-intertidal zones. These small snails, commonly known as littorines or periwinkles, live on rocky shores and in estuaries around the world, from the tropical through the boreal latitudes. They are often the highest-living marine invertebrates on the shore, commonly living above the height of the highest high tides and relying on wave splash

to wet them occasionally. Littorines are commonly exposed to the air for days or weeks on end, and must contend with both high and low temperatures, as well as severe desiccation. By virtue of their position on the shore, these snails should experience the most extreme temperature and desiccation conditions of any of the intertidal animals. As such, the littorine snails have been the subject of much attention by biologists interested in the evolution of strategies of marine organisms for coping with a nearly terrestrial existence. How do these species cope with extreme temperatures physiologically? Does their shell morphology allow them to regulate body temperature more efficiently than related groups? What morphological, physiological and behavioral adaptations allow the littorines to extend their zone of occupation on the sea shore beyond that of other marine organisms? To address some of the long-standing evolutionary and ecological questions concerning the littorine snails, I developed a heat-budget model to predict the temperature of these snails from local weather data. The heat-budget model is then employed to test the effects of physical characteristics of the shells such as shape, size, or color on body temperature, as well as exploring the role of behavior in regulating body temperature.

This work shows that much of the variation in shell morphology, long thought to affect the temperature stresses experienced by these snails, may be of little consequence for regulating body temperature. However, a unique behavioral adaptation shared by littorine snails - removing their foot from the substratum - creates large reductions in body temperature that may allow these snails to avoid lethal thermal stress while at the same time minimizing desiccation during prolonged aerial exposure.

The third chapter is concerned with the limpet *Lottia gigantea,* an important member of the mid-intertidal community on wave-exposed rocky shores in California and Baja California. Utilizing data from a heat-budget model for this species created by Denny and Harley (2006), I created a new series of laboratory stress exposures designed to accurately mimic conditions found in the field. Much of the existing work on thermal stress in intertidal organisms has used methodologies that expose organisms to stress

in a manner very different from what they might experience in the field. The newly-developed high-temperature exposure methods, coupled with the development of an assay for sub-lethal stress markers in *L. gigantea*, gives new insight into the frequency and severity of stress events experienced by this species. The combination of biomechanics (via the heat-budget model) and physiology (via the laboratory stress experiments) allow me to use historical weather records for Hopkins Marine Station and make predictions about where and when limpets might have experienced sub-lethal or lethal stress exposures.

The fourth chapter returns to the other major stress of intertidal life, disturbance caused by large waves, and how organisms might combine both morphological and behavioral adaptations to successfully cope with high water velocities. The subject of this study is the barnacle *Chthamalus fissus,* a common inhabitant of the mid- and high-intertidal zones along the California coast. Barnacles cement themselves to the rock permanently, and must feed by capturing food particles from the water. They build strong shells capable of withstanding large, crashing waves, and withdraw their delicate feeding legs into the shell when conditions become unfavorable. The question is how these barnacles balance the size and feeding efficiency of their legs with the need to avoid damage from high velocity flows. Morphological plasticity in leg form allows for some compensation to the local flow conditions, but I find that at extremely wave-exposed sites, behavior takes over to allow efficient utilization of the time spent submerged in order to feed. By making the first video observations of barnacle feeding behavior under breaking waves, it became clear that barnacles are extremely adept at reacting quickly to high flows and withdrawing into the protection of the shell, while also being able to quickly resume feeding in between peak flows. These unique observations provide insight into how barnacles have been so successful across the entire gradient from calm, protected harbors to the most wave-exposed open coast sites. A version of this chapter was published in the *Marine Ecology Progress Series* (Miller, 2007).

The range of topics in this dissertation provides a number of new avenues and techniques for future research. The heat-budget model for littorine snails tests a number of long-standing hypotheses about the evolution of snail morphology and shows how the behavior and physiology of these snails makes them well-suited to survival in the extremes of the environment in the intertidal zone. With the work on *L. gigantea*, I hope to encourage future researchers to strive to employ more realistic methods when making physiological measurements so that these data can be directly used in ecological studies of organismal distributions or climate change. Traditional comparative physiology studies have given us a plethora of comparative data on species' relative physiological capabilities, but when we take the critical step from the laboratory to the field, these data may be of dubious utility. Instead, the methods I have outlined here give us data that can be directly applied to field measurements or predictions from heat-budget models. Finally, the ability to observe barnacle feeding behavior *in situ* on the rocky shore leaves us with a more complete picture of how barnacles utilize their time in the waves, but also opens up further questions about the tradeoff between leg morphology and the flow environment.

Ultimately, the work carried out in the course of this dissertation has served to further reinforce my own amazement with the variety of adaptive strategies that can succeed in a harsh environment. With more time, more work, more technology, and most importantly, more ideas, I hope that the information in this dissertation can be expanded and incorporated into both pure and applied research on this unique environment and its inhabitants.

Chapter 1

Predicting the body temperature of littorine snails

1.1 Introduction

A trip to the seashore on a warm, sunny, low tide typically makes for a pleasant outing. Trampling over rocks and splashing through tidepools, visitors find a world of unique animals and algae exposed for all to see, but only briefly until the next high tide creeps back up the shore to bathe everything in cooling seawater. While low tides might provide pleasant conditions for humans to explore the ocean's edge, warm days may have severe consequences for the organisms living on the shore.

Save for a few interloping insects and birds that visit at low tide, everything living in the intertidal zone requires wetting by the ocean in order to survive. Because of this basic requirement, the intertidal zone is often characterized as a stressful environment, a place where organisms live at the limits of their physiological capabilities due to the wide swings in environmental conditions that accompany the waxing and waning tides. Despite this assumed stressfulness, we are struck by the diversity and productivity of such an "extreme" environment. Low on the shore, nearly every available surface is covered by some species of alga or animal, an ever-changing patchwork of neighbors vying for space to settle, grow, and reproduce. Moving up the shore, away from the nearly constant splash of the waves, the dense mosaic of different species often gives way to less diverse assemblages, zones where only a few species can survive well enough to reproduce. The oft-cited culprit for this winnowing of species diversity as one moves up the shore is the imposition of severe thermal and desiccation stress brought on by prolonged emersion. Only a select number of the algae and animals that occupy the intertidal zone can withstand the wide swings in temperature made possible by the absence of the thermal buffering of the ocean waters. High shore levels can be subjected to regular temperature excursions of 15-

20°C in a day, occasionally more during heat waves. When the ocean swells recede, the substratum dries out and the local humidity in the intertidal zone may drop as well, exposing a previously-immersed organism to relative humidity levels below 50%, leading to desiccation, which can be further exacerbated by high temperatures.

In light of these general patterns of environmental severity and species distributions, the intertidal zone has long been a testing ground for questions about the evolution and ecology of intertidal organisms. Questions about the effects of temperature on the survival and performance of organisms have been particularly intriguing to both ecologists and evolutionary biologists. The goal of this chapter and the next is to employ a bio-physical modeling approach to address questions of how the morphology and behavior of some species of high-shore snails affect the thermal stresses that these snails must withstand during prolonged emersion during low tides (Porter *et al.*, 1973). More specifically, in this chapter I describe the theory and implementation of a heat-budget model to predict body temperatures of littorine snails. The subsequent chapter details a variety of questions that can be addressed using the heat-budget model approach, such as examining the effects of shell color, shell size, shore height, and behavior on the temperatures experienced by five species of littorine snails.

1.1.1 A word about behavior

Before describing the theory behind using a heat-budget model to predict the body temperature of littorine snails, it is necessary to introduce the reader to a behavior of these snails that has a considerable bearing on the function of the model. The majority of aquatic gastropods strive to keep their foot in contact with the substratum throughout the course of their adult lives. However, this is rarely true for littorine snails, which tend to share their terrestrial snail relatives' proclivity for withdrawing the foot into the shell and isolating themselves from the outside environment when conditions become unfavorable. As a result of living high on rocky shores and in estuaries, littorines can spend much of their lives emersed from the water in dry conditions which may be unsuitable for crawling and grazing behaviors. Their evolved solution is to wait out the unfavorable conditions by pulling into the shell and

occluding the opening of the shell with the horny operculum. To hold their shore position while the foot is out of contact with the substratum, the littorine snail deposits a mucus layer between the outer edge of the shell's aperture and the substratum. This mucus dries out and acts as a holdfast that maintains the position of the shell on the substratum quite effectively (Denny, 1984).

In addition to withdrawing the foot into the shell, many littorine species undergo the additional step of reorienting the shell relative to the substratum (Vermeij, 1971; Garrity, 1984). Instead of leaving the aperture of the shell against the substratum, the snail lifts the shell away from the substratum while the mucus holdfast dries (Figure 1-1). Throughout this chapter and the next, I refer to these two shell orientations as the "down" and "up" orientations. During the explanation of the components of the heat-budget model, it will become evident how the behavioral choice of withdrawing the foot and altering the shell orientation relative to the substratum can change several of the heat fluxes into and out of a snail.

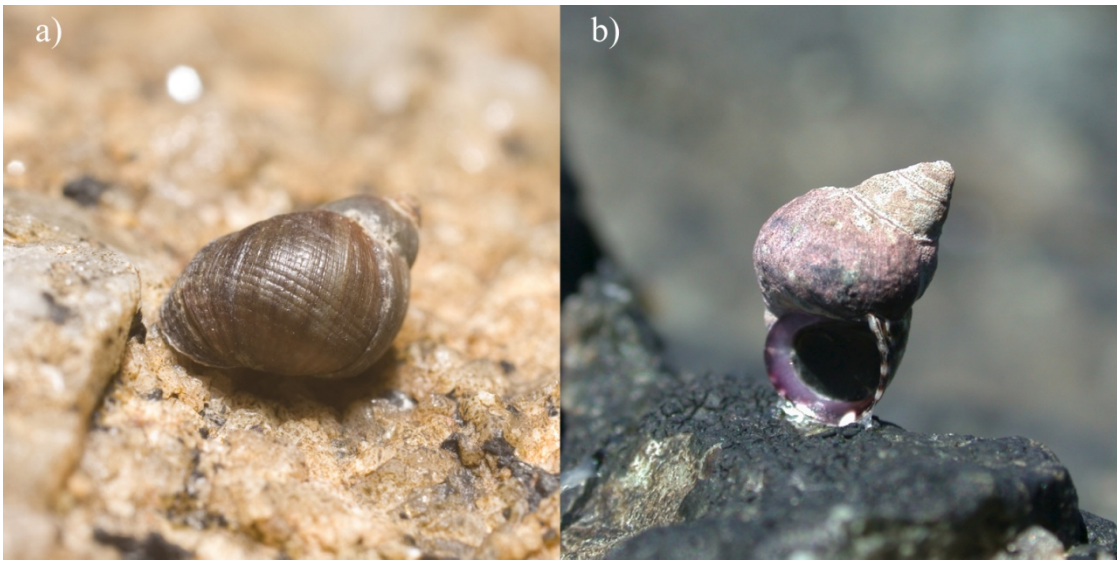

Figure 1-1. a) Littorine snails, such as the *Littorina scutulata* shown here, are commonly found at low tide with the foot withdrawn into the shell and the shell sitting down on the substratum, attached by a dried mucus holdfast. b) On occasion, littorine snails can be found with the shell elevated up off of the substratum, using dried mucus to hold the shell's position until high tide returns.

1.1.2 The heat-budget model

At any point in time, the total heat energy in an organism is a function of the sum of all of the heat fluxes between the organism and its surrounding environment. By adding up all of the ways that heat enters or leaves the organism, it is possible to calculate the temperature at which the organism is at thermal equilibrium. Heat energy enters or leaves the organism through solar irradiance, evaporation (or condensation) of water, convection, conduction, long-wave (infrared) radiation, and the metabolism of the organism (Gallucci, 1973; Gates, 1980). By convention, I define any heat entering the organism to be a positive flux, W_{in} (units of Watts, or Joules s^{-1}) and heat leaving the organism to be a negative flux, W_{out}. In addition to heat fluxes in and out of the organism, there is also heat stored in the organism, W_{stored}. Energy in this system is conserved, so that the sum of all the heat fluxes in and out of the organism, along with the heat stored in the organism, must equal zero:

$$W_{\text{in}} + W_{\text{out}} + W_{stored} = 0 \,. \tag{1}$$

The pathways of heat energy flux in and out of the organism listed above can be substituted for W_{in} and W_{out} as

$$W_{\text{sw}} \pm W_{\text{evap}} \pm W_{\text{conv}} \pm W_{\text{cond}} \pm W_{\text{lw}} + W_{\text{met}} = W_{\text{stored}} \tag{2}$$

where W_{sw} is shortwave radiation from the sun, W_{evap} is heat energy gained or lost via evaporation and condensation, W_{conv} is heat energy exchanged with the surrounding air via convection, W_{cond} is heat energy exchanged with the substratum via conduction, W_{lw} is long-wave radiation exchanged between the organism its surroundings, and W_{met} is heat energy produced internally by the metabolism of the organism.

Because the thermal mass of the organism is relatively small, and contact with the air and rock is large (the organism is not well insulated), I can legitimately set the value of W_{stored} equal to zero. I then describe how to calculate the value of each of the other heat fluxes using measured environmental variables and the physical properties of the components of the system. With one exception, each of these heat fluxes is a function

of body temperature, which in the end (as we will see), allows us to calculate the temperature of the body, T_{body}.

Table 1-1. Symbols used in the text. The equation where the symbol first appears is listed in the Equation column.

Symbol	Definition	Units	Equation
a	Nusselt-Reynolds proportionality coefficient	None	(23)
b	Nusselt-Reynolds exponent	None	(23)
c_{Ag}	Specific heat of silver	J kg^{-1} K^{-1}	(18)
c_{rock}	Specific heat of granite	J kg^{-1} K^{-1}	(29)
A_{cond}	Area available for conduction to the substratum	m^2	(7)
A_{conv}	Area available for convective heat transfer	m^2	(6)
A_{evap}	Area available for evaporation	m^2	(5)
A_l	Area available for long-wave heat energy exchange	m^2	(9)
A_{proj}	Projected area of shell facing the sun	m^2	(3)
D_{rock}	Thermal diffusivity	m^2 s^{-1}	(27)
h_c	Heat transfer coefficient	W m^{-2} K^{-1}	(6)
h_m	Mass transfer coefficient	m s^{-1}	(5)
K_{air}	Thermal conductivity of air	W m^{-1} K^{-1}	(19)
K_{rock}	Thermal conductivity of substratum	W m^{-1} K^{-1}	(7)
K_{shell}	Thermal conductivity of shell	W m^{-1} K^{-1}	(30)
m	Mass	g	(18)
Nu	Nusselt number	None	(19)
q_{sol}	Solar irradiance	W m^{-2}	(3)
R	Radius of shell or sphere	m	(19)
Re	Reynolds number	None	(21)
t	Time	s	(4)
T_{air}	Temperature of the air	K	(10)
T_{body}	Temperature of the snail body	K	(9)
T_{rock}	Temperature at rock surface	K	(7)
u	Velocity	m s^{-1}	(21)
W_{cond}	Conductive heat transfer rate	W	(2)
W_{conv}	Convective heat transfer rate	W	(2)
W_{evap}	Evaporative heat transfer rate	W	(2)
W_{in}	Heat transfer rate in to animal	W	(1)
W_{lw}	Long-wave heat transfer rate	W	(2)
$W_{lw,in}$	Long-wave heat transfer rate in from surroundings	W	(8)
$W_{lw,out}$	Long-wave heat transfer rate to surroundings	W	(8)
W_{met}	Metabolic heat production rate	W	(2)
W_{out}	Heat transfer rate out of animal	W	(1)
W_{stored}	Heat energy storage rate in animal	W	(1)
W_{sw}	Short-wave heat transfer rate	W	(2)
α_{sw}	Short-wave absorptivity	None	(3)
$\alpha_{lw,shell}$	Long-wave absorptivity of shell	None	(10)
Γ	Latent heat of evaporation of water	J kg^{-1}	(4)
$\epsilon_{lw,sky}$	Long-wave emissivity of the sky	None	(10)
$\epsilon_{lw,shell}$	Long-wave emissivity of shell	None	(9)
ν	Kinematic viscosity of air	m^2 s^{-1}	(21)
ρ_{rock}	Density of granite rock	kg m^3	(29)
$\rho_{V,air}$	Vapor pressure density of air	kg m^3	(5)
$\rho_{V,body}$	Vapor pressure density of saturated air at body surface	kg m^3	(5)
σ	Stefan-Boltzmann constant	W m^{-2} K^{-4}	(9)

1.1.3 Short-wave heat flux

The sun is the primary input of heat energy into the organism on sunny days. Shortwave solar radiation heats the air, the surrounding substratum, and the organism directly. For the purposes of this study, short-wave radiation is defined as light with wavelengths between 300 nm and 1500 nm. Radiated heat energy at longer wavelengths is considered long-wave radiation. Here we concern ourselves with solar radiation falling on the organism itself, so that the heat energy flux from short-wave radiation is

$$W_{\mathrm{sw}} = \alpha_{\mathrm{sw}} A_{\mathrm{proj}} q_{\mathrm{sol}} . \quad (3)$$

The short-wave absorptivity, α_{sw}, of the shell is a function of its color and reflectance, and is empirically measured. Absorptivity is a dimensionless number that varies between 0 and 1, where an ideal black body has a value of 1 and an ideal mirror has a value of 0. The projected area of the shell facing the sun, A_{proj} (units of m^2), can be empirically measured or, for some organisms, mathematically approximated. Finally, the solar irradiance, q_{sol} (units of Watts m^{-2}), is a measure of the heat energy from the sun falling on the organism. The short-wave heat energy entering an organism is independent of body temperature, unlike the remaining heat fluxes.

1.1.4 Evaporation and Condensation

The process of evaporating water from a wet surface of an organism results in a flux of heat energy out of the organism. The loss of water through evaporation can be an important heat flux for organisms with a large surface area for evaporation (Ramsay, 1935). Conversely, condensation of water onto the surface of an organism results in heat flux into the organism, warming it. W_{evap} represents both evaporation and condensation heat energy flux. The components of W_{evap} are

$$W_{\mathrm{evap}} = \Gamma \frac{d(\mathrm{mass})}{dt} \quad (4)$$

where Γ is the latent heat of evaporation of water (at 30 °C, $\Gamma = 2.465 \times 10^6$ J kg^{-1}), and $\frac{d(\text{mass})}{dt}$ is the rate of mass transfer of water onto or away from the surface of the organism. The rate of mass transfer is further equal to

$$\frac{d(\text{mass})}{dt} = -h_{\text{m}} A_{\text{evap}} (\rho_{\text{V,body}} - \rho_{\text{V,air}}) \quad (5)$$

where h_{m} (units of m s^{-1}) is a mass transfer coefficient that must be empirically measured, A_{evap} (units of m^2) is the surface area open to evaporation, $\rho_{\text{V,body}}$ (units of kg m^{-3}) is the water vapor density of saturated air at the surface of the organism, and $\rho_{\text{V,air}}$ is the water vapor density of the surrounding air. During the warm periods of interest here, littorine snails withdraw the body into the shell and occlude the aperture of the shell with a horny operculum, which effectively minimizes water loss due to evaporation (Garrity, 1984; McMahon and Britton, 1985; Britton and McMahon, 1986).

In preliminary experiments, I recorded average evaporation rates of *L. keenae* held in 33% relative humidity air at a constant temperature of 35°C. The water loss rate during the first three hours, when evaporation rate should be highest, was 0.00198 g hr^{-1}. This value can be combined with Newell's (1976) figure of 2277.6 J g^{-1} of energy released when water evaporates at 33°C to calculate an instantaneous heat flux for evaporation of 1.25 mW. For comparison, heat flux due to shortwave radiation or convection may exceed 100 mW for a snail of the size used here. The energy flux due to evaporation will decrease over time as the evaporation rate of the snail slows further. For the purposes of this study, I simplify the heat-budget equation by setting the heat energy flux due to evaporation and condensation equal to zero, which implies that the organisms neither lose water to evaporation nor experience condensation during cool periods.

1.1.5 Convection

When an organism has a body temperature different than that of the fluid surrounding it, heat energy is exchanged between the fluid and the organism. For the purposes of this heat-budget model, the fluid is the air moving around the organism at low tide.

Convection can either cool or warm the organism, depending on the relative temperatures of organism and air. Newton's law of cooling states that

$$W_{\text{conv}} = h_{\text{c}} A_{\text{conv}} \left(T_{\text{air}} - T_{\text{body}} \right) . \quad (6)$$

The heat flux between an object and the fluid around it is governed by the heat transfer coefficient, h_{c} (units of W m^{-2} K^{-1}), the area of the object available for convective heat transfer, A_{conv} (units of m^2), and the temperatures of the air and body of the organism (T_{air} and T_{body} respectively, units of K). The heat transfer coefficient is a function of the size and shape of the shell, as well as of the wind speed, and can be measured empirically in a wind tunnel (see below).

1.1.6 Conduction

As with convection, if a temperature differential exists between the organism and the substratum that it sits on, heat energy is exchanged via conduction. The rate of conductive flux is described as

$$W_{\text{cond}} = K_{\text{rock}} A_{\text{cond}} \frac{d(T_{\text{rock}})}{dz} . \quad (7)$$

The thermal conductivity of the substratum, K_{rock} (units of W m^{-1} K^{-1}), can be measured empirically. The area of conduction, A_{cond} (units of m^2), is the contact area between the rock and the organism. The temperature gradient in the substratum is represented by $\frac{d(T_{\text{rock}})}{dz}$ where T_{rock} is the temperature of the surface of the rock and z is depth into the rock over which a temperature gradient exists (z is positive into the rock). This form of the equation assumes that the rate-limiting step in conduction is between the substratum and the organism, rather than within the organism itself. Because the snails examined here actively circulate fluids through the body, the transfer of heat throughout the tissues of the body should be relatively fast.

1.1.7 Long-wave radiation

Long-wave radiation can be exchanged between the organism and several parts of the environment. Here I consider exchange between the organism and the sky, though the

concepts are the same for long-wave heat flux between the organism and the surrounding substratum or ocean, both of which are included in the actual heat-budget model (Walsberg, 1992).

For a body at a given absolute temperature, the net long-wave radiation in, $W_{\mathrm{lw,in}}$, and out, $W_{\mathrm{lw,out}}$, of the organism (in Watts m^{-2}) can be described as

$$W_{\mathrm{lw}} = W_{\mathrm{lw,in}} - W_{\mathrm{lw,out}} . \quad (8)$$

The long-wave radiation out of the shell to the sky, $W_{\mathrm{lw,out}}$, is a function of the area of the shell facing the sky, A_{l}, the long-wave emissivity of the shell, $\epsilon_{lw,shell}$, and the temperature of the organism, T_{body}:

$$W_{\mathrm{lw,out}} = A_{\mathrm{l}} \epsilon_{\mathrm{lw,shell}} \sigma {T_{\mathrm{body}}}^{4} . \quad (9)$$

Here, σ represents the Stefan-Boltzmann constant (5.67×10 W m^{-2} K^{-4}; Gates, 1980).

The long-wave radiation from the sky absorped by the shell can be expressed in a form similar to Eqn. (9):

$$W_{\mathrm{lw,in}} = A_{\mathrm{l}} \alpha_{\mathrm{lw,shell}} \epsilon_{\mathrm{lw,sky}} \sigma {T_{\mathrm{air}}}^{4} \quad (10)$$

where $\alpha_{\mathrm{lw,shell}}$ is the long-wave absorptivity of the organism, $\epsilon_{\mathrm{lw,sky}}$ is the emissivity of the air, and T_{air} is the temperature of the air around the organism.

To simplify Eqn. (10) for the following algebraic operations, we draw on the fact that the long-wave absorptivity of an object is equivalent to its long-wave emissivity, and substitute $\epsilon_{\mathrm{lw,shell}}$ for $\alpha_{\mathrm{lw,shell}}$ (Nobel, 1999). This substitution allows us to rewrite Eqn. (8) as:

$$W_{\mathrm{lw}} = A_{\mathrm{l}} \epsilon_{\mathrm{lw,shell}} \epsilon_{\mathrm{lw,sky}} \sigma {T_{\mathrm{air}}}^{4} - A_{\mathrm{l}} \epsilon_{\mathrm{lw,shell}} \sigma {T_{\mathrm{body}}}^{4} , \quad (11)$$

which can be further simplified to

$$W_{\mathrm{lw}} = A_{\mathrm{l}} \epsilon_{\mathrm{lw,shell}} \sigma \left(\epsilon_{\mathrm{lw,sky}} {T_{\mathrm{air}}}^{4} - {T_{\mathrm{body}}}^{4} \right) . \quad (12)$$

The heat-budget model used in this experiment solves for body temperature, so it is desirable to express Eqn. (12) in terms of T_{body} rather than T_{body}^4. To accomplish this, Eqn. (12) can be expressed as a Taylor series expansion for T_{body} near T_{air}, so that retaining the first two terms results is an approximation for W_{lw} of the form

$$W_{lw} \cong A_l \epsilon_{lw,shell} \sigma {T_{air}}^4 \left(\epsilon_{lw,sky} - 1\right) + 4 A_l \epsilon_{lw,shell} \sigma {T_{air}}^3 \left(T_{air} - T_{body}\right). \quad (13)$$

Using the first two terms of the Taylor series expansion is reasonably accurate for T_{air} and T_{body} within 10 – 15 K of each other (Tracy *et al.*, 1984; O'Connor and Spotila, 1992). The same procedure can be used to calculate the long-wave heat flux between the organism and the ocean or substratum by substituting appropriate values for the emissivity of the ocean or rock along with the surface area of the organism that is facing these other sources.

1.1.8 Metabolic heat production

Living organisms, both ectothermic and endothermic, produce heat from metabolic processes. However, the total contribution of metabolic heat production to the heat budget of a small ectothermic animal may be quite small (Edney, 1951, 1953; Parry, 1951; Newell, 1976). Metabolic heat production of small animals such as littorine snails can be directly measured non-invasively in a calorimeter. Published rates of metabolic heat production during aerial exposure for *Littorina saxatilis*, a high-shore member of the genus from Europe, are quite low relative to the calculated rates of heat flux from environmental sources (Kronberg, 1990). When placed in air inside a calorimeter, *L. saxatilis,* which were in the same size class as the *L. scutulata, L. plena,* and *E. natalensis* used in this study, produce only ~1 to 2.5 mW g^{-1} (ash free dry weight). Shortwave radiation impinging on a snail of the same size at midday may routinely be as high as 900 mW g^{-1} (ash free dry weight). For the purposes of the current heat-budget model, I assume that the contribution of metabolism to the overall temperature of the organism is negligible, and set $W_{met} = 0$.

1.2 Methods

1.2.1 Species collections

Five species were used in these experiments, collected from a number of locations (Figure 1-2, Figure 1-3). *Littorina keenae* (Rosewater, 1978, formerly *L. planaxis* Philippi, see (Rosewater, 1978)) and *L. scutulata* (Gould, 1849) were collected at Hopkins Marine Station (HMS, 36°37.3'N, 121°54.25'W). *L. sitkana* (Philippi, 1846) shells were collected from the shores at the Friday Harbor Laboratories (48°32.8'N, 123°0.6'W) on San Juan Island, in the Puget Sound of Washington State, during a visit in the summer of 2002. *L. plena* (Gould, 1849) shells were generously provided by Dr. Chris D. G. Harley, and were originally collected from the high intertidal zone of Tatoosh Island (48°39.17'N, 124°73.66W), at the top of the Olympic Peninsula in Washington State. The final species, *Echinolittorina natalensis* (Philippi, 1847, formerly *Nodilittorina natalensis,* see Williams *et al.*, 2003)*,* is found in sub-tropical eastern South Africa. With the help of Dr. Kerry J. Sink, I collected specimens of *E. natalensis* from the Natal region of South Africa, north of Durban at Cape Vidal (28°13'S, 32°56'E), during a visit to the region in 2002.

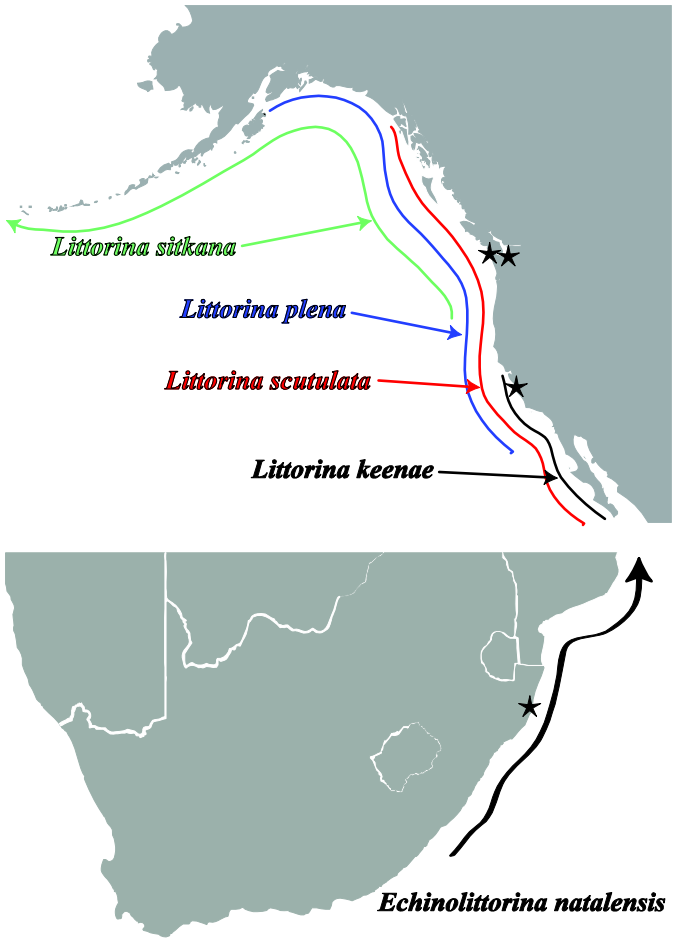

Figure 1-2. Distribution maps for the species used this study. The range of *Littorina sitkana* extends into the western Pacific Ocean to Japan. The range of *Echinolittorina natalensis* extends north to Kenya. Stars indicate the collection sites for the shells. Precise collection locations are listed in the text. Distributions based on (Reid, 1996) and (Williams and Reid, 2004).

Figure 1-3. Littorine snail shells used in this study. From left to right: *Littorina keenae*, *L. scutulata*, *L. plena*, *L. sitkana* and *Echinolittorina natalensis*.

1.2.2 Heat-budget model parameters

The physical parameters used to create the heat-budget model were collected via a variety of methods. Some values, such as those for color and conductivity of the shell, were calculated for representative samples, while other parameters were collected for each individual shell. The methods detailed below are arranged according to the heat flux components of the heat-budget model. In addition to measuring parameters for the snail shells, the various heat flux parameters were also measured or estimated for brass spheres for use as a point of comparison with the snails.

1.2.2.1 Short-wave flux parameters

The short-wave absorptivity, α, of a material is a function of the color of the material. Lighter colors such as white tend to reflect a greater portion of the visible wavelengths of light, while dark colors such as black absorb more of the incoming shortwave energy. Therefore the color of a shell affects the absorbance of shortwave radiation from the sun, which in turn affects the temperature of the organism inside the shell. Littorine snails occur in a range of colors within and among species. *L. sitkana* shells are typically black or dark brown, but there may be color banding including shades of white, orange, green, yellow etc. (Harger, 1972; Reid, 1996). *L. scutulata* and *L. plena* shells are nearly identical in shape (Hohenlohe and Boulding, 2001), and are typically black or dark green, but can contain a variety of tessellated color patterns over the dark background (Mastro *et al.*, 1981; Chow, 1987a). Eroded individuals may be much lighter in color. *E. natalensis* shells are brown with white flecks, especially on the tips of the nodules. *L. keenae* contains a substantial amount of shell color variation, even within local populations, with individuals laying down shell material that ranges in color from white to brown to green to black, along with mottled combinations of those colors. Eroded shells of *L. keenae* typically are dull brown. Examples of shell colors used for measurements in this experiment are show in Figure 1-4.

Figure 1-4. Shell fragments used to measure short-wave absorptivity. Colors were classified from left to right as black, green, brown, and white. For reference, the photograph was taken in full sunlight, and the surrounding gray border represents the reading from a standard 18% reflective gray card photographed under the same light. The black, brown and white shell fragments came from *L. keenae*, the green fragments came from *L. scutulata*. Both species were collected at HMS.

Shortwave absorbance measurements were made using a spectroradiometer (LI-COR model 1800 with integrating sphere, LI-COR Biosciences, Lincoln, Nebraska, USA). Because the aperture of the integrating sphere of the spectroradiometer is larger than a single snail shell, I broke a number of shells into large flakes, and glued those pieces to cardstock. This produced a flat sample specimen > 15.2 mm diameter, which could then be inserted into the spectroradiometer. To cover the range of shell colors, four cardstock sample specimens were made, one each for black, green, brown, and white shells.

The area of the shell that absorbs shortwave radiation, the projected area, varies through the day as the sun traverses the sky. Because littorine snail shells are not simple shapes, it is difficult to approximate the projected area with purely mathematical expressions. In order to calculate the projected area of a shell as the sun moves across the sky, it was necessary to empirically measure the projected area, A_{proj}, of each shell from a number of perspectives.

To this end, each shell was attached to a platform that could be rotated through 180 degrees. I positioned a digital camera at a fixed position facing the shell, and placed a ruler next to the shell for scale. I then took a picture of the shell to measure projected area, and rotated the platform a set number of degrees. The ruler was repositioned parallel with the center of the shell for each position, and a series of either 18 or 12

(corresponding to 10° and 15° rotation steps) photographs was taken as the platform was rotated through a full 180 degrees. Each shell was oriented in one of four directions: head facing the camera, left side facing the camera, head turned 45° clockwise from the camera, and head turned 45° counterclockwise from the camera. Additionally, I shot a series of pictures while rotating the shell on the horizontal plane, every 15 degrees for a complete rotation. Every image of the shell was then loaded into the image analysis program Image-J (National Institutes of Health,Rasband, 1997-2007) and the projected area was calculated using the ruler in each image as a size reference.

Although the shell was rotated to take the pictures for the projected area calculations, it is perhaps more intuitive to conceptualize the process from a different viewpoint. If we treat the shell as being fixed in space, on a horizontal plane with the anterior end facing north (as a starting point), and treat the camera as the moving portion of the system, it should make sense to treat the camera like a "sun", moving over the shell much as the sun would transit the sky during the day (Figure 1-5). Each picture of the projected area of the shell represents the projected area that would be facing the sun at a particular solar altitude and azimuth.

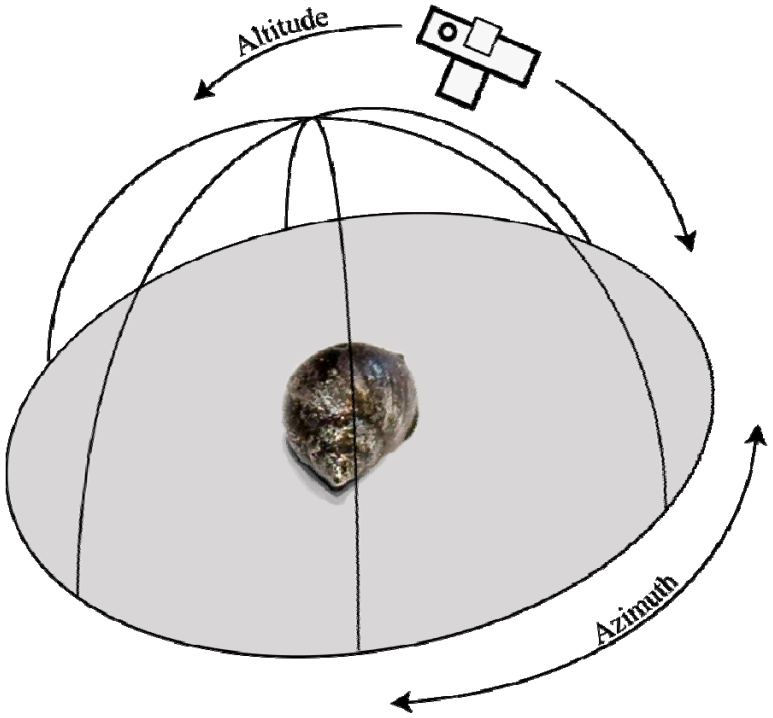

Figure 1-5. Measuring projected area of a littorine shell. The camera traversed a number of transects over the shell to provide images of the shell from different directions. The images were used for calculating the projected area of the shell facing the sun at any given solar altitude and azimuth.

The projected-area pictures of each shell represent only a small fraction of the positions in the sky that the sun travels through during a day, so it was necessary to interpolate projected areas between each measured point, using a triangle-based cubic interpolation routine implemented in Matlab software (The Mathworks, Inc., Natick, Massachusetts, USA). As before, the shell was treated as if it were facing north on a horizontal plane, and the position of the camera for each picture was mapped onto a grid of x,y coordinates, calculated as if the camera were always at a fixed distance (= 1 unit) from the shell and moving in a hemisphere above the shell. Each picture had an altitude and azimuth assigned to it in this coordinate space, and those values were converted to radians and mapped onto the planar projection of the x,y grid using the equations:

$$x = \sin(\text{azimuth}) \times \cos(\text{altitude}) \quad (14)$$

and

$$y = \cos(\text{azimuth}) \times \cos(\text{altitude}) \; . \quad (15)$$

Each x,y coordinate then had a projected area value assigned to it. The resulting three-dimensional array of coordinates (equivalent to solar altitude and azimuth) and the associated projected areas were then saved as an input to the heat-budget model. Separate arrays of projected area values were produced for each shell in the "down" and "up" orientations.

For the standard spheres, projected area was calculated based on the standard equation for the area of a circle using the radius, R, of the sphere:

$$A_{\text{proj}} = \pi R^2. \quad (16)$$

1.2.2.2 Convective flux parameters

Convective heat flux is a function of the size and shape of the organism, and wind speed, all of which determine the value of the heat transfer coefficient, h_c. To determine h_c, a silver-alloy cast was made for each shell used in this study (Figure 1-6). Silver is an efficient conductor of heat, which helps homogenize the flow of heat energy to all surfaces of the model and allows a temperature measurement taken at one point to be representative of the overall temperature of the model. The silver casting was fitted with a 0.08 mm copper-constantan thermocouple lead (Omega Engineering, Stamford, Connecticut, USA) to measure the temperature of the model, T_b, and placed on a piece of insulating Styrofoam inside a wind tunnel. A series of plaster tiles cast in the form of a piece of granite from the shore of HMS were placed upstream of the silver models in order to provide a boundary layer flow of air similar to that in the field. Each model was heated to 30°C above ambient temperature, and cooled by pulling air through the wind tunnel. Five air speeds were used, ranging from 0.25 m s^{-1} to 5 m s^{-1}. Air speed was measured using a model 441S thermistor anemometer (Kurz, Inc., Monterey, California, USA) mounted 20 cm above the floor of the wind tunnel.

The wind speed and temperature of the air, T_{air}, and model, T_{body}, were recorded on a datalogger (21X, Campbell Scientific Inc., Logan, Utah, USA). Each silver model was run in four orientations: anterior end facing into wind, posterior end facing into wind, left and right sides facing into wind. The heating and cooling cycle was replicated three times at each wind speed for each orientation of the shell, and each set of runs was carried out with the shell sitting down on the substratum or up off the substratum with only the lip of the shell attached.

Figure 1-6. Representative littorine snail shells and their silver casts. *Littorina scutulata* and a silver cast are shown on the left. *Echinolittorina natalensis* and a silver cast are shown the right.

Despite the insulating properties of the Styrofoam under the silver model, there was some heat loss through conduction. To correct for this, each silver model was placed on the Styrofoam, heated to 30°C above ambient temperature, and capped with an additional piece of Styrofoam to minimize convective heat transfer. The heat transfer coefficient calculated in this situation was then subtracted from the value of h_c at all other wind speeds.

The surface area of the silver model exposed to the air for convective heat exchange, A_{conv}, was calculated as follows. Each silver model was glued to the head of a pin which was then inserted into a fixture that could rotate the pin. A digital camera was set up in a fixed position relative to the silver model, and a ruler was included in the picture for scale. The silver model was rotated through 360° a number of times, and pictures were taken at haphazard intervals. The silver model was then removed from

the pin and reattached in another orientation (spire pointing up, spire horizontal, spire elevated 45° from horizontal) and another series of pictures was taken. At least 120 images were shot for each silver model. The images were imported into Image-J and the projected area was calculated for each image. To aid in the processing of the large number of images in Image-J, the images for each model were combined into a stack, and the scale (pixels per meter) was set using the ruler. Each image in the stack was then thresholded so that the background was white and the silver model was black. Extraneous objects, such as the mounting pin, were manually erased. When each image was ready, the entire stack was processed automatically using the "Analyze Particles" routine in Image-J. Only particles larger than 4 $x10^{-6}$ m^2, i.e. the black silhouettes of the silver models, were included in the analysis. Image-J could then automatically calculate the projected area of the silver model silhouette in each image.

The projected areas from all photographs of a silver model were averaged, and the total surface area of the model was calculated by the method of Johnsen and Widder (1999) for calculating the surface area of a convex polyhedron:

$$A_{\mathrm{conv}} = 4 \times \text{average projected area} . \qquad (17)$$

When the snail shell was sitting with the aperture down against the substratum, the surface area available for convective cooling was reduced. Using photographs of the aperture area of each shell, a value for the surface area that would be obstructed from the air flow, equivalent to the aperture area, was calculated and subtracted from the total surface area of the shell to give a modified value of A_{conv}. When the shell was perched on its lip and had minimal contact with the substratum, the total surface area of the shell was used as the value for A_{conv}.

The mass, m, of each silver model was measured on a balance, and the specific heat of the sterling silver in the model, c_{Ag}, was 251 J kg^{-1} K^{-1}. Using the mass of the silver model, the specific heat of silver, surface area of the shell, and expressing the rate of heat loss of the silver model in the wind tunnel as the natural logarithm of (T_{body} - T_{air}), the value for the heat transfer coefficient, h_{c}, could be obtained from the equation:

$$h_c = -\frac{m\, c_{Ag}}{A_{conv}} \times \frac{\ln (T_{body} - T_{air})}{t} \quad (18)$$

To calculate h_c for wind speeds other than those used in the wind tunnel, it was convenient to construct a plot of the Nusselt number (*Nu*) as a function of the Reynolds number (*Re*) (Johnson, 1975). Nusselt number is calculated as

$$Nu = \frac{Lh_c}{K_{air}} \quad (19)$$

where L is the characteristic length of the shell in the direction of flow, and K_{air} is the conductivity of air (W m^{-1} K^{-1}). K_{air} is a function of the air temperature, T_{air}, based on the relationship given in (Denny, 1993):

$$K_{air} \cong 0.005010 + 7.2 \times 10^{-5} T_{air} \,. \quad (20)$$

Reynolds number is calculated as

$$Re = \frac{Lu}{\nu} \quad (21)$$

where u is the wind speed (m s^{-1}) , ν is the kinematic viscosity of air (m^2 s^{-1}) , and L is the characteristic length of the shell, as for the Nusselt number. The value of ν is calculated as (Denny, 1993):

$$\nu \cong -1.25 \times 10^{-5} + 9.2 \times 10^{-8} T_{air}. \quad (22)$$

By expressing the relationship between *Nu* and *Re* in the form

$$Nu = aRe^b \quad (23)$$

and estimating the values of a and b with a curve fitting routine in Matlab software, it is possible to estimate a value of h_c for any shell size and wind speed combinations that fall on the curve. The r^2 values for the estimates of a and b were all > 0.99. To estimate h_c, *Nu* and *Re* in Eqn. (23) can be substituted with the equivalent values from Eqns. (19) and (21):

$$\frac{Lh_{\mathrm{c}}}{K_{\mathrm{air}}} = a\left(\frac{Lu}{\nu}\right)^{b}, \tag{24}$$

which can be rearranged to solve for h_{c}:

$$h_c \cong aK_{\mathrm{air}}\left(\frac{u}{\nu}\right)^{b} L^{b-1}. \tag{25}$$

Values for *a* and *b* were calculated for each silver model of a shell facing in each of four directions. Additionally, different values of *a* and *b* were calculated for shells modeled in the "down" and "up" positions.

To compare snail shells to a standard sphere, it was necessary to measure h_{c} for spheres in the wind tunnel. In order to account for potential changes in h_{c} among different sized spheres due to the thickness of the boundary layer of air flowing over the floor of the wind tunnel (Mitchell, 1976), a range of brass sphere sizes was used, from 4.75 mm to 25.4 mm diameter (brass alloy 260, McMaster-Carr Supply Co., Los Angeles, California, USA). Each sphere was drilled so that a thermocouple lead could be inserted into the center of the sphere. Spheres were placed on Styrofoam in the wind tunnel in the same manner as the silver snail shells, and were run at a range of wind speeds from 0.1 to 5 m s^{-1}. Conductive heat loss to the Styrofoam was measured in the same manner as for the silver snail shells. The area for convection, A_{conv}, was calculated using the radius of the sphere, *R*, and the standard equation for the surface area of a sphere:

$$A_{\mathrm{conv}} = 4\pi R^2. \tag{26}$$

The heat transfer coefficient, h_{c}, was calculated for each sphere using equation (18) and a specific heat for brass of 383 J kg^{-1} K^{-1}. The relationship between the Nusselt number and the Reynolds number was calculated for each brass sphere using equations (19) and (21), and then fitting a curve to the resulting data to estimate the coefficients *a* and *b* in equation (23).

Wind speeds in the wind tunnel were measured at a fixed height of 20 cm above the substratum, but the silver snails and brass spheres were sitting down on the substratum in the boundary layer of slower-moving air flowing over the rough plaster tiles. To characterize the profile of the boundary layer, the anemometer was moved through a range of heights from 2.5 mm to 140 mm above the substratum while holding the free-stream wind velocity in the wind tunnel constant. These profiles were measured for each of the wind speeds utilized in the wind tunnel experiments.

1.2.2.3 Conductive heat flux parameters

The area in contact with the substratum, A_{cond}, consisted of three separate values, depending on the behavior of the snail (Figure 1-7): 1) Snails with the foot extended out of the shell have maximal contact with the substratum. 2) Snails may withdraw the foot into the shell and glue the outer lip of the shell to the rock, leaving portions of the shell resting on the substratum. 3) Snails may withdraw the foot and elevate the shell up off the substratum, using dried mucus to position the shell so that only a portion of the outer lip of the shell is in contact with the rock.

For snails with the foot extended, foot contact area was estimated via photogrammetry. Shells were placed with the aperture facing upwards and a ruler was placed adjacent to the shell and on the same plane as the aperture opening, so that both could be photographed from directly overhead with a digital camera. The digital image was transferred to a computer and opened in Image-J, where the area of the aperture, approximately equal to the area of the foot, could be calculated.

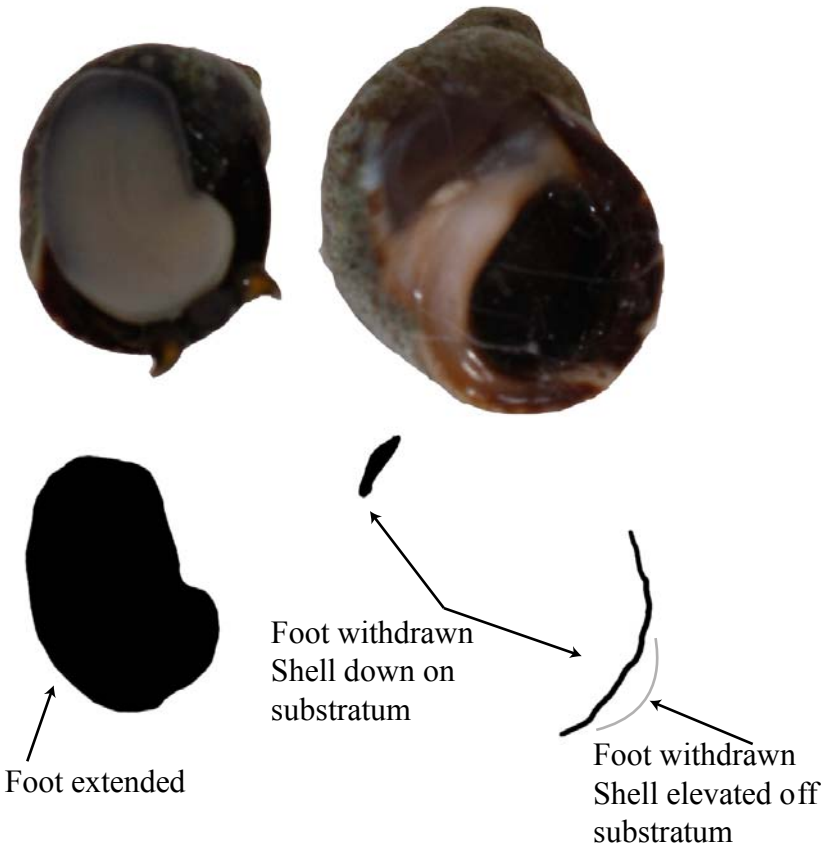

Figure 1-7. Illustration of contact area with substratum in various body positions. The silhouettes demonstrate the change in contact area when snails remove the foot from the substratum and withdraw into the shell. When the shell is elevated up off the substratum, only the silhouette in the lower right contacts the rock.

The contact area of the shell with the foot withdrawn was made by taking each shell and rolling it on an ink pad. The shell was then transferred to a piece of copier paper, where it was pressed down onto the surface lightly. Every effort was made to minimize rolling the shell on the paper or otherwise artificially increasing the size of the ink mark left behind. This operation was carried out three times for shells in each of two positions: shell sitting down with the aperture against the substratum, and shell sitting up on its lip. After photographing the resulting marks with a scale bar in the picture, the same digital image analysis routine was carried out in Image-J to calculate contact area as described for the foot area.

As part of the calculation to determine the heat flux due to conduction, W_{cond}, the heat-budget model calculates the surface temperature of the rock and the temperature gradient in the rock substratum, $\frac{d(T_{\text{rock}})}{dz}$. The temperature gradient in the rock is calculated using a 1-dimensional heat equation. The 1-D heat equation has the form

$$\frac{dT_{\text{rock}}}{dt} = D_{\text{rock}} \frac{d^2T_{\text{rock}}}{dz^2} \tag{27}$$

where D_{rock} (units of $m^2\ s^{-1}$) is the thermal diffusivity of the substratum, and $\frac{d^2T_{\text{rock}}}{dz^2}$ is the 2nd derivative of the change in temperature with distance into the rock substratum (Incropera and DeWitt, 2002). The model is initialized with a uniform temperature gradient throughout the substratum, from the surface to a depth of 0 m above Mean Lower Low Water, where the rock temperature is assumed to always equal sea surface temperature. The distance from the surface to the lowest depth is divided into a series of evenly spaced steps, 1 cm apart. At each time step in the model, a new set of temperature values for the depth steps is calculated using a finite difference solution. The first derivative of Eqn. (27) is approximated as the difference in temperature between pairs of evenly spaced points located halfway between each of the depth steps in the rock. The 2nd derivative is then approximated as the difference in temperature between pairs of points located halfway between the 1st derivative points, which results in these points aligning with the original depth steps (Figure 1-8). The new temperature at each depth step is then calculated as

$$\text{new } T = \text{old } T + \left(D_{\text{rock}} \frac{d^2T}{dz^2} \times \Delta t\right) \tag{28}$$

where Δt is the time step. The calculation of new rock temperatures at each depth step is repeated at short time intervals until the main time step of the model has elapsed.

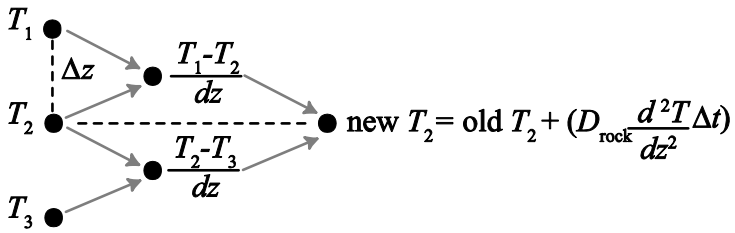

Figure 1-8. Conceptual diagram of the method used to calculate the temperature gradient in the substratum. At the left are known temperatures, T_1, T_2, and T_3, at discrete depths in the rock. Following a time step Δt, a new temperature at T_2 is calculated by approximating the first derivative of the temperature gradient at points spaced between T_1, T_2, and T_3, followed by approximating the second derivative at points spaced between the first derivative points. This arrangement of spatial steps results in the second derivative in this example being calculated at the same depth as the original T_2, allowing calculation of a new temperature, T_2, using the equation shown at the right of the diagram.

The thermal diffusivity of the rock, D_{rock}, is a function of its thermal conductivity, K_{rock}, its density, ρ_{rock}, and the specific heat capacity of the rock, c_{rock} (Carslaw and Jaeger, 1959):

$$D_{\text{rock}} = \frac{K_{\text{rock}}}{\rho_{\text{rock}} c_{\text{rock}}}. \quad (29)$$

The complete calculation of the temperature gradient in the rock requires knowledge of the temperature of the rock at the surface. This temperature is calculated in a manner similar to the body temperature of the snail, using estimates of W_{sw}, W_{lw}, W_{conv}, and W_{cond} at the rock surface. Rock temperature is calculated for a circular disk of rock with radius 2.08 cm (see Denny and Harley, 2006).

The conductive length, d_s, over which heat energy must travel to reach the body of the organism, changes depending on the orientation of the body (Figure 1-9). When the snail foot is in contact with the rock, I assume that the circulation system of the snail quickly moves heat throughout the body. In this case, the conductive length is a short distance step, Δz, into the rock, and Eqn. (7) is used to calculate W_{cond}. If the snail's foot is withdrawn, d_s can be one of two distances depending on the orientation of the shell. For a shell sitting down on the substratum, d_s is the thickness of the shell on the

main body whorl separating the tissue of the body from the substratum. When the shell is elevated up off the substratum with only the lip of the shell touching the rock, d_s was measured as the length of shell from the substratum to the body withdrawn inside the shell. The thermal conductivity of the shell, K_{shell}, is substituted into Eqn. (7), and the temperature gradient is calculated across the thickness of the shell, resulting in the new version of the equation for conductive heat flux:

$$W_{cond} = K_{shell} A_{cond} \frac{d(T_{rock})}{d_s} . \quad (30)$$

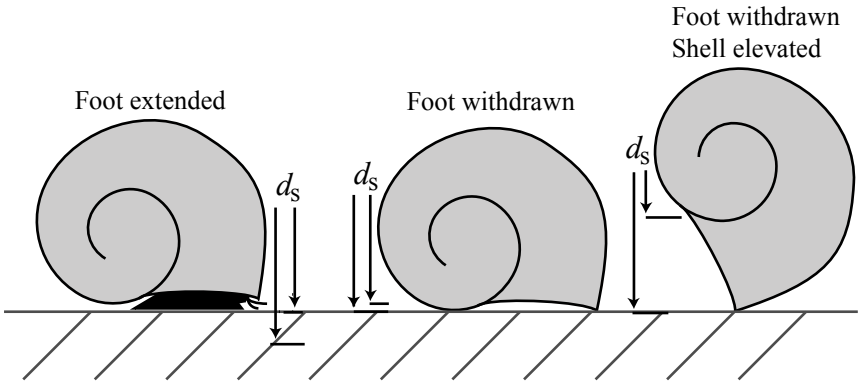

Figure 1-9. Diagram of conductive length, d_s, distances used in the heat-budget model for various shell positions. When the foot is out in contact with the rock, the conductive length is a short step from the rock surface across the mucus layer under the foot and into the body, where circulation should distribute heat energy relatively quickly throughout the body. If the snail withdraws the foot into the shell, the conductive length is the thickness of the main body whorl of shell. When the shell is additionally elevated up off the substratum, conductive length is measured as the distance between the substratum and the closest point to where the body sits inside the shell.

When modeling spheres using the heat-budget model, the contact area of the sphere with the substratum was estimated based on the substratum contact area of *L. keenae* shells with total shell surface areas ranging from 9.9×10^{-5} m^2 to 3.5×10^{-4} m^2 (maximum shell lengths from 7.6 mm to 14.6 mm). Contact area was measured using the ink-and-paper method described above, and the scaling relationship between shell (or sphere) surface area and contact area was estimated as

$$A_{\text{cond}} = 0.133(A_{\text{conv}})^{1.11}. \quad (31)$$

1.2.2.4 Long-wave flux

Values for the average long-wave emissivity of snail shells and granite substratum were taken from Denny and Harley (2006) as determined for the shell of *Lottia gigantea* and the granite rocks at HMS. The model assumes the long-wave emissivity, $\epsilon_{\text{lw,sky}}$, of air on a clear, cloudless day is 9.2 x $10^7 T_{\text{air}}{}^2$ (Campbell and Norman, 1998) where T_{air} is the temperature of the air. During cloudy and foggy periods the emissivity of the sky approaches 1, but unfortunately the environmental data collected for the model do not contain a record of cloud or fog cover. As the goal of the heat-budget model was to calculate accurate body temperatures during warm periods, the night time long-wave heat exchange with the sky was simplified by using a constant value for $\epsilon_{\text{lw,sky}}$ of 0.95, which suits the foggy conditions often found during the early morning hours before sunrise at HMS.

Because littorine snail shells are roughly spherical objects, the upper portions of the shell faces up towards the sky, while the lower side of the shell faces the substratum, and the long-wave heat flux between those sources and the shell may be quite different.

To produce an approximate measurement of the surface area of the shell facing the sky or substratum, a picture taken from directly overhead was used to calculate the projected area of the shell. If the shell is approximated as a sphere, the surface area of the hemisphere facing the camera should be two times the projected area. This hemispherical surface area was used in the model as the surface area that exchanged long-wave heat energy with the sky. The same value was also used as the surface area for the lower portion of the shell facing the rock substratum. Shells were photographed in both the "down" and "up" orientations, so that two separate values of surface area available for long-wave exchange with the surroundings were produced for each shell. Though this method is simplistic in that it treats the shell as a sphere, the overall contribution of long-wave heat flux to the temperature of the organism is relatively

low compared to other sources of heat flux, in large part because the temperatures of the sky and substratum are close to the temperature of the shell during warm daylight hours. Due to this small contribution, the simple method of calculating surface area for long-wave heat exchange was deemed sufficient.

1.2.2.5 Behavioral shifts

The cue that caused snails to withdraw the foot and glue the shell to the substratum was determined with a combination of laboratory and field trials. In the laboratory, three groups of twenty *L. keenae* were placed in a temperature controlled wind tunnel. The temperatures of the substratum and air were raised at a steady rate of 8°C hr^{-1} from an initial temperature of 14°C, and the behavior of the snails was observed. The temperature at which half of the snails had withdrawn the foot was recorded and used as an input parameter for controlling "behavior" in the heat-budget model.

In the field, groups of twenty *L. keenae* were placed on a rock in the high intertidal of HMS on the nights of July 20, 21, and 22nd, 2007. The rock surface was wetted with seawater at the start of the deployment, and the snails were monitored every half hour. The air and rock temperatures during these trials did not exceed 16°C. The time at which half the snails had withdrawn the foot and glued the shell to the rock was determined and used as a second input parameter (time-of-emersion) used to control the behavior of the modeled snails.

1.2.3 Heat-budget model operation

The code of the heat-budget model used here is derived from the model of Denny and Harley (2006) for *Lottia gigantea*. The model was supplied with a continuous record of environmental conditions sampled at 10 minute intervals. Solar irradiance (LI-200SZ, LI-COR Biosciences, Lincoln, Nebraska, USA), wind speed (Wind Monitor 05103-5, R.M. Young Co., Traverse City, Michigan, USA), and air temperature (Viasala HMP45C, Campbell Scientific Inc., Ogden, Utah, USA) are measured at a pair of weather stations deployed on the point at HMS, using Campbell 23X dataloggers to store the data (Campbell Scientific Inc.). Water temperature data are

interpolated from a daily sea surface temperature measurement made every morning on Agassiz Beach at HMS. Significant wave height data, used to calculate the extent of wave swash up the shore, are collected by a SeaBird SBE-26 wave gauge mounted at 12 m depth approximately 50 m north of the point at HMS (SeaBird Electronics, Bellevue, Washington, USA). Measured tidal level is taken from a NOAA tide gauge station located approximately 1 km south of HMS at the Monterey Municipal Harbor. The environmental data set used in this project covers seven years from 1 August, 1999 to 31 July, 2006.

In operation, the heat-budget model steps through the environmental data set in 10 minute increments. At each time point, the effective height of the tide (tide height + swash due to waves) is calculated and compared to the shore level of the organism. When the effective height of the tide is equal to or higher than the shore height of the organism, the model sets the body temperature of the organism and the surface temperature of the rock substratum equal to ocean temperature, and updates the temperature gradient within the rock.

When the effective tide height is less than the shore height of the organism, a body temperature for the organism is calculated on the basis of the environmental parameters and the calculated temperature of the rock surface beneath the organism. The simplest case is for night time, when solar irradiance (and therefore short-wave heat flux) is zero. The temperature of the organism is calculated based on the sum of the remaining heat flux components: long-wave radiation, conduction with the substratum, and convection with the air.

During daylight hours, short-wave heat flux depends on the position of the sun relative to the organism and the substratum. The position of the sun in the sky is calculated using the time of day, the latitude and longitude of the site, and standard celestial equations (Gates, 1980). The short-wave heat flux into the rock substratum is calculated from the position of the sun relative to the substratum and the irradiance value from the pyranometer. The short-wave heat flux into the organism requires knowing the projected area of the shell facing the sun at its current position. The

position of the sun is fed into the supplied matrix of projected area values measured for the snail shell, and an interpolated projected area value is returned. Short-wave heat flux into the shell can then be calculated in the same manner as for the rock.

The behavior of the littorine snail impacts all of the heat fluxes in and out of the body. Unlike limpets and many other snail species, littorine snails may alter their foot contact with the rock and change the orientation of the shell relative to the substratum and sun. The heat-budget model contains options for adjusting the "behavior" of snails in response to rising temperatures and prolonged emersion. Instead of simply keeping the foot in contact with the substratum at all times, the model allows control over the threshold body temperature or time-of-emersion threshold (the elapsed time since the effective tide level dropped below the shore height of the snail), above which a snail withdraws the foot and glues the shell to the rock. Withdrawing the foot reduces the contact area with the substratum by an order of magnitude, reducing conductive heat exchange (Figure 1-7). When the foot is withdrawn, the model also allows the snail to either remain with the shell down on the rock, or to assume a position where only the outer lip of the shell is glued to the substratum and the spire of the shell points up away from the substratum (Figure 1-1). All of the heat fluxes change as the shell position is altered.

When the shell transitions from down against the rock to standing up on the lip of the shell, the projected area of the shell towards the sun changes, altering A_{proj} and changing the short-wave heat flux, $W_{sw,}$ as a result. Depending on the orientation of the substratum and the time of year, this may either raise or lower the projected area relative to the shell sitting down on the rock. Raising the shell up off the rock also changes the components of convective heat exchange, W_{conv}, by: 1) altering the area, A_{conv}, available for convection, 2) moving the shell further up into the boundary layer of air flowing over the substratum, which changes the heat transfer coefficient, h_c, and 3) changing the characteristic length of the shell, which also shifts h_c. Long-wave radiative heat flux, $W_{lw,}$ can be changed by altering the area of the shell facing the sky or surrounding substratum. Finally, conductive heat exchange, W_{cond}, is further

reduced by limiting contact with the substratum to the lip of the shell and increasing the conductive length over which heat energy must travel to reach the body of the snail.

The heat-budget model for spheres operated in the same manner as the model for the snails, but with a slightly simplified set of features. Spheres were modeled as inanimate objects with no behavior, so that the contact area between the sphere and the substratum never changed. The conductive length and thermal conductivity of the sphere were set equal to the values of a snail shell of nearly the same diameter (d_s and K_{shell}, respectively). Contact area was estimated using the relationship in equation (31). Short-wave heat flux was calculated using a constant projected area based on the radius of the sphere and a short-wave absorptivity equivalent to a snail shell. Long-wave flux was calculated in the same manner as for the snail shells, with the area facing the sky and substratum each being half of the total surface area of the sphere. Convective heat flux was calculated using the surface area of the sphere minus the contact area with the substratum. The heat transfer coefficient for a sphere of a given size was estimated from the relationship between sphere diameter and the coefficients *a* and *b* from the Reynolds-Nusselt number data for each sphere size.

1.2.4 Heat-budget model verification

A series of trials was carried out to ensure that the body temperatures predicted by the heat-budget model were accurate. A mixture of snail mimics and live snails were fitted with thermocouples and monitored in the field and the laboratory

1.2.4.1 Field trials

Each of the shells used to create the silver casts was used as a snail mimic in the field. A mixture of epoxy resin and silver was used to fill the body cavity of each shell, and once dried, the mixture was drilled to insert a 0.08 mm thermocouple lead. The snail mimics were deployed on a granite bench in the high intertidal zone at HMS, above the height where waves would reach the models. Because the granite surface at this high shore site is extremely friable, I first smoothed the granite with a masonry

grinding wheel. The resulting surface more closely matched the surface texture of the intertidal rocks on which the snails typically live. Each snail mimic was placed on the rock in either the "up" or "down" position, with the anterior end facing north. A minimal amount of water-based lubricating jelly was placed between the lip of the shell and the granite to substitute for the layer of mucus used by snails to attach the shell to the rock. The thermocouple wire was also employed as a brace to help hold shells in the "up" position when necessary. The very thin thermocouple wire has no measurable influence on the temperature of the snail mimic. The thermocouple from each snail mimic was hooked to a multiplexing thermocouple reader and electronic datalogger (Models AM416 and 23X, Campbell Scientific Inc., Logan, Utah, USA).

To test the accuracy of rock surface temperature predictions, a pair of thermocouple leads was inserted into shallow grooves ground into the rock surface. The grooves were filled with silver-filled thermal conductive paste (Arctic Silver 5, Arctic Silver Inc., Visalia, California, USA) and a covering of granite particles was sprinkled over the groove to match the color to the surrounding granite. Solar irradiance was measured with a LI-200SB pyranometer (LI-COR Biosciences, Lincoln, Nebraska, USA) and wind speed was measured with a cup anemometer (Wind Sentry, R. M. Young Co., Traverse City, Michigan, USA). The anemometer was placed approximately 20 cm above the snail mimics, the same height as the anemometers used in the wind tunnel when measuring the heat transfer coefficient for the silver models. Air temperature was measured with a shaded thermocouple mounted approximately 10 cm above the height of the snail mimics. Measurements of weather conditions and snail mimic temperatures were made during two periods, April 23-29 and June 3-7, 2007. Temperatures, wind speed, and solar irradiance were recorded once a minute continuously during those times. Some days had fog or clouds for part of the day, which changes the emissivity of the sky, so data from those days were discarded. Fog often settled over this site from the middle of the night until sunrise, so the emissivity of the sky was set to 1.0 for those periods. During the April deployment half of the snail mimics were placed with the shell down on the rock and the other half were placed with the shell perched on its lip. These positions were reversed for the

June deployment so that every shell mimic was tested in both the "down" and "up" positions at some point.

During the June deployment, a pair of live *L. keenae* was fitted with thermocouples and deployed alongside the snail mimics. These live snails, which were similar in size to the larger *L. keenae* snail mimic, had a hole ground into the main body whorl of the shell with a rotary grinder. When the shell was almost ground through, a pair of forceps was employed to break through the last layer of shell. A 0.08 mm diameter thermocouple lead was then inserted into the shell where it sat in contact with the body of the snail. To minimize evaporative water loss, the thermocouple lead was glued in place with cyanoacrylate glue which closed over the hole. The snails were placed on a wetted portion of the granite bench and allowed to position themselves as they liked. As the rock surface dried, both snails withdrew the foot into the shell, glued the lip of the shell to the rock with the shell in the "down" position, and sealed the operculum. The temperature of these two snails was monitored from June 9 -10.

The heat-budget model used to test the deviations between measured and predicted temperatures for snail mimics in the field implemented a moving average filter to smooth the short term temperature fluctuations contained in the 1-minute-sampling-frequency data. Because the heat-budget model attempted to calculate an instantaneous body temperature based on the previous body temperature and the environmental conditions at the current time point, it did not account for time lags in the temperature response of the live and model snails over short time periods. The equation for the time scale of convective heat transfer:

$$t = \frac{\pi \rho_b R Q_s}{3 h_c} \tag{32}$$

where ρ_b is the density of the snail body, R is the radius of a spherical body, Q_s is the specific heat of the body, and h_c is the heat transfer coefficient of the snail, shows that for calm wind periods where h_c is low, a time scale of up to 15 minutes is appropriate. The model implemented a 10 minute moving average window to account for time lags in the response of the temperature of the snails. The two live *L. keenae* deployed in the

field during the June trial were larger than the two *L. keenae* shells for which model parameters existed, so it was necessary to alter the input parameters of the model to suit the live snails. The shell length and contact areas input into the model were taken from measurements of the live snails, and a simple multiplier was applied in the model to scale the projected areas and surface areas to be closer to the values of the live snails. Values for the heat transfer coefficient from a particular model shell ("*Littorina keenae* 2") were used for the two live snails.

1.2.5 Laboratory trials

Due to the high shore position of the granite bench, testing the accuracy of the heat-budget model in the field precluded the measurement of snail body temperatures when the foot was out in contact with the substratum. When a snail extends its foot out of the shell and crawls on the substratum, the contact area available for conductive heat exchange increases by an order of magnitude. The overall contribution of conduction to the heat flux into the snail body can change drastically as a result. To validate the model's accuracy for times when the snail was crawling around on the substratum, a temperature-controlled wind tunnel in the laboratory was employed (see Chapter 3 for description of the wind tunnel). A live *L. keenae*, chosen to be as close as possible in size to one of the *L. keenae* shells ("*Littorina keenae* 2") for which model parameters existed, was fitted with a thermocouple as described in the previous section. The snail was placed on the wetted surface of the wind tunnel heating plate. The temperature of the heating plate and the air in the wind tunnel could be independently controlled. The temperature of the live snail was recorded on a datalogger as the temperatures of the substratum and air were raised and lowered. A reduced version of the heat-budget model, where substratum temperature was a direct input to the model rather than being calculated from the other environmental parameters, was used to compare predicted temperatures with the measured body temperature of the snails crawling on the heating plate.

1.2.6 Sensitivity analyses

The sensitivity of the heat-budget model to changes in input parameters was tested by varying selected parameters by ± 10% while holding all other parameters constant. The change in the maximum body temperature predicted over a seven year set of environmental data from HMS was recorded. The selected input parameters were: the long-wave emissivity of the snail shell, $\epsilon_{lw,shell}$, the conductivity of the granite, K_{rock}, the thermal diffusivity of the rock, D_{rock}, and the value of the proportionality coefficient *a* in the Nusselt-Reynolds relationship.

Changes in the value of the proportionality coefficient *a* are accompanied by a change in the value of the scaling exponent *b* in the Nusselt-Reynolds relationship. Using the coefficients for all of the silver shells measured in the wind tunnel, a correlation analysis showed that a 10% increase in the value of *a* was accompanied by a 1.7% decrease in the value of *b* ($r^2 = 0.813$, $p < 0.001$, n = 18). Consequently, each the sensitivity analyses of the proportionality coefficient *a* involved a simultaneous alteration of the scaling exponent *b.*

In addition to the shell and substratum parameters tested above, the sensitivity of body temperature to two of the behavioral parameters in the model was tested. In the model, the decision to withdraw the foot into the shell and glue the shell to the substratum is based on either the accumulated time since the start of the emersion cycle, or on the body temperature of the snail rising above a threshold temperature. In separate trials, the time-of-emersion threshold was varied between 1 hr and 12 hr while keeping the body temperature threshold at 25°C, and the body temperature threshold for foot withdrawal was varied between 18 and 32°C, while keeping the time-of-emersion threshold at 3 hr. The maximum temperature achieved during the model run was recorded as the response variable. When the model was run for each snail using the standard parameter values, approximately 1% of the predicted body temperatures in the 7-year dataset were above 30°C for each snail. The cumulative time spent above this 30°C threshold was chosen as a second response variable for the analysis of the sensitivity of the behavior parameters.

Changes in the contact area of the shell, size of the shell, absorptivity, behavioral choices, shell orientation relative to the substratum, and other parameters are treated as experimental variables in the model, and are discussed in the next chapter.

1.3 Results

1.3.1 Model parameters

The values of model parameters for the environmental and substratum portions of the model are given in Table 1-2. The parameters used for each modeled shell are arranged by species in Tables 1-3, 1-4, 1-5, 1-6, and 1-7. Where parameter values could differ due to the behavior of the snail, such as when the shell is elevated up away from the substratum, the parameter values for each situation are given.

Table 1-2. Values for environmental, substratum, and common shell parameters used in the model

Parameter	Units	Value
α_{sw} (black shell)	None	0.85
α_{sw} (brown shell)	None	0.80
α_{sw} (white shell)	None	0.67
$\alpha_{lw,shell}$	None	0.97
$\epsilon_{lw,shell}$	None	0.97
a*	None	0.320
b*	None	0.478
c_{rock}	J kg^{-1} K^{-1}	788.8
D_{rock}	m^2 s^{-1}	$1.49x10^{-6}$
K_{rock}	W m^{-1} K^{-1}	3.06
K_{shell}	W m^{-1} K^{-1}	3.00
R	mm	20.8
$\epsilon_{lw,rock}$	None	0.95
$\epsilon_{lw,sky}$ (night)	None	0.95
ρ_{rock}	kg m^3	2601

*a and b were calculated for a disk of granite cut from the shore at HMS that retained the typical surface rugosity of the rock in the field.

Table 1-3. *Littorina keenae*. Values for parameters used in the heat-budget model.

		Shell	
Parameter	Units	*Littorina keenae 1*	*Littorina keenae 2*
A_{cond} (foot extended)	mm^2	37.3	58.5
A_{cond} (shell down)	mm^2	1.45	2.20
A_{cond} (shell up)	mm^2	0.31	0.34
A_{conv} (shell down)	mm^2	197.9	287.4
A_{conv} (shell up)	mm^2	236.4	347.8
d_s (shell down)	mm	0.41	0.42
d_s (shell up)	mm	2.23	2.57
L (shell down)	mm	9.20	10.82
L (shell up)	mm	8.34	9.56
a (shell down)	None	0.204	0.190
b (shell down)	None	0.568	0.580
a (shell up)	None	0.240	0.238
b (shell up)	None	0.567	0.565

Table 1-4. *Littorina scutulata.* Values for parameters used in the heat-budget model.

		Shell	
Parameter	Units	*Littorina scutulata 1*	*Littorina scutulata 2*
A_{cond} (foot extended)	mm^2	10.3	12.8
A_{cond} (shell down)	mm^2	1.02	0.78
A_{cond} (shell up)	mm^2	0.14	0.12
A_{conv} (shell down)	mm^2	69.92	89.48
A_{conv} (shell up)	mm^2	81.1	102.9
d_s (shell down)	mm	0.31	0.31
d_s (shell up)	mm	1.41	1.43
L (shell down)	mm	6.06	6.54
L (shell up)	mm	4.6	5.04
a (shell down)	None	0.060	0.041
b (shell down)	None	0.855	0.770
a (shell up)	None	0.118	0.064
b (shell up)	None	0.647	0.728

Table 1-5. *Littorina sitkana.* Values for parameters used in heat-budget model.

		Shell	
Parameter	Units	*Littorina sitkana 1*	*Littorina sitkana 2*
A_{cond} (foot extended)	mm^2	15.50	10.30
A_{cond} (shell down)	mm^2	1.02	1.04
A_{cond} (shell up)	mm^2	0.29	0.22
A_{conv} (shell down)	mm^2	106.9	78.71
A_{conv} (shell up)	mm^2	123.1	89.83
d_s (shell down)	mm	0.63	0.61
d_s (shell up)	mm	1.44	1.40
L (shell down)	mm	6.64	5.90
L (shell up)	mm	5.94	5.06
a (shell down)	None	0.098	0.088
b (shell down)	None	0.659	0.617
a (shell up)	None	0.109	0.128
b (shell up)	None	0.651	0.57

Table 1-6. *Echinolittorina natalensis.* Values for parameters used in the heat-budget model.

		Shell	
Parameter	Units	*Echinolittorina natalensis 1*	*Echinolittorina natalensis 2*
A_{cond} (foot extended)	mm^2	11.40	10.30
A_{cond} (shell down)	mm^2	0.71	0.73
A_{cond} (shell up)	mm^2	0.25	0.25
A_{conv} (shell down)	mm^2	67.19	82.13
A_{conv} (shell up)	mm^2	85.64	99.28
d_s (shell down)	mm	0.55	0.67
d_s (shell up)	mm	1.32	1.45
L (shell down)	mm	6.29	7.00
L (shell up)	mm	4.74	5.34
a (shell down)	None	0.065	0.068
b (shell down)	None	0.766	0.735
a (shell up)	None	0.107	0.087
b (shell up)	None	0.682	0.618

Table 1-7. *Littorina plena.* Values for parameters used in the heat-budget model.

Parameter	Units	*Littorina plena*
A_{cond} (foot extended)	mm^2	10.90
A_{cond} (shell down)	mm^2	0.84
A_{cond} (shell up)	mm^2	0.10
A_{conv} (shell down)	mm^2	65.37
A_{conv} (shell up)	mm^2	77.01
d_s (shell down)	mm	0.32
d_s (shell up)	mm	1.25
L (shell down)	mm	5.66
L (shell up)	mm	4.22
a (shell down)	None	0.057
b (shell down)	None	0.730
a (shell up)	None	0.092
b (shell up)	None	0.684

A representative distribution of projected areas for the *Littorina keenae* 2 shell in both the "down" and "up" shell positions is shown in Figure 1-10. When the shell is sitting down on the substratum (Figure 1-10a), the maximal projected surface area is exposed when the sun in high in the sky. In contrast, when the shell is elevated up off the substratum with the spire of the shell pointing approximately normal to the plane of the substratum, the projected surface area is minimized when the sun is high in the sky (Figure 1-10b).

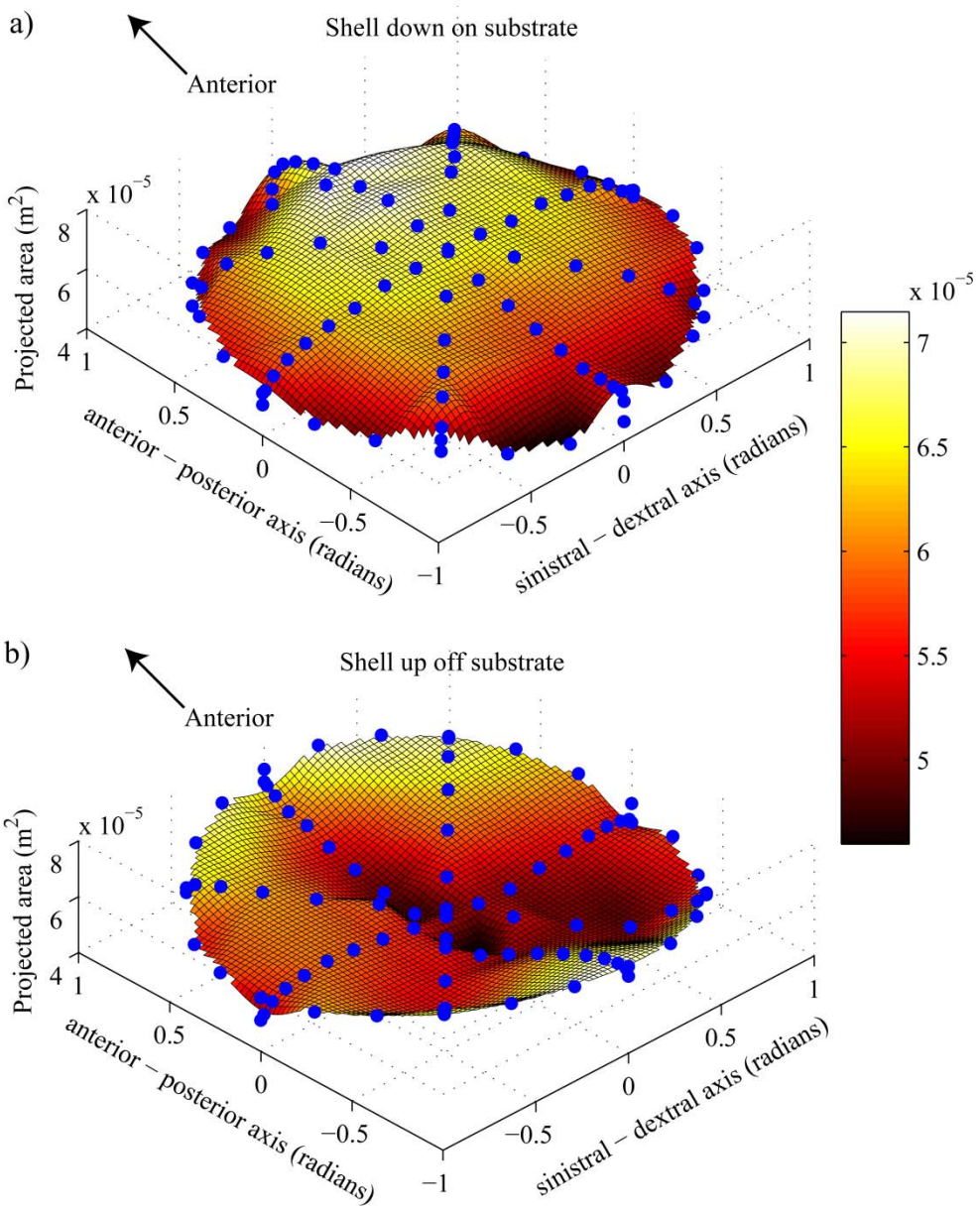

Figure 1-10. Projected area of a *Littorina keenae* shell from multiple angles. Circles represent measured points and the surface is interpolated between points. a) Shell positioned with the aperture down against the substratum. In this position, projected area is generally maximized when the sun is overhead. b) Shell lifted up off the substratum, with the spire normal to the plane of the substratum. In this orientation, projected area is maximal when the sun is low on the horizon, and at a minimum when the sun is high in the sky.

For the Nusselt-Reynolds number relationship produced using the silver model snails in the wind tunnel, there was little variation between the four tested directions (anterior end oriented upwind, anterior end oriented downwind, anterior end oriented to the right or left of oncoming wind) for each shell (Figure 1-11). Because of the small variation in h_c with wind direction and the fact that the wind in the field may come from many different directions through time, the decision was made to pool the heat transfer coefficients from the four directions to produce the Nusselt-Reynolds curve fits for each shell used to generate parameters *a* and *b*.

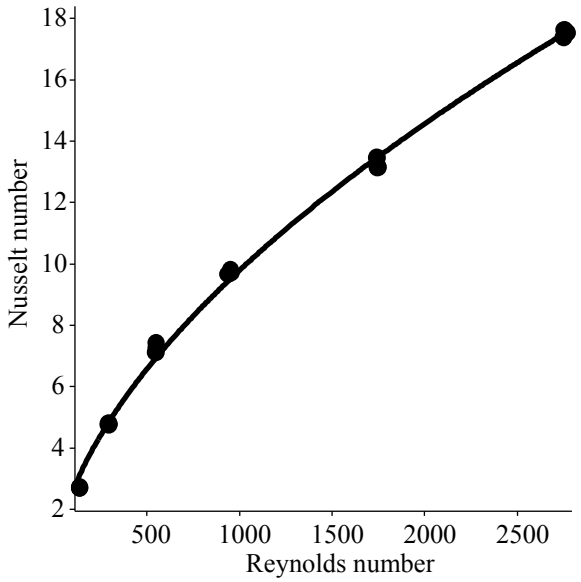

Figure 1-11. Example of the relationship between the Reynolds number and Nusselt number for a *Littorina keenae* shell. The points represent data collected in the wind tunnel in each of four shell directions, with three replicates at each Reynolds number value. A curve of the form $y = a * x^b$ is fit to the data to estimate the heat transfer coefficient for wind speeds that were not empirically measured.

The measured sphere diameters, areas, and coefficients for the Nusselt-Reynolds number relationship are shown in Table 1-8. The values of *a* and *b* for the Nusselt-Reynolds relationship changed as sphere diameter changed. The shift in values is shown graphically on a $\log_{10}$-$\log_{10}$ plot of the Nusselt-Reynolds relationship in Figure 1-12. A test for homogeneity of the $\log_{10}$-$\log_{10}$ transformed slopes by analysis of

covariance demonstrated that the slopes were significantly different among the sphere diameters ($F_{(7,299)} = 18.59$, $p << 0.001$).

Table 1-8. Parameters for brass spheres. The proportionality coefficient, *a*, and scaling coefficient, *b*, are derived from the curve fit to the relationship between the Nusselt number and Reynolds number according to the equation $Nu = aRe^b$.

Sphere diameter (mm)	Surface area (m^2)	Projected area (m^2)	Proportionality coefficient, *a*	Scaling coefficient, *b*
4.75	$7.09x10^{-5}$	$1.77x10^{-5}$	0.077	0.697
5.55	$9.68x10^{-5}$	$2.42x10^{-5}$	0.107	0.659
6.35	$1.27x10^{-4}$	$3.17x10^{-5}$	0.122	0.642
7.95	$1.98x10^{-4}$	$4.96x10^{-5}$	0.138	0.621
9.52	$2.85x10^{-4}$	$7.12x10^{-5}$	0.168	0.599
11.09	$3.86x10^{-4}$	$9.66x10^{-5}$	0.189	0.581
12.73	$5.09x10^{-4}$	$1.27x10^{-4}$	0.227	0.565
25.4	$2.03x10^{-3}$	$5.07x10^{-4}$	0.374	0.513

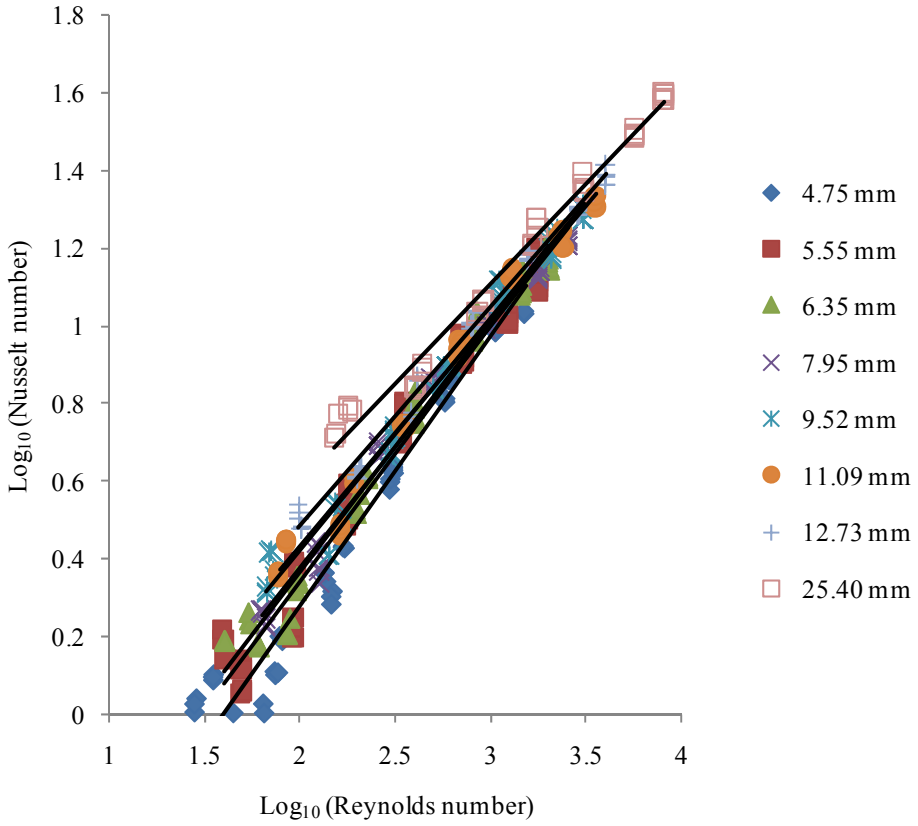

Figure 1-12. Relationship between the Nusselt number and Reynolds number of eight brass spheres in the wind tunnel. The change in the slope and intercept of the linear fit for each sphere size indicates that the calculated heat transfer coefficient will differ between sphere sizes for a given wind speed.

The boundary layer established by wind flowing over the rough plaster tiles in the wind tunnel reduced velocities close to the substratum by up to 90% (Figure 1-13). Snails or spheres sitting further down in this slower-moving air shed heat more slowly, leading to the changing Nusselt-Reynolds number relationship found for the different sphere sizes.

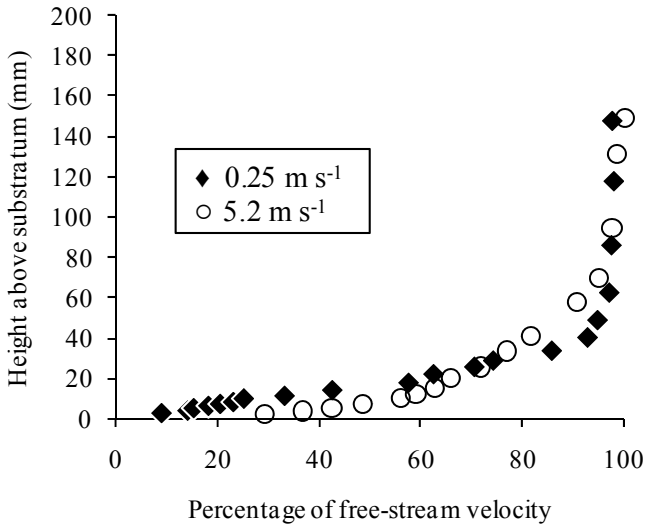

Figure 1-13. Boundary layer profiles for two wind speeds in the wind tunnel. A reference anemometer at 200 mm height above the substratum provided the measurement of the free-stream velocity.

1.3.2 Field tests

The predicted temperatures of the silver-filled snail shells deployed in the field were generally in close agreement with the measured temperatures. The modeled temperatures tended to deviate from measured temperatures more at low temperatures and during the night.

Table 1-9 lists the mean difference between modeled and measured temperatures for all of the shells during the deployment, along with the difference between modeled and measured temperatures for the hottest 5% of temperatures during the time series. Across all of the modeled shells, the mean difference between modeled and measured temperatures was 0.58°C, while the difference improved to 0.28°C when considering only the hottest 5% of all temperatures. Figure 1-14 shows the correspondence between measured and predicted body temperatures for each of the modeled shells when the shell was positioned with the aperture down against the rock; Figure 1-15 shows the same data for periods when the shells were positioned with the shell lifted away from the rock (spire aligned normal to the substratum).

Table 1-9. Comparison of measured temperatures of snail shells in the field and modeled snail temperatures using weather data from the same time period. Average differences between measured and modeled temperatures are given for both the whole range of temperatures in the field and for the highest 5% of measured temperatures in the field.

Species	Mean difference between all modeled and measured temperatures (°C ± 1 SD)	Mean difference between modeled and measured temperatures for top 5% of temperatures (°C ± 1 SD)
Shell down		
Littorina keenae 1	-0.28 (± 1.14)	0.21 (± 0.55)
Littorina keenae 2	-1.13 (± 1.51)	0.64 (± 0.63)
Littorina scutulata 1	0.20 (± 1.31)	0.05 (± 0.46)
Littorina scutulata 2	-0.35 (± 0.83)	-0.99 (± 0.44)
Littorina sitkana 1	-0.75 (± 0.95)	-0.09 (± 0.19)
Littorina sitkana 2	0.08 (± 0.67)	-0.52 (± 0.41)
Littorina plena	0.17 (± 0.88)	-0.07 (± 0.24)
Echinolittorina natalensis 1	-0.21 (± 1.07)	0.00 (± 0.41)
Echinolittorina natalensis 2	-0.09 (± 1.15)	0.13 (± 0.80)
Shell up		
Littorina keenae 1	No data	No data
Littorina keenae 2	-1.47 (± 2.40)	0.45 (± 0.78)
Littorina scutulata 1	-1.03 (± 1.14)	0.11 (± 0.63)
Littorina scutulata 2	-0.71 (± 1.23)	0.36 (± 0.38)
Littorina sitkana 1	-0.10 (± 0.79)	-0.21 (± 0.28)
Littorina sitkana 2	-1.00 (± 1.28)	0.38 (± 0.74)
Littorina plena	-0.73 (± 1.28)	0.16 (± 0.81)
Echinolittorina natalensis 1	-0.55 (± 0.89)	-0.17 (± 0.62)
Echinolittorina natalensis 2	-1.11 (± 1.18)	-0.19 (± 0.34)

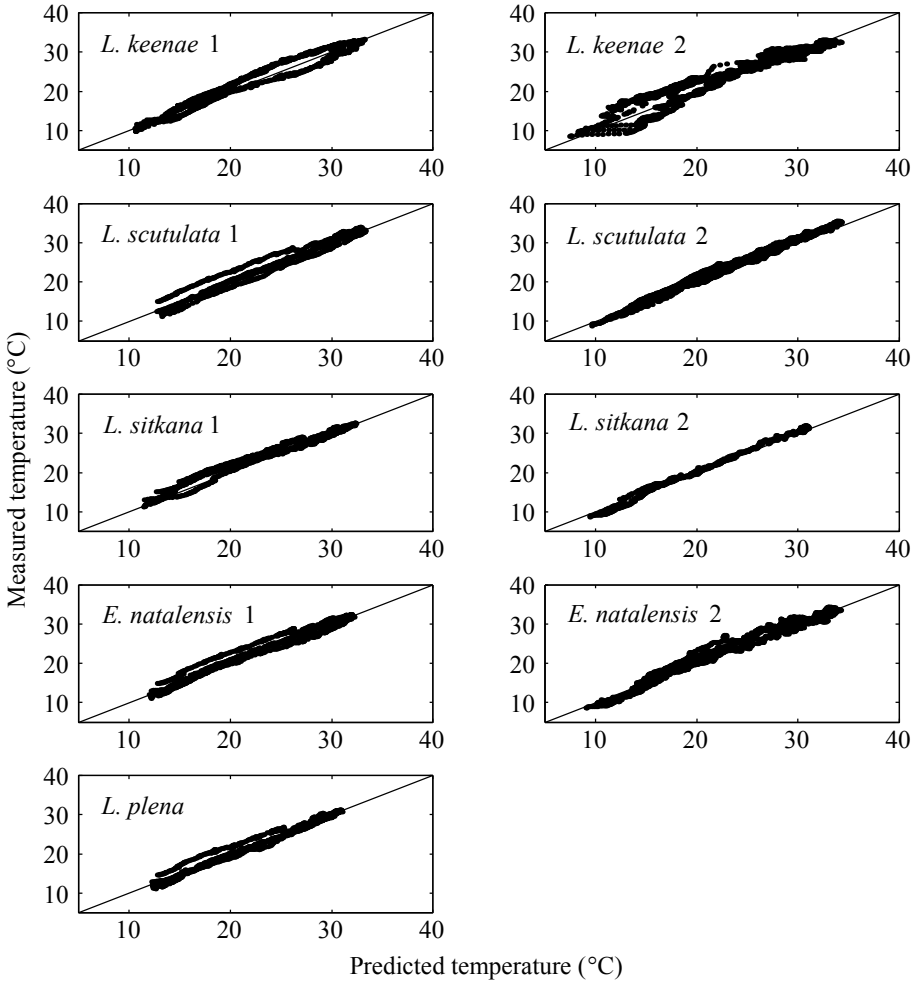

Figure 1-14. Measured *versus* predicted temperatures for silver-filled shells set out in the field, with the aperture of the shell down against the substratum. The line of unity is plotted to show deviations between the model predictions and measured temperatures. Field data were collected during April and June of 2007.

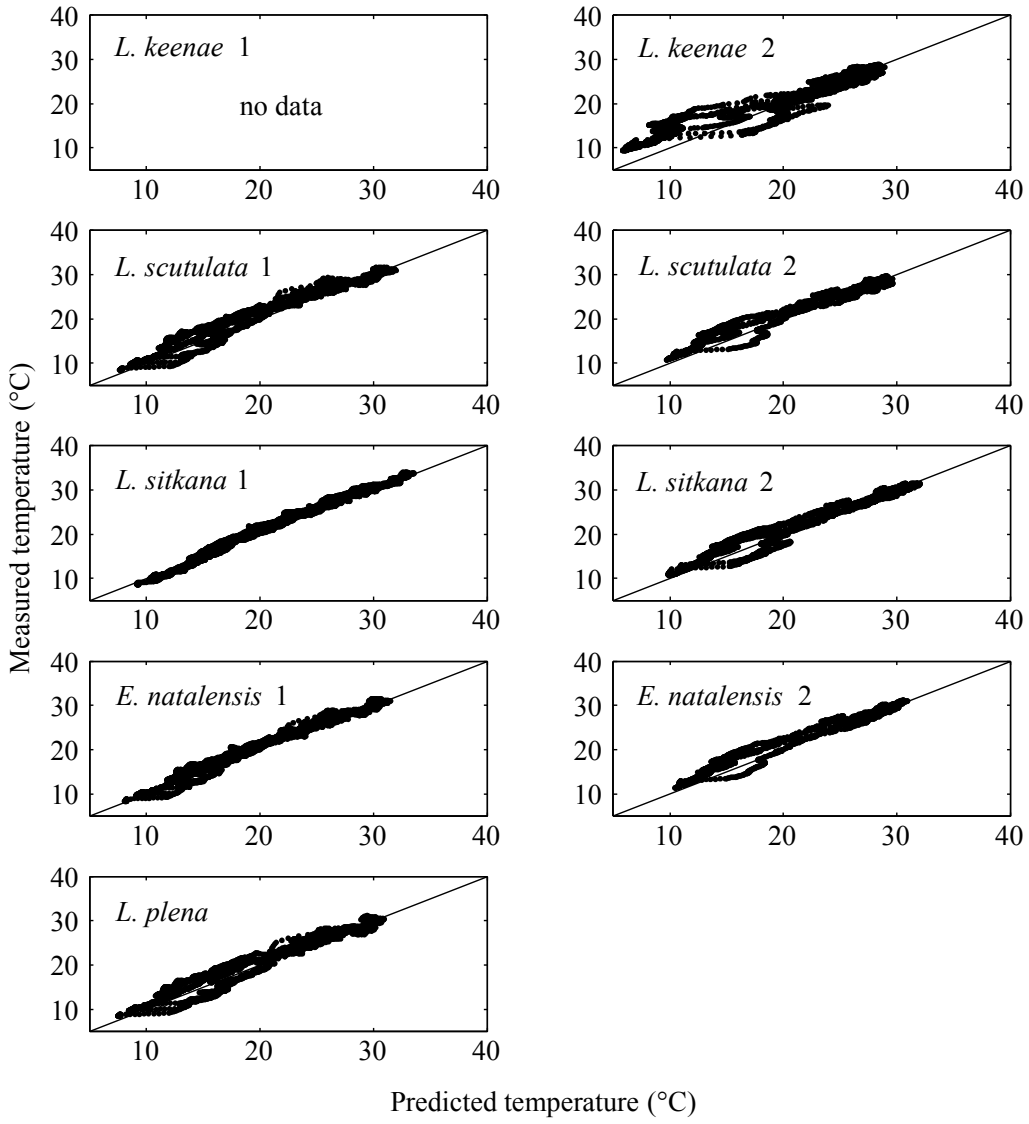

Figure 1-15. Measured *versus* predicted temperatures for silver-filled shells set out in the field, with the spire of the shell approximately normal to the substratum and only the outer lip of the aperture of the shell in contact with the substratum. The line of unity is plotted to show deviations between the model predictions and measured temperatures. Field data were collected during April and June of 2007. The comparison for *Littorina keenae* 1 was not possible due to corrupted field data.

The modeled and measured temperatures for the two live *Littorina keenae* deployed in the field on June 9 and 10, 2007, are shown in Figure 1-16. Because the model parameters for these two snails had to be adapted from one of the existing silver-filled

Littorina keenae shells, the correspondence between the modeled and measured body temperatures is not as close as it was for some of the silver-filled shells. The mean difference between the measured and predicted temperatures for the first live *Littorina keenae* was -0.74°C (± 1.21°C) across all time periods and -0.10°C (± 0.34°C) for the hottest 5% of all time points. For the second live *Littorina keenae*, the average difference between measured and predicted temperatures for all time points was -1.00°C (± 0.87°C) and 0.17°C (± 0.29°C) for the hottest 5% of time points.

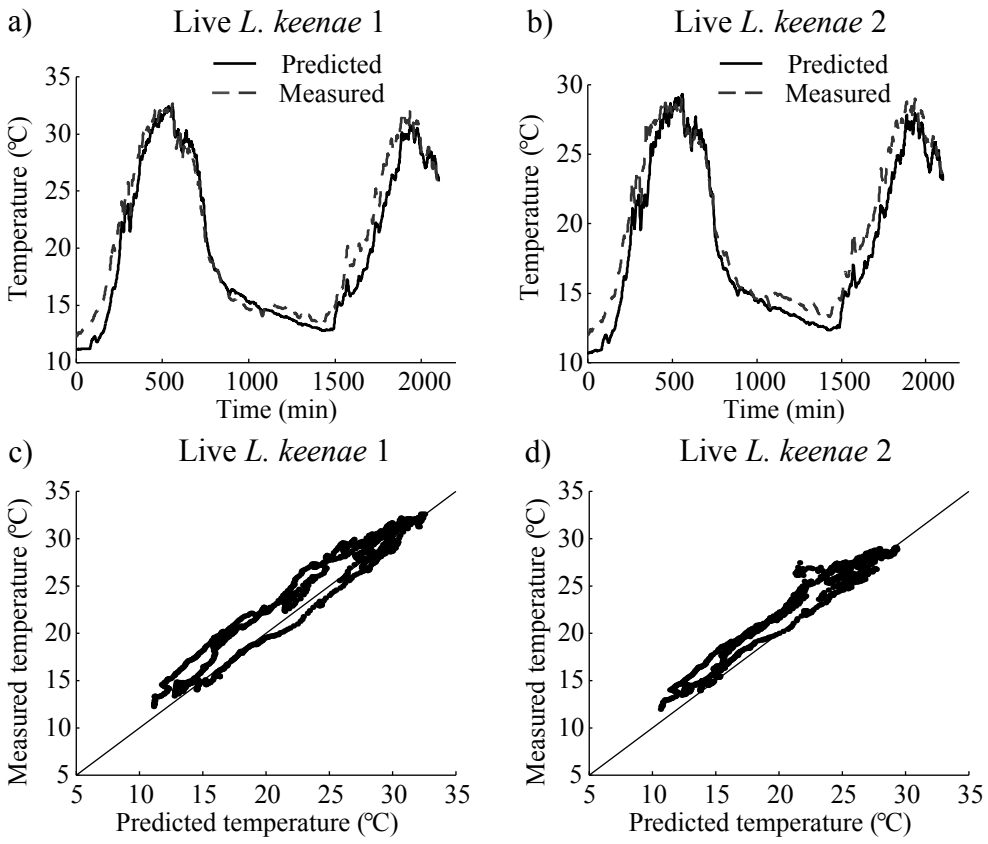

Figure 1-16. Measured and predicted temperatures for two live *Littorina keenae* fitted with thermocouples in the field. a) Predicted and measured time series for snail 1. b) Predicted and measured temperature time series for snail 2. c) Comparison of predicted and measured body temperatures during the deployment of snail 1 shown in (a). A line of unity is plotted. d) Comparison of predicted and measured body temperatures for snail 2 during the deployment depicted in (b).

1.3.3 Laboratory validation

Model predictions of body temperature for the live *Littorina keenae* placed in the environmental chamber in the laboratory followed the measured temperatures very closely (Figure 1-17). When snails had the foot extended, the difference between the predicted and measured temperatures was -0.18°C (±0.27). After the snails withdrew into the shell, the difference between the predicted and measured temperatures was 0.02°C (±0.40) over the range of experimental temperatures.

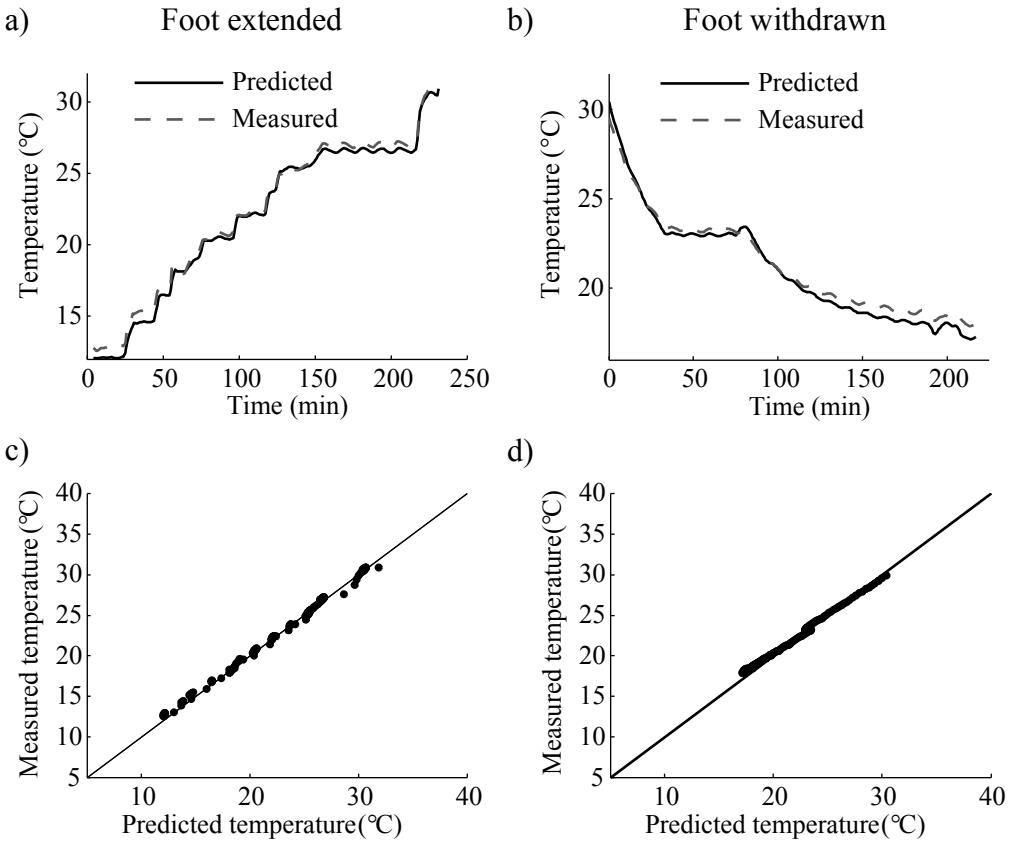

Figure 1-17. Predicted and measured body temperatures for a live *Littorina keenae* fitted with an internal thermocouple. The snail was placed in a temperature controlled chamber in the lab, and the temperatures of the air and substratum were changed through time. a) Predicted and measured body temperatures through time when the foot was extended and in contact with the substratum. b). Predicted and measured temperatures for times when the snail had the foot withdrawn so that only the shell rested on the substratum. c) Comparison of deviations between measured and predicted body temperatures for the snail with the foot extended. A line of unity is plotted. d) Comparison between measured and predicted body temperatures when the snail's foot was withdrawn into the shell.

1.3.4 Sensitivity Analyses

The results of the sensitivity analysis are given in Table 1-10. Of the measured parameters, the predicted body temperature of the snails responded most strongly to changes in the thermal conductivity of the rock, K_{rock}, and the thermal diffusivity of the rock, D_{rock}.

Table 1-10. Sensitivity analyses for heat-budget models of five littorine snail species. Values given are change in maximum body temperature during a 7-year period. The mean result from two modeled shells is reported for each species, except *Littorina plena*, for which there is only one shell modeled.

Parameter		Change in 7-year maximum body temperature (°C)	
		+10%	-10%
Littorina keenae			
$\epsilon_{lw,shell}$	long-wave emissivity	-0.04*	0.14
K_{rock}	thermal conductivity of rock	-0.96	1.06
D_{rock}	thermal diffusivity of rock	-0.50	0.55
a	Proportionality coefficient†	-0.02	0.03
Littorina scutulata			
$\epsilon_{lw,shell}$	long-wave emissivity	-0.04*	0.12
K_{rock}	thermal conductivity of rock	-0.97	1.06
D_{rock}	thermal diffusivity of rock	-0.53	0.59
a	Proportionality coefficient†	0.00	0.01
Littorina sitkana			
$\epsilon_{lw,shell}$	long-wave emissivity	-0.04*	0.15
K_{rock}	thermal conductivity of rock	-1.02	1.12
D_{rock}	thermal diffusivity of rock	-0.53	0.59
a	Proportionality coefficient†	-0.01	0.02
Littorina plena			
$\epsilon_{lw,shell}$	long-wave emissivity	-0.04*	0.13
K_{rock}	thermal conductivity of rock	-1.08	1.18
D_{rock}	thermal diffusivity of rock	-0.56	0.62
a	Proportionality coefficient†	-0.01	0.00
Echinolittorina natalensis			
$\epsilon_{lw,shell}$	long-wave emissivity	-0.03*	0.09
K_{rock}	thermal conductivity of rock	-1.10	1.20
D_{rock}	thermal diffusivity of rock	-0.57	0.63
a	Proportionality coefficient†	-0.01	0.01

*The long-wave emissivity of the shell is normally 0.97, so the +10% value used is 1.0 for these calculations.
†An increase of 10% in the proportionality coefficient, *a,* of the Nusselt-Reynolds number relationship is accompanied by a 1.7% decrease in the scaling exponent, *b*.

The maximum body temperature and cumulative time above a threshold temperature of 30°C over the seven year dataset showed almost no response to variations in the parameters used to trigger withdrawal of the foot into the shell. When the body temperature threshold used to trigger foot withdrawal was varied between 18°C and 32°C, there was no change in the maximum body temperature, and the cumulative time above 30°C increased by 1% over the whole 7-year dataset. When the time-of-emersion threshold was varied between 1 hr and 12 hr, there was no change in maximum body temperature or cumulative time above 30°C during the 7-year dataset.

1.4 Discussion

The heat-budget model developed here for five species of littorine snails makes excellent predictions of body temperature in a variety of conditions. The field and laboratory tests of the model demonstrate that while there are some environmental conditions under which model predictions deviate from live snail body temperatures, the output of the model during warm periods is acceptably close to measured temperatures. The model and parameters described here form the basis for addressing the questions about morphology and behavior of littorine snails in the next chapter.

1.4.1 Heat-budget model parameters

Previous studies have postulated that the orientation of the shell relative to the substratum might have significant effects on the amount of short-wave heat energy absorbed by littorine snails (Vermeij, 1973; Garrity, 1984). The data collected on projected area here can be used to begin to address the question of how much altering shell position impacts heating by the sun.

The measurements of projected area for shells in both the “down” and “up” positions (Figure 1-10) show that the choice of shell orientation by the snail can substantially alter the potential short-wave heat flux into the shell as the sun travels through the sky. When the shell sits down on the substratum, the short-wave radiation from a noon sun high in the sky impinges on a larger surface area than a shell with the spire pointing up

at the sun. The difference between the two shell orientations for all azimuth/altitude positions of the sun is shown in Figure 1-18, using *Littorina keenae* shell 1 as an example. *Littorina keenae* shell 1 had a maximum projected area of 72.08 mm^2. Normalizing the difference between the "down" and "up" orientations to the maximum projected area shows that there can be differences in projected area as large as 25% when the sun is shining nearly straight down on the shell.

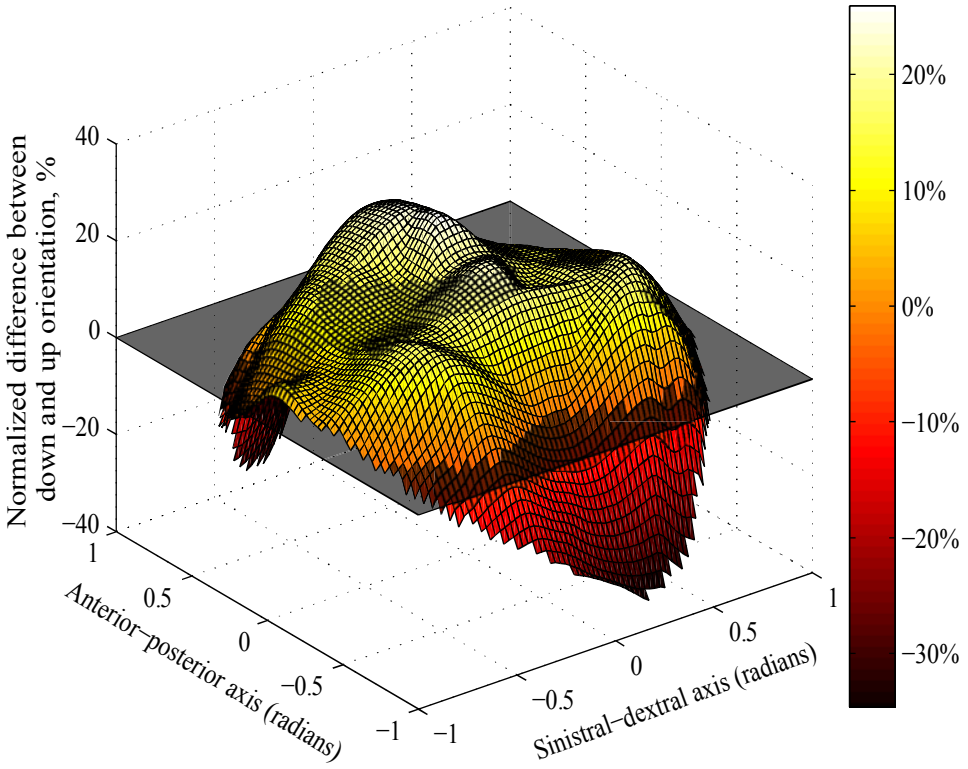

Figure 1-18. Difference in projected area facing the sun for two shell orientations of a *Littorina keenae* shell. The projected area for a shell elevated up off the substratum is subtracted from the projected area for a shell sitting down on the substratum for each solar position above the shell, and normalized by the maximum projected area of the shell. Values above the plane at 0 indicate that the shell sitting down on the substratum has a higher projected area when the sun shines down from the indicated position above the shell. The maximum projected surface area of the shell was 72.08 mm^2.

For the Nusselt-Reynolds number relationship used to calculate the heat transfer coefficient, h_c, for each shell, the position of the shell relative to the substratum

("down" *versus* "up") altered the relationship between wind speed and convective heat exchange (Tables 1-3, 1-4, 1-5, 1-6, and 1-7). The differences in the heat transfer coefficient can be due to a number of factors, such as the surface area of the shell exposed to the air, the height of the shell within the boundary layer of air flowing over the substratum, and differences in the characteristic length in some orientations. When the characteristic length of the shell is held constant by placing a shell broadside to the oncoming wind and measuring h_c for the shell in the down and up positions, the change in surface area and height above the substratum still contribute to differences in h_c (Figure 1-19).

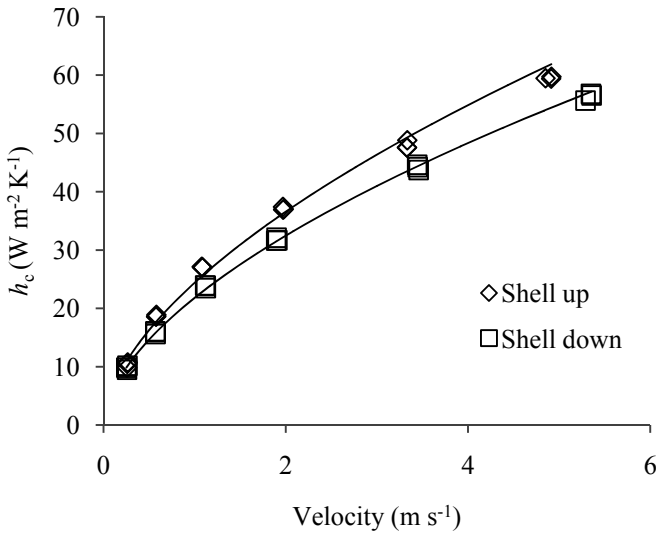

Figure 1-19. Effect of shell orientation on the heat transfer coefficient, h_c, for a *L. keenae* shell at various wind speeds. The heat transfer coefficient is higher when the shell is elevated up off the substratum, so that only the outer lip of the shell is in contact with the ground.

The combination of all of these changes in heat flux in and out of the snail shell resulting from altering shell orientation can have substantial effects on the body temperature achieved by a snail. The following chapter will address these issues more thoroughly.

1.4.2 Heat-budget model verification

The correspondence between predicted body temperatures and the internal temperatures of the silver-filled snail shells was quite good in most situations (Figure 1-14 and Figure 1-15). The largest deviations between the predicted and measured results occurred at lower temperatures, particularly during the night, with the model typically underestimating the temperature of the shell during the very early morning hours. The differences in predicted and measured temperatures for the two live *Littorina keenae* set out in the field alongside the snail mimics showed the same pattern of deviations (Figure 1-16), but were augmented by the difference in size between the live and modeled snails, which necessitated the use of estimated parameters values for the Nusselt-Reynolds relationship and surface area.

The deviations, both high and low, between predicted and measured temperatures for the snail mimics and live snails at low temperatures and at night may be due to multiple factors, primarily the convective heat exchange at low wind speeds and long-wave heat exchange with the sky.

Accurate prediction of convective heat exchange between the snail and the surrounding air relies on an accurate measurement of wind speed at the site. The cup anemometer used to gather wind speed data in the field does not register wind speeds below ~20 cm s^{-1}, instead recording a zero value. In the environmental datasets, these zero values are changed to 20 cm s^{-1} due to the fact that the air is rarely completely still during the day. However, during the very still periods of the early morning common at HMS, wind speeds may drop substantially below 20 cm s^{-1}. If the wind speed during these calm, cool periods in the early morning is over-estimated in the model, the predicted rate of convective heat exchange between the shell and the air will be high as well, leading to higher predicted rates of heat exchange, which cause deviations between the model and the measured temperature values in the field. The effect of this discrepancy in convective heat exchange will vary depending on the weather conditions. On clear, cold nights, shell temperature could drop below air temperature, in which case convective heat exchange would warm the shell, biasing

predictions higher than measured values. Conversely, if the shell stays warmer than the air during the night, such as by conduction with the larger thermal mass of the rock, over-estimating wind speeds and convection will lead to the model biasing predictions below measured values.

The long-wave heat exchange predictions will be influenced by the presence of clouds or fog during both day and night. As explained in the methods, the model uses a value for the long-wave emissivity of the sky, $\epsilon_{lw,sky}$, of 0.95 during the hours of darkness to account for the occurrence of fog or clouds. If the night-time sky remains clear, the deviation between the predicted and actual long-wave heat exchange with the sky may be quite large, leading to lower body temperatures than would be predicted by the model. While this difference certainly exists in the dataset, it is difficult to assess its magnitude without detailed records of cloud and fog cover.

Because the goal of the model is primarily to predict body temperatures during warm, sunny periods, the deviations that occur during the night are deemed acceptable. If the goal of the model was instead to examine the impact of low temperature events on snail body temperature, the discrepancies described here would have to be addressed in order to ensure accurate predictions during cold and dark periods.

1.4.3 Sensitivity analyses

Of the parameters subjected to sensitivity analysis, the thermal conductivity and thermal diffusivity of the modeled granite substratum had the largest effect on body temperature of the snail (Table 1-10). Increasing the conductivity, K_{rock}, or thermal diffusivity, D_{rock}, of the rock results in lower rock temperatures on hot days, due to stronger coupling with the colder temperatures further down inside the rock. Lower rock surface temperature decreases the heat energy flux into the shell of the snail through conduction.

The behavioral components of the model subjected to sensitivity analyses showed very little response to the range of values tested. When examining the time course of exposures to high temperatures produced with the model, it becomes clear that both

the time-of-emersion threshold and the body temperature threshold used to trigger withdrawal of the foot into the shell have little impact on snail temperatures on hot days. Typically the time-of-emersion threshold comes into play first, because these snails live high on the shore and are only wetted by the higher high tides. Extremely hot days are commonly accompanied by low wave heights, and the hottest body temperatures are reached on days with low tides occurring near midday. As a result, when the cooling effects of wave splash are removed, snails living high on the shore are typically emersed many hours before low tide, prompting the withdrawal of the foot into the shell. The rate of heating, even on the hottest days, is typically slow enough in the morning that the time-of-emersion threshold is reached before the body temperature threshold is achieved.

This does not mean that snail behavior has no effect on the body temperatures achieved during hot periods. While the time-of-emersion threshold and body temperature threshold have little effect on the temperatures reached, the decision to pull the foot in and the decision to alter the orientation of the shell relative to the substratum do have substantial impacts on body temperature, as will be shown in the next chapter.

1.4.4 Summary

The intertidal zone is typically considered to be a harsh environment, due in part to the large swings in temperature that accompany the cycling of the tides. For animals of marine origin, low tide can be a period of stressful temperature and desiccation, stresses that might have affected the evolution of these animals and may set limits on the current ecological niche they occupy. One method for addressing questions about the evolution and ecology of organisms subjected to thermal stress is to employ a heat-budget model to predict body temperatures.

In this chapter I have described the function of such a heat-budget model, and detailed the implementation and verification of the model for five species of high-shore littorine snails. Using a variety of empirically-measured physical characteristics and behavioral traits of the snails, I have created a working model that can take

environmental data as inputs and output a time series of body temperatures. The correspondence between the predictions of the model and the measured temperatures of snail mimics and live snails deployed in the field or tested in the laboratory demonstrate that the model can make accurate predictions during warm periods, with typical deviations of less than 0.5°C at the highest temperatures.

Using with this model, I will address a number of questions in the following chapter about the evolution and ecology of high-shore littorine snails. The model can be used to examine the effects of shell color, shape, behavior, and shore height on the intensity, duration, and frequency of high temperature stress events over multiple years.

Chapter 2

The roles of morphology and behavior in regulating body temperature in littorine snails

2.1 Introduction

The heat-budget model presented in the preceding chapter provides a powerful tool for examining the roles that behavior and morphology of littorine snails play in determining the severity of thermal stress. Through a careful accounting of the sources of heat flux into and out of a snail, the relative influence of solar radiation, conduction, convection, and long-wave radiation can be examined, and long-term hindcasts of body temperature can be produced for a simulated shoreline at Hopkins Marine Station. The goal of this chapter is to use these hindcasts to examine the role of morphological and behavioral variation among littorine snails in regulating their body temperature, and to discuss the role of these characteristics in littorine snail evolution and ecology.

The five species of littorine snails discussed here occupy a range of habitats in the intertidal zone, and are therefore subjected to different environmental conditions. *Littorina sitkana* typically lives in the low and mid intertidal zone where it is reliably submerged by high tides every day (Boulding and Van Alstyne, 1993; Rochette and Dill, 2000). At the latitudes where the species overlap (46°N to 60°N), *L. sitkana* lives lower on the shore than *L. plena* and *L. scutulata,* which occupy the mid and upper intertidal zones (Harger, 1972; Behrens Yamada, 1989, 1992). Further south, *L. plena* and *L. scutulata* live below *L. keenae,* which occupies the high intertidal and supralittoral zones, where high tides do not reliably wet the rock every day. The southern Africa species *E. natalensis* occupies the high intertidal zone up to the high water mark. The severity and predictability of the environmental conditions across this vertical range on the shore is thought to vary substantially (Southward, 1958;

McMahon, 1990), and the survival of these species may depend in part on the thermal stress they experience as a result of their behavior and morphology. Here I introduce several aspects of littoriniid behavior and morphology that can influence body temperature, and discuss how the heat-budget model can be utilized to test the efficacy of the proposed mechanisms for survival in stressful conditions.

2.1.1 Foot behavior

For most gastropods, maintaining shore position requires keeping the foot in adhesive contact with the substratum (Denny, 1984; Smith, 1992; Smith and Morin, 2002). However, in addition to serving as an adhesive appendage, the foot also forms a large conductive surface between the substratum and the body of the snail, tending to bring the two close to the same temperature, a potentially harmful situation on hot days (Denny and Harley, 2006). Among gastropods in the intertidal zone, a number of different strategies have arisen to help mitigate the effects of conduction on hot days (Vermeij, 1971; Garrity, 1984). Limpets may lift the shell and portions of the foot away from the substratum, reducing the contact area of the foot and increasing the area available for evaporation (Williams *et al.*, 2005). Some snails such as the tropical Neritids have evolved a relatively small foot for the size of the shell, reducing the contact area at the expense of stability in moving water (Vermeij, 1971).

Numerous authors have pointed out that littorine snails, as a group, have gone the furthest towards reducing contact with the substratum. Rocky shore, estuarine, and mangrove species of littorines around the world glue the lip of the shell to the substratum and withdraw the foot into the shell, sealing the opening of the shell with the horny operculum (Gowanloch and Hayes, 1926; Wilson, 1929; Broekhuysen, 1940; Newell, 1958; Markel, 1971; Vermeij, 1971; Bingham, 1972; Hamilton, 1978; Mitchell, 1980; Denny, 1984; Garrity, 1984; McQuaid, 1992; Lang *et al.*, 1998; Wada and Ito, 2000). This behavior minimizes desiccation (McMahon and Britton, 1985), and can result in a lower body temperature by reducing body contact with the hot substratum (McQuaid and Scherman, 1988). The snails typically do not re-emerge from the shell until they have been wetted by water, which usually produces a

vigorous extension of the foot and quick establishment of contact between the foot and the substratum. The strength of the mucus attachment of the shell is strong, but not sufficient for holding the shell steady in flowing water. For this reason, littorine snails need to grab hold of the substratum with their foot in order to hold their shore position when water washes over the site (Miller, 1974; Denny, 1984). I have observed these behaviors for each of the five species used in the current study.

The effect on body temperature of pulling the foot into the shell has been measured in the field for several tropical species, and the behavior generally results in a body temperature 1-2°C cooler than conspecifics with the foot on the substratum (Vermeij, 1971; Garrity, 1984; McQuaid and Scherman, 1988). In temperate species, the research focus has been on how snails avoid desiccation (Bush, 1964; Bingham, 1972; Atkinson and Newbury, 1984; McMahon, 1990; Behrens Yamada, 1992), so little is known about the effect of foot contact on body temperature for these species. The heat-budget model can be used to make predictions about the change in body temperature afforded by removing the foot from the substratum by altering the behavioral components of the model that control foot withdrawal. In this chapter, I explore the magnitude of temperature change created by foot withdrawal, as well as the resulting long-term differences in heat stress likely to be experienced over the course of several years.

Figure 2-1. *Littorina keenae.* Littorine snails may be found with the foot withdrawn and the shell perched on the lip of the aperture. This behavior is seen most commonly among snails on open rock faces exposed to the sun.

2.1.2 Shell orientation

In addition to removing the foot from the substratum during warm and dry periods, many littorines further reduce their conductive contact with the substratum by lifting the shell away from the substratum (Vermeij, 1971; Garrity, 1984)(Figure 2-1). The shell may be elevated so far that the spire of the shell is perpendicular to the plane of the substratum. This rather precarious position reduces contact with the substratum to the bare minimum, as well as raising the shell further into the boundary layer of wind flowing over the substratum (thereby facilitating convective heat loss), and may reduce the projected area of the shell facing the sun. These changes have the potential to lower body temperature by minimizing heat flux into the shell via solar insolation and conduction, and by maximizing heat flux out of the shell through convection. While this behavior has been shown to benefit littorine snails by lowering body temperatures on the hot tropical shores of Panama (Garrity, 1984), the heat-budget model can be used to examine the efficacy of lifting the shell off the substratum under other environmental conditions.

2.1.3 Shell color

The functional significance of shell color variation has long been of interest to evolutionary biologists. The hypotheses explaining shell color variation within and among species have typically centered on the role of color in determining the body temperature of a snail (Markel, 1971; Vermeij, 1971; Jones, 1973; Heath, 1975; Heller, 1981; Etter, 1988; McQuaid and Scherman, 1988; McQuaid, 1992; McQuaid, 1996a; Miura *et al.*, 2007) (Cook and Freeman, 1986; Sergievsky, 1992) or on the role of shell color in crypsis, providing protection from visual predators (Hoagland, 1977; Reid, 1987) (Reimchen, 1979; Heller, 1981; Atkinson and Warwick, 1983; Heller, 1984; Hughes and Mather, 1986; Reimchen, 1989; Johannesson and Ekendahl, 2002). The heat budget model developed for littorine snails allows me to test hypotheses concerning the effect of shell color on body temperature.

The interplay between color and temperature has received substantial attention. Dark colors absorb more short-wave radiation, increasing the heat energy flux into the body relative to a lighter color. This effect may be of particular importance in ectothermic animals where activity levels are often governed by the body temperature of the animal. Watt (1968) demonstrated that the darker pigmentation of the hind wings of *Colias* butterflies living high in the Rocky Mountains of the United States led to faster heating rates when exposed to the sun, allowing those individuals to reach the optimal body temperature for flight sooner than their more lightly colored relatives. In colder climates and at higher altitudes, the faster heating rate is beneficial to butterflies trying to gather food and find mates, especially when the thermal environment shifts quickly due to changing cloud cover.

In the molluscan literature, numerous authors have attributed differences in shell color to differences in survival in adverse conditions. Jones (1973) and Jones *et al*. (1977) argued that much of the cline in shell color among terrestrial *Cepaea* snails between warmer and cooler climes in Europe was due to the beneficial effects of lighter shell colors in avoiding heat stress in southern Europe. Conversely, for *Cepaea* living in the

colder regions of northern Europe, dark brown morphs benefited from faster heating and higher equilibrium body temperatures that allowed them to forage more actively during cold periods. Heath (1975) demonstrated that *Cepaea nemoralis* color variation led to measurable differences in body temperature (typically from 0.34°C to 0.6°C) among yellow, pink, and brown morphs. Adding a layer of black paint to *Cepaea* shells increased the temperature differential to 2.5°C.

The most extensive test of the effect of shell color on survival in intertidal molluscs was carried out by Etter (1988) on *Nucella lapillus* from New England. In the laboratory, brown morphs of *N. lapillus* reached temperatures that were on average 2°C warmer than white conspecifics when both groups were set out in the sun. Heating rates were also faster for the brown morph. In the field, the results were less clear, with brown morphs registering temperatures up to 3°C warmer than white morphs in specific microhabitats. However, on certain substratum types such as barnacle beds, the temperatures of the two color morphs were statistically indistinguishable. Etter concluded that the combination of higher body temperatures, coupled with increased evaporation due to the higher temperature, led to higher mortality in brown morphs on hot shorelines. The natural distribution of the white and brown color morphs followed the pattern of thermal stress present along the environmental gradient from wave-exposed, algae-covered sites to wave-protected, barnacle-dominated sites.

The heat-budget model presented here can be used to address the potential role of shell color in affecting body temperatures of littorine snails. Two questions will be addressed: 1. Do dark shell colors lead to substantial differences in body temperature during high temperature periods, differences that could impact the survival of snails? 2. Do dark colored shells provide a benefit by raising body temperatures during cold periods, potentially allowing for higher activity levels?

2.1.4 Shore height

Littorine snails can be found occupying habitats from the low intertidal to the upper reaches of the supralittoral zone (Reid, 1989; Reid, 2002). Seasonal shifts in vertical distributions are common, especially in wave-swept temperate sites, as are ontogentic shifts in shore height (Smith and Newell, 1955; Bock and Johnson, 1967; Vermeij, 1972; Gendron, 1977). During the colder winter months, snails on wave-swept shores may move upshore while large waves splash higher on the shore, and then retreat downshore during calmer summer months (Bock and Johnson, 1967). The vertical distribution of each species may be driven by several factors, some of which the heat-budget model can be used to explore.

Thermal stress can vary with height on the shore due to the cycling of the tides and the effects of wave action. The magnitude of the variation in thermal stress with shore height is surprisingly understudied. Early interest in the effects of shore height on thermal stress implicated the role of "critical tidal levels", heights on the shore where the duration of aerial emersion shifted markedly relative to lower levels due to the frequency of submersion caused by semi-diurnal or mixed semi-diurnal tidal cycles (Colman, 1933; Doty, 1946; Evans, 1947; Southward, 1958). While the idea of the primacy of the tides in establishing zones occupied by species with differing tolerances for aerial emersion was intuitively attractive, the ability to rigidly define the extent of zones on a particular shore due solely to the tidal cycle was complicated by a plethora of confounding factors, chief among them the effects of wave action and biotic interactions such as grazing and predation (Underwood, 1978).

Critical tidal levels are of dubious benefit for describing the vertical limits of most intertidal organisms, but certain aspects of the critical tidal level concept have not been wholly discarded. McMahon (1990), concerned with physiological adaptations of high shore snails (including the littorines), simplified the concept and proposed that there was one important vertical boundary on the seashore, the height reached by the lower high tides. Above this height, the shore is not reliably wetted by tides, while the regions below this mark are submerged daily. As a result, organisms living above the

high tide mark must contend with unpredictable and often prolonged periods of aerial emersion, while organisms below can rely on being washed by the tide once within a day. McMahon argued that snails living in the high eulittoral fringe zone should show different patterns of temperature and desiccation tolerance, as well as having different behaviors, compared to snails living in the eulittoral zone that were reliably wetted.

Part of McMahon's (1990) hypothesis was that, regardless of shore height, eulittoral and eulittoral fringe gastropods should reach similar body temperatures while exposed to the sun, so that only the duration of the thermal stress should differ between shore heights. The heat-budget model can be used to make a simple test of this hypothesis, by comparing both the maximum temperatures and duration of high temperature exposures for snails living at different shore heights. The proposed threshold in stress at the high water mark can also be tested to reveal how severe the transition from the eulittoral to the eulittoral fringe zones may be.

2.1.5 Shell size and shape

The size of an organism will affect the body temperature it achieves during the course of a hot day (Vermeij, 1972; Newell, 1976; O'Connor and Spotila, 1992; Helmuth, 1998, 1999). Larger organisms have a larger projected area with which to absorb short-wave radiation, along with a larger surface area for conduction from the substratum and for convection (Vermeij, 1973), all of which can affect body temperature. Larger organisms also have more thermal inertia, resulting in slower heating and cooling rates relative to a smaller organism of the same basic shape (Helmuth, 2002). However, the heat-budget model in the form used here ignores the contribution of stored heat, removing the effect of thermal inertia from the prediction of body temperature. As noted in the previous chapter, the size of the organisms modeled here is small, and they are poorly insulated, resulting in a small heat storage term. As a result, thermal inertia has only a negligible effect on body temperature.

Littorine snails change shape as they grow; a fact that makes simple scaling of the empirically measured parameters of the shells in the previous chapter potentially inaccurate. Heat transfer coefficients, projected areas, surface areas, and contact areas

all scale non-linearly as the shape of the snail changes throughout its life. To simplify the examination of the role of size in thermal stress, I instead use simple spheres as replacements for the littorine snails. The physical parameters measured for brass balls in the preceding chapter can be used in the heat budget model to examine how size influences body temperature of snails.

The predicted temperatures from the spheres can also be used as a standard of comparison allowing us to explore how effectively the shape of the shell and behavior keeps snails cool on hot days. Littorine snails can be found with varying amounts of sculpturing on the shell, different shell thicknesses, and different spire heights that affect the overall shape of the shell. These differences have been hypothesized to arise for a number of reasons, such as temperature regulation (Vermeij, 1973), wave action (Struhsaker, 1968; Currey and Hughes, 1982), and predation pressure (Vermeij, 1982; Trussell, 2000, 2002; Trussell and Nicklin, 2002). I can estimate temperatures for spheres that share similar physical dimensions, such as characteristic length or surface area, to the snail shells studied here. With these data I can also compare temperatures for the idealized spheres and real snails under identical conditions.

2.2 Methods

The tests in this chapter were conducted using the littorine heat-budget model described in the previous chapter. Wherever necessary, the parameters of the model were altered to address specific questions and body temperatures were predicted using a seven year data set (1999-2006) of weather and sea conditions for Hopkins Marine Station in Pacific Grove, CA.

2.2.1 Foot behavior

The effect of leaving the foot in contact with the substratum, or removing it when temperatures or emersion time increased beyond a certain threshold, could be modeled by adjusting the threshold conditions for withdrawing the foot. The basic model assumed that snails pulled the foot into the shell and glued the shell to the substratum

when substratum temperatures exceeded 25°C or when the snails had been emersed for more than three hours. Adjusting the model to raise these thresholds yielded temperature predictions for snails that never removed the foot from the substratum (see Chapter 1). In all cases the shell remained oriented with the aperture of the shell down against the substratum. For this test, snails were modeled on a horizontal surface at 2 m above Mean Lower Low Water (MLLW, tides measured at Monterey, CA, tide gauge, National Tidal Datum Epoch 1983-2001) on a wave-protected shore (wave swash up the shore = 0.5 x significant wave height). Each species was modeled using the most common shell color(s) for that species.

Time series outputs from the models for each species were sorted according to temperature and the top 1% of all temperatures during each model run was recorded. At each time point in the 1% sample, the temperature of the snail with the foot pulled in was subtracted from that of the snail with the foot on the substratum. The mean difference, standard deviation, and maximum difference were all calculated for this subset of the temperature data.

In addition to comparisons of temperature differences at each time point, the total degree-minutes above a threshold temperature was calculated. To calculate degree-minutes, every time point with a body temperature above 30°C was selected (for all of the modeled snail shells, a 30°C cutoff represented approximately the top 1% of all predicted temperatures). The difference between the predicted temperature and the 30°C threshold was calculated and multiplied by the duration of the time step. Degree-minutes are meant to act as a measure of the combined intensity and duration of thermal stress. The average degree-minutes above 30°C for the six complete years (2000 - 2005) in the long term data set were calculated, along with the total degree-minutes for the entire data set (1 August 1999 – 31 July 2006).

2.2.2 Shell orientation

When a littorine snail withdraws the foot into the shell, the snail can either glue the shell with the aperture against the rock, or orient the shell with the aperture lifted away from the substratum. The effect of this behavioral choice on the body temperature of a

snail was examined by running identical snails through the model, in one instance keeping the shell down against the substratum while the foot was withdrawn into the shell, and in the other instance lifting the shell off the substratum every time the foot was withdrawn. All shells were modeled on a horizontal substratum 2.0 m above MLLW on a wave-protected shore.

The projected area of *L. scutulata* and *L. plena* in the "down" and "up" orientations was surveyed in the field at the Friday Harbor Laboratories (FHL) in the summer of 2002. Due to the morphological similarity of the two species and the fact that they co-occur on the shores of FHL, the two species were grouped for the purpose of this survey (Hohenlohe and Boulding, 2001; Hohenlohe, 2003). Snails were photographed *in situ* with a camera oriented in line with the sun, so that the area facing the camera was the same as the area facing the sun. A ruler was placed in the frame at half the height of the shell along the axis facing the camera. All photographs were taken between 11:45 and 14:30 on July 12, 2002 and 10:15 and 13:00 on July 14, 2002 (solar noon at this site on these dates was ~12:15pm, peak body temperatures are typically reached around 13:00 to 14:00). After each photograph, the snail was removed from the rock and the maximum shell length from the spire to the outer edge of the aperture was measured with calipers to the nearest 0.02 mm. The projected area for each shell was measured using Image-J software (NIH, Rasband, 1997-2007).

A representative group of 8 snails spanning the range of sizes found in the field was returned to the lab and photographed from multiple angles. The maximum and minimum projected area for each shell was determined, and the relationship between $\log_{10}$(shell length) and $\log_{10}$(projected area) was calculated. These relationships were used to calculate an approximate maximum and minimum projected area for each snail photographed in the field.

2.2.3 Shell color

Shell color was adjusted by changing the absorbance value, α, of each modeled shell. Three shell colors were tested: a "black" color such as that normally found on *L. scutulata, L. plena* and *L. sitkana* (α = 0.84), a "brown" color typically found on

weathered shells of *L. keenae* or *E. natalensis* (α = 0.80), and "white" shells like those of some *L. keenae* and *E. natalensis* (α = 0.67). Green colored shells were left out of these analyses due to their having an absorbance (α =0.82) so close to that of the black and brown shells that temperature differences were minimal. All simulations were run with snails sitting on a horizontal surface at 2 m above MLLW on a simulated wave-protected shore. Two sets of models were run, one with the shell in contact with the substratum, and a second set in which the snail glued only the lip of the shell to the substratum and lifted the rest of the shell up.

2.2.3.1 Shell color at high temperatures

The seven-year time series of temperatures was saved from each model run. To compare the effect of shell color at high temperatures, the temperature data at each time point for the black shell color (which was always the hottest) were sorted from high to low temperature. The highest 1% of all temperatures was chosen, and the temperatures of the brown and white shells at the same time points were recorded. Because the model parameters for each species were identical save for the shell's absorptivity, a predicted temperature for the black shell at a specific time point could be directly compared to the temperature for the brown or white shell at the same time, as the environmental conditions in the model are identical across all three models.

2.2.3.2 Shell color at lower temperatures

To examine the potential beneficial effect of dark shell coloring at low temperatures, the time-series of body temperatures for the modeled snails was divided up into four seasons of three months each, based on the typical meteorological divisions (i.e., winter runs from 1 December to 1 March, spring from 1 March to 1 June etc). Within these four seasons, the predicted body temperatures were recorded for each of the three shell colors at each time period during daylight hours when the effective tidal level was below the simulated shore height (2 m). Dividing the seasons in this fashion was chosen to accentuate any potential temperature differences between the color morphs during certain conditions, such as cooler winter temperatures. Because shell color should have no effect on body temperature during darkness or when the snail is

awash at high tide, excluding these periods should further highlight the potential beneficial effect of dark colors.

2.2.4 Shore height

The effect of shore height on body temperature of snails was measured for one shell from each species. Each simulated snail was modeled at six shore heights ranging from 1.5 m to 2.75 m above MLLW at 0.5 m intervals, on a wave-protected shore. In addition to predictions of maximum temperature and degree-minutes above a 30°C threshold, the relative time available for "foraging" was recorded. Foraging time was counted as any time step where the snail was either submerged or was emersed but still had the foot in contact with the substratum. The criteria used for triggering foot withdrawal were the standard 3 hr time-of-emersion threshold or the 25°C temperature threshold. Foraging time was expressed as the average percentage of a year spent with the foot on the substratum.

2.2.5 Shell size and shape

The effect of increasing body size on body temperature was tested by modeling a series of spherical "snails" ranging in diameter from 4.75 to 25.4 mm using the parameter data collected for brass spheres in the preceding chapter. The heat-budget model was run with each of the eight sizes of sphere sitting on a horizontal substratum 2.0 m above MLLW, on a wave-protected shore. The contact area between the sphere and the substratum was calculated using the relationship between contact area and shell surface area determined for *L. keenae* in the preceding chapter. There was no behavioral component to this version of the model, so the contact area of the sphere did not change as it did for model snails that could extend and withdraw the foot. The heat transfer coefficient was calculated based on the empirically measured heat transfer coefficients for each brass sphere. Short-wave absorptivity was set equal to that of a black shell. The maximum temperature and cumulative time spent above a threshold temperature of 30°C were recorded for each sphere size. The average temperature difference during all emersion times and during the hottest 1% of all time periods was calculated for each pair of sphere sizes.

Comparisons of spheres and snail shells of similar sizes were carried out by estimating temperatures of spheres that were similarly sized to the individual snail shells used elsewhere in this chapter. Because snails are not perfect spheres, it was necessary to choose a characteristic dimension to match the sphere size to. The chosen characteristic dimensions could be the characteristic length of the shell, as used in the standard snail heat-budget models (see Tables 1-3, 1-4, 1-5, 1-6, and 1-7), or another dimension of the shell such as the surface area, volume, or average projected area. Each of these dimensions was converted to a characteristic length that was then used to calculate the sphere size and resultant heat-budget parameters.

The surface area of each littorine shell was previously calculated for use in the heat transfer coefficient calculations (see Chapter 1.2.2.2). The characteristic length, *L*, of a sphere with a given surface area was calculated using the equation for the surface area of a sphere:

$$L = 2 \times \sqrt{\frac{\text{Surface area}}{4\pi}}. \quad (33)$$

The volume of a snail shell was measured via displacement by dropping the silver-filled littorine shells of each species into small syringe graduated at 0.01 cm^3. The error of this process was ±0.01 cm^3, which translates to an error in characteristic length calculation of 1 mm for a spherical object. The volume calculated for each shell was translated into a characteristic length, *L*, using the equation for the volume of a sphere:

$$L = 2 \times \sqrt[3]{\frac{3}{4} \times \frac{\text{Volume}}{\pi}}. \quad (34)$$

The average projected area of a snail shell was calculated using the image data used to calculate the projected area of the shell in various orientations (see Chapter 1.2.2.1). The average projected area of a snail shell was converted to a length, *L*, using the equation for the area of a circle:

$$L = 2 \times \sqrt{\frac{\text{projected area}}{\pi}}\,. \tag{35}$$

The characteristic length, L, calculated using each of these methods was then used to calculate the surface area and projected area of the sphere. The surface area of the sphere was then used to calculate the contact area with the substratum, using the relationship in Eqn. (31) from Chapter 1. Because of the non-linear change in heat-transfer coefficient with change in sphere size, the coefficients a and b for the Nusselt-Reynolds number relationship were estimated by fitting curves to the empirically measured data from spheres of different diameters (Table 1-8), as shown in Figure 2-2.

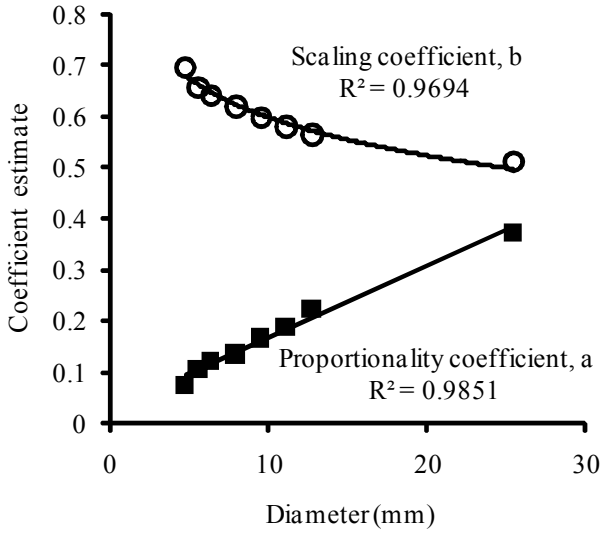

Figure 2-2. Scaling relationship of sphere diameter with the coefficients *a* and *b*, from the Nusselt-Reynolds number relationship (Nu = aRe^b) for brass spheres in the wind tunnel.

With the parameters for the snail-sized sphere calculated, the heat-budget model was run with the sphere on a horizontal platform 2.0 m above MLLW on a wave protected shore. The temperature data for the sphere and the snail on which it was based could be compared under identical conditions. Temperatures were compared for the shell in both the down and up shell orientations, using all time periods where the objects were emersed, or the hottest 1% of all time periods in the seven year dataset.

2.3 Results

2.3.1 Foot behavior

Model snails forced to keep the foot in contact with the substratum at all times had higher predicted body temperatures than snails that could withdraw the foot and minimize contact with the hot substratum (Table 2-1). Snails with the foot always extended accumulated more time above the 30°C threshold on both a per-year basis and over the whole seven year data set (Table 2-2, Figure 2-3).

Table 2-1. Effect of foot position on body temperature. Snails were modeled either with the foot always in contact with the substratum, or retracted into the shell to minimize substratum contact during hot periods. The mean difference (± 1 SD) and maximum difference between the two foot positions were calculated for the upper 1% of all predicted temperatures during the seven year model period. Data are from shells modeled on a horizontal substratum at 2.0 m shore height, on a wave-protected shore.

Species (shell color)	Foot behavior	Maximum temperature (°C)	Mean difference (°C ± 1 SD)	Maximum difference (°C)
L. keenae (black)	Extended Retracting	40.66 38.99	2.32 (± 0.38)	3.39
L. keenae (brown)	Extended Retracting	40.65 38.89	2.40 (± 0.38)	3.47
L. keenae (white)	Extended Retracting	40.63 38.64	2.64 (± 0.37)	3.69
L. scutulata (black)	Extended Retracting	40.57 38.81	2.61 (± 0.59)	4.38
L. plena (black)	Extended Retracting	40.37 38.42	3.26 (± 0.74)	5.37
L. sitkana (black)	Extended Retracting	40.58 38.81	2.53 (± 0.43)	3.82
E. natalensis (brown)	Extended Retracting	40.58 38.80	2.70 (± 0.52)	4.20

Table 2-2. Time spent above 30°C threshold body temperature during 1999 - 2006. Snails were modeled on a horizontal surface 2 m above MLLW on a wave-protected shore. Snails either had the foot constantly extended onto the substratum, or withdrawn during warm periods.

Species (shell color)	Foot behavior	Degree-minutes yr^{-1} above 30°C (mean ± 1 SD)	Total degree-minutes above 30 ºC
L. keenae (black)	Extended Retracting	13,379 (± 8,549) 3,088 (± 2,661)	87,268 19,716
L. keenae (brown)	Extended Retracting	13,302 (± 8,504) 2,920 (± 2,574)	86,731 18,602
L. keenae (white)	Extended Retracting	13,078 (± 8,388) 2,523 (± 2,277)	85,242 15,990
L. scutulata (black)	Extended Retracting	9,164 (± 6,299) 2,155 (± 1,990)	59,596 13,804
L. plena (black)	Extended Retracting	8,660 (± 6,046) 1,637 (± 1,689)	56,334 10,340
L. sitkana (black)	Extended Retracting	12,308 (± 7,976) 2,602 (± 2,330)	80,219 16,600
E. natalensis (brown)	Extended Retracting	11,803 (± 7,722) 2,388 (± 2,162)	76,915 15,274

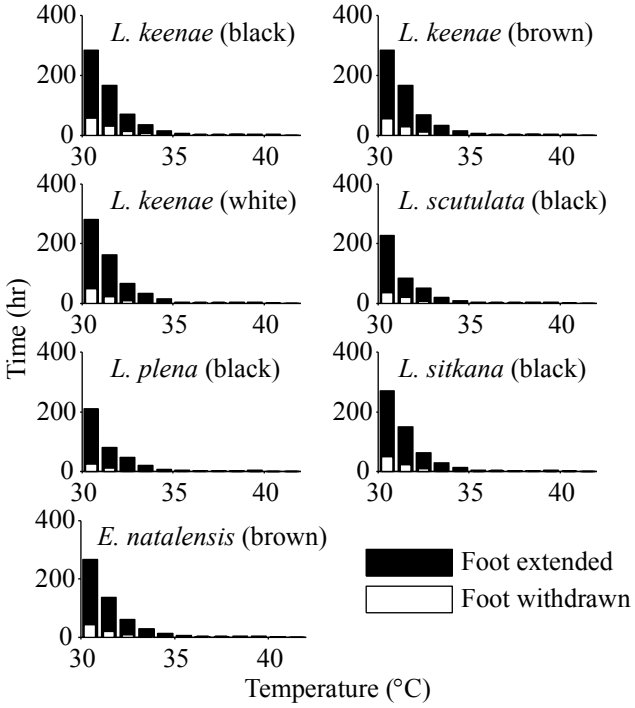

Figure 2-3. Cumulative hours spent above 30°C for snails modeled with the foot always extended or withdrawn during warm periods, using weather data from Hopkins Marine Station from 1999 to 2006. Predicted temperatures were binned in 1°C increments, and the cumulative time for each temperature increment is shown. The shell color for each modeled snail is listed next to the species name.

2.3.2 Shell orientation

When a littorine snail withdraws the foot into the shell, the snail has a choice of whether to glue the shell with the aperture sitting down against the rock, or to orient the shell with the aperture lifted away from the substratum. The effect of this behavioral choice on the body temperature of a snail was examined by running identical snails through the model, in one instance keeping the shell down against the substratum while the foot was withdrawn into the shell, and in the other instance lifting the shell off the substratum every time the foot was withdrawn.

Model snails that reoriented the shell to minimize contact with the substratum were 1.5 to 2.4°C cooler on average than the same snail with the shell sitting on the hot rock

surface, and achieved lower maximum body temperatures under the same extreme weather conditions (Table 2-3). The cumulative time spent above 30°C by snails oriented up off the substratum was less than half that of snails sitting on the substratum (Figure 2-4) and the total degree-minutes accumulated under the same conditions were reduced by 2 to 3 times (Table 2-3). Representative temperature profiles on two hot days are shown in Figure 2-5. By all of these measures, the duration and intensity of thermal stress endured by snails oriented up away from the substratum was markedly reduced.

Table 2-3. Comparison of predicted body temperatures for simulated snails in one of two shell orientations. Snails in the "Down" shell position withdraw the foot and leave the shell sitting down on the substratum during low tide. Snails in the "Up" position withdraw the foot into the shell, and elevate the shell up off the substratum, leaving only the lip of the shell in contact with the rock. Results are for shells modeled on a horizontal bench at a 2.0 m shore height on a wave-protected shore. The mean differences are calculated for the hottest 1% of all temperatures during the model run.

Species	Shell position	Maximum Temperature (°C)	Degree-minutes above 30°C	Mean difference, Down-Up (°C ± 1 SD)	Maximum difference, Down-Up (°C)
L. keenae (black)	Down	38.99	19,716	1.49 (± 0.27)	2.16
	Up	37.82	8,839		
L. keenae (brown)	Down	38.89	18,602	1.54 (± 0.27)	2.21
	Up	37.68	8,180		
L. keenae (white)	Down	38.64	15,990	1.68 (± 0.25)	2.32
	Up	37.30	6,639		
L. scutulata (black)	Down	38.81	13,804	1.94 (± 0.40)	3.00
	Up	37.17	5,561		
L. plena (black)	Down	38.42	10,340	1.53 (± 0.35)	2.57
	Up	36.89	5,170		
L. sitkana (black)	Down	38.81	16,600	2.18 (± 0.53)	3.39
	Up	37.28	5,993		
E. natalensis (brown)	Down	38.71	14,012	2.37 (± 0.55)	3.48
	Up	36.87	5,049		

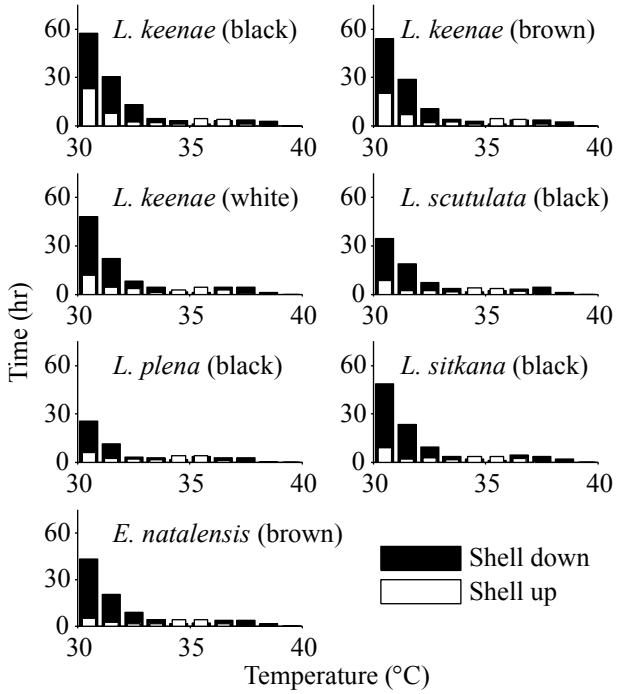

Figure 2-4. Cumulative hours spent above 30°C for modeled shells that remain down on the substratum, or elevated up off the substratum during warm periods, using weather data from Hopkins Marine Station for 1999 to 2006. Predicted body temperatures were sorted into 1°C increments, and the cumulative time for each temperature interval is plotted. The shell color of each modeled shell is listed next to the species name.

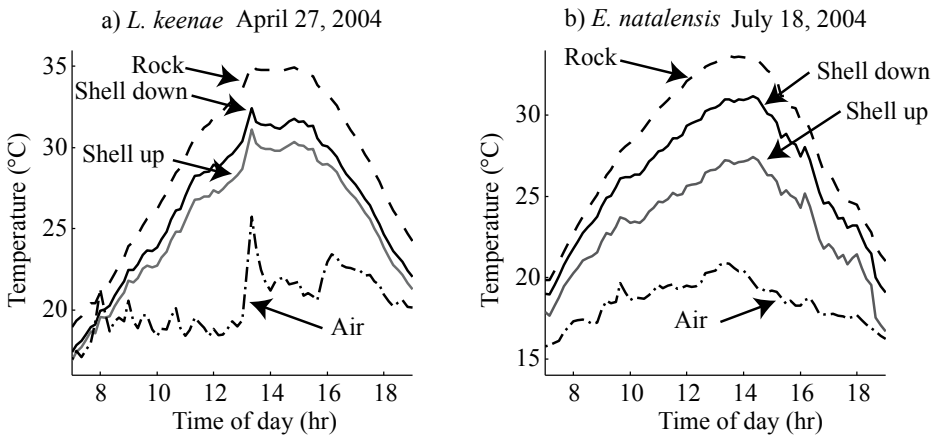

Figure 2-5. Simulated temperatures from two representative days for two snails on a horizontal platform at 2.0 m shore height, on a wave-protected shore. a) Temperatures for a white *Littorina keenae* shell, modeled with the shell down against the substratum at all times (black solid line), or with the shell elevated up off the substratum during low tide (gray solid line). Temperatures (dashed lines) for the rock surface (predicted) and air temperature (measured) are shown. b) Temperatures for a brown *Echinolittorina natalensis*, modeled with the shell down or elevated up off the substratum.

Snails measured in the field at Friday Harbor did not orient the shells to minimize the projected area towards the midday sun. The relationship between the reference shell lengths and minimum projected area was

$$\text{projected area} = 0.299 \times \text{length}^{2.02} \,. \tag{36}$$

The average difference between the measured projected area and predicted minimum area for each snail was significantly greater than zero (one-tailed t-test, "down" snails, n = 25, $p < 0.001$; "up" snails, n = 86, $p < 0.001$) and the two groups were not significantly different from each other (t-test, df = 109, $p = 0.359$). Snails in both the "down" and "up" orientations spanned the range of projected areas between the maximum and minimum predicted areas for each size of snail (Figure 2-6).

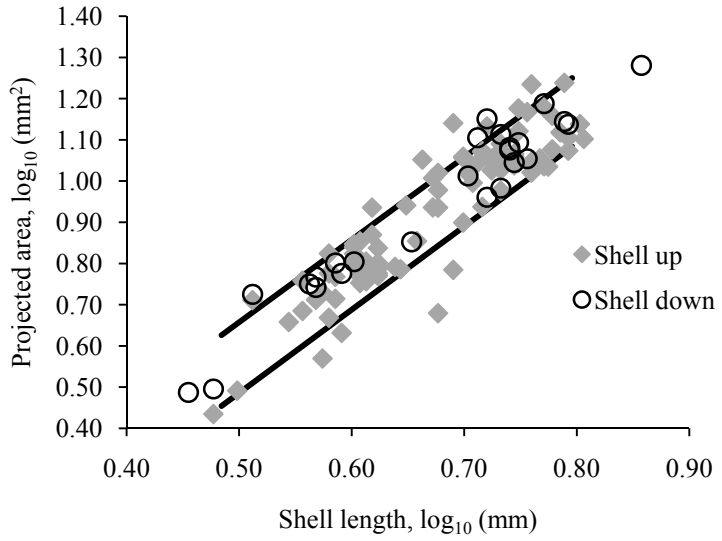

Figure 2-6. Projected area measured at midday for *Littorina scutulata* or *L. plena* in the field. Snails were sitting down on the rock (○) or elevated up off the rock (♦). The black lines represent the calculated maximum and minimum projected areas based on fitted relationships of projected area on shell length from eight snails collected from the field.

2.3.3 Shell color effects

2.3.3.1 Shell color at high temperatures

The mean temperature difference between the black and brown, or black and white, shell colors was calculated for the top 1% of temperatures. The results for snails sitting with the shell against the substratum are given in Table 2-4. In all cases, the black shell had the highest predicted body temperature, and the temperature difference between the black and white shell colors was greater than the temperature difference between the black and brown shells. For all of the species, the maximum difference between black and white shells was between 0.20°C and 0.39°C. A representative temperature trace for the same shell modeled as a black or white color is shown in

Table 2-4. Temperature differences between shell colors of littorine snails when shell sat down on the substratum. Mean temperature differences among shell colors are calculated for the hottest 1% of all body temperatures predicted from seven years of weather data. All models were run with the snail positioned on a horizontal surface, 2 m above MLLW in a wave-protected site.

Species	Shell color comparison	Mean difference (°C ± 1SD)	Maximum difference (°C)	Maximum temperature (black shell, °C)
L. keenae	Black – brown	0.10 (± 0.01)	0.13	38.99
	Black – white	0.35 (± 0.02)	0.49	
L. scutulata	Black – brown	0.04 (± 0.01)	0.05	38.81
	Black – white	0.15 (± 0.01)	0.20	
L. plena	Black – brown	0.05 (± 0.02)	0.07	38.42
	Black – white	0.20 (± 0.02)	0.27	
L. sitkana	Black – brown	0.10 (± 0.01)	0.13	38.81
	Black – white	0.37 (± 0.03)	0.49	
E. natalensis	Black – brown	0.09 (± 0.01)	0.12	38.80
	Black – white	0.33 (± 0.03)	0.43	

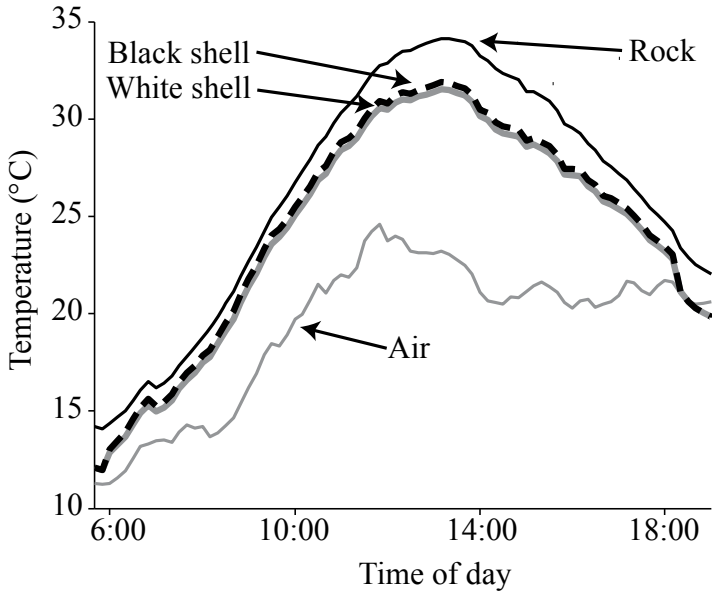

Figure 2-7. *L. keenae*. Representative temperature predictions from April 25, 2004, for a snail shell colored black or white. The shell was modeled sitting down on the substratum with the foot withdrawn, on a horizontal platform 2 m above MLLW on a wave-protected shore at HMS. The black morph (dashed black line) was 0.17°C warmer on average through the daylight hours than the white morph (thick gray line). Measured air temperatures and predicted rock temperatures are also indicated.

The temperature difference between different shell colors was larger for models where the snail shell was lifted off the substratum (Table 2-5). In this case, white shells were maximally 0.6°C to 0.75°C cooler than black shells. The average difference between black shells and brown or white shells was also larger compared to the situation in which shells were kept down in contact with the rock surface.

Table 2-5. Temperature differences between shell colors of littorine snails when shell was lifted away from substratum. Mean temperature differences among shell colors are calculated for the hottest 1% of all body temperatures predicted from seven years of weather data. All models were run with the snail positioned on a horizontal surface, 2 m above MLLW in a wave-protected site. During hot periods snails reduced contact with the rock surface by gluing only the lip of the shell to the substratum.

Species	Shell color comparison	Mean difference (°C ± 1SD)	Maximum difference (°C)	Maximum temperature (black shell, °C)
L. keenae	Black – brown	0.15 (± 0.01)	0.20	37.83
	Black – white	0.55 (± 0.04)	0.75	
L. scutulata	Black – brown	0.12 (± 0.02)	0.17	37.17
	Black – white	0.43 (± 0.06)	0.63	
L. plena	Black – brown	0.11 (± 0.02)	0.16	36.89
	Black – white	0.39 (± 0.07)	0.61	
L. sitkana	Black – brown	0.12 (± 0.02)	0.18	37.28
	Black – white	0.46 (± 0.06)	0.68	
E. natalensis	Black – brown	0.11 (± 0.02)	0.17	36.98
	Black – white	0.40 (± 0.07)	0.63	

2.3.3.2 Shell color at low temperatures

The results of the shell color analysis for daylight hours at low tide in each season are shown in Table 2-6 and Table 2-7. There was slight variation in the mean difference between shell colors through the four seasons, but in all cases the temperature differential was quite small. The simulated *Littorina keenae* shell showed the greatest deviation between black and white shell morphs, and the distributions are shown in Figure 2-8.

Table 2-6. Temperature differences between shell colors of littorine snails. Shells were modeled sitting down against the substratum at all times. The mean differences are given for all time points during daylight hours when the tide was below the simulated shore level of the snail, separated into each season.

Species	Shell color comparison	Mean difference, all temperatures (°C ± 1 SD)			
		Winter	Spring	Summer	Autumn
L. keenae	Black – brown	0.07 (± 0.04)	0.09 (± 0.03)	0.08 (± 0.03)	0.07 (± 0.03)
	Black - white	0.27 (± 0.13)	0.32 (±0.12)	0.28 (± 0.12)	0.27 (± 0.12)
L. scutulata	Black – brown	0.03 (± 0.01)	0.03 (± 0.01)	0.03 (± 0.01)	0.03 (± 0.01)
	Black - white	0.10 (± 0.05)	0.11 (± 0.04)	0.10 (± 0.04)	0.10 (± 0.04)
L. plena	Black – brown	0.03 (± 0.01)	0.03 (± 0.01)	0.03 (± 0.01)	0.03 (± 0.01)
	Black - white	0.11 (± 0.05)	0.12 (± 0.04)	0.10 (± 0.05)	0.11 (± 0.05)
L. sitkana	Black – brown	0.05 (± 0.03)	0.06 (± 0.02)	0.06 (± 0.02)	0.05 (± 0.02)
	Black - white	0.23 (± 0.09)	0.21 (± 0.09)	0.19 (± 0.08)	0.21 (± 0.09)
E. natalensis	Black – brown	0.04 (± 0.02)	0.05 (± 0.02)	0.04 (± 0.02)	0.04 (± 0.02)
	Black - white	0.15 (± 0.07)	0.18 (± 0.07)	0.16 (± 0.07)	0.15 (± 0.07)

Table 2-7. Temperature differences between shell colors of littorine snails. Simulated shells were elevated up off the substratum and attached with a film of mucus during aerial emersion. The mean differences are given for all time points during daylight hours when the tide was below the simulated shore level of the snail, separated into each season.

Species	Shell color comparison	Mean difference, all temperatures (°C ± 1 SD)			
		Winter	Spring	Summer	Autumn
L. keenae	Black – brown	0.14 (± 0.07)	0.13 (± 0.05)	0.11 (± 0.05)	0.12 (± 0.05)
	Black - white	0.51 (± 0.26)	0.47 (±0.17)	0.40 (± 0.17)	0.44 (± 0.20)
L. scutulata	Black – brown	0.09 (± 0.05)	0.08 (± 0.03)	0.06 (± 0.03)	0.08 (± 0.04)
	Black - white	0.33 (± 0.17)	0.28 (± 0.11)	0.23 (± 0.10)	0.29 (± 0.13)
L. plena	Black – brown	0.09 (± 0.05)	0.07 (± 0.03)	0.06 (± 0.03)	0.07 (± 0.03)
	Black - white	0.32 (± 0.17)	0.28 (± 0.11)	0.23 (± 0.10)	0.27 (± 0.13)
L. sitkana	Black – brown	0.05 (± 0.03)	0.06 (± 0.02)	0.06 (± 0.03)	0.05 (± 0.02)
	Black - white	0.19 (± 0.09)	0.23 (± 0.09)	0.21 (± 0.09)	0.20 (± 0.09)
E. natalensis	Black – brown	0.10 (± 0.05)	0.09 (± 0.04)	0.08 (± 0.03)	0.09 (± 0.04)
	Black - white	0.38 (± 0.19)	0.34 (± 0.13)	0.29 (± 0.12)	0.33 (± 0.15)

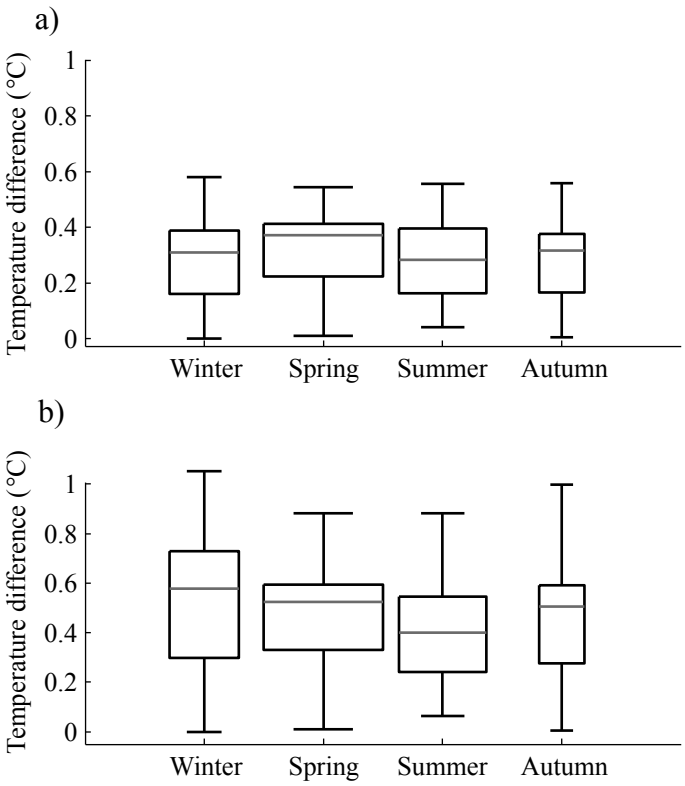

Figure 2-8. Temperature differences between color morphs of a *Littorina keenae* shell. a) Temperature differences between black and white shell colors during daylight hours when the simulated snail was emersed. The shell was modeled so that it was always held down against the substratum. The center line in the box represents the median temperature deviation, and the top and bottom of the box denote the 75th and 25th percentiles, respectively. b) Temperature difference for black and white shell colors for a *L. keenae* shell elevated up off the substratum when emersed. All other parameters were equivalent to those in (a). Box widths represent relative sample size in each season, with the spring sample size equal to 16,776 time points. Sample size varies between seasons due to timing of the low tides, wave action, and day length.

2.3.4 Shore height

The standard form of the heat-budget model allows snails to keep the foot in contact with the rock, and thus able to forage, for three hours after the final wetting by wave splash. The interaction of the tidal regime and wave conditions with shore height lead to snails living lower on the shore having a substantially greater fraction of time available for foraging every year (Figure 2-9). The greater amount of time spent wetted at lower shore heights also reduces the severity of high temperature periods as

measured by total degree-minutes spent above 30°C and maximum predicted temperature (Figure 2-10 and Figure 2-11).

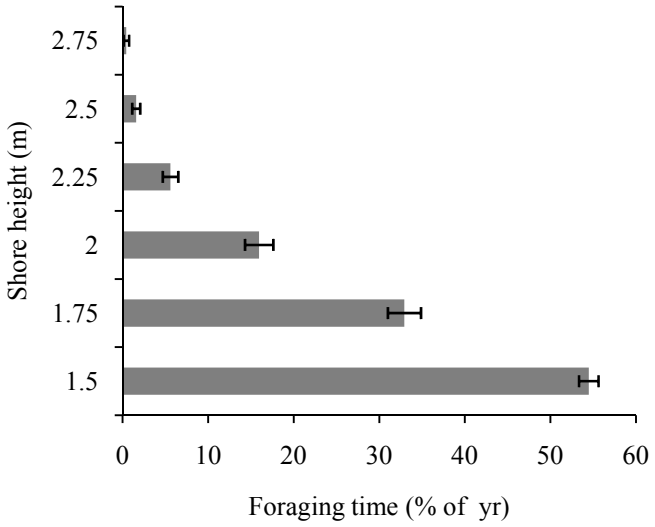

Figure 2-9. *Littorina scutulata*. Mean percent of year available for foraging at different shore heights for the period 1999-2006, on a simulated horizontal platform on a wave-protected shore. The model assumes that foraging ceases 3 hr after aerial emersion. Error bars are ±1 SD.

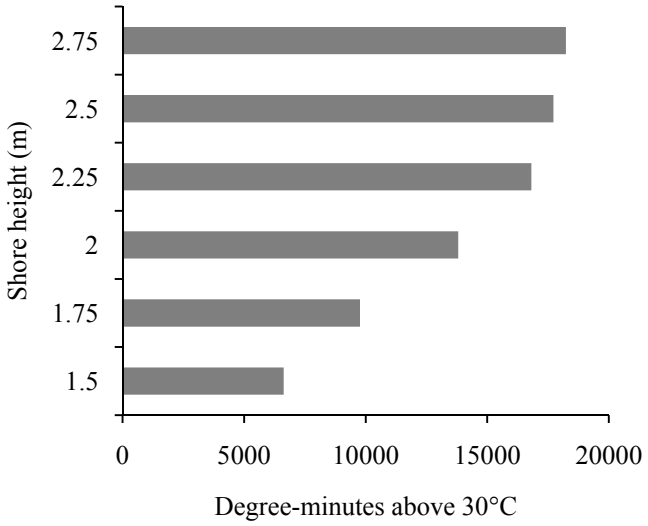

Figure 2-10. *Littorina scutulata*. Total degree-minutes above 30°C at different shore heights for the period 1999-2006. The snail was modeled with a black shell, sitting down on a horizontal platform on a wave-protected shore.

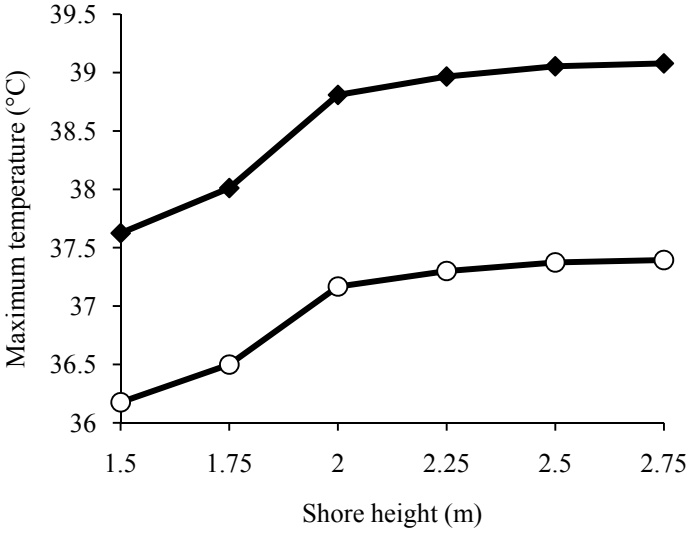

Figure 2-11. *Littorina scutulata*. Maximum body temperature predicted during the period 1999-2006 for several shore heights (m above MLLW). Snails were modeled on a horizontal substratum on a wave protected shore. Diamonds (♦) represent a black shell that remains down against the substratum, circles (○) represent the same shell elevated up off the substratum during emersion.

The maximum temperature achieved during a day and the duration of high temperature events at each shore height varied with the tidal regime and wave climate on each particular day. Three examples of these effects are shown in Figure 2-12. During calm days with neap tides, there was virtually no effect of shore height on temperature (Figure 2-12a), while days with higher tides or larger waves allowed snails at lower shore heights to spend more time submerged, reducing the severity of the environmental conditions (Figure 2-12b + c).

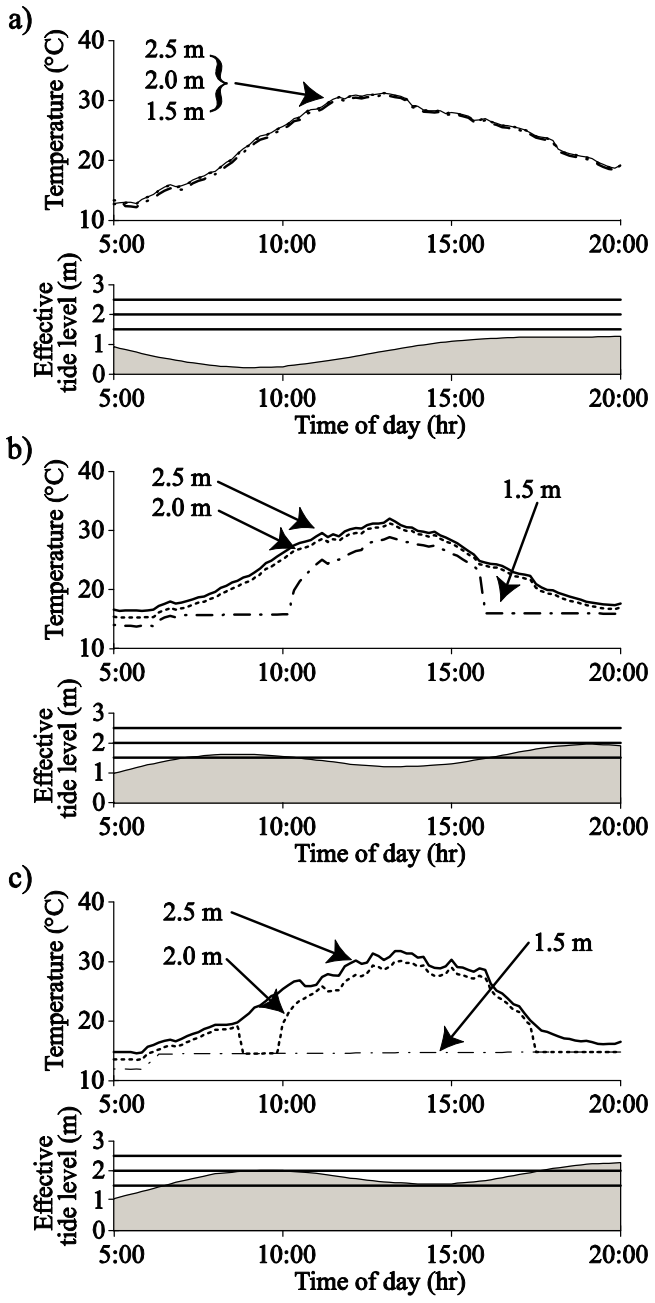

Figure 2-12. *Littorina scutulata.* Representative temperature traces for identical model snails at three shore heights (2.5, 2.0, 1.5 m above MLLW). The lower graph of each pair shows the effective tidal height (tide + wave splash) and the 3 modeled shore heights. a) April 25, 2004. Tide height was low for the entire day, and snails at all three shore heights experienced similar body temperatures. b) September 22, 2003. The 1.5 m shore height is submerged for part of the day, resulting in a lower body temperature and shorter duration of exposure relative to the two higher shore positions. c) August 30, 2005. The 1.5 m shore height is submerged the entire day, while the 2.0 m shore height is submerged briefly in the morning and evening, resulting in a lower body temperature than the snail modeled at 2.5 m shore height.

2.3.5 Body size scaling and temperature

Among the sizes of spheres modeled here, body temperature varied very little as sphere size changed. The maximum temperature achieved over the course of seven years of predicted temperatures varied by less than 0.1°C (Figure 2-13a) and cumulative time above 30°C rose by 6.5 h (Figure 2-13b). When predicted sphere temperatures were compared for the hottest 1% of all modeled time periods, the average difference between spheres ranged from approximately 0 to 0.5°C, with the larger spheres tending to be warmer than small spheres (Table 2-8).

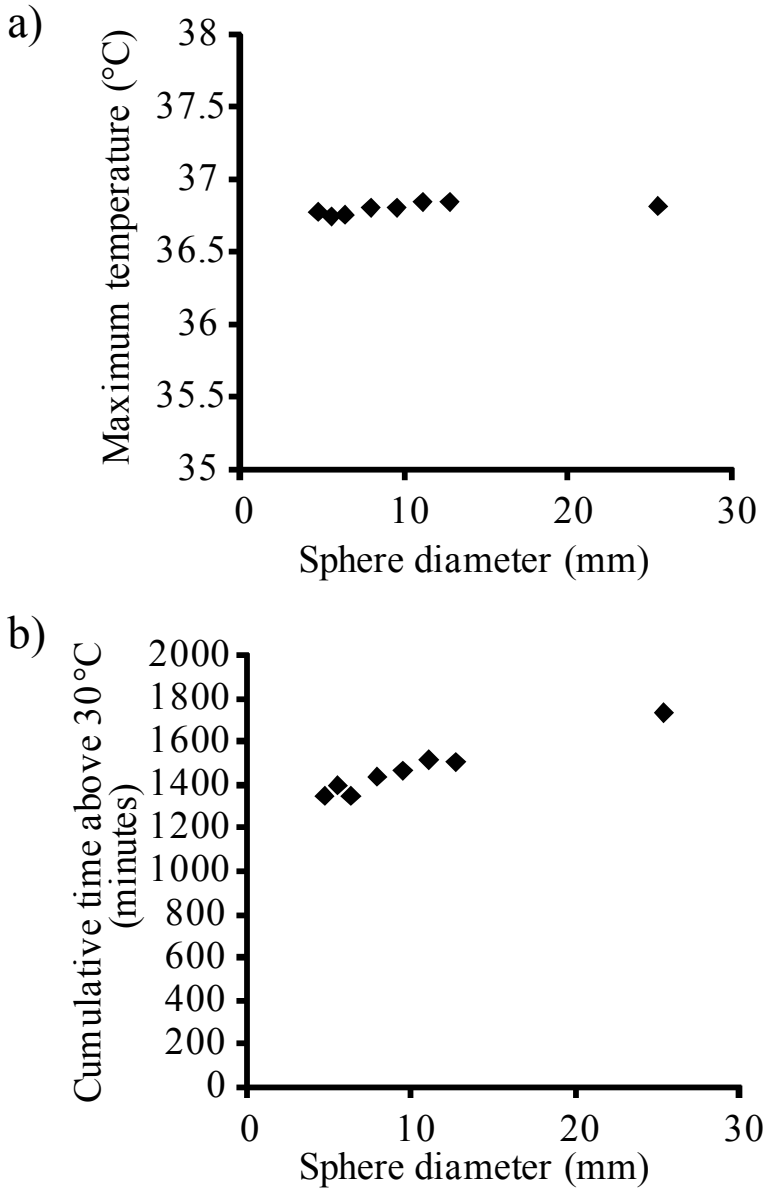

Figure 2-13. Results from heat-budget models of eight sizes of spheres modeled on a horizontal platform 2.0 m above MLLW on a wave protected shore. a) Maximum temperature achieved by spheres of different diameters during seven years. b) Cumulative time spent above 30°C for sphere of different sizes of the course of seven years.

Table 2-8. Average temperature difference between spheres of different diameters for the hottest 1% of temperatures during a seven year period. The temperature of the sphere in each column was subtracted from the temperature of the sphere in each row for each time point. The spheres were modeled sitting on a horizontal platform 2.0 m above MLLW on a wave-protected shore.

Diameter (mm)	4.75	5.55	6.35	7.95	9.52	11.09	12.73	25.40
4.75								
5.55	-0.02							
6.35	0.03	0.05						
7.95	0.17	0.18	0.14					
9.52	0.21	0.23	0.18	0.04				
11.09	0.31	0.33	0.28	0.13	0.09			
12.73	0.31	0.32	0.27	0.13	0.09	-0.01		
25.40	0.53	0.55	0.49	0.34	0.30	0.20	0.21	

Calculating the characteristic length of spheres based on the chosen four characteristic dimensions of a snail shell (average length, surface area, volume, projected area) resulted in very small changes in the characteristic length of the theoretical spheres (Table 2-9). The effect of these small shifts in characteristic length on predicted temperature may be inferred from the data in Figure 2-13, where shifts of 1 – 2 mm in sphere diameter shift the maximum temperature by only 0.1 – 0.2°C at most.

Table 2-9. Representative calculated characteristic length values used to compare spheres to snail shells. The four dimensions of each shell were measured using methods outlined in the text. Characteristic lengths derived from the surface area, volume, and projected area were approximated using the equations for the dimensions of a sphere.

	L. keenae 2		*E. natalensis* 1	
Shell dimension	Measured shell value	Calculated characteristic length	Measured shell value	Calculated characteristic length
Average length	10.19 mm	10.19 mm	6.17 mm	6.17 mm
Surface area	348 mm^2	10.53 mm	99.5 mm^2	5.63 mm
Volume	0.51 mm^3	9.89 mm	0.08 mm^3	5.28 mm
Projected area	86.5 mm^2	10.49 mm	24.9 mm^2	5.63 mm

Due to the very small effect of the different methods of measuring characteristic length of the snail shells, only spheres with a characteristic length derived from the average length of each snail shell were compared to the shell temperatures. When snail shells were modeled with the aperture down against the substratum, they were between 1.5 and 2.4°C warmer than the equivalently-sized sphere on the warmest days (Table 2-10). When the same shell was lifted away from the substratum so that only

the outer lip of the shell contacted the warm rock, all snail species were closer in temperature to the sphere, with the small *L. plena* and *E. natalensis* snails maintaining body temperatures roughly equal to the spheres during the warmest periods (Table 2-10, Figure 2-14).

Table 2-10. Average temperature difference between littorine snail and sphere with an equivalent characteristic length. Results are given for comparisons to snails with the shell oriented down against the substratum or oriented up off the substratum. Temperature differences are calculated for the hottest 1% of all time periods during a seven year time period.

	Shell – sphere average difference (±1 SD)	
Species	Shell down	Shell up
L. keenae	2.33 (± 0.12)	0.87 (± 0.18)
L. scutulata	2.06 (± 0.27)	0.16 (± 0.46)
L. sitkana	2.16 (± 0.20)	0.18 (± 0.34)
L. plena	1.51 (± 0.38)	-0.06 (± 0.45)
E. natalensis	1.99 (± 0.21)	-0.14 (± 0.46)

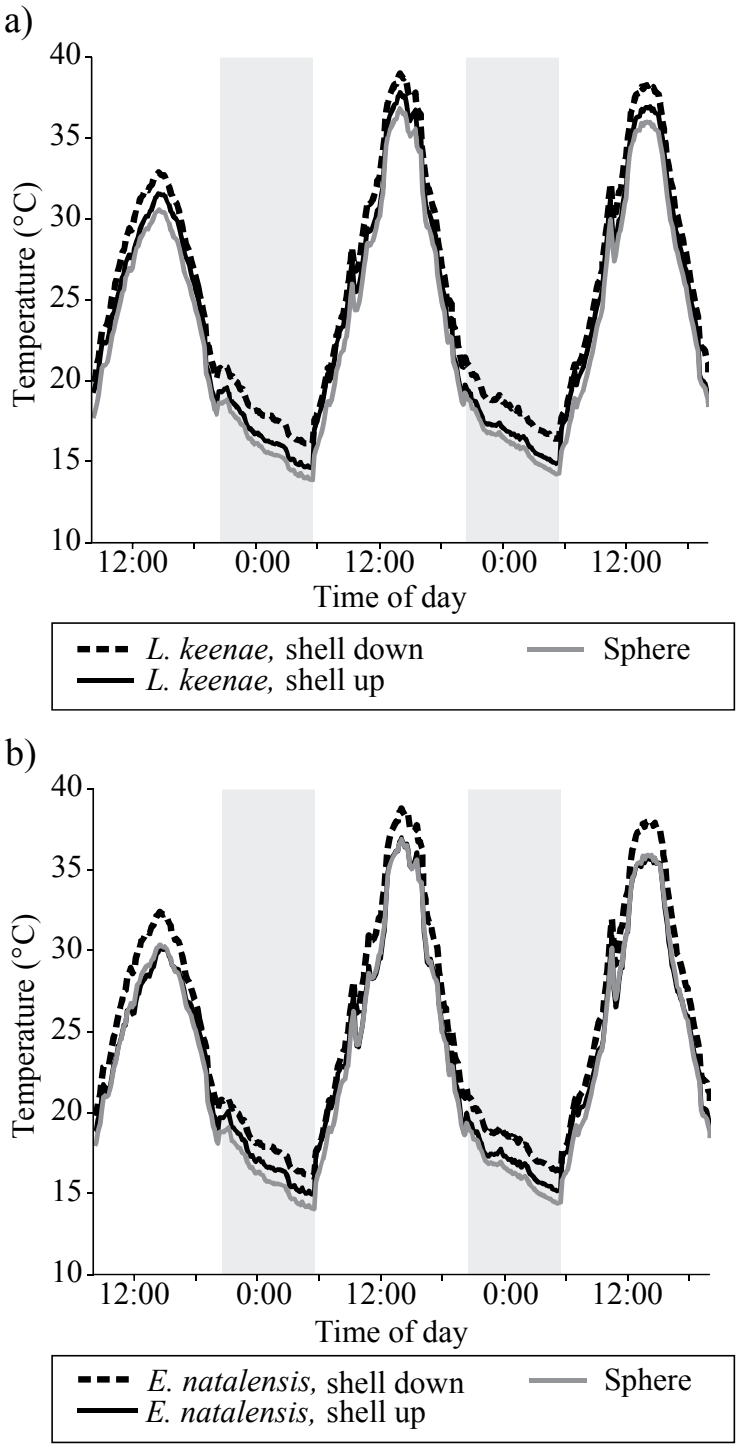

Figure 2-14. Representative body temperatures for snail shells with the aperture down against the substratum or oriented up off the substratum, and spheres with characteristic lengths equal to the snail shells. a) *L. keenae* and sphere predicted temperatures from June 24 – 26, 2003, for individuals modeled at 2.0 m above MLLW on a wave-protected shore. b) *E. natalensis* and equivalent-sized sphere modeled under the same conditions as *L. keenae*.

2.4 Discussion

The heat-budget model, combined with a long-term weather data set, demonstrates the utility of a modeling approach for answering questions about the efficacy of behavioral and morphological characteristics of littorine snails for regulating body temperature. Questions of the effect of color, shell orientation, withdrawing the foot, shape and size can all be addressed in a controlled manner not possible in the field. The results presented here call into question earlier hypotheses about the role of color and shell sculpture as adaptations to surviving high temperatures, but they also show that behavioral choices made by snails can strongly affect body temperature. The results and potential causes of the temperature differences for each comparison are discussed below, as well as a treatment of the broader implications of the model results for littorine biology.

2.4.1 Foot behavior

Schmidt-Nielsen (1971) demonstrated that the ability of terrestrial snails to become dormant and withdraw the foot into the shell was a major advantage for survival, especially in the extreme temperatures of desert habitats. While the soil on the desert floor heated to 65°C, the body of the snail reached a temperature of only 50°C. This reduction in temperature relative to the ground was enough to keep the snails alive for the duration of an 8 hr exposure, while snails stressed at 55°C began dying after 30 minutes. Temperature conditions in the temperate intertidal zone do not approach the severity of the desert, but, for snails, the advantage of removing the foot from the substratum remains. For each of the littorine snails modeled here, removing the foot from the substratum during the warmest days dropped body temperatures by more than 2°C on average, and maximum differences were approximately twice that value. These predicted differences agree with the data of McQuaid and Scherman (1988), who found a similar reduction in body temperature upon withdrawal of the foot for live *Afrolittorina africana* and *A. knysnaensis* in the field in South Africa.

Solar radiation remains the dominant heat flux into the animal during daylight hours whether the foot is extended or withdrawn, and the heat transfer coefficient for convective cooling is not affected by the position of the foot (assuming the shell remains in the same orientation relative to the rock surface). As a result, it is the change in area of contact with the substratum, typically around one order of magnitude, resulting from foot extension and retraction that controls body temperature. With the foot extended, the heat flux from the hot substratum into the snail is increased, an increase that is only partially offset by the increased flow of heat out of the shell by convection.

For snails regularly exposed to warm conditions, the reduction in body temperature due to removing the foot from the substratum results in drastically less time spent at high temperatures over the lifetime of a snail (Figure 2-3). The average degree-minutes per year spent above 30°C for snails modeled at the 2 m shore height was reduced from approximately 11,000 to approximately 2,300 degree-minutes, indicating a substantial change in the duration and severity of high temperature exposures for each of the modeled species (Table 2-2). High temperatures beyond the scope of the normal temperature range to which snails are acclimated can have detrimental effects on the physiological function of snails and can impose substantial metabolic costs for repairing damaged cellular machinery (Roberts *et al.*, 1997; Somero, 2002). Therefore, withdrawing the foot into the shell appears to be a major benefit for littorine snails avoiding thermal stress, even before considering the additional benefit of the reduction in desiccation that can be accomplished by sealing the aperture of the shell closed to the outside air (Garrity, 1984).

2.4.2 Shell orientation

Withdrawing the foot into the shell provides a marked thermal benefit to the snail. Taking the extra step of elevating the shell off the substratum provides an additional, although smaller, temperature reduction. During the hottest periods, snails modeled with the shell elevated up off the substratum were at least 1.5 to 2°C cooler on average than snails modeled with the shell sitting on the substratum (Table 2-3). This reduction

in body temperatures is accompanied by a reduction in the total time spent at elevated temperatures (Figure 2-4). These results agree qualitatively with field measurements made for tropical littorines exhibiting the same behavior by Vermeij (1971) and Garrity (1984). For the tropical species *L. aspera* and *L. modesta* studied by Garrity, simply reorienting shells to sit down on the horizontal substratum led to measurable mortality rates under warm field conditions.

It should be noted that while the advantage of lifting the shell away from the substratum in terms of reducing conduction and increasing convection should hold for all cases, the change in projected area facing the sun will not always be beneficial. On a horizontal surface during summer, pointing the spire of the shell normal to the substratum should reduce the projected area during the middle of the day, when solar insolation will be at its peak. If the substratum is tilted away from horizontal though, a shell oriented normal to the plane of the surface can present a larger projected area towards a midday sun. Thus, orientation relative to the sun and orientation relative to the substratum can present conflicting demands. The data from south-facing slopes at Friday Harbor indicate that neither the snails sitting down on the rock nor those elevated up off the rock managed to consistently minimize the projected area facing the midday sun as a group (Figure 2-6). Individual snails did manage to orient the shell so that the spire pointed towards the midday sun and minimized projected area, but this was likely a chance combination of shell orientation and the orientation of the rock where a snail was sitting. McQuaid and Scherman (1988) reached the same conclusion for high shore littorines in South Africa. However, Muñoz *et al.* (2005) have shown that *Echinolittorina peruviana* in Chile reorient the shell so that the longitudinal axis of the shell faces towards the sun on sunny summer days. *E. peruviana* snails do not necessarily lift the shell away from the substratum while orienting themselves, but they do show a preference for minimizing solar exposure on potentially stressful days. Based on the observations here and the lack of data to the contrary, it is probably the case that the littorine snails in this study are elevating the shell off the substratum in order to minimize contact and increase convective cooling; any reduction in projected area is likely a coincidence. This is not meant to discount

the contribution of reducing projected area to keeping the snail cool, but is meant encourage caution when outlining the benefits of altering shell orientation.

2.4.3 Shell color

From the predictions of the model, it is unclear whether the body temperature differences produced by different shell color morphs would be meaningful to a snail in the field. The average and maximum temperature differences at high temperatures (Table 2-4 and Table 2-5) between black and white shells are less than 1°C in all cases. Shells lifted up off the substratum, so that only the lip of the shell was glued to the rock, had larger differences between color morphs. Similar small differences in temperatures between color morphs have been predicted and measured in insects (Willmer and Unwin, 1981; Forsman, 1997; Forsman *et al.*, 2002) and snakes (Forsman, 1995), and those temperature differences were also overshadowed by the greater effects of behavior on temperature regulation (Ahnesjö and Forsman, 2006).

For the bulk of the time during the year, when air, rock, and body temperatures are all much lower than during extreme heat waves, the effect of darker shell morphs is again questionable. Brown shells reach higher body temperatures than white shells, and black shells reach even higher temperatures under identical conditions, but these differences amount to fractions of a degree Celsius. It is doubtful that such small differences would lead to substantially altered activity levels during cold periods or to higher metabolic rates and growth during all time periods.

The results of the color comparisons for *Littorina* species do not lend support to the hypothesis that dark colors should be beneficial at low temperatures or detrimental at high temperatures. The temperature differences between dark and light morphs are not as extreme as those measured for the larger whelk *Nucella lapillus* used by Etter (1988), nor are *Littorina* as susceptible to high temperatures as *Nucella*, making the temperature differences measured here seem to be of dubious benefit for survival at high temperatures, at least at HMS. Attempting to find color morph benefits during high temperature periods is difficult at a notoriously "cold" site such as HMS (Helmuth *et al.*, 2002), so it remains possible that under more extreme conditions dark

colors would in fact be detrimental to survival. Markel (1971) found that darker *L. aspera* in Central America were between 1 and 3°C warmer than the lighter colored *L. modesta* living on the same shores. McQuaid and Scherman (1988) found that for the two South African species *A. africana* and *A. knysnaensis*, painting the shells black resulted in extremely high mortality rates in the field for both species, while control snails painted with a clear paint experienced very little mortality under the same conditions. It should be noted that using black paint to alter shell color could artificially increase the short-wave heat flux into the animal beyond that of a naturally dark-colored shell. Commercial flat black paints have a short-wave absorptivity, α_{sw}, of approximately 0.95. This short-wave absorptivity is higher than the value measured for black shells of *L. keenae* and *L. scutulata* ($\alpha_{sw} = 0.85$). From Chapter 1, the heat flux (W_{sw}, units of Watts) into a shell due to short-wave solar radiation can be calculated as

$$W_{sw} = \alpha_{sw} A_{proj} q_{sol} \quad (37)$$

where A_{proj} is the projected area (m^2) facing the sun and q_{sol} is the solar irradiance (W m^{-2}). For snails under identical field conditions, increasing α_{sw} increases the heat flux into the shell by a proportional amount. Running the heat-budget model with an α_{sw} value of 0.955 for the same *L. keenae* described above (positioned down on the substratum on a horizontal platform 2.0 m above MLLW on a wave-protected shore) increased the average body temperature 0.2°C over the naturally black shell ($\alpha_{sw} = 0.85$) and 0.56°C over the white shell color ($\alpha_{sw} = 0.67$). The short-wave absorptivity of some white shells may also be markedly lower than the white shells reported here. Schmidt-Nielsen (1971) reported a short-wave reflectivity of approximately 90% for the desert snail *Sphincterochila boissieri*, equal to a short-wave absorptivity of 0.10. Using this very low absorptivity in the heat-budget model for *L. keenae* results in a body temperature 1.45°C cooler on average than a black shell and 1.1°C cooler than a white shell.

A similar shift in body temperatures could be expected for the black-painted snails used by McQuaid and Scherman, and the effect could be magnified if the natural white

shells of *A. africana* and *A. knysnaensis* have α_{sw} values closer to that of *S. boissieri* than the white *L. keenae* shells measured here. The black paint raised body temperatures enough to induce substantial thermal mortality, indicating that these species were living very close to their thermal limits. The slightly lower absorptivity of natural black shells might still have been sufficient to induce the same thermal mortality in populations of *A. africana* and *A. knysnaensis*. These examples from tropical and semi-tropical regions indicate that environmental conditions in warmer regions might accentuate the effect of shell color enough to provide a measurable benefit for snails in the field.

The crypsis hypothesis for explaining shell coloration in *Littorina* may be more important than hypotheses regarding body temperature for the temperate species in this study (McQuaid, 1996a; Forsman and Appelqvist, 1999). Among some species of *Littorina*, a role has been demonstrated for apostatic selection by visual predators driving color variations in populations of snails (Reimchen, 1979; Hughes and Mather, 1986; Reid, 1987; Reimchen, 1989). Similar processes may occur within other *Littorina* species. Crab and bird predation on *Littorina keenae*, the species with the largest color variation in this study, has not been examined in any great detail. A cursory examination of the shoreline at HMS demonstrates that the majority of *Littorina keenae* are a dull brown color that matches the color of the granite substratum. This may be a result of visual predation, and merits further investigation.

In cases where selection via thermal stress and visual predators is hard to prove (Ekendahl, 1994, 1995, 1998), the maintenance of shell color variation in a population may be a result of linkage with another unidentified gene under heavy selection (Jones, 1973; Jones *et al.*, 1977; Sokolova and Berger, 2000; Forsman *et al.*, 2008). Shell color in some gastropods, including some littorine species, is a simple system with one or a few loci and only a few alleles (Ekendahl and Johannesson, 1997). With more information about the genes under selection in these snails, we may eventually come to a better understanding of the role of shell color in littorine snail ecology and evolution.

2.4.4 Shore height

The comparisons of various shore heights are necessarily simplistic in the current form of the model, but they do reveal some general patterns with regard to temperature stress and foraging time at increasing shore heights. The level of Mean High Water at the Monterey Harbor tide gauge (approximately 1.5 km south-east of HMS) is 1.45 m above Mean Lower Low Water (National Tidal Datum Epoch, 1983-2001). With no wave action, this level should roughly correspond to the threshold described by McMahon (1990) for the shore level that is reliably wetted every day. However, any attempt to define a sharp boundary in tidal level at HMS is confounded by the effect of wave action, which tends to drive the effective tide level higher. Because littorine snails are content to forage on rocks that are merely wetted by wave splash, the effective tide level on a particular rock is tightly coupled to the wave exposure and offshore wave height at that site.

Despite the difficulties of delineating a boundary between the eulittoral zone and eulittoral fringe as defined by McMahon, there are patterns in predicted body temperature and foraging time that correspond to shore height at HMS. The maximum body temperature predicted at each shore height for the period 1999-2006 levels off above the 2 m shore height (Figure 2-11), and the percentage of time available for foraging varies substantially only below the 2 m mark (Figure 2-9). Because littorine snails can be important grazers of algal species, the amount of foraging time available for littorine snails may have important effects on the microalgal and macroalgal communities up and down the shore (Castenholz, 1961; Roberts and Hughes, 1980; Chow, 1987b, 1989; McQuaid, 1996b). The 2 m shore height corresponds to the upper portion of the zone where *L. keenae* and *L. scutulata* or *L. plena* overlap at HMS, with *L. keenae* becoming the dominant species higher on the shore (Bock and Johnson, 1967; Vermeij, 1973; Behrens Yamada, 1992). However, the transition from *L. plena* and *L. scutulata* to *L. keenae* on the high shore is not a result of temperature and desiccation limitation, but is due to competitive interactions between the species. Behrens Yamada (1992) demonstrated that *L. scutulata* survive when transplanted above its normal upper limit, as long as *L. keenae* is excluded. *L. keenae* is the

dominant competitor for food resources, and can survive on lower food supplies than *L. plena* or *L. scutulata*. The limited foraging time available at high shore heights, coupled with the lower settlement and growth rates of algae and diatom food sources, leaves *L. keenae* with a competitive advantage in mixed-species assemblages. While this division of the habitat between the species is perhaps ultimately tied to temperature and emersion time, the partitioning results from an indirect effect on a limiting food resource rather than a direct effect on the physiology of the littorine snails.

2.4.5 Shell size and shape

The allometry of shell growth makes direct scaling of the parameters used in the heat budget model difficult. As snails grow from juvenile to adult sizes, the shape of the shell changes, which alters the relationship between the Reynolds and Nusselt numbers for the shell. Therefore, the Reynolds - Nusselt relationship used to calculate heat transfer coefficients for convective heat exchange for one shell size cannot be used to calculate the heat transfer coefficients for a different sized shell. Additionally, changes in shell shape do not allow for simple scaling of the projected areas of a shell. Finally, as the animal grows in length, the area in contact with the substratum (both the foot and shell) may not scale as length squared. To demonstrate these difficulties, a group of 6 *L. keenae* shells ranging from 7.6 mm to 14.6 mm maximum shell length was collected from HMS. The shells were photographed to measure projected area using the same method described in Chapter 1. The scaling relationship between shell length and projected area was calculated for each orientation of the shell. The average scaling exponent (± 1 SD) was 1.84 (± 0.087), with a maximum value of 2.01 and a minimum value of 1.68 depending on the particular orientation of the shell. The same photographs were used to calculate the total surface area of each shell (see Chapter 1), which produced a scaling exponent of 1.83. The area of shell in contact with the substratum when the shell was sitting with the aperture down against the substratum had a scaling exponent of 1.11. Based on these scaling relationships, it would be difficult to make comparisons among different body sizes of snails without making

empirical measurements of all of the parameters outlined above, a time-consuming task that was not attempted here.

2.4.5.1 Size scaling using spheres

With these difficulties in mind, I elected to use spheres to explore the effect of increasing body (sphere) size on predicted temperatures. Because the surface area and projected areas of spheres scale with the diameter using known mathematical relationships, the effort to measure these variables is minimized. It was, however, still necessary to measure the heat transfer coefficients for each size of sphere in the wind tunnel in the same manner as the snail shells were measured. When a sphere is suspended in space, away from the ground or nearby obstructions, it has a consistent Nusselt-Reynolds number relationship across all sizes, but placing a sphere within a turbulent boundary layer of air flowing over a surface changes the Nusselt-Reynolds relationship (Mitchell, 1976). The manner in which wind speeds were measured in the wind tunnel, using a fixed anemometer height set 20 cm above the substratum in the free-stream flow, further complicates the measurement of the true Nusselt-Reynolds relationship, but allows for a standardized measurement protocol that can be compared directly with wind speeds measured in the field. The empirically measured relationship between the Nusselt number and Reynolds number for the various sizes of spheres in the preceding chapter showed that smaller spheres have higher heat transfer coefficients as wind speeds increase, though at slow wind speeds of 0.2 to 0.5 m s^{-1} heat transfer coefficients were within 2 – 10% of each other across the range of sphere sizes (Figure 2-15).

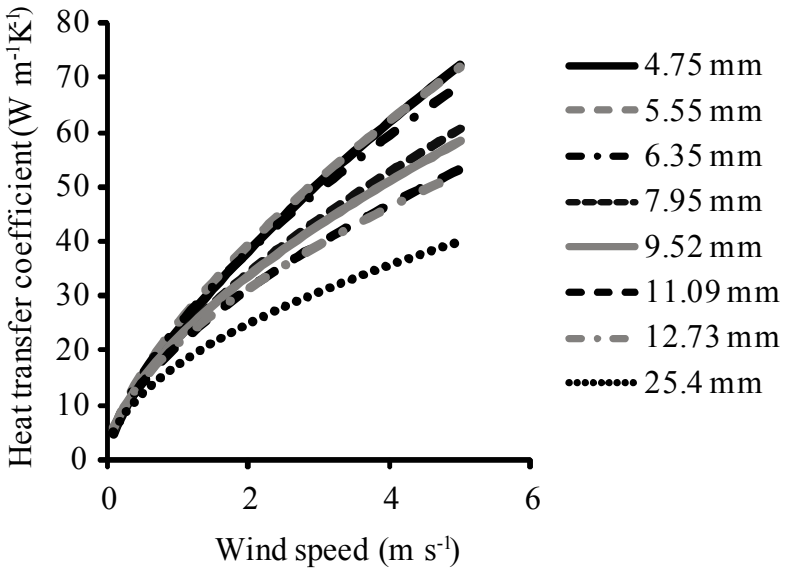

Figure 2-15. Heat transfer coefficients for spheres, calculated based on the Nusselt-Reynolds number relationships given in Chapter 1, for air at 25°C. At high wind speeds, the heat transfer coefficients of larger spheres are lower than those for smaller spheres. Sphere diameters are noted in the legend.

Results from the heat budget model using simple spheres indicate that the effect of increasing size on sphere temperature should be fairly small, typically less than 0.5°C (Figure 2-13, Table 2-8). Based on these data, I hypothesize that although real snails exhibit allometric changes in shell shape and contact area with increasing size, the effect of increasing shell size between juvenile and adult snails of any of the species studied here should result in minimal differences in temperatures achieved on hot days and resultant levels of thermal stress. It should be reiterated that this version of the model assumes that the modeled objects reach thermal equilibrium quickly, so the effect of thermal inertia is ignored. For these small snails this assumption should hold, but for larger body sizes the thermal inertia of the body may begin to affect the heating rate and maximum temperatures achieved. Helmuth (1998) used a heat-budget model for *Mytilus* mussels to predict that larger 10 cm length mussels should reach higher temperatures than small 5 cm length mussels under constant environmental conditions. The form of the high temperature exposure in the field matters though, as Helmuth (2002) found that smaller 4.2 cm mussel mimics would reach higher temperatures than larger 7.7 cm and 13.5 cm mimics during days with fast heating rates, while the larger

7.7 cm and 13.5 cm mussel mimics hit higher peak temperatures during slow, prolonged heating in the field (but see Jost and Helmuth, 2007, for a case where mussel size did not affect body temperature).

While the modeled spheres typically stayed cooler than the equivalently-sized snail shell, under certain conditions the snails were able to achieve temperatures equivalent to the spheres. Based on the shape of a shell, a snail with the shell oriented with the aperture down on the substratum and foot withdrawn has a larger contact area on the rock and smaller surface area exposed to the air than a sphere. While only a small portion of the shell may be contacting the rock, the entire area of the aperture of the shell may be occluded by the rock, minimizing air flow to that surface of the shell and operculum. The area of the shell held against the substratum can comprise a large portion of the total surface area of the shell (10-20%), and consequently decreases the convective heat flux relative to a sphere. As convective heat flux is the primary avenue by which snails shed heat during warm days, this reduction in convection results in higher body temperatures. The projected area of a shell sitting down on the substratum during the middle of the day, when the sun is high in the sky and shortwave radiation is at its peak, will often be equal to or larger than the projected area of a sphere sharing the same characteristic dimensions. The larger projected area increases the heat flux into the shell, helping to increase the temperature of the shell relative to that of the sphere.

The situation changes when a snail lifts the shell up away from the substratum. In this case, the shell maintains a small contact area with the substratum, minimizing conduction compared to the sphere. The orientation of the shell also helps increase convective heat loss, and minimizes absorption of shortwave radiation during the warmest time of the day (assuming the snail is on a horizontal or nearly-horizontal surface). Each species of littorine stayed much closer to the temperature of the equivalently-sized sphere during warm periods, and in some cases was the same temperature or cooler than the sphere (Figure 2-14).

Distributional patterns of different sized snail species or different life stages of littorine snails along the vertical axis of intertidal shorelines have been hypothesized to be related to thermal stress in some instances. Vermeij (1973) described a general pattern for tropical littorines that high shore species tend to be smaller than species living lower on the shore. The pattern is attributed to the potential for smaller species to have a greater contribution of convective cooling relative to large species, helping keep body temperature down. Tropical species may be living closer to their thermal tolerance limits (Stillman and Somero, 2000), making the regulation of their body temperatures particularly important (Garrity, 1984; McQuaid and Scherman, 1988). However, the temperate species *L. keenae*, *L. scutulata*, and *L. scutulata* reverse the pattern of the tropical species, with the largest species, *L. keenae* living at the highest reaches of the intertidal zone. In the case of these temperate species, thermal stress may be relatively less important than the ability to survive prolonged emersion and desiccation, making larger body sizes advantageous. Scaling relationships demonstrate that the larger shells hold a larger volume of water while the size of the aperture of the shell (which governs evaporative water loss) grows more slowly (Vermeij, 1972). Under the same conditions, a larger snail should lose a smaller percentage of its total body water, enabling survival for longer periods (Behrens Yamada, 1992).

2.4.5.2 Consider a spherical snail

O'Connor and Spotila (1992), referencing the earlier work of Mitchell (1976), asked us to "consider a spherical lizard" as an entry point into developing heat-budget models for animals. Mitchell (1976) reviewed much of the existing heat-budget work up to that time and demonstrated that for a wide array of organisms with a wide variety of shapes, the heat transfer coefficient of the animal, which is so important for balancing incoming heat from shortwave radiation, could be reasonably approximated by using heat transfer coefficients based on a simple sphere. In the case of littorine snails, this approximation seems especially appropriate (Figure 2-16). Indeed, using the heat transfer coefficients derived from spheres in the wind tunnel produced temperature predictions that were within 1.5 to 2.3°C of the snail predictions on

average, and even closer for snails elevated up off the substratum (Figure 2-14). Certainly as a first attempt, it would be appropriate to use data from spheres to make approximations of snail body temperatures without having to undertake the time-consuming measurements of the heat-transfer coefficient, surface area, and projected areas. Where greater accuracy is desired, these shell characteristics should still be measured, but for some questions and conditions the simpler spherical model would be sufficient.

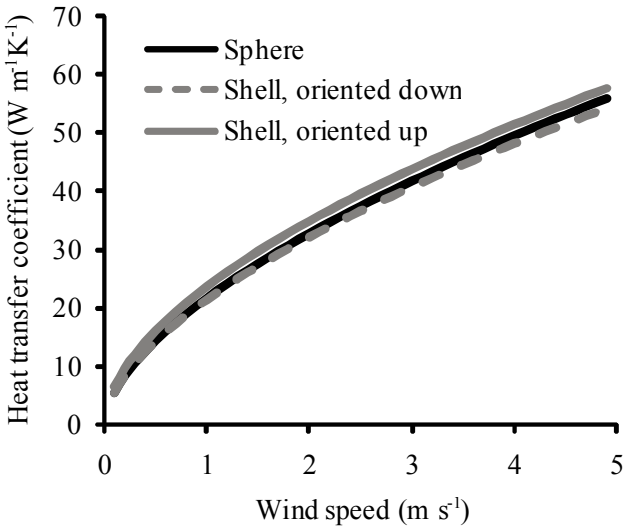

Figure 2-16. *Littorina keenae*. Representative predicted heat transfer coefficients for a snail and sphere sharing the same characteristic length. Heat transfer coefficients were calculated based on the Nusselt-Reynolds number relationships given for spheres and *L. keenae* in Chapter 1. Values are given for the snail shell sitting down on the substratum or oriented up away from the substratum. All calculations are for an air temperature of 25°C.

2.4.6 Lethal temperatures and beyond

Based on the results presented here, and the known habits of the species described, temperature stress alone would be unlikely to cause frequent mortality at HMS for the littorine snail species in this study. The species living lowest on the shore, *Littorina sitkana*, also shows a strong preference for congregating in cracks and crevices or under macroalgae, habitats which remain moist and shaded for longer periods than open rock faces (Behrens, 1972; Behrens Yamada, 1992). *L. sitkana* should be able to

avoid severe thermal stress by its choice of microhabitats. The species living highest on the shore, *L. keenae,* can often be found in congregations of a great number of individuals, and in crevices (Bock and Johnson, 1967), conditions that should reduce temperature and desiccation stress. However, *L. keenae*, *L. scutulata*, and *L. plena* can often be found out on the open faces of rocks, exposed to more severe temperature and desiccation stress.

The majority of tests of littorine thermal tolerance carried out to date exposed the animals to high temperatures while submerged (Evans, 1948; Fraenkel, 1961; Fraenkel, 1968; Stirling, 1982; Clarke *et al.*, 2000a; Clarke *et al.*, 2000b). This protocol likely produces different values for the lethal temperature than would tests that more closely mimic field conditions (see Chapter 3 for an example with a limpet species) so we lack an exact measure of the thermal tolerance of most high shore littorine snails.

Somero (2002) provides the only published data for the thermal tolerance of *L. keenae* and *L. scutulata,* using snails from HMS. To determine the lethal temperature at which 50% of the snails died (LT50), snails were submerged in water at fixed temperatures for 3 hr, followed by a 45 min recovery in cold ocean water. The LT50 for *L. keenae* was 47°C and *L. scutulata* had a LT50 of 45°C under this exposure regime. Miller and Sorte (unpublished data) carried out thermotolerance experiments in air for *L. scutulata* and *L. plena* from Friday Harbor, WA. The snails were exposed to a constant high temperature for 3 hr in air, and allowed a 2 hr recovery in ocean-temperature water. Under these conditions, both *L. scutulata* and *L. plena* had an LT50 of 41°C.

The African species, *E. natalensis,* has a higher thermotolerance than any of the Northeast Pacific *Littorina* species. Stirling (1982) placed *E. natalensis* in seawater and heated the snails at 6°C hr^{-1} to various target temperatures and judged both responsiveness and overall survival. Snails entered heat coma and became unresponsive at 46°C, while the LT50 was 53.5°C.

The thermotolerance data collected using the various methodologies all indicate that lethal temperatures would be extremely rare at HMS for any of the species used in the

heat-budget model. Lethal temperatures would only be approached if the snails were to leave the foot extended throughout the low tide. As soon as snails withdraw the foot into the shell, the maximum temperatures achieved during the 7 yr weather data set for HMS would likely be low enough to avoid thermally-induced mortality altogether. The highest temperature achieved by *L. keenae* with the foot withdrawn was 39°C, a full 8°C lower than the LT50 determined in water. *L. scutulata* and *L. plena* were not predicted to exceed 38.8°C and 38.4°C respectively, temperatures that were still at least 2.2°C lower than the LT50 measured in air.

The lack of lethal temperature exposures at HMS should not be taken to mean that littorine snails should never encounter lethal temperatures at other field sites. The Monterey peninsula is considered to be a 'cold' site relative to many other sites along the west coast of North America (Helmuth *et al.*, 2002). The influence of the local terrain and cool ocean temperatures leads to many foggy summer days, and the timing of the tides generally results in low tides occurring in the morning during the warmest times of the year. This combination of factors makes hot days in Monterey a comparative rarity. *Littorina* populations to the north in Oregon and Washington or to the south in southern California and Baja California may experience lethal temperatures more frequently by virtue of the particular combinations of local weather conditions and timing of the tides.

Of course, high temperatures do not act alone to stress snails at any site. Desiccation can have a major impact on the survival of littorines, especially littorines living high enough on the shore that they are left emersed for several days. The heat-budget model used here does not take evaporation into account when determining body temperatures, but body temperature will have an influence on the rate of evaporation during aerial emersion due to the relationship of saturation vapor density in air with temperature (see Eqn. (5) in Chapter 1).

Littorine snails are capable of withstanding prolonged desiccation and can survive losing more than 20 to 40% of their wet mass to evaporation over the course of several days (Britton, 1992; Britton, 1993). Hewatt (1937) reported that *L. keenae* from HMS

survived more than two months of continuous emersion on the desk in his office. Indeed, my own accidental "experiments" on my office desk (where the air temperature is between 22 and 25°C and relative humidity typically ranges between 40 and 60%) yielded 2 out of 10 *L. keenae* that survived continuous emersion from October 4 to December 6, 2007. Despite the general ability of the littorines to withstand such desiccation levels, mortality from desiccation and high temperatures can occur in the field. Chow (1989) reported mortality among *L. scutulata* and *L. plena* on the high shore at Bodega Head, CA, following a prolonged 10-day emersion with warm air temperatures and steady breezes.

Unfortunately, there is a paucity of data on the rates of evaporation in these littorine species under field conditions, and no rigorous tests of the LD50 for desiccation in the species studied here. Certainly each of the species should be able to withstand the loss of 20-30% of the total body water over the course of 2-3 days and recover fully when re-immersed in seawater (Bush, 1964). Better data on survival under various temperature and desiccation stress levels, coupled with a modified heat budget model that could account for evaporation, would allow for more robust predictions of mortality events in the field.

2.4.7 Metabolic responses to temperature

I now turn to potential effects of temperature on other aspects of the physiology of these snails. Temperature affects more than just the survival of a snail under acute exposures or the rate of desiccation over long emersions. Temperature also impacts the rate of metabolism of a snail, which will have cascading effects on growth and reproduction rates.

Changes in body temperature induce changes in the rate of metabolism, as temperature affects the rate of chemical reactions taking place in cells (Newell, 1976; Hochachka and Somero, 2002). In the most basic sense, as temperature rises, chemical reactions can proceed at a faster rate due to an increase in the number of molecules reaching the activation energy necessary to carry out a reaction. These changes in reaction rates propagate through metabolic pathways, leading to faster processing of substrates and

increases in respiration. Uncontrolled changes in reaction rates can be detrimental to an organism, so many physiological processes show some measure of temperature compensation.

Variation in biological rates as a function of temperature is often couched in the framework of the "Q_{10}" relationship (Hochachka and Somero, 2002). Briefly, the Q_{10} relationship states that as an organism goes through a temperature change, the ratio of some rate (e.g. respiration) at the two temperatures will vary according to the relationship:

$$Q_{10} = \left(\frac{R_2}{R_1}\right)^{\frac{10}{T_2 - T_1}} \tag{38}$$

where R_1 and R_2 are the rates at temperatures T_1 and T_2, respectively. Many physiological processes have a Q_{10} value of around 2, so that a temperature increase of 10°C results in a doubling of the rate of the process (Newell, 1969; Randall *et al.*, 1997). If the Q_{10} of a process is known for a given temperature interval, Eqn. (38) can be rearranged so that the rate R_2 can be calculated based on the initial rate R_1 and the temperature change of interest:

$$R_2 = R_1 \left(Q_{10}^{\frac{T_2 - T_1}{10}}\right). \tag{39}$$

While a consistent value for Q_{10} over the relevant range of biological temperatures would make calculations of the effect of temperature on the physiology of an organism simple, nature is rarely so straightforward. The value of $Q_{10} = 2$ listed above is an extremely generalized value, and there are myriad cases where the true Q_{10} of a physiological process varies widely through the range of temperatures an organism might experience (Newell, 1969, 1976; McMahon and Russell-Hunter, 1977; Sokolova *et al.*, 2000).

A particularly relevant example comes from studies on the *Littorina* species of the northern Atlantic Ocean. A number of studies have examined the respiration rate of *Littorina* species across a range of body temperatures that might be experienced in the

field (Newell and Pye, 1970b; Pye and Newell, 1973; McMahon and Russell-Hunter, 1977; Sokolova and Pörtner, 2001, 2003). Rather than having consistent Q_{10} values for respiration, the three species used in these studies, *Littorina saxatilis, L. obtusata,* and *L. littorea* all show variation in Q_{10} values as temperature rises, both for active snails submerged in water and for inactive snails exposed in air. Of particular note is the fact that all three species can hold the respiration rate fairly steady ($Q_{10} \sim 1$) across certain ranges of body temperatures when inactive. However, at other temperature ranges, the Q_{10} for respiration can be as high as 3.5. For example, in *L. littorea*, the aerial respiration rate of inactive snails held steady between 20°C and 30°C ($Q_{10} = 1$), but over the temperature range of 30°C to 35°C the Q_{10} jumped up to 3.5 (McMahon and Russell-Hunter, 1977). Above 35°C, the respiration rate of *L. littorea* dropped ($Q_{10} < 1$), presumably due to the animals beginning to enter heat coma. However, for the aerial respiration rates of inactive snails listed (McMahon and Russell-Hunter, 1977), the overall Q_{10} for respiration between the temperatures of 5°C and 35°C was around 2 (*L. saxatilis* = 2.6, *L. obtusata* = 1.9, *L. littorea* = 2.4).

The temperatures at which these changes in the respiration rate and Q_{10} take place vary among species (McMahon and Russell-Hunter, 1977), and within species depending on locality (Sokolova and Pörtner, 2003), body size (Newell and Pye, 1971), or time of year (Newell, 1969; Newell and Pye, 1970a; Newell, 1973). Based on this variation of Q_{10} with temperature, and the fact that respiration data or other measures of Q_{10} for physiological rates do not exist for the Northeastern Pacific *Littorina*, I will use the data from north Atlantic species as a rough guideline to make comparisons of the potential effects of temperature differences on the different morphologies or behaviors of the species discussed in this chapter.

While a high metabolic rate could be considered a benefit to an ectothermic snail attempting to process food for growth and reproduction, the benefit will only accrue when the snail is able to consume food and respire normally, as it can when the rocks are wetted and it is able to graze. On the other hand, when littorines are driven to withdraw inside the shell at low tide, the need to conserve body water and energy

stores until the next submersion, which may be days away, overrides the benefit of higher metabolic rates brought on by high temperatures. As a result, a high metabolic rate during aerial emersion could be considered a detriment to the overall survival of the snail if it increases the use of energy stores and drives production of metabolic end products that cannot be removed from the shell until re-immersion (Newell, 1976).

With these considerations in mind, I have plotted the effects of various values of Q_{10} for respiration rates of *Littorina* for the temperature range of 30°C to 40°C (Figure 2-17). From the data of McMahon and Russell-Hunter, a respiration rate of 1 µl O_2 hr^{-1} g^{-1} at 30°C is taken as a rough average (McMahon and Russell-Hunter, 1977). For a snail that can undergo metabolic depression at this temperature range (Q_{10} = 1), there is no change in the respiration rate, which can be beneficial if the goal is to minimize energy expenditures until the next submersion cycle when feeding can resume (Newell, 1976; Branch, 1978). For Q_{10} values above 1.0, the gradual increase in temperature from 30°C to 40°C results in an ever-increasing respiration rate that could be detrimental to the snail.

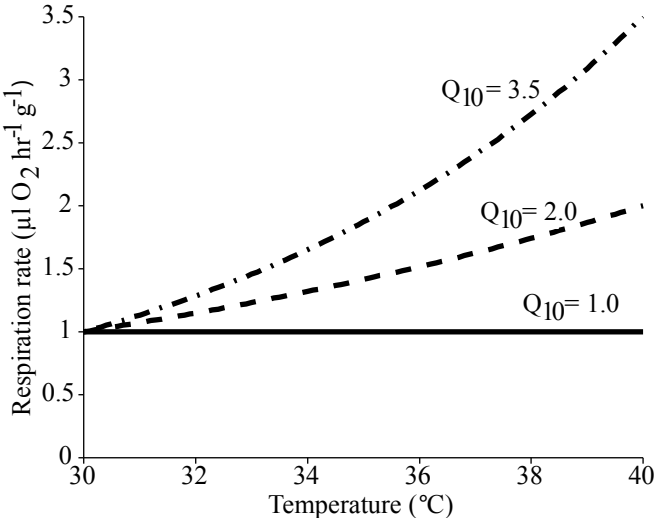

Figure 2-17. Illustration of the effect of Q_{10} value on respiration rate as temperature rises. The aerial respiration rate of 1.0 µl O_2 hr^{-1} g^{-1} (dry tissue weight) at 30°C is an approximation based on values from McMahon and Russell-Hunter (1977) for Atlantic *Littorina* species.

Building on the basic relationships expressed in Figure 2-17, let us return to the temperature predictions for the *Littorina* species described earlier. Using the Q_{10} values presented above, the relative respiration rates for different snails can be estimated based on differences in body temperature under equivalent environmental conditions.

Comparisons were carried out using predicted temperature data for modeled shells over the seven year extent of the weather data set. Respiration calculations were made separately for snails during periods when the foot was withdrawn into the shell and when snails had the foot out and were actively grazing. The respiration rate at each time point for each of the three Q_{10} values was calculated using Eqn. (39). The values of T_1 and R_1 used for the calculations varied depending on whether the snail had the foot out, in which case $T_1 = 10°C$ and $R_1 = 0.2$ µl O_2 hr^{-1} g^{-1}, or if the foot was withdrawn, so that $T_1 = 30°C$ and $R_1 = 1.0$ µl O_2 hr^{-1} g^{-1}. The cumulative "respiration" during the dataset for each value of Q_{10} is then summed and expressed relative to a Q_{10} of 1, for which there should be no difference between shells modeled under the same conditions.

When comparing the effects of shell color, the change in respiration rate resulting from differences in body temperature was relatively small (Table 2-11). During periods when the foot was extended and the snail could actively graze, the difference in cumulative respiration rate between the black and white morphs of *L. keenae* was predicted to be less than 1% for the warmer black-colored snail. This further reinforces the conclusion that there is little evidence that dark shell coloration would provide any meaningful benefit in terms of raising body temperature and metabolism during cold periods. When the snails were withdrawn into the shell, a time when higher respiration rates could be detrimental to the snail, black snails were predicted to have respiration rates up to 2.6% higher than the cooler white-colored morph. For time periods when minimizing respiration would be advantageous, lighter shell color might have a beneficial effect, but this benefit is small compared to the temperature change and subsequent change in respiration afforded by lifting the shell up away from the

substratum. The choice to elevate the shell up off the substratum had a much larger effect on body temperature and the resulting respiration rates, so that snails remaining down on the rock got hotter and could have respiration rates up to 16% higher than snails lifting the shell away from the rock (Table 2-11).

Table 2-11. *Littorina keenae*. Percentage increase in respiration for two values of Q_{10} using predicted body temperatures for the period 1999-2006. Data for each comparison represent all time periods when the foot was either withdrawn into the shell or extended for grazing, as denoted in each column. Shells were modeled on a horizontal platform 2.0 m above MLLW on a wave-protected shore.

	Shell color Black vs. white		Shell position Down vs. up
	Foot extended	Foot withdrawn	Foot withdrawn
$Q_{10} = 2$	0.04	1.11	8.71
$Q_{10} = 3.5$	0.09	2.58	16.65

If littorine snails cannot stabilize or depress metabolic rates when withdrawn into the shell at high temperatures, then the differences in body temperature created by various morphologies or behaviors will result in higher metabolic rates for hotter animals. This will happen during intervals where a higher metabolic rate and greater usage of energy stores would be disadvantageous to the animal. Conversely, if the species studied here are capable of depressing the metabolic rate while withdrawn into the shell, the Q_{10} effect on metabolic rates can be reduced or even reversed at high temperatures (i.e. $Q_{10} < 1.0$), removing the potential detriment to the energy consumption of the snail. Clearly there remains a substantial amount of work to be done to be able to adequately resolve the importance of the temperature shifts associated with different morphologies and behaviors on the overall metabolic state of high shore littorine snails during high temperatures and prolonged desiccation stress.

2.4.8 Conclusions

The heat-budget model employed for five species of littorine snails demonstrates the potential importance of several characteristics of morphology and behavior. Withdrawing the foot into the shell and gluing the lip of the shell to the substratum results in substantial reductions in the predicted body temperature for all species. The

additional step of lifting the shell away from the substratum further reduces predicted body temperatures approximately 1 – 2°C. The shore height of a snail also results in major differences in the time available for foraging, as well as reductions in the frequency and intensity of high temperature exposures for snails living lower on the shore.

On the other hand, the role of shell color in modulating body temperature is quite minimal, resulting in temperature differences between black and white shells of less than 1°C, and even smaller differences between black and brown shells.

Based on the limited data for lethal temperatures of the five species studied here (Stirling, 1982; Somero, 2002), the temperatures at Hopkins Marine Station between 1999 and 2006 were predicted to rarely be stressful. Temperature alone is not predicted to be a substantial threat for littorine snails living at HMS.

The rarity of lethal temperatures at HMS does not remove the threat of mortality however, primarily due to the additional stress of desiccation. The shore height and exposure of a particular microhabitat could have significant impacts on the extent of desiccation that littorine snails undergo. Future studies should strive to better understand the interplay of temperature and desiccation rate on the survival of these littorine snails. The role of food supply has also not been addressed here. While littorine snails might be quite capable of surviving most conditions at HMS, their primary food supply of microalgae might be more susceptible to heat or desiccation than the snails, thereby restricting the vertical extent of the species that must graze on microalgae to survive (Behrens, 1974; Chow, 1987b; Behrens Yamada, 1992).

The data presented here provide insight into the role of evolved morphologies and behaviors for determining body temperature. The heat-budget model performs admirably for addressing those questions. The future role of the heat-budget model presented here relies on the availability of better physiological data on the thermal and desiccation tolerance of each of the species described. With realistic projections of the conditions that littorine snails can withstand, it will be possible to make more accurate

projections about the frequency of lethal or sub-lethal stress events, all of which will impact the demography and ecology of littorine snails.

Chapter 3

The role of thermal stress in limiting the distribution of the limpet, *Lottia gigantea*

3.1 Introduction

Identifying the factors that set the limits of distributions of organisms is one of the central goals in ecology. Across all ecosystems, organism abundances wax and wane due to a variety of influences, and knowledge of the relative importance of these factors is useful in formulating generalizations about what forces shape communities. Knowledge about what sets species distribution limits also has uses in formulating management strategies, setting aside protected areas, preserving biodiversity, and predicting the potential effects of climate change. For both basic and applied ecological studies, having a firm grasp on the processes that set species distributions is vital. The processes or factors that set species distributions can be broken down into four broad categories: (1) predation or herbivory, (2) competition for resources, (3) dispersal, and (4) the influence of the abiotic environment.

Examples of all four of these factors abound in the literature. The lower limits of mussel beds on the Pacific coast of North America are typically limited by the predatory activities of *Pisaster* seastars (Paine, 1966, 1974), while the lower limits of barnacle distributions may be limited by predatory whelks(Connell, 1961; Dayton, 1971). Grazing by herbivores can limit the distribution of algae and plants (Tansley and Adamson, 1925; Jones, 1948; Castenholz, 1961; Underwood, 1980). Competition for space, light, food, or other resources can set limits to where certain species can survive (Muller, 1966; Koplin and Hoffmann, 1968; Connell, 1975; Luken *et al.*, 1997; Clark *et al.*, 2004; Bertness *et al.*, 2006). The dispersal abilities of individual species (or lack thereof) can limit expansion into what might be favorable habitat (Behrens Yamada, 1977; Gaylord and Gaines, 2000; Zacherl *et al.*, 2003). Perhaps the

most obvious examples of this process come from the large number of invasive species that humans have introduced around the world (Sax and Brown, 2000; Carlton and Geller, 1993; Carlton, 1996; Kado, 2003; Branch and Steffani, 2004; Xavier *et al.*, 2007). Lastly, the abiotic environment can set limits on the ranges of species through a variety of means such as limiting resources, extreme temperatures, or disturbance caused by high winds or water flows (Broekhuysen, 1940; Connell, 1972; Kelsch, 1994; McAuliffe, 1994; Barry *et al.*, 1995; Whiles and Wallace, 1995; Porter *et al.*, 2002; Somero, 2002; Zacherl *et al.*, 2003; Bertness *et al.*, 2006).

The disciplines of biomechanics and physiology offer techniques to make possible quantitative measurements of organismal performance in the face of environmental stresses. If we can demonstrate proximal mechanisms of organismal failure, we can test those mechanisms and create models to predict the frequency and severity of environmental stresses that could limit the distribution of a species. In this chapter I describe a series of experiments designed to combine a bio-physical model of body temperature with physiological measurements of performance and survival under stressful environmental conditions, with the ultimate goal of using the model to test the hypothesis that environmentally-induced physiological stresses limit the distribution of species. Biophysical models for predicting body temperatures of organisms (heat-budget models) have been used in the terrestrial realm for more than three decades (Bartlett and Gates, 1967), and the outputs have been used to explain behaviors of individual organisms (Porter and Gates, 1969; Porter *et al.*, 1973) as well as broader distributional patterns of species (Heller and Gates, 1971), and potential effects of climate change (Porter *et al.*, 2002). Around the same time that heat-budget models began to appear in terrestrial studies, Vermeij (1973) and Johnson (1975) used certain parts of the heat-budget model to explain the relative importance of aspects of intertidal snail morphology and behavior, but operational heat budget models for intertidal organisms did not appear until much later. Simplified models that relied on correlations between measured body temperature and a subset of environmental variables were used briefly (Elvin, 1976; Elvin and Gonor, 1979), but it is difficult to use these methods to make generalized models that could function in different habitats

or conditions (Bakken, 1992). It was not until the 1990's that the methods described by terrestrial researchers (Gallucci, 1973; Porter *et al.*, 1973) were applied to intertidal organisms such as algae (Bell, 1995) and mussels (Helmuth, 1998, 1999).

The rocky intertidal zone is an obvious study system in which to address questions of physiological limitations in communities, primarily due to the steep environmental gradients that exist along both the horizontal and vertical axes of the shoreline. Along these axes we can find gradients in wave exposure and effective submersion time, both of which contribute to influencing the body temperature of organisms. Intertidal organisms are primarily of marine origin, and require occasional wetting or submersion in order to survive. When the tide drops and waves recede, the intertidal zone transforms into a terrestrial habitat, with the temperature-buffering capacity of the ocean no longer available to moderate the thermal environment and desiccation becoming a concern after prolonged exposure (Newell, 1964). The most extreme temperatures in the intertidal habitat are usually recorded during aerial exposure, when temperatures may dip towards freezing or shoot towards extreme highs as the effects of solar radiation, air temperature, and wind combine to produce large temperature swings relative to the ocean temperature (Grainger, 1969; Helmuth, 1999).

Small changes in vertical or horizontal position on the shore can potentially lead to large changes in the severity of temperature swings (Johnson, 1975; Helmuth and Hofmann, 2001; Harley and Helmuth, 2003). Along the vertical axis, shifts up and down the shore can change the duration of emersion due to tidal fluctuations and wave splash. Early research sought to define "critical tidal levels" that would separate intertidal communities based on the time spent emersed in air (Colman, 1933; Doty, 1946; Evans, 1947; Shotwell, 1950; Southward, 1958). Emersion consequently affects the thermal and desiccation stress experienced by organisms at each level. While the concept of "critical tidal levels" was confounded by the variability induced by waves and weather (Johannesson, 1989), along with inaccurate calculations (Underwood, 1978), intertidal ecologists recognize that there is a continuum of emersion time and environmental severity as one moves up the shore (Harley and Helmuth, 2003; Finke

et al., 2007). On the horizontal axis, variation in the severity of the environment occurs at many scales. Historically, whole sites have been delineated as "wave-exposed" or "wave-protected", and the potential thermal stress at a site was often tied to its latitude and exposure to ocean waves. But even these simple divisions are complicated by processes occurring at smaller scales (Helmuth *et al.*, 2002). Within a site, small-scale refuges on the shore, such as crevices, algal canopies, or slopes facing away from the sun, have long been recognized as important factors influencing the distributions of organisms (Kensler, 1967; Behrens, 1972; Menge, 1978; Raffaelli and Hughes, 1978; Atkinson and Newbury, 1984; Gray and Hodgson, 2004; Denny *et al.*, 2004).

Studies of intertidal organisms have demonstrated that there can be vertical limits above which some species cannot survive, typically attributed to extreme temperatures and desiccation (Connell, 1961; Dayton, 1971; Foster, 1971; Paine, 1974; Stillman and Somero, 2002; Stenseng *et al.*, 2005; Bertness *et al.,* 2006; Bazterrica *et al.,* 2007). Rare high temperature events have been implicated in mortality events at a number of intertidal sites (Suchanek, 1978; Tsuchiya, 1983; Williams and Morritt, 1995). Additionally, studies on patterns of growth and reproductive effort along shore height gradients have shown that high shore organisms often grow slower and produce fewer gametes than conspecifics from lower on the shore (Blanchette *et al.*, 2007; Menge *et al.*, 2007; but see Sutherland, 1970). We have numerous examples from the intertidal zone demonstrating that life on the rocky seashore can be physically stressful for the organisms settling there.

The focus of this chapter will be the large intertidal limpet *Lottia gigantea* (Sowerby 1834) (Figure 3-1). This limpet, which commonly exceeds 50 mm in length, with some individuals exceeding 100 mm, has a northern population limit around Crescent City, CA (Fenberg, 2008) and a southern limit in Baja California (Morris *et al.*, 1980). In the range where *L. gigantea* is still abundant, primarily in areas protected from human harvesting (Pombo and Escofet, 1996; Fenberg and Roy, 2007), it is a co-dominant competitor for primary space with the sea mussel *Mytilus californianus*

(Conrad, 1837). Individuals of *L. gigantea* may be long-lived, commonly 5 to 10 yr, with some individuals potentially living up to 20 yr (Fenberg, 2008).

Figure 3-1. A *Lottia gigantea* grazing on its territory in the mid-intertidal zone at Hopkins Marine Station. The limpet is 60 mm long.

Large *L. gigantea* are territorial, creating cleared spaces on the rock from which they exclude conspecifics, neighboring mussels, macroalgae, and other limpet species (Stimson, 1970, 1973). They feed on a mat of microalgae that they graze while the rocks are wetted by the splash of waves at high tide (Connor and Quinn, 1984; Connor, 1986). In the mid intertidal zone at Hopkins Marine Station (HMS), *L. gigantea* is a conspicuous space-holder, especially on vertical or angled substratum on wave-exposed portions of the shore (Denny and Blanchette, 2000). Because of its importance in the mid-intertidal community, having robust predictive models and performance data for *L. gigantea* can be beneficial for making broader predictions about the developmental trajectory of the mid-intertidal community as a whole, especially following extreme abiotic conditions (Helmuth *et al.*, 2006).

To make these sorts of ecological predictions, we need information about the physiological limits of *L. gigantea*. While field sampling of body temperatures and

physiological stress markers can be useful for making these sorts of predictions, the very fact that stressful long, hot, dry, low tide periods are rare events makes gathering these sorts of data in the field extremely difficult. Given the amount of effort, and luck, required for collecting data in the field on limpet responses to high temperature and desiccation stress, it was necessary to adapt a variety of modeling and laboratory methods to address questions about how the abiotic environment limits the distribution of *L. gigantea*.

This work benefits from the existence of a heat budget model for *L. gigantea* developed by Denny and Harley (2006). The model, similar to the model described for littorine snails in the previous chapters, allows the user to make predictions of the body temperature of a limpet using weather and sea state data. The interpretation of these model results relies on the existence of physiological performance data for the focal species, which has been lacking for *L. gigantea* to date. In this chapter, I address several questions about the physiology of *L. gigantea*: how does the form and duration of exposure to high temperatures affect the physiological performance of *L. gigantea*? What is the response of *L. gigantea* to realistic stress regimes? Does the method by which animals are stressed in the laboratory result in potentially misleading conclusions about performance in the field? With knowledge of how *L. gigantea* might perform under stressful conditions in the field, I return to the heat budget model to incorporate these data and ask two further questions. How does the measured physiological performance of *L. gigantea* correspond with predicted stress events in the field? Is the upper limit of *L. gigantea* in the field potentially set by environmentally imposed physiological stresses?

3.2 Methods

3.2.1 Collections

All *Lottia gigantea* used in these experiments were collected from north and north-east facing vertical or near-vertical walls in the intertidal zone at Hopkins Marine Station

(36° 37.3' N, 121° 54.25'W). Collections were made in the winter months between December and March during 2006 and 2007. Limpets were removed from the substratum by forcing the blunted edge of a flexible knife under one edge of the shell and foot and prying slowly upwards. Ideally the knife would dig into the algal crust or friable rock surface rather than cutting the organism. If the removal process resulted in any visible damage to the limpet's foot or shell, the organism was discarded. Preliminary tests demonstrated that injured limpets subsequently failed to fully adhere to the substratum in aquaria, while healthy limpets adhered strongly to their new substratum and crawled and grazed normally.

Prior to all experiments, *L. gigantea* were held in an outdoor seawater table for a minimum of five days. High shore *Lottia* species typically respond poorly to being submerged constantly, so I devised a simple system to spray the limpets at intervals. A lawn sprinkler solenoid controlled the spray of seawater over the water table. The solenoid was activated for three seconds to spray water over the limpets, and shut off for ten seconds in between sprayings. This protocol was meant to mimic the periodicity of ocean waves, and allowed the limpets to be submerged for a few seconds as the water slowly drained away after each spray. The entire spray cycle was further augmented with a simple "tidal" cycle which shut off the supply of water altogether for a six hour period, followed by a six hour cycle of spraying. Limpets grazed on a film of algae and diatoms that grew on the ceramic tiles placed in the bottom of the seawater table. This holding arrangement was sufficient to keep limpets alive for more than six months. In addition to *L. gigantea*, the seawater spray table was used to hold *L. austrodigitalis* (Murphy, 1978), *L. digitalis* (Rathke, 1833), *L. scabra* (Gould, 1846), *L. scutum* (Rathke, 1833), *L. limatula* (Carpenter, 1864), and *L. pelta* (Rathke, 1833). Of these species, *L. austrodigitalis* and *L. scabra* are most similar to *L. gigantea* in that they react poorly to being held fully submerged for long periods, with seemingly healthy, uninjured limpets dying after a few days of submersion in a typical aquarium.

The water temperature of seawater in the holding table was the same as the ambient seawater temperature off HMS, typically between 11 and 14°C. The outdoor aquaria were shaded from the sun, and air temperatures ranged between approximately 8 and 20°C.

3.2.2 Laboratory heat stress profiles

Heating rates and exposure regimes used in the laboratory experiments were chosen based on the results of the *L. gigantea* heat budget model of Denny and Harley (2006). The body temperature of a limpet sitting on a horizontal surface at a shore height of 2 m above Mean Lower Low Water (MLLW) was modeled using seven years of weather and sea data from HMS. All days where the limpet body temperature was predicted to rise above 30°C were recorded and examined. The fastest rate of temperature increase among those days was 10.75 °C hr^{-1}, with most of the temperature increase rates between 15°C and 30°C falling between 6 and 9°C hr^{-1} (Figure 3-2). A temperature rise rate of 8°C hr^{-1} was chosen as a value that would allow for realistic heating stress while keeping trial durations to a reasonable length. On hot days, air temperature rarely exceeded 30°C, so this was chosen as a maximum air temperature for the trials in which air temperature was independently controlled. Air temperature was raised at the same rate as the substratum temperature.

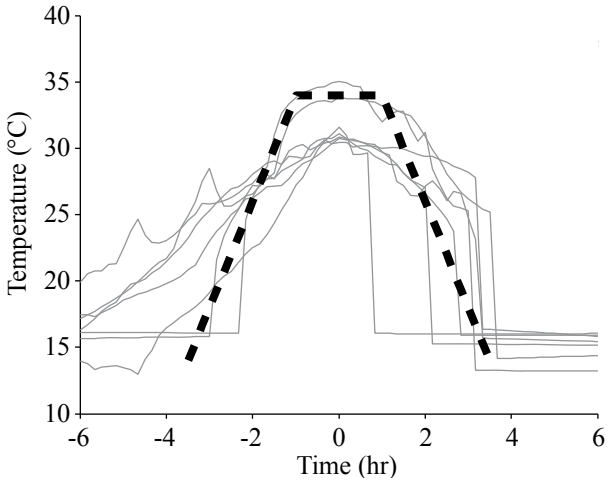

Figure 3-2. Predicted high temperature events for *Lottia gigantea* sitting on a horizontal platform at 2.0 m shore height on a wave-protected shore (gray lines). The dashed black line represents an experimental exposure regime used in the laboratory, with an 8°C hr^{-1} temperature rise and fall rate.

The heat budget model results further revealed that there were two common modes of heat exposure (Denny *et al.*, 2006). The first consisted of a rapid rise to a peak temperature followed by a rapid return to seawater temperature as the high tide returned, resulting in a relative short overall exposure. The second common exposure pattern was a rapid rise to a peak temperature followed by a period of time at the peak temperature, finally followed by a decrease back to ocean temperature. These longer temperature exposures generally lasted between 7 and 12 hr. A maximum exposure length of 7 hr was chosen for these experiments, and a short exposure time of 3.5 hr was chosen to recreate the short duration exposures (Figure 3-3). Each trial started with substratum and air temperatures of 14°C, close to seawater temperature. For the 3.5 hr trials, the temperature of the substratum and air were raised at 8°C hr^{-1} until the chosen limpet body temperature was achieved. Because the heating rate was fixed, trials with lower maximum temperatures reached the maximum temperature before 3.5 h had elapsed, at which point the air and substratum temperatures were held constant so that the limpet maintained the desired body temperature until the end of the 3.5 hr trial. The longer 7 hr trials mirrored the 3.5 hr trials, so that the limpets held the

desired body temperature until the appointed time, at which point the temperatures of the substratum and air were lowered to cool the limpet back to 14°C at a rate of 8°C hr^{-1} (Figure 3-3).

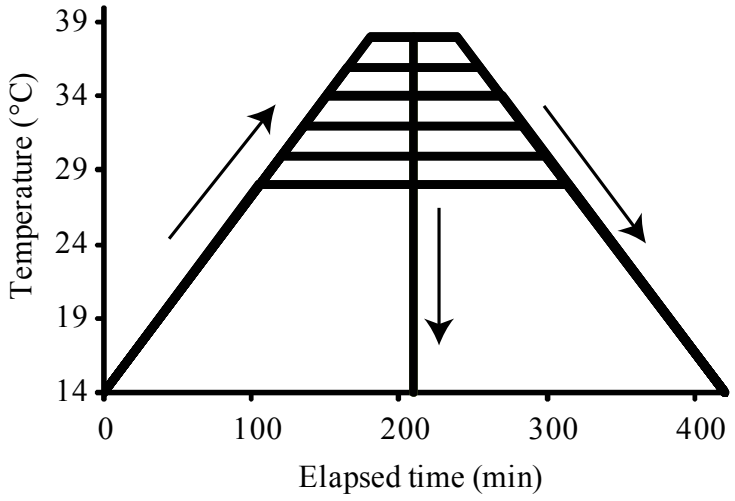

Figure 3-3. Illustration of the temperature profiles used in the environmental chamber. The temperature was raised at a rate of 8°C hr^{-1}. Once the temperature reached the target value, the temperature held steady for the remainder of the allotted time. The vertical line at 210 min denotes trials where limpets were returned immediately to seawater after 3.5 hr. The 7 hr trials finished with a 8°C hr^{-1} temperature drop back to the initial temperature.

3.2.3 Lethal temperatures

Lethal temperature distributions for *L. gigantea* were determined using environmental chambers in the laboratory. These chambers allowed for groups of limpets to be exposed to repeatable heating regimes with known environmental parameters. While the chambers simplified the control of conditions, they permitted the use of realistic rates of heating and duration of exposure.

3.2.3.1 High humidity tests

Many traditional tests of intertidal organism thermal tolerance either place the organism directly into already-hot water, or place them in closed volumes of air that are heated, resulting in high humidity within the chamber that limits evaporative

cooling and the effects of desiccation. For comparison to the low-humidity results described later, I carried out a series of high humidity thermal stress exposures using a closed chamber to maintain relative humidity values at or near 100%.

The chamber consisted of an acrylic box, filled with a quantity of seawater in the bottom, and an aluminum plate mounted above the water reservoir. The water in the lower section of the box was heated and cooled using a coiled copper heat exchanger hooked to a programmable water bath (Polystat 12108-30, Cole-Parmer, Vernon Hill, IL, USA). The water was stirred using a magnetic stir bar. The aluminum platform had a finned heat sink attached to its bottom that was partially submerged in the water in the lower chamber to enhance the conduction of heat from water to platform. The temperatures of the platform and the air in the chamber were monitored using thermocouples attached to an electronic datalogger (23X, Campbell Scientific, Logan, UT, USA). The entire heating chamber was placed in an insulating Styrofoam container to buffer the chamber from the temperature of the air in the room. The temperature of the chamber was raised and lowered at 8°C hr^{-1}, and all trials lasted for 7 hrs.

Limpets generally started off tightly adhered to the aluminum plate, but as temperatures increased some individuals lifted the shell from the substratum, a behavior previously described as "mushrooming" (Branch, 1978; Chelazzi *et al.*, 1999; Williams *et al.*, 2005). At the end of a trial, each limpet was assessed for signs of heat coma, which manifested as mushrooming behavior, retraction of the mantle, and poor attachment to the substratum (Figure 3-4). Limpets were then returned to the seawater holding table and immersed in seawater for recovery. Each limpet was surveyed 24 hr later to determine whether it was capable of firmly attaching to the substratum. Individuals which were easily picked off of the substratum were scored as "ecologically dead" in the manner of Wolcott (1973), and further observations beyond the 24 hr recovery period demonstrated that these individuals eventually died. Animals which could adhere firmly to the substratum after 24 hr were scored as "alive", and these individuals generally resumed feeding in the holding tanks as normal.

Figure 3-4. *Lottia gigantea* after thermal stress trials. a) The limpet on the left has retracted the mantle from the edge of the shell, and the edges of the foot have begun to curl upwards, both signs of heat coma. The limpet on the right has not been subjected to heat stress. b) Mushrooming behavior at the end of a thermal stress trial.

3.2.3.2 Low humidity tests

To examine the effects of high temperature and desiccation on limpets in realistic field conditions, lethal temperature distributions for *L. gigantea* were measured using an environmental chamber to mimic stressful field conditions in the laboratory. The chamber allowed for independent control of air temperature, substratum temperature, humidity, light level and wind speed.

The environmental chamber consisted of a closed wind tunnel that recirculated air continuously (Figure 3-5). The working section of the chamber where the organisms were placed was 35 cm wide and 13 cm in height. Unidirectional air flow of 0.5 m s^{-1} was created with a fan. Limpets sat on an aluminum plate that was heated by an array

of electric heating pads mounted to the underside of the plate. The temperature and heating rate of the aluminum plate were controlled by a computer that cycled the heating pads as necessary. Air temperature was controlled by a programmable water bath (Polystat 12108-30, Cole-Parmer, Vernon Hill, IL, USA) plumbed into a heat exchanger mounted in the lower section of the chamber (1978 Econoline E-150, Ford Motor Company, Dearborn, MI, USA). Relative humidity was controlled manually by opening and closing an access door to the outside air, allowing mixing of the relatively dry air in the room with the moist air inside the environmental chamber.

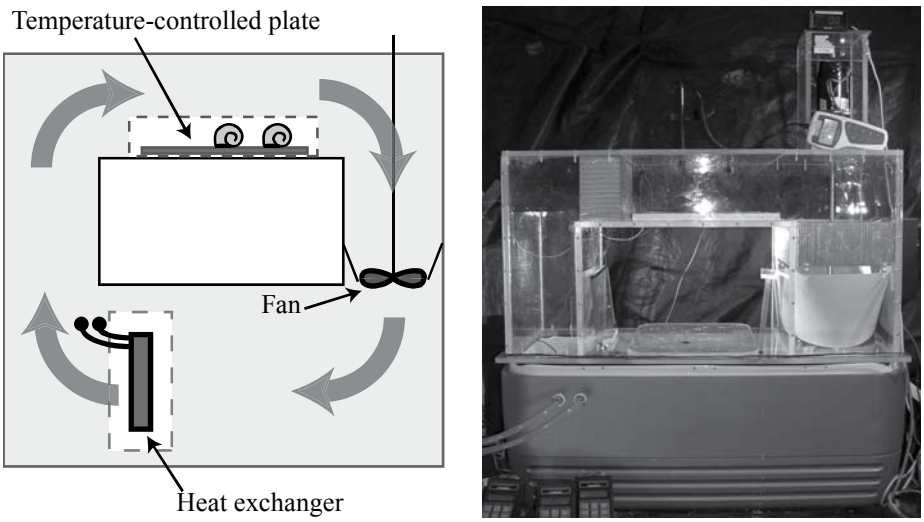

Figure 3-5. Environmental chamber used to mimic field conditions for thermal tolerance experiments. The fan housed on the right side of the chamber circulates air through the top and bottom sections. Air is heated or cooled through a heat exchanger in the lower section supplied by an external water bath (not pictured). Limpets are placed on the heated aluminum plate located in the middle of the upper section. Dry air could be admitted from the outside through the access hole in the middle of the lower section.

Air, substratum, and organismal temperatures were monitored with 40 gauge copper-constantan thermocouples. Relative humidity was monitored with an electronic thermohygrometer, calibrated against standard salt solutions (35612 series, Oakton, Vernon Hills, IL, USA). Temperature and humidity measurements were recorded with a datalogger (23X, Campbell Scientific, Logan, UT, USA). The chamber differed from field conditions due to the fact that solar irradiance was not used as a primary source of heat input to the limpets in the chamber. Heat budget modeling by Denny and

Harley (2006) demonstrated that the intimate contact between limpets and the substratum resulted in body temperatures very close to rock surface temperatures. Due to the close connection between substratum temperature and body temperature, it was decided that the primary heat source for limpets in the environmental chamber would be from the heated aluminum substratum, which allowed for much simpler control of limpet body temperature. As the ultimate goal of the experiments was to examine the effect of high body temperatures on limpet survival, this simplified heating methodology was deemed appropriate.

To determine a realistic humidity value for the trials, I used the thermohygrometer to measure relative humidity values in the field at HMS during warm low tide periods during the spring and summer of 2004. On sunny days when the rock surface was dry, the relative humidity at the rock surface was typically between 50 and 60%, with occasional excursions to between 30 and 40%. The range between 50 to 60% was the most common relative humidity, so this range was the target used in the heating trials.

Following the initial collection and holding period in the water tables, a group of *L. gigantea* was haphazardly chosen to be used in a heating trial. The shell of each limpet was dried and numbered with a tag to facilitate later measurements. The maximum length of each limpet was recorded, and each trial contained a mixture of limpet lengths between 25 mm and 65 mm. To avoid desiccation prior to the start of the trial, limpets were held in seawater while the numbering and length measurements were carried out. Heating trials of 3.5 h duration used groups of 10 limpets, while the 7 hr trials used sample sizes of 5 limpets. *L. gigantea* were placed on the wetted aluminum plate and allowed to attach to the plate at the beginning of each trial. The environmental chamber was then closed and the temperature ramps began. Outside air was fed into the chamber as necessary to regulate the relative humidity in the chamber, which rose as the temperatures inside the chamber rose.

At the conclusion of the 3.5 hr or 7 hr trials the limpets were returned to running seawater in the holding tanks. Survival was determined 24 hr after the end of each trial using the same criteria as for the 100% relative humidity trials.

The number of limpets in each trial that survived the lethal temperature trials was noted and expressed as the fraction surviving, *S*. The fraction surviving was averaged for the three replicates at each temperature. The lethal temperature, *T,* at which 50% of the limpets in a trial died (LT50) was determined by a fitting a sigmoidal curve to the survival data:

$$S = 1 - \frac{1}{1+\exp\left(-\frac{T-a}{b}\right)} \quad (40)$$

where *a* and *b* represent coefficients determined by a curve-fitting routine implemented in Matlab software (The Mathworks, Natick, Massachusetts, USA). The value of *a* is equal to the LT50 temperature.

3.2.4 Sublethal stress

In addition to measuring lethal limits for *L. gigantea*, the environmental chamber was used to expose limpets to sub-lethal temperature and desiccation stress. The intensity of sub-lethal stress was measured using a common physiological stress marker, heat shock protein 70 (Hsp70). Groups of five *L. gigantea* were processed in the environmental chamber up to temperatures ranging from 24 to 36°C, for either 3.5 hr or 7 hr durations, using the same parameters as the low-humidity lethal temperature determinations. To control for the effects of handling and exposure in the environmental chamber, control groups of five limpets were placed in the environmental chamber and held at 14°C for 3.5 hr and 7 hr. These control limpets remained wetted for the entire duration, so that desiccation was likely a minor stress. The limpets targeted for protein expression work recovered in seawater for one hour, and were then frozen in liquid nitrogen. An additional field control sample of five *L. gigantea* was collected from the field at HMS while still submerged by the tide and immediately frozen. The frozen limpets were stored at -70°C until they could be processed.

Hsp70 assays were carried out using a protocol similar to that of Hofmann and Somero (1995). Each limpet was partially thawed and a small portion of the pallial gills and mantle tissue (~1 – 2 mg) was dissected from the edge of the mantle (Fisher,

1904). The tissue was placed into 200 µl of homogenization buffer and boiled for 5 minutes. A stainless steel bead was then placed in each tube, and the tissue was homogenized using an automatic homogenizer (Tissuelyser, Qiagen, Valencia, CA, USA). The samples were boiled and homogenized twice more before centrifugation at 14,000 g for 15 min. The supernatant was pipetted to a new microfuge tube and stored at -20°C.

After sitting in the freezer for 24 hours, the samples were quickly thawed in a dry bath at 60°C, and centrifuged at 14,000 g for 5 min. Any congealed solid materials were removed from the tubes. The freeze, thaw, and centrifuge process was repeated twice for all samples, after which the appearance of solids during thawing was markedly reduced.

Quantification of the total protein content of each sample was carried out using the BCA Pierce protocol (BCA Protein Assay Kit, Pierce, IL, USA) in 200 µl well plates. Each sample was loaded in triplicate, and each plate contained a set of pre-diluted bovine serum albumin (BSA) standards, also loaded in triplicate. Absorbances were measured in a SpectraMax 340pc spectrophotometer (Molecular Devices, Sunnyvale, California, USA). A standard curve was calculated from the absorbance of the standards, and the average of the three replicates of each sample was taken as the protein concentration for that sample. The protein quantification was carried out two times in order to determine if concentrations changed appreciably due to freeze and thaw cycles, but no change was detected.

SDS-PAGE gel electrophoresis was used to separate proteins for Western blotting. After boiling for 3 minutes at 100°C and centrifuging at 14,000 g for one minute, a sample of 7 µg of total protein from each limpet (with the remaining volume up to 7 µl made up with distilled water, and 7 µl of Laemmli sample buffer) was loaded into each lane of a 10% Tris-HCl pre-cast gel (Ready-Gel Polyacrylamide gel, Bio-Rad Laboratories, Hercules, CA, USA). In addition to the heat-shocked samples, a molecular weight standard was loaded (Precision Plus Protein Standard, Bio-Rad Laboratories, Hercules, CA, USA), along with 30 ng of human Hsp70 in another lane

(NSP-555, StressGen – Assay Designs, Ann Arbor, MI, USA). Gels were submerged in Tris-glycine running buffer with 0.1% SDS. The gels were placed in a 4°C cold room and electrophoresed at 200 V for 50 min.

The proteins were then electrophoretically transferred from the gel to the solid phase on nitrocellulose membranes. Each gel was sandwiched with the nitrocellulose membrane between four pieces of filter paper and submerged in transfer buffer (Tris-glycine and 20% methanol). The transfer was carried out in the 4°C cold room at 80 V for 75 min.

Membranes were stored dry between Kim-wipes before the start of the immunoassay. Each membrane was incubated with gentle shaking in blocking buffer (5% non-fat dried milk) for 1 h. After three 5 min washes in phosphate-buffered saline (PBS), four membranes were incubated for 1 hour with gentle shaking in primary antibody mixed 1:5000 in PBS with 5% BSA (antibody MA3-008, clone 2A4, mouse monoclonal, Affinity BioReagents, Golden, CO, USA). The membranes were washed six more times for 5 min each prior to incubation in the secondary antibody (SAB-100, 1:5000 dilution in PBS with 5% BSA, StressGen – Assay Designs, Ann Arbor, MI, USA) . The incubation in secondary antibody lasted for 1.5 h and was followed by three, 5 min washes in PBS with 0.1% Tween-20.

Each membrane was laid out flat on a piece of Parafilm and covered with 3.5 ml of enhanced chemiluminescence (ECL) reagent for 1 min (GE Healthcare Bio-Sciences Corp, Piscataway, NJ, USA). The ECL bound to the horseradish peroxidase that was conjugated to the secondary antibody on the membrane and emitted light around the 430 nm wavelength in proportion to the density of secondary antibody present. Membranes were then wrapped in plastic wrap and placed in an x-ray exposure cassette. In the darkroom, each membrane was exposed to x-ray film. Because the dynamic range of the film is limited, it was necessary to test multiple exposure times for each membrane to find a suitable exposure. X-ray film exposes linearly in relation to the output of the ECL reagent within a certain range of exposure values, but can easily saturate if exposed for too long. Exposure time varied between 30 s and 20 min

as necessary in order to avoid overexposing bands with a high density of protein while yielding measurable bands for low-expression samples.

The exposed x-ray film was digitally scanned on a transparency scanner. The image files were transferred to the image analysis program Image-J for densitometry (National Institutes of Health, USA). Using the "gel analysis" routine in Image-J, the density of each sample's band at 70 kDa was measured relative to the density of the 30 ng human Hsp70 standard on each gel. The presence of the human standard on all gels allowed for comparison of relative density values across multiple Western blots. Data were log transformed to better conform to assumptions of normality and tested for homogeneity of variances using Cochran's test. Analysis of variance was carried out in Matlab software.

3.2.5 Desiccation

During the thermal tolerance trials in the environmental chamber, limpets lost body water via evaporation, which should increase the osmolality (moles of solute dissolved in a kilogram of solvent) of the internal and extracorporeal fluids of the limpet. A subset of the limpets used in the thermal tolerance trials were used to measure the post-exposure osmolality levels of extracorporeal mantle water.

Following the 3.5 hr or 7 hr exposure in the environmental chamber, each limpet was removed and a portion of the free water in the mantle cavity above the head was sampled with a pipette. The sample of water was placed in a 200 µl microfuge tube until it could be analyzed. No sample was held for more than 1 hr prior to analysis.

Osmolality of the mantle water was measured with a vapor pressure osmometer (5500, Wescor Inc., Logan, Utah, USA). The osmometer was calibrated ahead of each trial using 290 and 1000 mmol kg^{-1} standards. A total of five, 10 µl samples from each limpet were measured. In addition to the experimental samples, control samples were collected from the seawater holding table, from the mantle cavity of limpets in the holding table, and from limpets sampled during high tide in the field at HMS.

3.2.6 Heat budget modeling

The heat budget model of Denny and Harley (2006) was used to produce hindcasts of *L. gigantea* body temperatures on a number of hypothetical shore positions at HMS. The model, written and run using Matlab software, used the same parameters as the previously published model. Seven years of historical weather data, from 1 August 1999 through 31 July 2006, were used to produce a time series of body temperatures at 10 min intervals for the seven year period. The modeled limpet was 42 mm long, and was positioned in one of 5 orientations: on a horizontal surface, or on a sloped surface elevated 45° above horizontal facing north, west, south, and east. The limpets were modeled at elevations of 0.5 m to 2.25 m above MLLW on a wave-protected shore so that wave splash did not extend above the tide level. These conditions were meant to produce a "worst-case scenario" for *L. gigantea* on the shore at HMS.

3.3 Results

3.3.1 High humidity lethal temperatures

When *L. gigantea* were subjected to a 7 hr aerial exposure regime at 100% relative humidity, the median lethal temperature was 37.4°C (Figure 3-6). Limpets died at temperatures as low as 34°C, and all limpets died when the maximum temperature was 42°C.

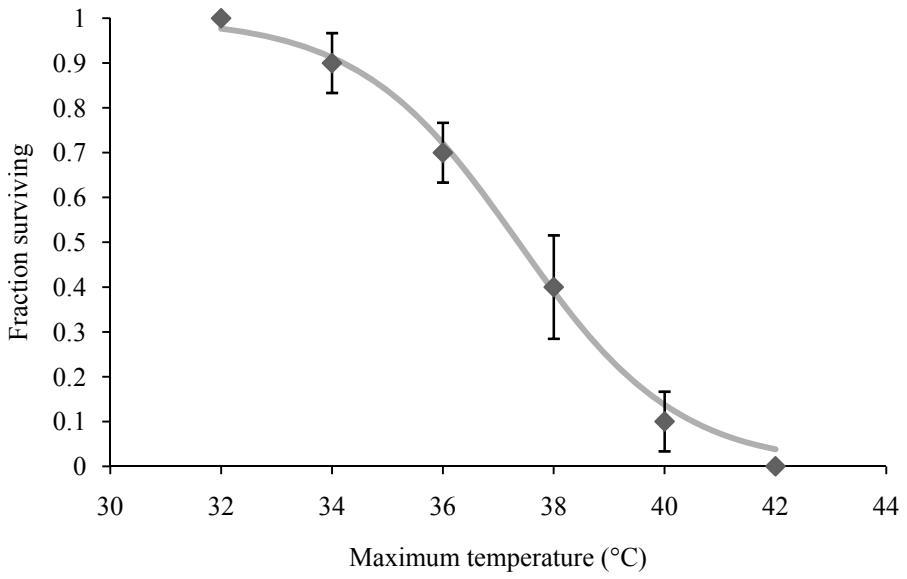

Figure 3-6. Survival of *L. gigantea* after exposure to thermal stress at 100% relative humidity. Exposure times were 7 hr, and the exposure profiles followed those depicted in Figure 3-3. Ordinate values are fraction of surviving limpets in each trial ± 1 SEM. Sample sizes were 5 limpets in each trial, and every trial was replicated three times. The curve is drawn according to Equation (40).

3.3.2 Low humidity lethal temperatures

Exposing *L. gigantea* to high temperatures at realistic humidity levels resulted in lower survival rates than those measured in the 100% relative humidity chamber. The temperature at which 50% of *L. gigantea* were predicted to die after the 3.5 h treatments at 50-60% RH was 36.7°C, and the onset of thermal death occurred between 34°C and 36°C. For limpets exposed in the wind tunnel for 7 h, the LT50 was 32.5°C, and the onset of death occurred between 30°C and 32°C. Survivorship data and survivorship curves are plotted in Figure 3-7.

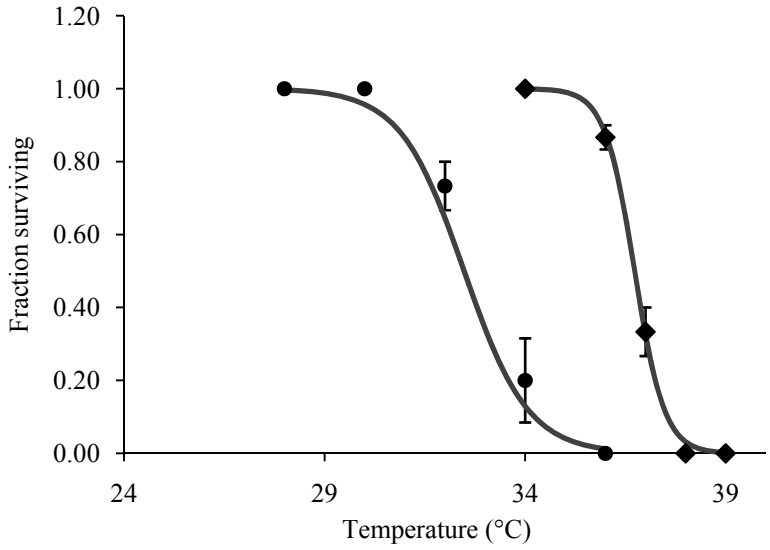

Figure 3-7. Survival of *Lottia gigantea* after exposure to thermal stress. Circles (●) represent limpets exposed for 7 hr, and diamonds (♦) represent limpets exposed for 3.5 hr. The thermal stress profiles used in these trials are explained in the text. Values are mean survival ± 1 SEM for 3 replicates, except for the 39°C point, for which there is one sample. The curves are drawn according to Equation (40). Sample sizes were 10 limpets for the 3.5 hr trials and 5 limpets for the 7 hr trials, and each trial was repeated three times.

3.3.3 Desiccation

Measurements of osmolality of mantle water samples from the aerial exposure limpets revealed substantial variation between treatment groups (Figure 3-8). All groups had elevated quantities of dissolved solids relative to samples of sea water from the aquaria system or from limpets being actively splashed by seawater in the holding tanks. For the 7 hr exposures at 24, 28, 32 and 36°C, one limpet in each group had an osmolality value higher than 2000 mmol kg^{-1}, which was above the limits of measurement for the osmometer. Additionally, one individual in the 28°C 3.5 hr treatment did not yield enough mantle fluid to make osmolality measurements. Due to these limitations, the data were not deemed appropriate for tests of significance of the treatments.

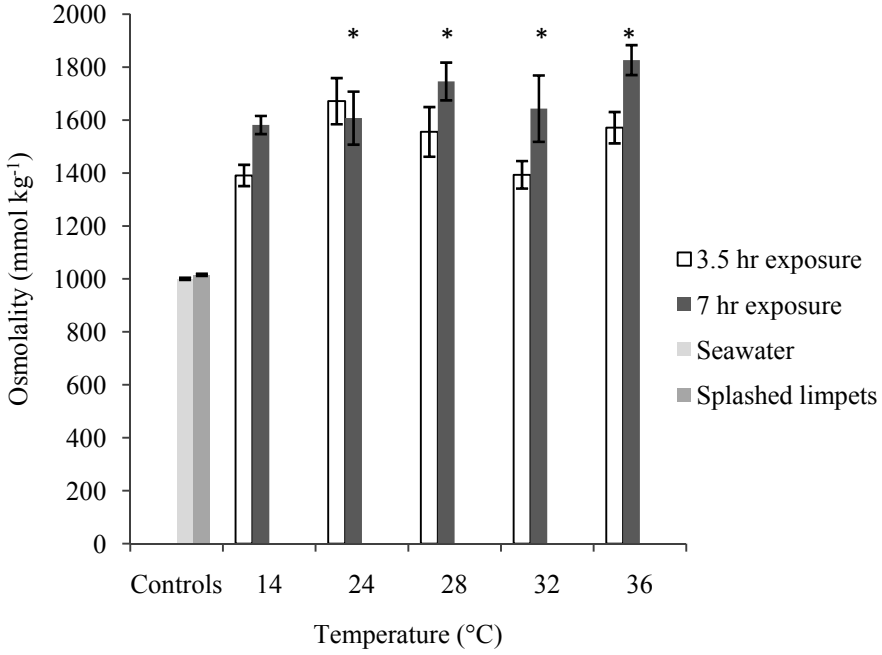

Figure 3-8. Osmolality of extracorporeal mantle water sampled from *L. gigantea* after aerial exposure for 3.5 hr or 7 hr at the indicated maximum temperature. The control values were taken from the sea water in the holding aquaria and from the mantle cavity of non-stressed limpets being splashed in the holding aquaria. Mean ± 1 SEM, n = 5 for each treatment. 7 hr data points marked with asterisks (*) denote groups where one of the sampled limpets had an osmolality value in excess of the 2000 mmol kg^{-1} limit of the instrument.

3.3.4 Hsp70 expression

The primary antibody (MA3-008) used in these experiments resolved one band of 70 kDa that showed low levels of constitutive expression and was strongly induced by temperature stress (Figure 3-9). The mean intensity of the Hsp70 band increased in treatments with a higher maximum temperature until the 36°C treatment (Table 3-1, Figure 3-10). The decrease in induced Hsp70 expression at 36°C in both time trials is likely correlated with the onset of heat coma in these limpets. Field control limpets exhibited the lowest levels of inducible Hsp70 expression, though they were not included in the statistical analysis due to the difference in exposure protocol for those limpets.

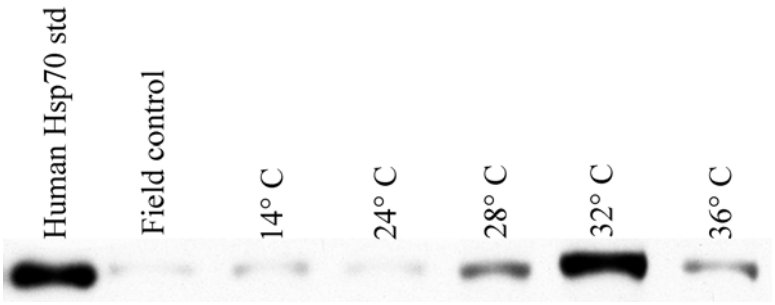

Figure 3-9. Representative expression of Hsp70 from limpets exposed for 3.5 hr. Temperature labels represent the maximum temperature reached in the trial. The standard was 30 ng of human Hsp70.

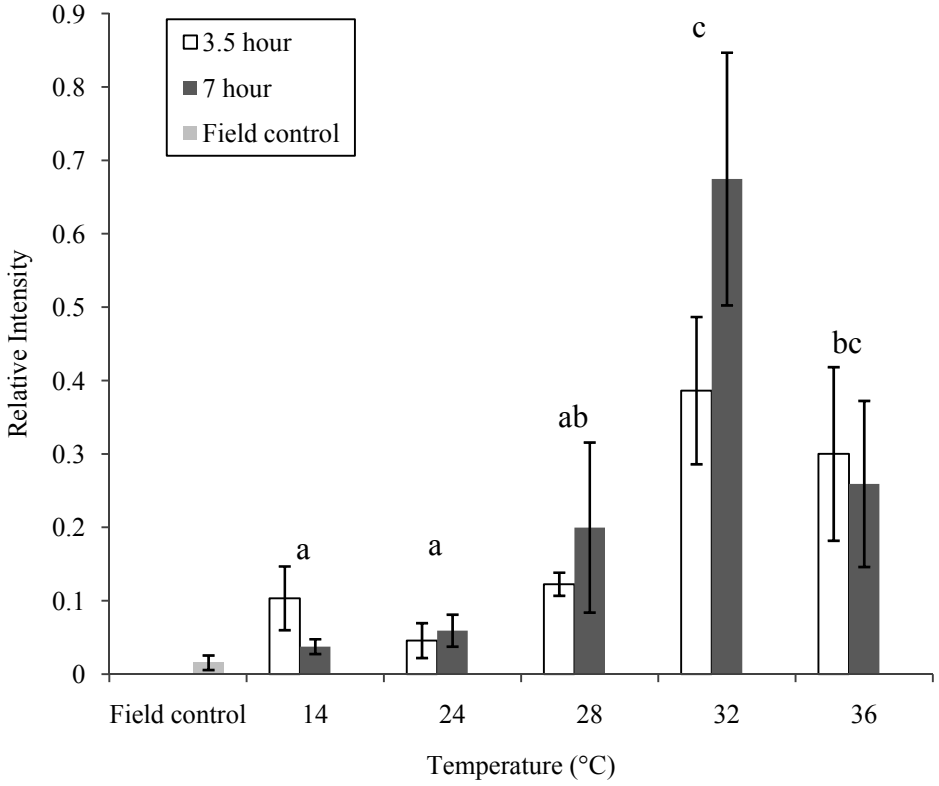

Figure 3-10. Induced expression of Hsp70 in *Lottia gigantea* relative to a 30 ng standard of human hsp70 after aerial exposure to high temperatures for 3.5 hr or 7 hr. Values are average expression of five individuals ± 1 SEM. Letters above each temperature treatment denote groups that are not significantly different in Bonferroni-adjusted post-hoc pairwise comparisons. The field control samples are provided for comparison, but were not included in the statistical analysis due to the difference in treatment protocol.

Table 3-1. Analysis of variance tests of temperature and time on expression of Hsp70 for *L. gigantea* during aerial exposure trials at 50-60% relative humidity in the wind tunnel chamber.

Source	SS	d.f.	Mean Square	F - ratio	*p*
Temperature	8.229	4	2.057	9.531	**<0.001**
Time	0.032	1	0.032	0.147	0.703
Temperature x Time	0.451	4	0.113	0.522	0.720
Error	8.634	40	0.216		

3.3.5 Heat budget model results

Modeling a *Lottia gigantea* on the shore at Hopkins Marine Station yielded multiple stress events during the course of the seven year data set (Figure 3-11). Two threshold conditions were chosen to define "stressful" days. The threshold for the onset of Hsp70 expression was calculated as any day where the limpet body temperature exceeded 28°C for more than 210 minutes, which corresponded to the experimental regime in the wind tunnel that produced a significant increase in Hsp70 expression relative to control conditions (Figure 3-10). The mortality threshold in the heat-budget model was defined as any day where limpet body temperature was predicted to exceed 32°C for more than 150 minutes, based on the lowest-temperature conditions expected to produce mortality in the low-humidity wind tunnel trials (Figure 3-7). The cumulative number of stress events varied with the altitude, azimuth and shore height of the modeled substratum, with a south-facing site angled 45° above horizontal producing the largest number of high temperature days, and higher shore heights producing higher temperatures.

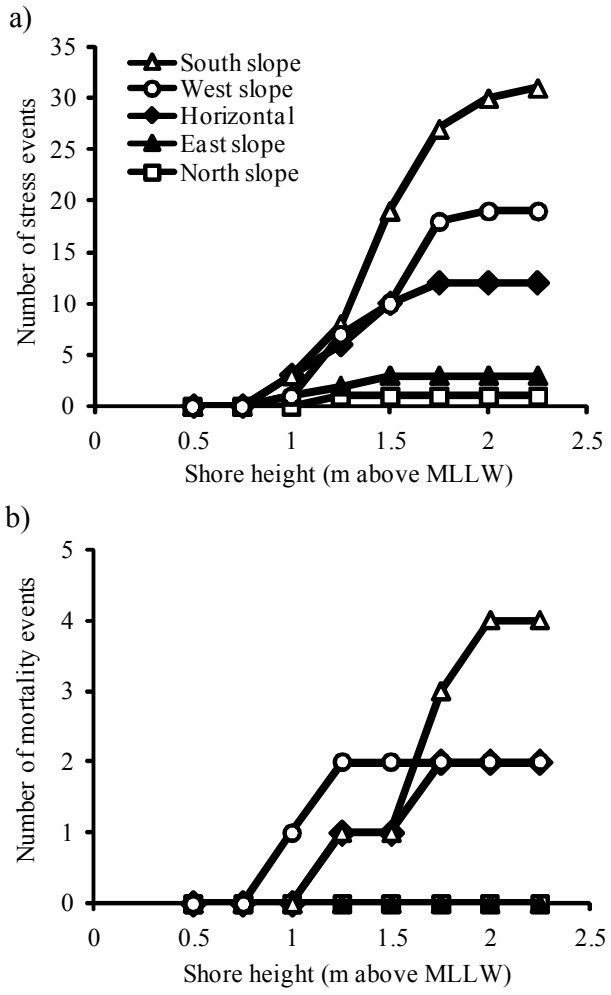

Figure 3-11. Cumulative predicted occurrence of stress and mortality events for *L. gigantea* modeled on the shore at HMS during the time period 1999-2006. A horizontal surface and four sloped surfaces angled 45° above the horizontal were modeled, facing each of the cardinal directions. a) Number of hot days where conditions were predicted to induce Hsp70 expression by raising limpet body temperature above 28°C for more than 3.5 hrs. b) Number of hot days where conditions could cause mortality in a portion of the limpet population when body temperatures exceeded 32°C for 2.5 hrs.

A representative set of temperature traces for the most stressful orientation, a south-facing slope at 2.25 m above MLLW, are shown in Figure 3-12. The threshold for the onset of Hsp70 production was exceeded 31 times at this model site, and many of these exposures lasted for longer than 3.5 hr. The prolonged exposure conditions should further increase the thermal and desiccation stress on the limpet, resulting in

more protein damage and subsequent Hsp70 production to repair the damage done. In the seven years, only 4 days were predicted to exceed the mortality threshold of *L. gigantea* on that same south-facing slope, but those included two days with exposures sufficient to kill 70-90% of the limpets at the modeled site (body temperatures in excess of 34°C for more than 120 min).

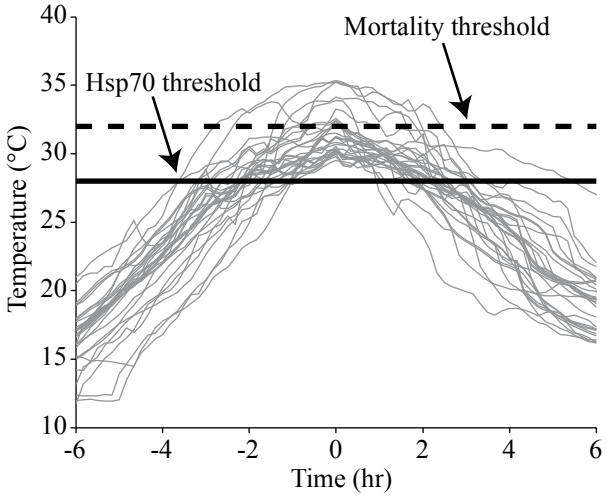

Figure 3-12. Predicted body temperatures (gray lines) for a *Lottia gigantea* modeled at 2.25 m above MLLW on a south-facing slope, on a wave-protected shore at HMS for the time period 1999-2006. The solid line represents the threshold above which Hsp70 expression should be induced. The dashed line represents the temperatures that could result in more than 10% mortality in the limpet population at this modeled site. Each gray line represents predicted body temperatures from a day in the dataset where the body temperatures exceeded 28°C for more than 3.5 hr.

3.4 Discussion

Predicting how intertidal organisms will cope with prolonged aerial exposure during low tide requires experimental methods that reasonably recreate conditions in the field (Newell, 1976; Branch, 1981; Jost and Helmuth, 2007). While simplified laboratory stress protocols work well for comparative physiological studies, making the transition from idealized conditions to the extremely variable real world introduces a number of

concerns that must be addressed before we can produce a meaningful measure of thermal and desiccation tolerance for an intertidal species.

3.4.1 Thermal stress methods

L. gigantea were able to survive at much higher temperatures when kept in saturated air, a condition that is extremely unlikely to occur in the field at HMS. Clearly, the method by which lethal temperature determinations are made has substantial effects on the resulting survival data. Comparing the median lethal temperatures for the 7 hr exposures in the 100% relative humidity chamber and the 50% relative humidity wind tunnel shows that the LT50 drops nearly 5°C in the latter trial (Figure 3-13).

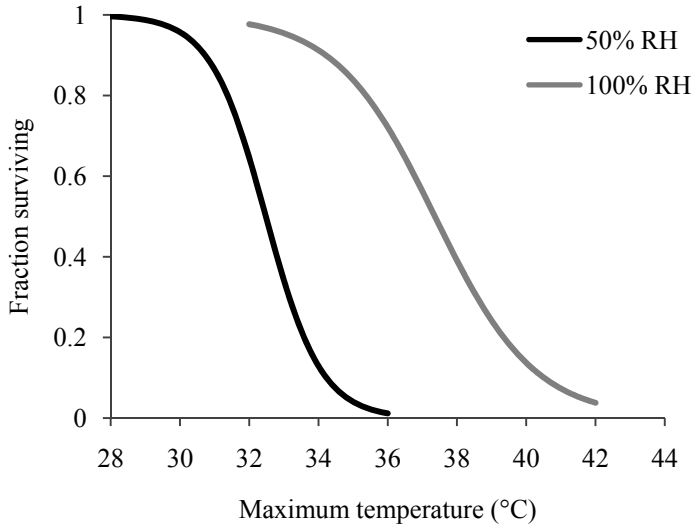

Figure 3-13. Survival of *Lottia gigantea* after exposure to high temperatures in 100% or 50% relative humidity air for 7 hr. The time course of the exposure was identical for the two experiments, with a temperature rise of 8°C hr^{-1} from 14°C to the indicated maximum temperature, followed by a return to 14°C at the same rate.

Much of the existing literature on thermal stress in intertidal organisms relies on lethal temperature data derived from high humidity trials in closed chambers or while organisms are submerged in seawater (Broekhuysen, 1940; Orr, 1955; Fraenkel, 1961; Fraenkel, 1968; Stirling, 1982; McMahon and Britton, 1985; Cleland and McMahon, 1986; McMahon, 1991; Sanders *et al.*, 1991; Clarke *et al.*, 2000a; Clarke *et al.*, 2000b;

McMahon, 2001; Davenport and Davenport, 2005). The prevalence of these protocols is understandable from a practical standpoint because the submerged or 100% RH methodologies can be carried out with only a water bath, as opposed to the need for a temperature-controlled wind tunnel to accurately replicate field conditions at lower humidity. Because much of the work on thermal tolerance in intertidal organisms has been focused on comparisons across species, in an attempt to correlate thermal tolerance with shore height, these standardized methods allow researchers to remove some of the variability of the natural system (Tomanek and Somero, 1999; Davenport and Davenport, 2005). There are cases where these simpler methods might also be informative for field studies of organismal survival during stress events, especially when the natural history of the organism is considered. Conditions similar to the high humidity trials do occur in some parts of the world, particularly in tropical regions where hot periods may be accompanied by relative humidity values in excess of 90% (McMahon and Britton, 1985; McMahon and Cleland, 1986; Williams and Morritt, 1995). In these situations the ability to lose heat via evaporation is substantially reduced, while also lowering the rate of desiccation. It should be noted that the concentration of metabolic by-products will still rise during aerial exposure at high humidity, which can constitute a stress that would not be replicated in a submerged trial where the organism would have the opportunity to circulate water as needed to eliminate these waste products (Smith, 2001). These comments do not apply to intertidal flora and fauna found in tidepools, where experiments with submerged organisms are quite appropriate.

Based on the large shift in lethal temperatures between the 100% RH trials and the 50% RH trials, it seems prudent to discard the survival data from the 100% relative humidity trials and focus on the more realistic low-humidity trials when attempting to make predictions about the survival of *L. gigantea* in the field. For days in the field where body temperatures are likely to reach lethal temperatures, the added stress of desiccation during the prolonged aerial exposure is a substantial stress that cannot be overlooked.

3.4.2 Length of exposure

The original heat-budget model data used to create the laboratory exposure trials showed that there were two general forms of aerial exposure at high temperatures, the short exposure with an abrupt return to seawater temperature, and the long exposure with a gradual return to seawater temperature. Both types of exposure can be stressful for *L. gigantea*, but there was a clear effect of the duration of the aerial exposure on the survival of the limpets (Figure 3-7). Doubling the exposure time for the limpets resulted in a nearly 4°C drop in the median lethal temperature for *L. gigantea*, as well as a downward shift in the lowest temperature at which individuals started to enter heat coma and die. Clearly the total time of exposure, as well as the maximum temperature achieved, has strong effects on the survivability of a limpet on the seashore.

The longest exposure used in the laboratory trials, a total of 7 hr, was short compared to many of the exposures predicted by the heat-budget model. This short exposure regime was chosen in part because it represented some of the fastest heating and cooling rates predicted by the heat-budget model, and it also made running many replicates logistically feasible. Unfortunately, we still have only a very small sampling of the many possible exposure regimes that limpets might be expected to experience in the field. To further improve the generality of the results from the heat-budget model, it would be desirable to run limpets under a larger variety of exposure durations (Newell, 1976). Many of the high temperature days predicted in the model had heating and cooling rates as slow as 2-3°C hr^{-1}, but exposure times in excess of 12 hr. Body temperatures were still predicted to exceed 30°C on these long-exposure days, and it remains unknown how this sort of exposure will impact the survival of *L. gigantea*.

3.4.3 Humidity and desiccation

The laboratory physiology trials demonstrated that relative humidity and desiccation have strong effects on the survival of limpets. At the most basic level, these data speak to the need for realistic stress protocols in laboratory trials. For animals and algae living outside of tidepools, the air around them is not saturated with water, which

allows for some evaporative cooling, but also leads to desiccation (Wolcott, 1973). For these reasons, stressing organisms in water or in closed, high-humidity chambers potentially alters both lethal temperatures and the onset of sublethal stress, leading to potentially incorrect conclusions about the susceptibility of that organism to realistic stressful field conditions (Figure 3-13).

As with the comparison of exposure time, the small number of humidity experiments described here only begins to address the large variety of possible exposure regimes a *L. gigantea* might face in the field. It is difficult to draw strong conclusions about the isolated effect of desiccation on the survival and performance of *L. gigantea*, in large part because the rate of desiccation shows so much potential variation. In the wind tunnel trials, where evaporative water loss was possible, individual variation in behavior likely had strong effects on the rate of water loss and measured osmolality of extracorporeal mantle water in *L. gigantea*. As shown in Figure 3-8, the variability in water loss, measured as osmolality of mantle water, was extremely high within a given temperature and time treatment.

Part of the large variability in desiccation rate could be due to the peculiar "mushrooming" behavior exhibited by *L. gigantea* and many other limpet species under high temperature stress (Segal and Dehnel, 1962; Williams *et al.*, 2005). Mushrooming limpets lift the shell away from the substratum, thereby increasing the surface area available for evaporative water loss and convective heat exchange with the surrounding air flow (Figure 3-4b). The typical behavior of a limpet during low tide under benign conditions is to pull the shell down against the substratum, essentially creating a gasket between the shell and the substratum sealed by a thin strip of mantle tissue. When pulled down against the substratum, water loss rates are minimized by reducing the surface area of moist tissue exposed to the dry air outside the shell (Lowell, 1984). Water loss is further reduced in some species by creating a mucus curtain between the shell and substratum as *L. digitalis* does, or by growing the margins of the shell to perfectly fit the contours of the rock surface at the home scar, as in *L. scabra* (Wolcott, 1973; Collins, 1977). However, on extremely hot days at

HMS, I have observed *L. gigantea* mushrooming in the field, sitting with a substantial gap between the shell and the rock. During these periods, measured body temperatures were 33-34°C, air temperature was 27°C, the rock temperature next to the limpets was 34-35°C, and the relative humidity was 33-48%.

Figure 3-14. A 'mushrooming' *L. gigantea* in the field at HMS on April 26, 2004. The body temperature of the limpet was 33.8°C, close to the rock temperature of 34°C.

While mushrooming is rare in the field, some of the *L. gigantea* used in the wind tunnel trials spent much of the time mushrooming. When limpets were restrained from mushrooming during pilot experiments, restrained limpets were 0 to 0.5°C warmer than limpets allowed to mushroom. When temperature differences existed, they could be due to increased evaporation or to the reduced area of contact between the limpet and substratum. The mushrooming behavior may have been responsible for much of the variance in desiccation rates measured in the wind tunnel. Some individuals began mushrooming at temperatures as low as 24°C, while others did not mushroom until reaching temperatures above 30°C. The distance lifted away from the substratum also varied among individuals, as did the duration of the mushrooming behavior. All of these factors likely contributed to the wide range of osmolality values measured for *L. gigantea* in the wind tunnel.

3.4.4 Sublethal stress

For both the long 7 hr exposures and the short 3.5 hr exposures in the wind tunnel, the onset of Hsp70 expression occurred between 24 and 28 °C (Figure 3-10). While the occurrence of lethal stress events was predicted to be quite rare, the much lower threshold temperature for the expression of these molecular chaperones indicates that sublethal stress events are much more common for *L. gigantea* in the field at HMS than lethal stresses.

Expression of Hsps carries metabolic costs, as well as indicating that the limpet likely sustains cellular damage due to protein denaturation during the temperature exposure (Hofmann and Somero, 1996; Tomanek, 2002). Prolonged exposure and higher temperatures increase the quantity of Hsp produced, until a time/temperature threshold is crossed where the limpet enters into heat coma (Cleland and McMahon, 1986). For the 7 hr trials, there was a marked decrease in the expression of Hsp70 for limpets exposed to a 36°C maximum temperature (Figure 3-10), indicating that these limpets had gone beyond the point where recovery was possible, and death was imminent.

The range of onset temperatures for Hsp70 production resembles the expression profiles of other intertidal gastropods living at HMS. Two species of turban snails, *Tegula funebralis* (now *Chlorostoma*) and *T. brunnea*, induce Hsp production between 20°C and 30°C, with the mid-shore species *T. funebralis* delaying Hsp expression until higher temperatures relative to the low shore *T. brunnea* (Tomanek and Somero, 2000; Tomanek and Sanford, 2003). Sanders *et al.* (1991) measured Hsp expression in two species of *Lottia* from southern California and found that the mid-shore species *L. pelta* induced Hsp production at 25°C while the higher-living species *L. scabra* did not begin production of Hsps until 29°C. At HMS these two species co-occur with *L. gigantea*, with *L. pelta* overlapping the lower vertical range of *L. gigantea* and *L. scabra* occupying the same zone as *L. gigantea* or higher on the shore.

3.4.5 Predictions of stress events in the field

With the new determinations of lethal and sublethal temperature thresholds for *L. gigantea*, it is time to return to the heat budget model to compare the predicted body temperatures for *L. gigantea* with the known tolerance limits of the species.

The frequency, intensity, and duration of thermal and desiccation stress events in the intertidal zone are intimately associated with the particular microhabitat of an organism (Grainger, 1969; Denny *et al.*, 2006). Organisms living low on the shore spend more time submerged, and thus have a smaller chance of reaching high temperatures. Organisms that seek refuge in crevices, under an algal canopy, or in the interstices of a biogenic structure such as a mussel bed also experience fewer hot days due to shading and retention of moisture (Kensler, 1967; Raffaelli and Hughes, 1978; Halpin *et al.*, 2002; Gray and Hodgson, 2004; Bazterrica *et al.*, 2007). But for organisms that choose to live out in the open and higher on the shore, weather conditions can raise body temperatures into the danger zone (Breen, 1972; Roberts *et al.*, 1997; Gilman, 2006; Berger and Emlet, 2007; Jost and Helmuth, 2007). Horizontal benches and sloped surfaces facing south or west are the most stressful habitats from this standpoint, with the heat-budget model predicting body temperatures greater than 28°C multiple times every year for shore heights at 1.5 m or higher above MLLW (Figure 3-11). Conversely, east-facing and north-facing rock faces are relatively benign habitats, with sub-lethal stress events predicted to occur every two to three years on average. These sublethal stress events are energetically costly for *L. gigantea* due to the need to produce Hsps to refold heat-damaged proteins, and may lead to increased ubiquitination of damaged proteins marked for degradation (Hofmann and Somero, 1995; Hofmann and Somero, 1996). Hsp expression can also come at the expense of the production of other proteins important for maintaining homeostasis in the cell (Feder and Hofmann, 1999). In *Drosophila melanogaster* tissue cultures undergoing heat stress, the production of Hsps may constitute 75 – 90% of the total protein production in the cell (Lindquist, 1980). Therefore, the overall cost to the organism includes not only the cost of producing Hsps to stabilize and repair proteins damaged by heat-induced denaturation, but also the added cost of degrading damaged

proteins and upsetting the normal function of the cells due to insufficient "normal" protein production. Because heat stress will not be homogenous across the microhabitats at a field site, only a subset of the population of *L. gigantea* might be expected to experience thermal stress on a given day and incur these costs, as has been shown in other limpet species (Halpin *et al.*, 2002).

Unfortunately, there are no good data on the energetic cost to a limpet to produce Hsps, so it remains unclear how much of a fitness cost the heat-stressed portion of the population might incur, or how repeated stress events might influence the long-term success of limpets in a particular microhabitat. Thermal stress events can combine with other characteristics of the microhabitat to make survival, growth, and reproduction relatively difficult (Frank, 1965; Breen, 1972). The frequency of occurrence of sublethal stress events rises with increasing height on the shore, while the amount of time for grazing should decrease along the same height gradient (Sutherland, 1970). *L. gigantea* does not graze unless washed by waves, leaving less time for grazing at higher shore heights where the fraction of time spent submerged shrinks (Stimson, 1970). Additionally, the growth of algal food resources may be slower at higher shore heights, reducing the caloric intake of the limpets compared to conspecifics living lower on the shore (Castenholz, 1961).

Beyond sublethal stresses, from which *L. gigantea* can recover, the occurrence of lethal thermal stress events can have immediate impacts on the *L. gigantea* population and the surrounding community. On horizontal benches and south or west-facing slopes, multiple days during the seven year dataset registered high temperature events that lasted long enough to induce mortality in at least 10% of the population on each slope (i.e. limpets with body temperatures greater than 32°C for 180 minutes, Figure 3-11b). Of those stress events, a subset was hot enough to kill 70-90% of the limpets at the horizontal bench and south- or west-facing slope sites with body temperatures of 34°C or greater for more than 2 hr. These mortality events were predicted to occur both on wave-protected and wave-exposed shores due to the fact that the hottest days in the dataset were accompanied by very calm ocean swell conditions which did not

allow waves to splash and cool the high shore sites. Extreme lethal temperature exposures were restricted to shore heights above 1.75 m above MLLW, a shore height that is occupied by *L. gigantea* at wave-exposed portions of the shore at HMS.

The frequency of lethal temperature events predicted here differs from the earlier predictions of Denny *et al.* (2006) (three lethal temperature events in five years), for two reasons. The lethal temperature thresholds in Denny *et al.* were based only on data from the shorter 3.5 hr temperature exposure trials, which put the median lethal temperature for *L. gigantea* at 36.7°C (Figure 3-7) while the extended 7 hr exposure trials resulted in a lower median lethal temperature of 32.5°C. The earlier results of Denny *et al*. also assumed mortality occurred any time body temperatures were predicted to reach a given temperature threshold, while the method used here requires that body temperatures remain above a given threshold for a period of time at least as long as that used in the wind tunnel lethal temperature trials (Figure 3-3). This conservative method would reduce the total number of days predicted to produce mortality events (until the new lower lethal limits are considered), but also provides a more definitive measure of the potential mortality induced in a population.

The severity of a temperature stress event and the magnitude of the resulting stress response can be influenced by the environmental conditions leading up to the stressful period. Seasonal variation in ocean and air temperatures, as well as emersion time, can lead to changes in the metabolic rate and thermal sensitivity of intertidal organisms (Newell and Pye, 1970b; Newell and Bayne, 1973; Segal *et al.*, 1953; Segal, 1956; Markel, 1974, 1976; Stillman and Somero, 2000; Helmuth and Hofmann, 2001). This acclimation process is known to shift the temperature threshold for the production of Hsps (Roberts *et al.*, 1997; Feder and Hofmann, 1999; Tomanek and Somero, 1999; Buckley *et al.*, 2001; Hamdoun *et al.*, 2003; Encomio and Chu, 2005; Osovitz and Hofmann, 2005). The current study only used limpets harvested during winter months, a time period when high temperatures are predicted to be rare. These data do not allow me to speak to the role of thermal acclimation in changing the tolerance of *L. gigantea*

to high temperatures, but I can use the heat-budget model output to characterize the environmental conditions leading up to temperature stress events

I used the predicted body temperatures for a limpet in a stressful microhabitat at 2.0 m above MLLW on a south-facing slope that was protected from wave swash to examine the two week period prior to each day where limpet body temperature exceeded a 30°C threshold. As shown in Figure 3-11, limpets in this habitat should see a number of sub-lethal and lethal hot days during the seven years of the weather data set. Two examples of the predicted temperatures are shown in Figure 3-15. Some high temperature events may be preceded by mild conditions for many days. In the example shown here (Figure 3-15a), one of the most stressful days in the record, June 15, 2000 (maximum temperature 35.2°C, body temperatures greater than 30°C for over 5 hr) was preceded by two weeks of cool days where body temperature was predicted to never exceed 24.5°C. Alternatively, some high temperature events were preceded by repeated warm days near or above 30°C that might allow limpets to acclimate and mount a more effective physiological response to subsequent stress events (Figure 3-15b).

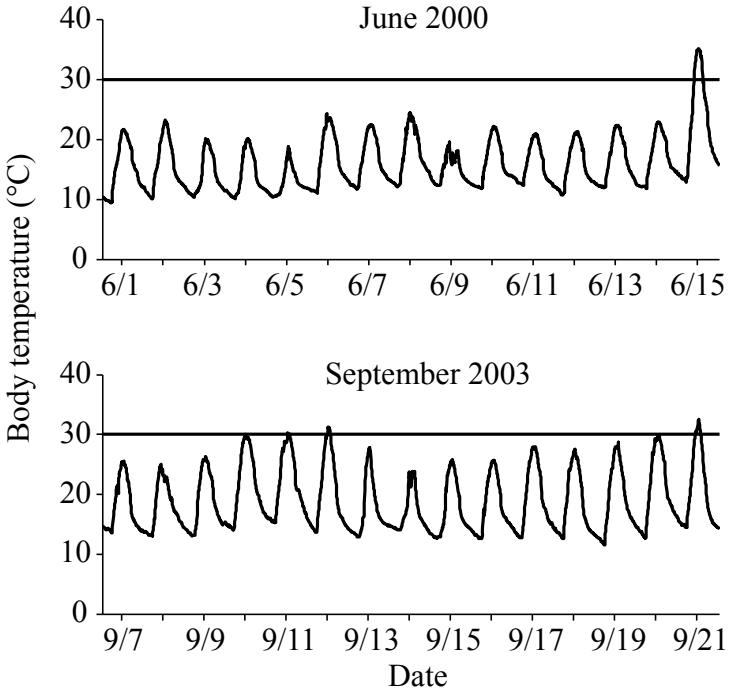

Figure 3-15. Representative body temperatures for a limpet modeled on a south-facing slope at 2.0 m above MLLW. Each panel shows temperatures for a two week time period leading up to a day where the limpet body temperature was predicted to exceed 30°C. The June 2000 series was marked by relatively mild temperatures leading up to June 15, when body temperature was predicted to reach 35.2°C and remain above 30°C for over three hours. The September 2003 series contains several warm days prior to the peak temperature on September 21.

The data for all of the two-week periods prior to high temperature events were analyzed by calculating the maximum temperature on each of the 14 days before the target date. The set of maximum temperatures for each day was bootstrapped 1000 times to produce a mean daily maximum temperature and 95% confidence limits. In addition, the difference between the maximum temperature on each day and the maximum temperature of the associated stressful day was bootstrapped in the same manner. The results (Figure 3-16) show that, on average, most of the days preceding a high temperature event reach maximum temperatures that are 6-8°C cooler than the target date, but as you approach the target date the difference decreases. The two to three days preceding a high temperature event often consist of days with maximum temperatures that equal or exceed the temperature on the target day (as shown by the

upper 95% confidence limits, Figure 3-16), reflecting instances where a multi-day heat wave set in over the site.

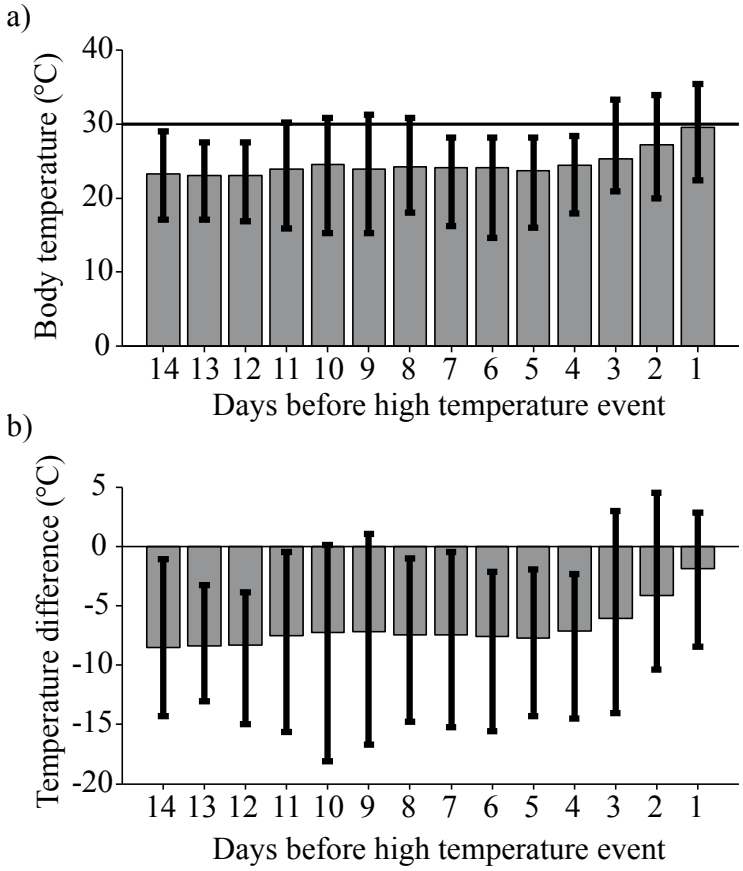

Figure 3-16. Predicted conditions for days leading up to a high temperature event. Temperature data were produced for a model limpet sitting on a south-facing slope at 2.0 m above MLLW. a) Average daily maximum body temperatures (± 95% CI) on each day leading up to a high temperature event where limpet body temperature exceeded 30°C (horizontal line). b) Average (± 95% CI) of the differences between the maximum temperature during stress events and the maximum temperature on each day prior to the events. Averages and 95% confidence limits were calculated by bootstrapping the values produced by the heat-budget model for each day 1000 times.

L. gigantea may acclimate to long-term seasonal shifts in temperatures and to short-term temperature shifts. The seasonal distribution of high temperature events at a high-shore south-facing slope is shown in Figure 3-17. The majority of days with body temperatures above 30°C were predicted to occur during the fall at HMS, but isolated warm days occurred throughout much of the year. *L. gigantea* experiencing thermal

stress during February, March, or April might be acclimated to the colder water and air temperatures of the winter season, while those same limpets may be more "thermally hardened" during the fall months when temperatures on the Monterey Peninsula are often relatively warm. As with many of the other conspicuous members of the intertidal community at HMS, much more work remains to be done on the roles of seasonal and short-term thermal acclimation for the survival of *L. gigantea* during hot low tide periods.

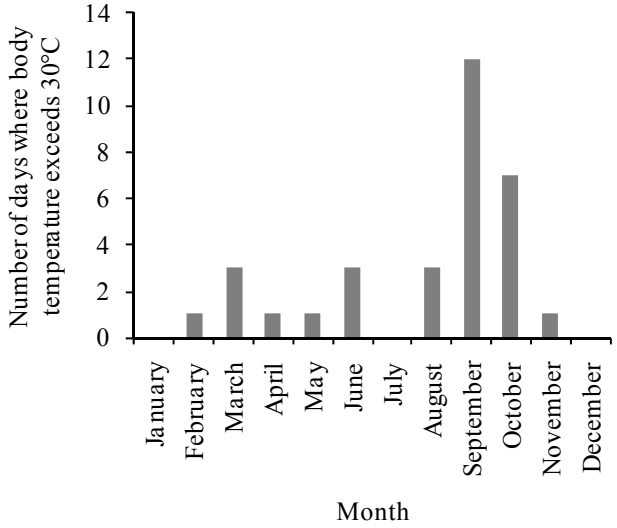

Figure 3-17. Distribution of predicted high temperature events during the period August 1, 1999 through August 1, 2006 for a limpet modeled at 2.0 m above MLLW on a south-facing slope.

3.4.6 Conclusions

The combination of lethal temperature data and model predictions shows that lethal temperature exposures for *L. gigantea* could occur at HMS. These events rely on a rare combination of calm sea state, still air, a midday low tide, and warm air temperatures, but this combination of conditions can clearly occur even at a "cool" site like HMS (Helmuth *et al.*, 2002). While these conditions might only occur every few years, the 20 year life span of *L. gigantea* makes it possible that an individual limpet could experience a stressful high temperature exposure during its lifetime. There is no

commonly accepted set of criteria for what frequency and intensity of disturbance constitutes an environmentally-imposed "limit" on a species' distribution, but multiple potentially lethal high-temperature events occurring at a site (such as south-facing slopes higher than 1.5-1.75 m above MLLW) within one generation of limpets should qualify.

Clearly the most important determinant for whether a limpet will eventually experience a lethal temperature exposure is the microhabitat choice of that limpet. *L. gigantea* that settle on north-facing or east-facing slopes, live in crevices, or live sufficiently low on the shore should be relatively safe from lethal and even most sub-lethal exposures. Minimizing the total emersion time and the time exposed to direct solar insolation by finding protected microhabitats removes the danger of thermal stress. These patterns in thermal stress correspond to the typical slopes and aspects occupied by *L. gigantea* at HMS, with most individuals of the species occupying sloped or vertical walls facing north or east at the wave-exposed end of the point. *L. gigantea* may also be added to the list of intertidal organisms that live near the upper limits of their thermal tolerance and have vertical distributional limits set by physiological stresses (Stillman and Somero, 2000; Tomanek, 2001; Somero, 2002; Tomanek and Sanford, 2003; Stenseng *et al.*, 2005; Gilman *et al.*, 2006).

The results of this study indicate that thermal stress may set the upper limits of *L. gigantea* in certain microhabitats by killing nearly all of the limpets every few years, while many other sites should be sufficiently protected from solar insolation to keep body temperatures from exceeding critical sublethal and lethal thresholds. It remains an open question of what factors set the upper limits of the distribution of *L. gigantea* in those microhabitats that are sheltered from high temperatures. As reported by Wolcott (1973), desiccation due to prolonged aerial emersion can be a danger to limpets even in habitats protected from high temperatures. Calm ocean conditions combined with neap tides can lead to prolonged exposure at sites that would normally be splashed or submerged, conditions that could endanger limpets that have ventured too far up shore during "normal" conditions (Orton, 1933; Frank, 1965; Breen, 1972).

The algal food supply of *L. gigantea* might also become limiting before temperature or desiccation stresses inhibit survival of the limpets. If settlement and growth rates of the algal food supply are limited at higher shore levels, due to reduced immersion time or high temperatures and desiccation, *L. gigantea* may not be able to graze enough algae to support its metabolic needs (Castenholz, 1961). The presence of other grazers may also reduce the standing algal crop (Castenholz, 1961; Frank, 1965; Wallace, 1972; Behrens Yamada, 1992), especially in situations where the submerged time is short enough to limit the effectiveness of the territorial behavior of *L. gigantea.* Little is known about the tolerance of the algae grazed by *L. gigantea* though, and the dietary requirements for maintenance and growth of *L. gigantea* remain unknown. Further study is needed to determine what factors set the upper limits of *L. gigantea* in cool microhabitats.

Figure 3-18. Apparatus for determination of wave impact forces on organisms. a) Approximately 120 m of 6.35 mm (1/4") diameter or larger steel wire cable should be procured and attached to the existing anchor offshore on the most southerly portion of Pete's Rock (end of red line). b) The landward end of the cable should be anchored to a heavy object that can be easily moved to set tension in cable. c) A tall, stable point should be chosen to support the cable above the ground. The height should be chosen to provide suitable ground clearance when larger organisms are suspended from the line. d) Organisms should be suspended from a low friction pulley. Final velocity on impact can be varied by accelerating the organism at the start of the descent and by varying tension in the wire cable. Impact force may be quantified by the relative change in tissue color (e.g. from pale pink to bright red) resulting from the collision of the body with the water surface. Obtain baseline tissue color measurements before beginning the trials.

Chapter 4

Feeding in extreme flows: behavior compensates for mechanical constraints in barnacle cirri

4.1 Introduction

Suspension feeders use a wide variety of methods to capture food items from the fluid in which they live. In many cases, some form of filter, net, or sieve-like structure is employed to intercept particles as they pass by the organism, such as the baleen of whales (Sanderson and Wassersug, 1993), gill rakers in fish (Lauder, 1983), modified mouth parts of invertebrates (Zhang, 2006), or other modified body parts such as legs (Crisp and Southward, 1961; Mauchline, 1989) and tube feet (LaBarbera, 1978). Trapping food particles in flowing water can place unique constraints on the form and function of feeding structures in suspension feeders. The size and form of the filtering apparatus must balance particle capture efficiency against mechanical constraints such as the drag created by fluids passing through and around the filter (Cheer and Koehl, 1987). While many suspension feeders (e.g. filter feeding vertebrates, or animals that actively pump water: Lauder, 1983; Sanderson and Wassersug, 1993; Vogel, 1994) dictate the rate of flow through their feeding apparatus, the subset of suspension feeders that extends the feeding apparatus into flowing fluids is somewhat at the mercy of the surrounding flow conditions. Because drag increases as the square of fluid velocity, the forces accompanying extreme flow speeds may impose limitations on the usefulness of the feeding structure at certain times.

Phenotypic plasticity in response to flow conditions has been reported in several phyla (Kaandorp, 1999; Okamura and Partridge, 1999; Arsenault *et al.*, 2001; Marchinko, 2003; von Dassow, 2005; Zhang, 2006). In habitats with relatively constant flow conditions, the form of the body, colony, or feeding apparatus may be tuned to suit the habitat. However, in habitats where flow speeds vary greatly over short time scales,

behavior may be a more important tactic for dealing with unpredictable changes in flow speed.

Barnacles extend their feeding legs (cirri) into flowing water to capture food particles. The size and shape of the cirri therefore affect the drag imposed on the feeding net. As flow speeds increase, barnacles may have difficulty keeping a large cirral net extended, limiting their ability to effectively feed (Marchinko, 2007). Barnacle cirral morphology varies plastically among habitats along a flow-speed gradient and has been correlated with maximum flow speeds experienced at sites over several weeks (Arsenault *et al.*, 2001; Marchinko and Palmer, 2003; Chan and Hung, 2005). Barnacles growing in slow-moving, wave-protected waters grow longer, thinner cirri than conspecifics growing at wave-exposed sites, and these cirral traits can be altered between moults in response to changing flow patterns (Marchinko, 2003).

There may be limits to the extent of the plastic response to flow. Li and Denny (2004) found that the correlation between cirral morphology and maximum water velocity at a site no longer held for barnacles from sites on the open coast. As peak water velocities at a site increase beyond 4 m s^{-1}, cirri do not continue to decrease in size or change shape. If the cirral net does not continue to get smaller as maximum flow speed, and consequently drag, increases, how do barnacles exposed to extreme flows maintain intact cirral nets and effectively feed? The proposed hypothesis is that behavior substitutes for further morphological variation and allows barnacles to avoid damaging flows, yet feed when flow speeds allow it (Marchinko and Palmer, 2003; Li and Denny, 2004). To address this hypothesis, I made observations of barnacle feeding behavior in the field. I sampled *Chthamalus fissus* barnacles along a wave-exposure gradient to determine whether they exhibit the same invariant cirral traits as previously studied species at high-flow sites, and gauged feeding behavior under breaking waves along with concurrent water velocity measurements to determine whether barnacles alter their feeding behavior to accommodate short-term changes in water velocity. An analysis of the distribution of water velocities at the wave-swept site was performed to

determine if barnacles might be using a measure of the environment besides maximum water velocity to dictate cirral morphology.

4.2 Methods

4.2.1 Cirral morphology

Chthamalus fissus barnacles were collected from eight sites on the Monterey Peninsula in California in October, 2006. Two protected sites in the Monterey Harbor were chosen to collect barnacles that see no breaking waves and contend only with slow surge and tidal currents. These two low-flow locations are where *Balanus glandula* barnacles were collected by Li and Denny (2004). Barnacles were also collected from sites along the wave-exposed Mussel Point at Hopkins Marine Station (HMS) in Pacific Grove, approximately 1.5 km from the harbor site (Figure 4-1). Mussel Point is exposed to the full force of incoming ocean swells. Water velocities in excess of 20 m s^{-1} have been measured at the wave-exposed end of Mussel Point (Denny et al., 2003). The six collection sites at HMS were chosen to encompass a broad range of wave exposure and resultant water velocities. *Chthamalus* were collected at sites along a horizontal transect 1.5 m above Mean Lower Low Water (MLLW). The relationship between offshore wave height and water velocity at each transect point has previously been described (Helmuth and Denny, 2003).

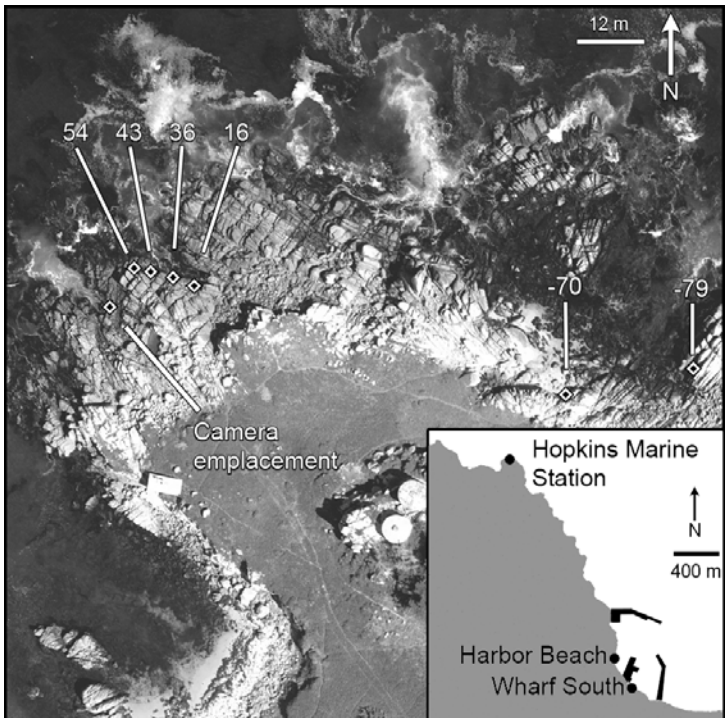

Figure 4-1. *Chthamalus fissus* collection sites. Sites at Hopkins Marine Station are marked on aerial image, and collection sites in Monterey Harbor are marked on inset map. Site of camera emplacement used in behavioral studies is also noted.

In the laboratory, the barnacle prosoma was dissected from the rest of the shell. Egg masses were removed, and the prosoma was blotted dry and weighed, following the protocol of Marchinko and Palmer (2003). The sixth biramus cirrus was then dissected from both the left and right sides of the cirral net and photographed under a dissecting microscope. The length of the ramus from the base to the tip, and the diameter of the ramus at the suture between the first and second articles, was measured using image analysis software (Image-J, NIH; Figure 4-2). An ordinary least squares regression was fitted to log (leg length) versus log (prosoma wet mass), as well as to log (ramus diameter) versus log (prosoma wet mass), in order to facilitate comparison of barnacle traits among sites. Analysis of covariance was carried out to compare ramus length and diameter among sites, with prosoma wet mass as the covariate.

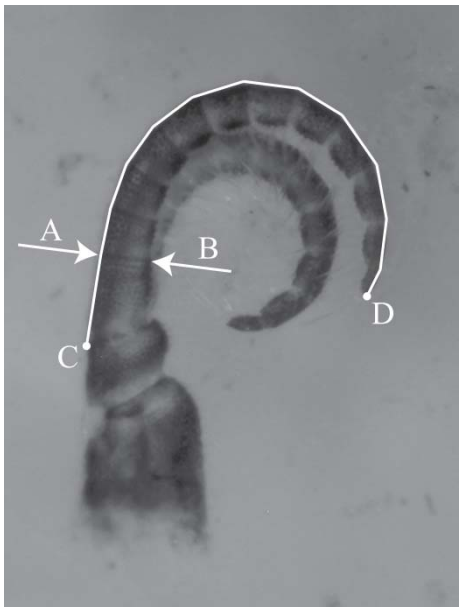

Figure 4-2. Diagram of measurements made on the sixth biramus cirrus of *Chthamalus fissus* collected from the Monterey Peninsula. The diameter of the ramus was measured between points A and B at the suture between the first and second articles. The length of the ramus was measured between points C and D by drawing straight line segments along the posterior edge of the ramus using an image analysis program. Terminal setae were not included in the ramus length measurement.

Average daily maximum water velocities at the collection sites were estimated for the 30 days prior to collection. Estimates were based on published relationships of average daily maximum water velocities at each site with the offshore significant wave height during the same time period (Helmuth and Denny, 2003; Li and Denny, 2004). The significant wave height was measured using a Seabird SBE-26 pressure gauge mounted at 10 m depth, 50 m off the point at HMS.

4.2.2 Feeding behavior

Barnacles used in the feeding behavior trials settled onto clear acrylic settlement plates deployed in the mid intertidal zone at HMS. The plates were attached to the rock surface on wave-exposed areas of the shore adjacent to existing *Chthamalus fissus* beds. After the initial deployment in the spring of 2004, the plates were left undisturbed until the spring of 2005. By this time, a mixture of *C. fissus* and *Balanus*

glandula barnacles had settled on the plates and grown to a basal shell diameter of 3 to 5 mm.

The clear acrylic settlement plates made the underside of the barnacles visible. *C. fissus* does not lay down a calcareous base plate, but instead grows a thin, partially transparent membrane. When the barnacles are still small, it is possible to see through the membrane, and observe the movement of the prosoma mass of the barnacle inside the shell.

A waterproof camera housing was constructed using plastic plumbing pipe to house a Watec 502B video camera. The camera housing mounted to the underside of a large aluminum plate with a hole bored through the middle. A settlement plate was then secured onto the top of the aluminum plate with the barnacles in view of the camera through the hole in the plate. An o-ring was placed between the settlement plate and the lens of the camera housing to provide a water-tight air space in the camera view path. This prevented water from getting between the camera and the settlement plate where it would obscure the view.

Prior to deployment in the field, the camera-and-settlement-plate apparatus was tested in an aquarium. Using a split-screen video system, the feeding behavior of the barnacles was observed from above and below simultaneously. These tests demonstrated that feeding movements viewed from above corresponded to movements of the prosoma within the barnacle test seen from below. The prosoma moved in time with the extension of the cirral net, and with the same rhythm of slow extension and fast withdrawal as described by other researchers (Crisp and Southward, 1961).

In the field, the entire apparatus was mounted in a concrete emplacement 1.5 m above MLLW, which exposed the barnacles to breaking waves (Figure 4-3). The emplacement was situated adjacent to the original deployment site of the settlement plates. Rocks offshore of the site caused the largest waves to break prior to impacting the barnacles, so that the majority of wave impacts were caused by turbulent bores rushing up the shore rather than by waves directly crashing on top of the barnacles.

Wave forces impacting a small sphere adjacent to the experimental barnacles were measured using a two-axis force transducer in a modified housing based on the basic design described by Boller and Carrington (2006). The force transducer had a 1.9 cm diameter roughened plastic sphere mounted on its post, and the transducer was bolted to the top surface of the aluminum mounting plate, 8 cm from the barnacles being filmed (Figure 4-3a). The transducer was calibrated prior to deployment by hanging known weights off of the drag sphere. Power, video data, and voltage data from the force transducer were run back to dry land by cable.

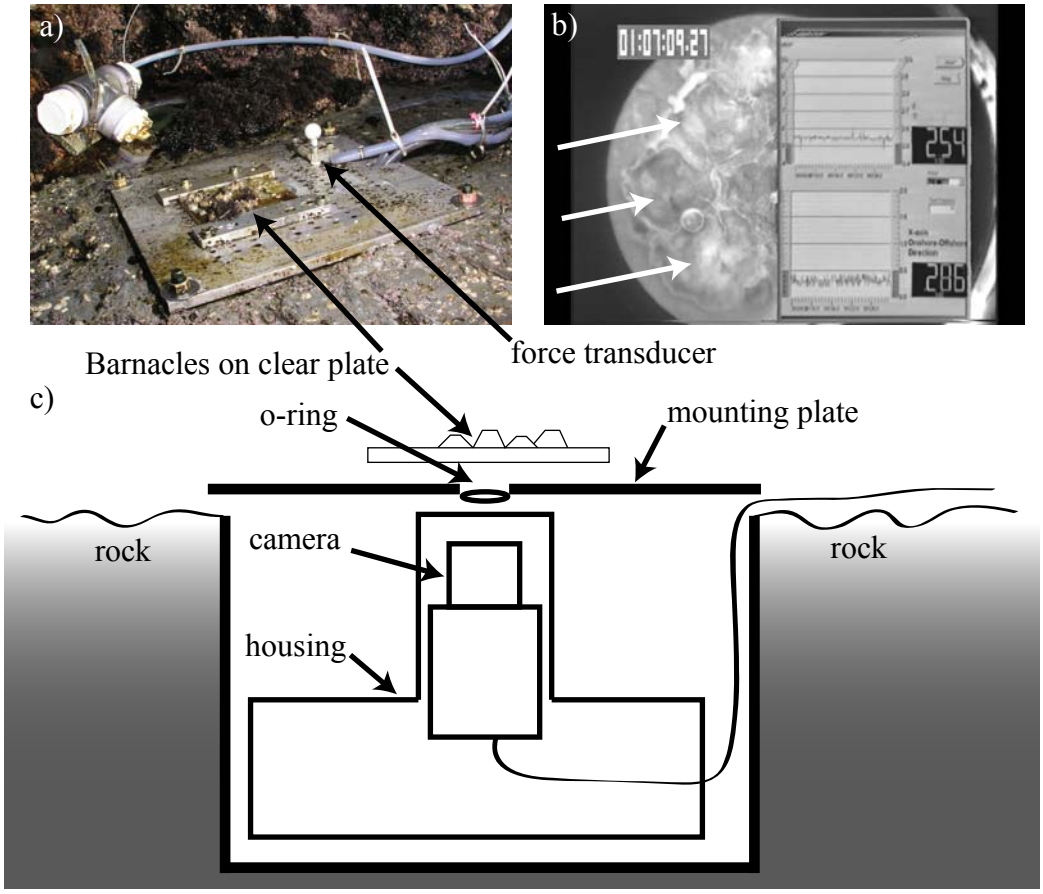

Figure 4-3. Apparatus used to monitor *Chthamalus fissus* feeding behavior in the field. (a) A view of the equipment deployed in the field, showing the barnacle settlement plate and wave force transducer. (b) Video frame capture with wave force data displayed on the inset graphs and three barnacles denoted by arrows. (c) Schematic of the camera housing emplacement.

The video and wave force data were simultaneously recorded onto video tape using a split-screen video camera arrangement (Figure 4-3b). A total of seven barnacles were deployed in the field on six days during October 2005 and three days during April 2006. Video recordings were made during high tide when the site was washed by waves.

Videotapes were analyzed with a video cassette player that allowed single frame stepping. A number of wave impacts were haphazardly selected for analysis from each two-hour-duration video tape. For each wave that impacted the barnacles and force transducer, a score was assigned to each barnacle in view. Prior to the wave hitting, the barnacle was scored as either feeding or not feeding. During the impact of the wave (generally 10 – 15 frames, or approximately ½ s) the barnacle was scored as either withdrawing from the impact or staying out in flow.

The maximum force recorded during each wave impact was recorded from the video playback and converted to a velocity using the equation:

$$U = \sqrt{\frac{2F}{A\rho C_d}} \tag{41}$$

where U is the velocity of the water, F is the force impacting the force transducer, A is the projected area of the drag sphere, ρ is the density of seawater, and C_d is the coefficient of drag of the drag sphere. C_d was assumed to be 0.45 based on data obtained in the laboratory (M. W. Denny, unpublished).

For each barnacle, a total of 600 individual waves were analyzed. Barnacles did not actively feed throughout each recording session, so the total number of waves that could be scored and used in the analysis (waves that hit a barnacle while it was feeding) was less than 600. The scored wave impacts were binned into velocity ranges with a minimum of thirty observations per bin, except for the highest water velocity bin where sample sizes ranged from 7 to 53, and the barnacles' feeding behavior was summarized as the fraction of waves in each velocity range for which they continued feeding uninterrupted.

Barnacle feeding behavior was also scored during intervals between wave impacts, while barnacles were still submerged. A series of 600 haphazardly selected time points from the various recording sessions was selected for each barnacle. This protocol was designed to measure the feeding activity of barnacles during the more benign flow conditions that make up the majority of submerged time.

4.2.3 Water flow conditions

In addition to scoring barnacle behavior, a random sample of water velocities was taken from each recording session used in this study in order to characterize the general water flow regime at this wave-exposed site. Water velocity was measured at 4000 haphazardly selected time points throughout the recorded sessions in order to produce a cumulative probability distribution. Due to limitations in the sensitivity of the force transducer, all velocities below 1.3 m s^{-1} had to be binned. Using Matlab software, a curve was fit to the cumulative probability distribution using a function from Gaines and Denny (1993):

$$\text{Cumulative probability} = e^{-\left[\frac{\alpha-\beta U}{\alpha-\beta\varepsilon}\right]^{\frac{1}{\beta}}}. \quad (42)$$

With U as the velocity, the resulting values for the parameters α, β, and ε allowed for the extrapolation of the cumulative probability distribution back to 0 m s^{-1} using the known cumulative probability distribution above 1.3 m s^{-1}. Taking the derivative of this curve yields the probability density function of water velocities during the recording sessions.

4.3 Results

4.3.1 Cirral morphology

Analysis of covariance tests of $\log_{10}$ (ramus length) on $\log_{10}$ (prosoma mass) and $\log_{10}$ (ramus diameter) on $\log_{10}$ (prosoma mass) revealed heterogeneous slopes among the sample sites (for ramus length: site x $\log_{10}$ (prosoma weight) interaction, $F_{7,139} = 2.92$,

$p = 0.007$; for ramus diameter: site x $\log_{10}$ (prosoma weight) interaction, $F_{7,139} = 2.96$, $p = 0.006$). The regressions are shown in Figure 4-4 and regression values are given in Table 4-1. At small and medium body sizes (0.1-1.2 mg prosoma mass), protected-site barnacles have longer rami than exposed-site barnacles, while they begin to overlap in ramus length at the largest body sizes sampled here (1.2 – 2.0 mg prosoma mass). However, barnacles from wave-exposed sites also grow thicker rami at those larger body sizes, which should lead to a stiffer overall structure, better able to withstand higher water velocities without bending.

An average body mass of 0.8 mg was used to compute representative ramus lengths and diameters for barnacles from the sample sites, which were then plotted against the average daily maximum water velocity at the sites (Figure 4-5).

Table 4-1. Ordinary least squares estimates of slope and intercept for $\log_{10}$ (ramus length) and $\log_{10}$ (ramus diameter) versus log (prosoma wet mass) (g). Sites are listed in order of increasing average daily water velocity. HMS: Hopkins Marine Station. The trait value (mean ± 95%CI) for a normalized body mass of 0.8 mg is given in the last column.

Site	Slope	Intercept	r^2	p	Trait value (mm)
Length					
WharfSouth	0.1490	0.6662	0.703	0.040	1.59 ± 0.258
HarborBeach	0.1651	0.7148	0.625	0.002	1.60 ± 0.249
HMS -79	0.1995	0.7186	0.675	<0.001	1.26 ± 0.073
HMS -70	0.2050	0.7841	0.764	0.005	1.41 ± 0.179
HMS 54	0.1844	0.6812	0.779	0.013	1.29 ± 0.185
HMS 36	0.2649	0.9361	0.884	<0.001	1.30 ± 0.227
HMS 43	0.1687	0.6635	0.726	<0.001	1.38 ± 0.186
HMS 16	0.2609	0.909	0.829	0.002	1.26 ± 0.115
Diameter					
WharfSouth	0.1452	-0.6122	0.792	0.012	0.079 ± 0.014
HarborBeach	0.1212	-0.7230	0.454	0.019	0.087 ± 0.013
HMS -79	0.2648	-0.1544	0.483	<0.001	0.107 ± 0.007
HMS -70	0.1881	-0.3693	0.734	0.008	0.112 ± 0.014
HMS 54	0.2280	-0.2749	0.835	0.004	0.104 ± 0.013
HMS 36	0.2147	-0.3436	0.787	0.004	0.098 ± 0.019
HMS 43	0.2038	-0.3432	0.755	<0.001	0.106 ± 0.015
HMS 16	0.2443	-0.2330	0.792	0.004	0.102 ± 0.009

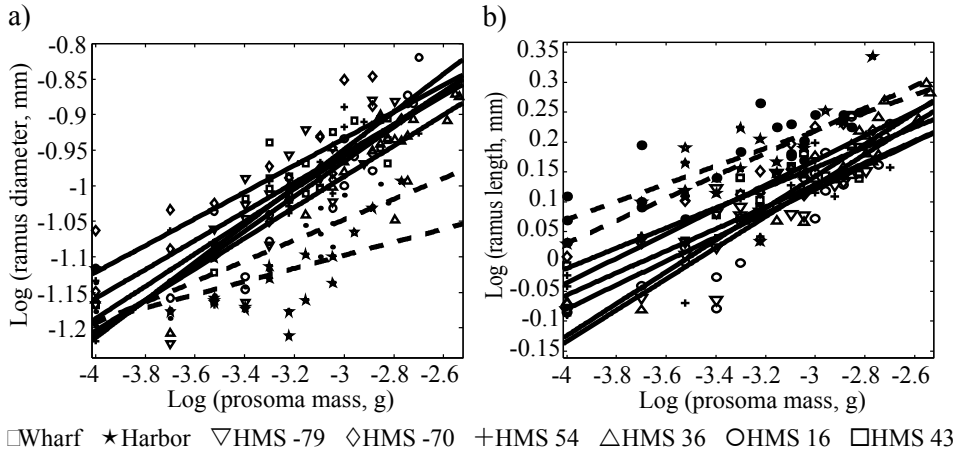

Figure 4-4. Ordinary least squares regressions of *Chthamalus fissus* sixth biramus cirrus traits against prosoma mass. (a) Log_{10} (ramus diameter, mm) vs. log_{10} (prosoma mass, g). (b) Log_{10} (ramus length, mm) vs. log_{10} (prosoma mass, g). The dashed lines represent regression fits for the two Monterey Harbor sites, solid lines are fits for Hopkins Marine Station sites.

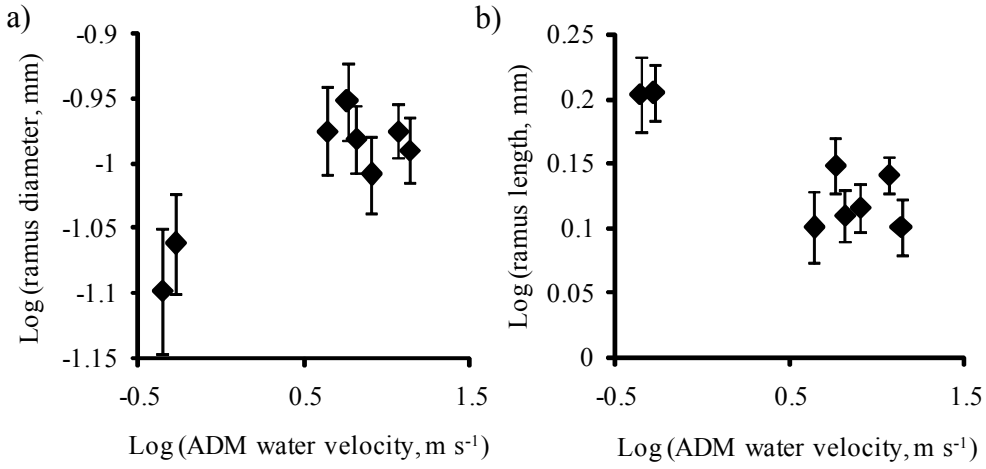

Figure 4-5. *Chthamalus fissus* ramus length and diameter at two wave-protected sites and six wave exposed sites on the Monterey Peninsula. (a) Log_{10} (ramus diameter, mm) vs. log_{10} (Average Daily Maximum water velocity, m s^{-1}) (b) Log_{10} (ramus length, mm) vs. log_{10} (Average Daily Maximum water velocity, m s^{-1}). Ramus length and diameter at each site are standardized to a common prosoma wet mass of 0. 8 mg based on the regression coefficients given in Table 1. Error bars represent 95% confidence limits.

4.3.2 Feeding behavior

As the wave size and peak water velocities increased, *Chthamalus fissus* chose to withdraw more often during wave impacts (Figure 4-6). There was substantial spread in the sensitivity of the barnacles to wave impacts. Five of the barnacles stayed open during more than eighty percent of the lowest measured velocity waves that impacted the site (less than 1.3 m s^{-1}). As water speeds increased above 2 to 3 m s^{-1} every barnacle withdrew for a greater fraction of the sampled waves, and they avoided nearly every high speed impact at water speeds above 4 to 5 m s^{-1}.

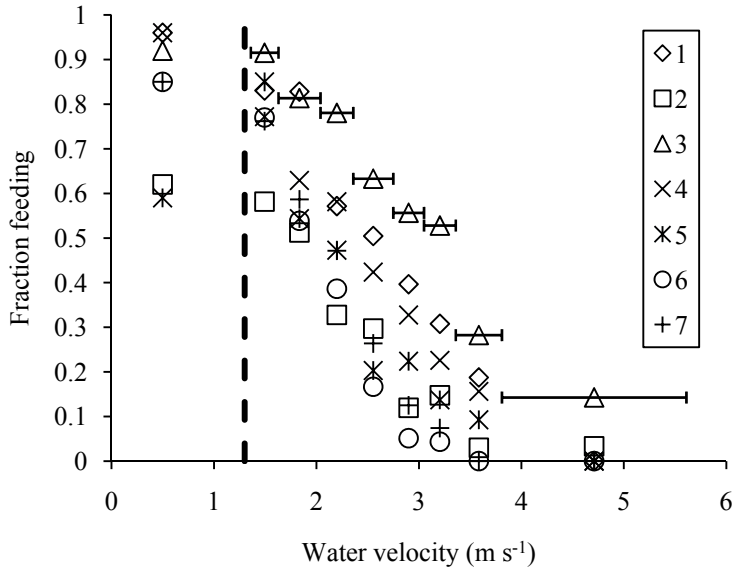

Figure 4-6. Feeding behavior of seven *Chthamalus fissus* barnacles under a variety of wave conditions in the field. Data points to the left of the dashed line represent the fraction of time spent feeding for water flow conditions below 1.3 m s^{-1} (n=600 time points for each barnacle). Data points to the right of the dashed line represent the fraction of wave impacts during which barnacles continued feeding, binned by velocity. The horizontal error bars for barnacle 3 indicate the width of the velocity bins. Sample size for each barnacle within each velocity bin ranged from 23 to 200, except for the two highest velocities for barnacles 6 and 7, where the sample sizes ranged from 7 to 12.

When the barnacles were not being impacted by waves but were still sitting submerged in slow moving water (less than 1.3 m s^{-1}), they spent at least half the time feeding, and in some cases more than ninety percent of the time (Figure 4-6). A representative record of 2 min of feeding behavior from barnacle 6 is depicted in

Figure 4-7. Waves washed over the site with a typical period of 8 to 12 s, and barnacle feeding paused during periods of high flow, but usually resumed quickly after the velocity decreased. There was no correlation between the water velocity of the wave impact and the time the barnacle spent retracted after the peak velocity had passed. The time periods between high water velocities consisted of many cirral extensions (gray shaded areas in Figure 4-7), mainly in the active feeding pattern but with some longer duration passive feeding extensions as well.

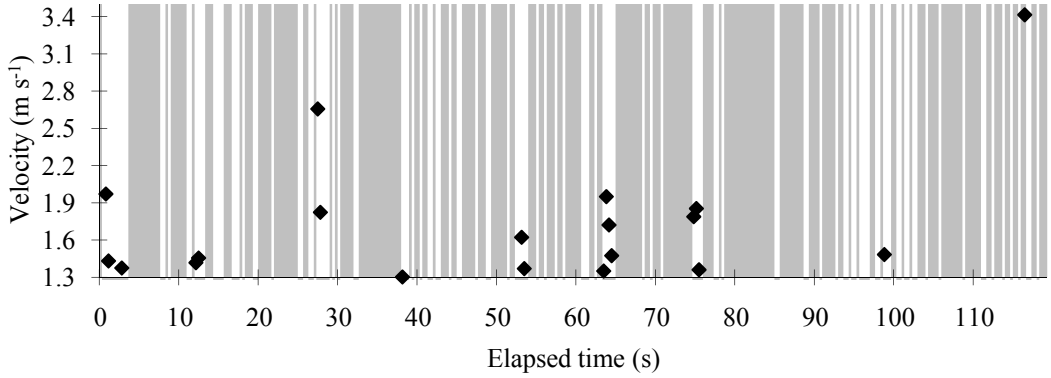

Figure 4-7. Feeding behavior of a representative barnacle and associated flow speeds during a 2 min interval, sampled every 10 frames (0.333 s). Shaded vertical bars: periods when the feeding cirri were extended into flow. Points on the graph: water velocity at each sample time. Velocity measurements <1.3 m s^{-1} were excluded due to limits in the sensitivity of the force transducer.

4.3.3 Water flow conditions

Figure 4-8a shows the cumulative probability distribution of water velocities during recording sessions at the wave-exposed HMS point. The probability that a randomly sampled water velocity is less than 1.31 m s^{-1} is greater than 87%, and climbs to 99% for a velocity below 2.3 m s^{-1}. The extrapolated probability density function of water velocities during the recording sessions (Figure 4-8b) has a mean water velocity of 0.98 m s^{-1}, and a mode of 0.52 m s^{-1}.

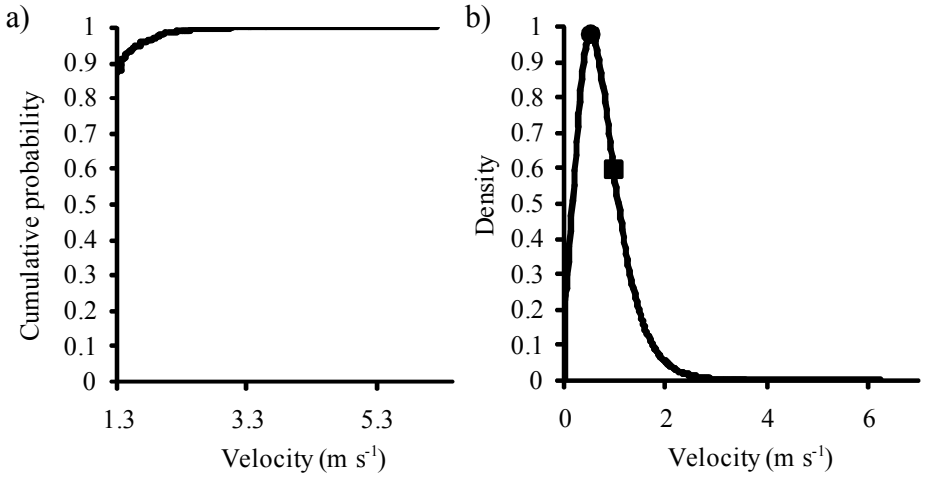

Figure 4-8. (a) Cumulative probability density function of water velocities during barnacle feeding observations. All velocities below 1.3 m s^{-1} were binned due to limits in the sensitivity and noise of the force transducer at low velocities. n=4000 (b) Probability density function of water velocities during the feeding behavior trials, based on a curve fit to the cumulative probability density function. The mode (closed circle) and mean (square) are denoted on the curve.

4.4 Discussion

4.4.1 Feeding vs. morphology

As in previous work on *Balanus glandula* from these same field sites, there is little variation in the morphology of the feeding cirri of *Chthamalus* among the wave-exposed sites at HMS (Li and Denny, 2004). This apparent limit to the extent of plastic change in cirral morphology at sites characterized by higher maximum water velocities is potentially compensated for by the ability of barnacles to alter feeding behavior as needed in response to the flow conditions. The field observations of *C. fissus* feeding behavior in a variety of flow conditions demonstrate that barnacles have the ability to withdraw and avoid individual breaking waves that generate high flow speeds. Barnacles at this wave-exposed site also continued feeding at flow speeds substantially faster than those used in previous laboratory tests of feeding behavior. Traditional laboratory flume experiments on feeding behavior have been limited to flow speeds below 50 cm s^{-1} (Trager *et al.*, 1990; Pullen and LaBarbera, 1991; Trager *et al.*, 1992; Sanford et al., 1994). Marchinko (2007) attempted to find the upper limit

of water flows that would cause barnacles to stop feeding, and given the constraints of the experimental equipment, this only occurred in his protected-shore individuals. Barnacles taken from high-flow field sites continued feeding at the 50 cm s^{-1} maximum velocity of Marchinko's flume. Observations made here in the field indicate that barnacles raised in this high-flow environment may occasionally leave their cirri extended in flows up to 3.5-4 m s^{-1}, though feeding drops off quickly in flows above 2 m s^{-1} (Figure 4-6). Based on the patterns of change in cirral morphology with wave exposure among barnacle species, I propose that a similar behavioral mechanism of high-flow avoidance may be operating in *B. glandula* and other barnacle species spanning a range of flow habitats.

4.4.2 Feeding behavior observations

Laboratory studies of barnacle feeding behavior have often focused on the method of feeding exhibited by barnacles in response to changing flow conditions. Crisp and Southward (1961) made the first detailed descriptions of the feeding behavior of several barnacle species in still water and slow flows. Among the various movement patterns exhibited by their barnacles were testing beats, pumping beats, active feeding, and passive feeding. Barnacles studied in flumes tend to switch from active beating of the cirri to passive extension as water speeds increase (Trager *et al.*, 1990; Pullen and LaBarbera, 1991), with passive feeding predominating at higher flow speeds in some species (Sanford *et al.*, 1994). The methods used in this study limited the different types of movements that could be clearly discerned, but it was possible to distinguish the full extension of active and passive feeding from the pumping and testing movements, based on the degree to which the prosoma shifted within the test. Based on initial observations made in the laboratory, pumping and testing movements in *C. fissus* were coupled with small movements in the prosoma, while the full extension of the cirri for feeding required the prosoma to shift from one end of the test to the other. In the field, *C. fissus* used the active feeding mode for the vast majority of the time and at all flow speeds measured in this experiment. Individual barnacles would occasionally switch to passive extension of the cirral net into flow for short periods of time (~3-5 s), but the switch happened only during long backwash periods as water

receded off the shore, and was not consistent across individuals. The constantly shifting nature of the turbulent flows at this site likely precludes the use of passive feeding much of the time.

Field feeding observations also demonstrated that the fast response time of barnacles to changes in flow speed allows them to feed for much of the time they are submerged (Figure 4-6, Figure 4-7). The high peak flows of breaking waves are extremely transient, often lasting for less than 1 second. The turbulent bore that continues up the shore and eventually washes back down moves much more slowly than the peak flows under the initial breaking wave. Barnacles in this study reacted quickly to the decelerating flows and began feeding again shortly (~ 0.5 – 2 s) after withdrawing to avoid the initial breaking wave. These behavioral observations match the predicted behavioral pattern postulated by previous researchers for barnacles living on wave-exposed shores (Marchinko and Palmer, 2003; Li and Denny, 2004). Barnacles growing in high-flow sites typically have faster growth rates than barnacles at protected sites (Sanford *et al.*, 1994; Sanford and Menge, 2001). If the feeding time lost to hiding from fast flows is a small fraction of the total time spent submerged, the proposed higher food delivery rates on exposed shores and headlands could lead to a higher food capture rate and growth rate for barnacles at those exposed sites (Sanford and Menge, 2001).

4.4.3 Characterizing the environment

Barnacles have the ability to withdraw into a robust shell that protects them from damage and dislodgement by high flow speeds (Denny *et al.*, 1985). For this reason, large waves impinging on a shoreline may be of little concern to barnacles when considering the plastic morphology of their feeding structures. Instead, barnacles may be tuning their cirral morphology to some other measure of their flow environment besides maximum water velocity. This point may be illustrated using the measured distribution of water velocities during the feeding observations in this study (Figure 4-8). The maximum water velocity measured during the time period of this experiment was 6.2 m s^{-1}, while the extrapolated probability density function in Figure 4-8b

indicates that the mean velocity was only 0.98 m s^{-1}, and the most common water velocity was predicted to be merely 0.52 m s^{-1}. The maximum water velocity measured was nearly 12 times faster than the most common water velocity at this site. The barnacles used in this experiment continued feeding at speeds well beyond 0.52 m s^{-1}. If we were to assume that the relationship between the maximum water velocity and most common water velocity was relatively consistent across wave-exposed sites, we would need to move to a site where the maximum water velocity was 30 m s^{-1} to increase the mode of water velocities to 2.5 m s^{-1}, the speed at which most barnacles in this study stopped feeding. Even at this hypothetical field site, we would assume that maximum water velocities must eventually drop below 30 m s^{-1} as the swell subsides, returning flow speeds to a range that permits barnacles to feed.

If barnacles on wave-exposed shores can ignore flows beyond a certain threshold velocity by withdrawing into the shell, it may be that in these exposed conditions they tune cirral morphology to another measure of the flow environment, such as mean or modal flow speeds. Therefore, the apparent lack of morphological change in barnacle cirri in response to increasing wave exposure along the HMS shore sites may be due not to a limit in the capacity for plastic change, but rather to a relatively invariant environmental cue. The gradient in maximum water velocities at the HMS sites sampled here for morphological measurements (4 to 13 m s^{-1}) might be accompanied by a relatively minor change in mean or modal flow speed. In wave-protected habitats, where there is a strong correlation between cirral morphology and maximum water velocity, flow speeds may never exceed the threshold that would require hiding inside the shell. These protected-shore barnacles can sample the entire distribution of velocities, including the maximum water velocities, and grow cirri to accommodate the full range of flow conditions.

References

Ahnesjö, J. and A. Forsman (2006) "Differential habitat selection by pygmy grasshopper color morphs; interactive effects of temperature and predator avoidance." *Evolutionary Ecology* **20**: 235-257.

Arsenault, D. J., K. B. Marchinko and A. R. Palmer (2001) "Precise tuning of barnacle leg length to coastal wave action." *Proceedings of the Royal Society of London Series B Biological Sciences* **268**: 2149-2154.

Atkinson, W. and S. Newbury (1984) "The adaptations of the rough winkle, *Littorina rudis*, to desiccation and to dislodgement by wind and waves." *Journal of Animal Ecology* **53**: 93-105.

Atkinson, W. D. and T. Warwick (1983) "The role of selection in the color polymorphism of *Littorina rudis* and *Littorina arcana* (Prosobranchia: Littorinidae)." *Biological Journal of the Linnean Society* **20**(2): 137-152.

Bakken, G. S. (1992) "Measurement and application of operative and standard operative temperatures in ecology." *American Zoologist* **32**: 194-216.

Barry, J. P., C. H. Baxter, R. D. Sagarin and S. E. Gilman (1995) "Climate-related, long-term faunal changes in a California rocky intertidal community." *Science* **267**: 672-675.

Bartlett, P. N. and D. M. Gates (1967) "The energy budget of a lizard on a tree trunk." *Ecology* **48**(2): 315-322.

Bazterrica, M. C., B. R. Silliman, F. J. Hidalgo, C. M. Crain and M. D. Bertness (2007) "Limpet grazing on a physically stressful Patagonian rocky shore." *Journal of Experimental Marine Biology and Ecology* **353**: 22-34.

Behrens, S. (1972) "The role of wave impact and desiccation on the distribution of *Littorina sitkana* Philipi, 1845." *Veliger* **15**(2): 129-132.

Behrens, S. (1974) "Ecological interactions of three *Littorina* (Gastropoda, Prosobranchia) along the west coast of North America." PhD thesis, Biology, University of Oregon, 111 pp.

Behrens Yamada, S. (1977) "Geographic range limitation of the intertidal gastropods *Littorina sitkana* and *L. planaxis*." *Marine Biology* **39**: 61-65.

Behrens Yamada, S. (1989) "Are direct developers more locally adapted than planktonic developers?" *Marine Biology* **103**: 403-411.

Behrens Yamada, S. (1992) "Niche relationships in northeastern Pacific littorines." *Proceedings of the Third International Symposium on Littorinid Biology*. J. Grahame, P. J. Mill and D. G. Reid (eds.) The Malacological Society of London**:** 281-291

Bell, E. C. (1995) "Environmental and morphological influences on thallus temperature and desiccation of the intertidal alga *Mastocarpus papillatus* Kutzing." *Journal of Experimental Marine Biology and Ecology* **191**(1): 29-55.

Berger, M. S. and R. B. Emlet (2007) "Heat-shock response of the upper intertidal barnacle *Balanus glandula*: thermal stress and acclimation." *Biological Bulletin* **212**: 232-241.

Bertness, M. D., C. M. Crain, B. R. Silliman, M. C. Bazterrica, M. V. Reyna, F. Hildago and J. K. Farina (2006) "The community structure of western Atlantic Patagonian rocky shores." *Ecological Monographs* **76**(3): 439-460.

Bingham, F. O. (1972) "The mucus holdfast of *Littorina irrorata* and its relationship to relative humidity and salinity." *Veliger* **15**(1): 48-50.

Blanchette, C. A., B. S. T. Helmuth and S. D. Gaines (2007) "Spatial patterns of growth in the mussel, *Mytilus californianus*, across a major oceanographic and biogeograpic boundary at Point Conception, California, USA." *Journal of Experimental Marine Biology and Ecology* **340**: 126-148.

Bock, C. E. and R. E. Johnson (1967) "The role of behavior in determining the intertidal zonation of *Littorina planaxis* Phillipi, 1847, and *Littorina scutulata* Gould, 1849." *Veliger* **10**(1): 42-54.

Boller, M. L. and E. Carrington (2006) "*In situ* measurements of hydrodynamic forces imposed on *Chondrus crispus* Stackhouse." *Journal of Experimental Marine Biology and Ecology* **337**: 159-170.

Boulding, E. G. and K. L. Van Alstyne (1993) "Mechanisms of differential survival and growth of two species of *Littorina* on wave-exposed and on protected shores." *Journal of Experimental Marine Biology and Ecology* **169**: 139-166.

Branch, G. M. (1978) "The responses of South African Patellid limpets to invertebrate predators." *Zoologica Africana* **13**(2): 221-232.

Branch, G. M. (1981) "The biology of limpets: physical factors, energy flow, and ecological interactions." *Oceanography and Marine Biology: an Annual Review* **19**: 235-380.

Branch, G. M. and C. N. Steffani (2004) "Can we predict the effects of alien species? A case-history of the invasion of South Africa by *Mytilus galloprovincialis* (Lamarck)." *Journal of Experimental Marine Biology and Ecology* **300**: 189-215.

Breen, P. A. (1972) "Seasonal migration and population regulation in the limpet *Acmaea* (*Collisella*) *digitalis*." *Veliger* **15**(2): 133-141.

Britton, J. C. (1992) "Evaporative water loss, behaviour during emersion, and upper thermal tolerance limits in seven species of eulittoral-fringe Littorinidae (Mollusca: Gastropoda) from Jamaica." *Proceedings of the Third International Symposium on Littorinid Biology*. J. Grahame, P. J. Mill and D. G. Reid (eds.) The Malacological Society of London, London**:** 69-83

Britton, J. C. (1993) "The effects of experimental protocol and behaviour on evaporative water loss during emersion in three species of rocky shore gastropods." *Proceedings of the Fifth International Marine Biological Workshop: The Marine Flora and Fauna of Rottnest Island, Western Australia*. F. E. Wells, D. I. Walker, H. Kirkman and R. Lethbridge (eds.) Western Australia Museum, Perth, **2:** 601-619

Britton, J. C. and R. F. McMahon (1986) "The relationship between vertical distribution evaporative water loss rate behavior and some morphometric parameters in four species of rocky intertidal gastropods from Hong Kong." *Proceedings of the Second International Marine Biological Workshop: The Marine Flora and Fauna of Hong Kong and Southern China, Hong Kong, 1986*. B. Morton (ed.) Hong Kong University Press, Hong Kong, **3:** 1153-1171

Broekhuysen, G. J. (1940) "A preliminary investigation of the importance of desiccation, temperature and salinity as factors controlling the vertical distribution of certain intertidal marine gastropods in False Bay, South Africa." *Transactions of the Royal Society of South Africa* **28**: 255-291.

Buckley, B. A., M.-E. Owen and G. E. Hofmann (2001) "Adjusting the thermostat: the threshold induction temperature for the heat-shock response in intertidal mussels (genus *Mytilus*) changes as a function of thermal history." *Journal of Experimental Biology* **204**: 3571-3579.

Bush, P. S. (1964) "Effects of desiccation on *Littorina planaxis*." Undergraduate thesis, Hopkins Marine Station, Stanford University, 17 pp.

Campbell, G. S. and J. M. Norman (1998) *An Introduction to Environmental Biophysics*. Springer-Verlag, New York, 286 pp.

Carlton, J. T. (1996) "Biological invasions and cryptogenic species." *Ecology* **77**(6): 1635-1655.

Carlton, J. T. and J. B. Geller (1993) "Ecological roulette: the global transport of nonindigenous marine organisms." *Science* **261**: 78-82.

Carslaw, H. S. and J. C. Jaeger (1959) *Conduction of Heat in Solids (2nd edition)*. Clarendon Press, Oxford, 510 pp.

Castenholz, R. W. (1961) "Effect of grazing on marine littoral diatom populations." *Ecology* **42**(4): 783-794.

Chan, B. K. K. and O. S. Hung (2005) "Cirral length of the acorn barnacle *Tetraclita japonica* (Cirripedia: Balanomorpha) in Hong Kong: Effect of wave exposure and tidal height." *Journal of Crustacean Biology* **25**(3): 329-332.

Cheer, A. Y. L. and M. A. R. Koehl (1987) "Paddles and rakes: Fluid flow through bristled appendages of small organisms." *Journal of Theoretical Biology* **129**: 17-39.

Chelazzi, G., G. A. Williams and D. R. Gray (1999) "Field and laboratory measurement of heart rate in a tropical limpet, *Cellana grata*." *Journal of the Marine Biological Association of the United Kingdom* **79**: 749-751.

Chow, V. (1987a) "Morphological classification of sibling species of *Littorina* (Gastropoda: Prosobranchia): discretionary use of discriminant analysis." *Veliger* **29**(4): 359-366.

Chow, V. (1987b) "Patterns of growth and energy allocation in northern California populations of *Littorina* (Gastropoda: Prosobranchia)." *Journal of Experimental Marine Biology and Ecology* **110**: 69-89.

Chow, V. (1989) "Intraspecific competition in a fluctuating population of *Littorina plena* Gould (Gastropoda: Prosobranchia)." *Journal of Experimental Marine Biology and Ecology* **130**: 147-165.

Clark, R. P., M. S. Edwards and M. S. Foster (2004) "Effects of shade from multiple kelp canopies on an understory algal assemblage." *Marine Ecology Progress Series* **267**: 107-119.

Clarke, A. P., P. J. Mill and J. Grahame (2000a) "Biodiversity in *Littorina* species (Mollusca: Gastropoda): A physiological approach using heat-coma." *Marine Biology* **137**(3): 559-565.

Clarke, A. P., P. J. Mill, J. Grahame and R. F. McMahon (2000b) "Geographical variation in heat coma temperatures in *Littorina* species (Mollusca: Gastropoda)." *Journal of the Marine Biological Association of the United Kingdom* **80**(5): 855-863.

Cleland, J. D. and R. F. McMahon (1986) "Upper thermal limit of nine intertidal gastropod species from a Hong Kong rocky shore in relation to vertical distribution and desiccation associated with evaporative cooling." *Proceedings of the Second International Marine Biological Workshop: The Marine Flora and Fauna of Hong Kong and Southern China, Hong Kong, 1986* B. Morton (ed.) Hong Kong University Press, Hong Kong, **3:** 1141-1152

Collins, L. S. (1977) "Abundance, substrate angle, and desiccation resistance in two sympatric species of limpets." *Veliger* **19**(2): 199-203.

Colman, J. (1933) "The nature of the intertidal zonation of plants and animals." *Journal of the Marine Biological Association of the United Kingdom* **18**(2): 435-476.

Connell, J. H. (1961) "Effects of competition, predation by *Thais lapillus*, and other factors on natural populations of the barnacle *Balanus balanoides*." *Ecological Monographs* **31**(1): 61-104.

Connell, J. H. (1972) "Community interactions on marine rocky intertidal shores." *Annual Review of Ecology and Systematics* **3**: 169-192.

Connell, J. H. (1975) "Some mechanisms producing structure in natural communities: a model and evidence from field experiments." *Ecology and Evolution of Communities*. M. L. Cody and J. M. Diamond (eds.) Belknap Press of Harvard University, Cambridge, Massachusetts**:** 460-490.

Connor, V. M. (1986) "The use of mucous trails by intertidal limpets to enhance food resources." *Biological Bulletin* **171**(3): 548-564.

Connor, V. M. and J. F. Quinn (1984) "Stimulation of food species growth by limpet mucus." *Science* **225**: 843-844.

Cook, L. M. and P. M. Freeman (1986) "Heating properties of morphs of the mangrove snail *Littoraria pallescens*." *Biological Journal of the Linnean Society* **29**: 295-300.

Crisp, D. J. and A. J. Southward (1961) "Different types of cirral activity of barnacles." *Philosophical Transactions of the Royal Society of London, Series B.* **243**(705): 272-307.

Currey, J. D. and R. N. Hughes (1982) "Strength of the dogwhelk *Nucella lapillus* and the winkle *Littorina littorea* from different habitats." *Journal of Animal Ecology* **51**: 47-56.

Davenport, J. and J. L. Davenport (2005) "Effects of shore height, wave exposure and geographical distance on thermal niche width of intertidal fauna." *Marine Ecology Progress Series* **292**: 41-50.

Dayton, P. K. (1971) "Competition, disturbance, and community organization - Provision and subsequent utilization of space in a rocky intertidal community." *Ecological Monographs* **41**(4): 351-389.

Denny, M. W. (1984) "Mechanical properties of pedal mucus and their consequences for gastropod structure and performance." *American Zoologist* **24**: 23-36.

Denny, M. W. (1993) *Air and Water*. Princeton University Press, Princeton, 341 pp.

Denny, M. W. and C. A. Blanchette (2000) "Hydrodynamics, shell shape, behavior and survivorship in the owl limpet *Lottia gigantea*." *Journal of Experimental Biology* **203**(17): 2623-2639.

Denny, M. W., T. L. Daniel and M. A. R. Koehl (1985) "Mechanical limits to size in wave-swept organisms." *Ecological Monographs* **55**(1): 69-102.

Denny, M. W. and C. D. G. Harley (2006) "Hot limpets: predicting body temperature in a conductance-mediated thermal system." *Journal of Experimental Biology* **209**: 2409-2419.

Denny, M. W., B. Helmuth, G. Leonard, C. D. G. Harley, L. J. H. Hunt and E. K. Nelson (2004) "Quantifying scale in ecology: lessons from a wave-swept shore." *Ecological Monographs* **74**(3): 513-532.

Denny, M. W., L. P. Miller and C. D. G. Harley (2006) "Thermal stress on intertidal limpets: long-term hindcasts and lethal limits." *Journal of Experimental Biology* **209**: 2420-2431.

Denny, M. W., L. P. Miller, M. D. Stokes, L. J. H. Hunt and B. S. T. Helmuth (2003) "Extreme water velocities: Topographical amplification of wave-induced flow in the surf zone of rocky shores." *Limnology and Oceanography* **48**(1): 1-8.

Doty, M. S. (1946) "Critical tide factors that are correlated with the vertical distribution of marine algae and other organisms along the Pacific coast." *Ecology* **27**(4): 315-328.

Edney, E. B. (1951) "The body temperature of woodlice." *Journal of Experimental Biology* **28**: 271-280.

Edney, E. B. (1953) "The temperature of woodlice in the sun." *Journal of Experimental Biology* **30**: 331-349.

Ekendahl, A. (1994) "Factors important to the distribution of colour morphs of *Littorina mariae* Sacchi and Rastelli in a non-tidal area." *Ophelia* **40**(1): 1-12.

Ekendahl, A. (1995) "Microdistribution on the field and habitat choice in aquaria by colour morphs of *Littorina mariae* Sacchi & Rastelli." *Journal of Molluscan Studies* **61**: 249-256.

Ekendahl, A. (1998) "Colour polymorphic prey (*Littorina saxatilis* Olivi) and predatory effects of a crab population (*Carcinus maenas* L.)." *Journal of Experimental Marine Biology and Ecology* **222**: 239-246.

Ekendahl, A. and K. Johannesson (1997) "Shell colour variation in *Littorina saxatilis* Olivi (Prosobranchia: Littorinidae): a multi-factor approach." *Biological Journal of the Linnean Society* **62**: 401-419.

Elvin, D. W. (1976) "Seasonal growth and reproduction of an intertidal sponge, *Haliclona permollis* (Bowerbank)." *Biological Bulletin* **151**: 108-125.

Elvin, D. W. and J. J. Gonor (1979) "The thermal regime of an intertidal *Mytilus californianus* Conrad population on the central Oregon coast." *Journal of Experimental Marine Biology and Ecology* **39**: 265-279.

Encomio, V. G. and F.-L. E. Chu (2005) "Seasonal variation of heat shock protein 70 in eastern oysters (*Crassostrea virginica*) infected with *Perkinsus marinus* (Dermo)." *Journal of Shellfish Research* **24**(1): 167-175.

Etter, R. J. (1988) "Physiological stress and color polymorphism in the intertidal snail *Nucella lapillus*." *Evolution* **42**(4): 660-680.

Evans, R. G. (1947) "The intertidal ecology of selected localities in the Plymouth neighbourhood." *Journal of the Marine Biological Association of the United Kingdom* **27**: 173-218.

Evans, R. G. (1948) "The lethal temperatures of some common British littoral molluscs." *Journal of Animal Ecology* **17**(2): 165-173.

Feder, M. E. and G. E. Hofmann (1999) "Heat-shock proteins, molecular chaperones, and the stress response: evolutionary and ecological physiology." *Annual Review of Physiology* **61**: 243-282.

Fenberg, P. B. (2008) "The effects of size-selective harvesting on the population biology and ecology of a sex-changing limpet species, *Lottia gigantea*." PhD thesis, Biology, University of California, San Diego, 114 pp.

Fenberg, P. B. and K. Roy (2007) "Ecological and evolutionary consequences of size-selective harvesting: how much do we know?" *Molecular Ecology* **17**(1): 209-220.

Finke, G. R., S. A. Navarrete and F. Bozinovic (2007) "Tidal regimes of temperate coasts and their influences on aerial exposure for intertidal organisms." *Marine Ecology Progress Series* **343**: 57-62.

Fisher, W. K. (1904) "The anatomy of *Lottia gigantea* Gray." *Zoologische Jahrbucher. Abteilung fur Anatomic und Ontogenie der Tiere* **20**: 1-66.

Forsman, A. (1995) "Heating rates and body temperature variation in melanistic and zigzag *Vipera berus*: does colour make a difference?" *Annales Zoologici Fennici* **32**: 365-374.

Forsman, A. (1997) "Thermal capacity of different colour morphs in the pygmy grasshopper *Tetrix subulata*." *Annales Zoologici Fennici* **34**: 145-149.

Forsman, A., J. Anhnesjö, S. Caesar and M. Karlsson (2008) "A model of ecological and evoutionary consequences of color polymorphism." *Ecology* **89**(1): 34-40.

Forsman, A. and S. Appelqvist (1999) "Experimental manipulation reveals differential effects of colour pattern on survival in male and female pygmy grasshoppers." *Journal of Evolutionary Biology* **12**: 391-401.

Forsman, A., K. Ringblom, E. Civantos and J. Ahnesjö (2002) "Coevolution of color pattern and thermoregulatory behavior in polymorphic pygmy grasshoppers *Tetrix undulata*." *Evolution* **56**(2): 349-360.

Foster, B. A. (1971) "On the determinants of the upper limit of intertidal distribution of barnacles (Crustacea: Cirripedia)." *Journal of Animal Ecology* **40**: 33-48.

Fraenkel, G. (1961) "Resistance to high temperatures in a Mediterranean snail, *Littorina neritoides*." *Ecology* **42**(3): 604-606.

Fraenkel, G. (1968) "The heat resistance of intertidal snails at Bimini, Bahamas; Ocean Springs, Mississippi; and Woods Hole, Massachusetts." *Physiological Zoology* **41**(1): 1-13.

Frank, P. W. (1965) "The biodemography of an intertidal snail population." *Ecology* **46**(6): 831-844.

Gaines, S. D. and M. W. Denny (1993) "The largest, smallest, highest, lowest, longest, and shortest: Extremes in ecology." *Ecology* **74**(6): 1677-1692.

Gallucci, V. F. (1973) "On the principles of thermodynamics in ecology." *Annual Review of Ecology and Systematics* **4**: 329-357.

Garrity, S. D. (1984) "Some adaptations of gastropods to physical stress on a tropical rocky shore." *Ecology* **65**(2): 559-574.

Gates, D. M. (1980) *Biophysical Ecology*. Dover Publications, Mineola, NY, 635 pp.

Gaylord, B. and S. D. Gaines (2000) "Temperature or transport? Range limits in marine species mediated solely by flow." *American Naturalist* **155**(6): 769-789.

Gendron, R. P. (1977) "Habitat selection and migratory behaviour of the intertidal gastropod *Littorina littorea* (L.)." *Journal of Animal Ecology* **46**: 79-92.

Gilman, S. E. (2006) "Life at the edge: an experimental study of a poleward range boundary." *Oecologia* **148**: 270-279.

Gilman, S. E., D. S. Wethey and B. S. T. Helmuth (2006) "Variation in the sensitivity of organismal body temperature to climate change over local and geographical scales." *Proceedings of National Academy of Sciences, USA* **103**(25): 9560-9565.

Gowanloch, J. N. and F. R. Hayes (1926) "Contributions to the study of marine gastropods I. The physical factors, behaviour, and intertidal life of *Littorina*."

Contributions to Canadian Biology and Fisheries: Being Studies from the Biological Stations of Canada **3**: 135-165.

Grainger, J. N. R. (1969) "Factors affecting the body temperature of *Patella*." *Verhandlungen der Deutschen Zoologischen Gesellschaft* **3**(7): 479-487.

Gray, D. R. and A. N. Hodgson (2004) "The importance of a crevice environment to the limpet *Helcion pectunculus* (Patellidae)." *Journal of Molluscan Studies* **70**(1): 67-72.

Halpin, P. M., C. J. Sorte, G. E. Hofmann and B. A. Menge (2002) "Patterns in variation in levels of Hsp70 in natural rocky shore populations from microscales to mesoscales." *Integrative and Comparative Biology* **42**: 815-824.

Hamdoun, A. M., D. P. Cheney and G. N. Cherr (2003) "Phenotypic plasticity in HSP70 and HSP70 gene expression in the Pacific Oyster (*Crassostrea gigas*): implications for thermal limits and induction of thermal tolerance." *Biological Bulletin* **205**: 160-169.

Hamilton, P. V. (1978) "Intertidal distribution and long-term movements of *Littorina irrorata* (Mollusca: Gastropoda)." *Marine Biology* **46**: 49-58.

Harger, J. R. E. (1972) "Competitive coexistence among intertidal invertebrates." *American Scientist* **60**(5): 600-607.

Harley, C. D. G. and B. S. T. Helmuth (2003) "Local- and regional-scale effects of wave exposure, thermal stress, and absolute versus effective shore level on patterns of intertidal zonation." *Limnology and Oceanography* **48**(4): 1498-1508.

Heath, D. J. (1975) "Colour, sunlight, and internal temperatures in the land-snail *Cepaea nemoralis* (L.)." *Oecologia* **19**: 29-38.

Heller, H. C. and D. M. Gates (1971) "Altitudinal zonation of chipmunks (*Eutamias*): energy budgets." *Ecology* **52**(3): 424-433.

Heller, J. (1981) "Visual versus climatic selection of shell banding in the landsnail *Theba pisana* in Israel." *Journal of Zoology* **194**: 85-101.

Heller, J. (1984) "Shell colours of desert landsnails." *Malacologia* **25**(2): 355-359.

Helmuth, B. (1999) "Thermal biology of rocky intertidal mussels: quantifying body temperatures using climatological data." *Ecology* **80**(1): 15-34.

Helmuth, B. (2002) "How do we measure the environment? Linking intertidal thermal physiology and ecology through biophysics." *Integrative and Comparative Biology* **42**: 837-845.

Helmuth, B. and M. W. Denny (2003) "Predicting wave exposure in the rocky intertidal zone: Do bigger waves always lead to larger forces?" *Limnology and Oceanography* **48**(3): 1338-1345.

Helmuth, B., C. D. G. Harley, P. M. Halpin, M. O'Donnell, G. E. Hofmann and C. A. Blanchette (2002) "Climate change and latitudinal patterns of intertidal thermal stress." *Science* **298**(5595): 1015-1017.

Helmuth, B., N. Mieszkowska, P. Moore and S. J. Hawkins (2006) "Living on the edge of two changing worlds: forecasting the responses of rocky intertidal ecosystems to climate change." *Annual Review of Ecology, Evolution, and Systematics* **37**: 373-404.

Helmuth, B. S. T. (1998) "Intertidal mussel microclimates: predicting the body temperature of a sessile invertebrate." *Ecological Monographs* **68**(1): 51-74.

Helmuth, B. S. T. and G. E. Hofmann (2001) "Microhabitats, thermal heterogeneity, and patterns of physiological stress in the rocky intertidal zone." *Biological Bulletin* **201**(3): 374-384.

Hewatt, W. G. (1937) "Ecological studies on selected marine intertidal communities of Monterey Bay, California." *American Midland Naturalist* **18**(2): 161-206.

Hoagland, K. E. (1977) "A gastropod color polymorphism: One adaptive strategy of phenotypic variation." *Biological Bulletin* **152**(3): 360-372.

Hochachka, P. W. and G. N. Somero (2002) *Biochemical Adaptation: Mechanism and Process in Physiological Evolution*. Oxford University Press, New York, USA, 480 pp.

Hofmann, G. E. and G. N. Somero (1995) "Evidence for protein damage at environmental temperatures: Seasonal changes in levels of ubiquitin conjugates and hsp70 in the intertidal mussel *Mytilus trossulus*." *Journal of Experimental Biology* **198**(7): 1509-1518.

Hofmann, G. E. and G. N. Somero (1996) "Protein ubiquitination and stress protein synthesis in *Mytilus trossulus* occurs during recovery from tidal emersion." *Molecular Marine Biology and Biotechnology* **5**(3): 175-184.

Hohenlohe, P. A. (2003) "Distribution of sister *Littorina* species, I: tenacity and the wave-exposure gradient." *Veliger* **46**(2): 162-168.

Hohenlohe, P. A. and E. G. Boulding (2001) "A molecular assay identifies morphological characters useful for distinguishing the sibling species *Littorina scutulata* and *L. plena*." *Journal of Shellfish Research* **20**(1): 453-457.

Hughes, J. M. and P. B. Mather (1986) "Evidence for predation as a factor in determining shell color frequencies in a mangrove snail *Littorina* sp. (Prosobranchia: Littorinidae)." *Evolution* **40**(1): 68-77.

Incropera, F. P. and D. P. DeWitt (2002) *Fundamentals of Heat and Mass Transfer*. John Wiley and Sons, New York, 776 pp.

Johannesson, K. (1989) "The bare zone of Swedish rocky shores: why is it there?" *Oikos* **54**: 77-86.

Johannesson, K. and A. Ekendahl (2002) "Selective predation favouring cryptic individuals of marine snails (*Littorina*)." *Biological Journal of the Linnean Society* **76**: 137-144.

Johnsen, S. and E. A. Widder (1999) "The physical basis of transparency in biological tissue: ultrastructure and the minimization of light scattering." *Journal of Theoretical Biology* **199**: 181-198.

Johnson, S. E. (1975) "Microclimate and energy flow in the marine rocky intertidal." *Perspectives of Biophysical Ecology*. D. M. Gates and R. B. Schmerl (eds.) Springer-Verlag, New York**:** 559-587.

Jones, J. S. (1973) "Ecological genetics and natural selection in mollusks." *Science* **182**(4112): 546-552.

Jones, J. S., B. H. Leith and P. Rawlings (1977) "Polymorphism in *Cepaea*: a problem with too many solutions?" *Annual Review of Ecology and Systematics* **8**: 109-143.

Jones, N. S. (1948) "Observations and experiments on the biology of *Patella vulgata* at Port St. Mary, Isle of Man." *Proceedings and Transactions of the Liverpool Biological Society* **56**: 60-77.

Jost, J. and B. Helmuth (2007) "Morphological and ecological determinants of body temperatures of *Geukensia demissa*, the Atlantic ribbed mussel, and their effects on mussel mortality." *Biological Bulletin* **213**: 141-151.

Kaandorp, J. A. (1999) "Morphological analysis of growth forms of branching marine sessile organisms along environmental gradients." *Marine Biology* **134**: 295-306.

Kado, R. (2003) "Invasion of Japanese shores by the NE Pacific barnacle *Balanus glandula* and its ecological and biogeographical impact." *Marine Ecology Progress Series* **249**: 199-206.

Kelsch, S. W. (1994) "Lotic fish-community structure following transition from severe drought to high discharge." *Journal of Freshwater Ecology* **9**(4): 331-339.

Kensler, C. B. (1967) "Desiccation resistance of intertidal crevice species as a factor in their zonation." *Journal of Animal Ecology* **36**: 391-406.

Koplin, J. R. and R. S. Hoffmann (1968) "Habitat overlap and competitive exclusion in voles (*Microtus*)." *American Midland Naturalist* **80**(2): 494-507.

Kronberg, I. (1990) "Heat production in *Littorina saxatilis* Olivi and *Littorina neritoides* L. (Gastropoda: Prosobranchia) during an experimental exposure to air." *Helgoländer Meeresuntersuchungen* **44**: 125-134.

LaBarbera, M. (1978) "Particle capture by a pacific brittle star: experimental test of the aerosol suspension feeding model." *Science* **201**: 1147-1149.

Lang, R. C., J. C. Britton and T. Metz (1998) "What to do when there is nothing to do: The ecology of Jamaican intertidal Littorinidae (Gastropoda: Prosobranchia) in repose." *Hydrobiologia* **378**(0): 161-185.

Lauder, G. V. (1983) "Food capture." *Fish Biomechanics*. P. W. Webb and D. Weihs (eds.) Praeger Publishers, New York**:** 280-311.

Li, N. K. and M. W. Denny (2004) "Limits to phenotypic plasticity: flow effects on barnacle feeding appendages." *Biological Bulletin* **206**: 121-124.

Lindquist, S. (1980) "Varying patterns of protein synthesis in *Drosophila* during heat shock: implications for regulation." *Developmental Biology* **77**: 463-479.

Lowell, R. B. (1984) "Desiccation of intertidal limpets: effects of shell size, fit to substratum, and shape." *Journal of Experimental Marine Biology and Ecology* **77**: 197-207.

Luken, J. O., L. M. Kuddes and T. C. Tholemeier (1997) "Response of understory species to gap formation and soil disturbance in *Lonicera maackii* thickets." *Restoration Ecology* **5**(3): 229-235.

Marchinko, K. B. (2003) "Dramatic phenotypic plasticity in barnacle legs (*Balanus glandula* Darwin): magnitude, age dependence, and speed of response." *Evolution* **57**(6): 1281-1290.

Marchinko, K. B. (2007) "Feeding behavior reveals the adaptive nature of plasticity in barnacle feeding limbs." *Biological Bulletin* **213**: 12-15.

Marchinko, K. B. and A. R. Palmer (2003) "Feeding in flow extremes: Dependence of cirrus form on wave-exposure in four barnacle species." *Zoology* **106**(2): 127-141.

Markel, R. P. (1971) "Temperature relations in two species of tropical west American littorines." *Ecology* **52**(6): 1126-1130.

Markel, R. P. (1974) "Aspects of the physiology of temperature acclimation in the limpet *Acmaea limatula* Carpenter (1864): an integrated field and laboratory study." *Physiological Zoology* **47**(2): 99-109.

Markel, R. P. (1976) "Some biochemical responses to temperature acclimation in the limpet, *Acmaea limatula* Carpenter (1864)." *Comparative Biochemistry and Physiology* **53B**: 81-84.

Mastro, E., V. Chow and D. Hedgecock (1981) "*Littorina scutulata* and *Littorina plena*: sibling species status of two prosobranch gastropod species confirmed by electrophoresis." *The Veliger* **24**(3): 239-246.

Mauchline, J. (1989) "Functional morphology and feeding of euphausiids." *Functional morphology of feeding and grooming in Crustacea*. B. E. Felgenhauer, L. Watling and A. B. Thistle (eds.) A.A.Balkema, Rotterdam, **6:** 173-184.

McAuliffe, J. R. (1994) "Landscape evolution, soil formation, and ecological patterns and processes in Sonoran desert bajadas." *Ecological Monographs* **64**(2): 111-148.

McMahon, R. F. (1990) "Thermal tolerance evaporative water loss air-water oxygen consumption and zonation of intertidal prosobranchs: a new synthesis." *Hydrobiologia* **193**: 241-260.

McMahon, R. F. (1991) "Upper critical temperature limits, tissue temperatures during emersion and evaporative cooling at elevated temperatures in Western Australian intertidal gastropods: Evidence for a physiological barrier at the high tide mark." *Proceedings of the Third International Marine Biological Workshop: The Marine Flora and Fauna of Albany, Western Australia*. F. E. Wells, D. I. Walker, H. Kirkman and R. Lethbridge (eds.) Western Australia Museum, Perth, **2:** 661-673.

McMahon, R. F. (2001) "Acute thermal tolerance in intertidal gastropods relative to latitude, superfamily, zonation and habitat with special emphasis on the Littorinoidea." *Journal of Shellfish Research* **20**(1): 459-467.

McMahon, R. F. and J. C. Britton (1985) "The relationship between vertical distribution, thermal tolerance, evaporative water loss rate, and behavior on emergence in six species of mangrove gastropods from Hong Kong." *The Malacofauna of Hong Kong and Southern China. II, Vol. 1 and 2. Second International Workshop: Hong Kong, Hong Kong, Apr. 6-24, 1983.* B. Morton and D. Dudgeon (eds.) Hong Kong University Press, Hong Kong**:** 563-582

McMahon, R. F. and J. D. Cleland (1986) "Thermal tolerance evaporative water loss and behavior during prolonged emergence in the high zoned mangrove gastropod *Cerithidea ornata* evidence for atmospheric water uptake." *Proceedings of the Second International Marine Biological Workshop: The Marine Flora and Fauna of Hong Kong and Southern China, Hong Kong, 1986*. B. Morton (ed.) Hong Kong University Press, Hong Kong, **3:** 1123-1139

McMahon, R. F. and W. D. Russell-Hunter (1977) "Temperature relations of aerial and aquatic respiration in six littoral snails in relation to their vertical zonation." *Biological Bulletin* **152**: 182-198.

McQuaid, C. D. (1992) "Stress on the high shore: a review of age-dependent causes of mortality in *Nodilittorina knysnaensis* and *N. africana*." *Proceedings of the*

Third International Symposium on Littorinid Biology. J. Grahame, P. J. Mill and D. G. Reid (eds.) The Malacological Society of London, London**:** 85-89.

McQuaid, C. D. (1996a) "Biology of the gastropod family Littorinidae. I. Evolutionary aspects." *Oceanography and Marine Biology: an Annual Review* **34**: 233-262.

McQuaid, C. D. (1996b) "Biology of the gastropod family Littorinidae. II. Role in the ecology of intertidal and shallow marine ecosystems." *Oceanography and Marine Biology: an Annual Review* **34**: 263-302.

McQuaid, C. D. and P. A. Scherman (1988) "Thermal stress in a high shore intertidal environment: morphological and behavioural adaptations of the gastropod *Littorina africana*." *Behavioral Adaptation to Intertidal Life*. G. Chelazzi and M. Vannini (eds.) Plenum Press, New York**:** 213-224.

Menge, B. A. (1978) "Predation intensity in a rocky intertidal community: Relation between predator foraging activity and environmental harshness." *Oecologia* **34**: 1-16.

Menge, B. A., B. A. Daley, E. Sanford, E. P. Dahlhoff and J. Lubchenco (2007) "Mussel zonation in New Zealand: an integrative eco-physiological approach." *Marine Ecology Progress Series* **345**: 129-140.

Miller, L. P. (2007) "Feeding in extreme flows: behavior compensates for mechanical constraints in barnacle cirri." *Marine Ecology Progress Series* **349**: 227-234.

Miller, S. L. (1974) "Adaptive design of locomotion and foot form in prosobranch gastropods." *Journal of Experimental Marine Biology and Ecology* **14**(2): 99-156.

Mitchell, C. P. (1980) "Intertidal distribution of six trochids at Portobello, New Zealand." *New Zealand Journal of Marine & Freshwater Research* **14**(1): 47-54.

Mitchell, J. W. (1976) "Heat transfer from spheres and other animal forms." *Biophysical Journal* **16**: 561-569.

Miura, O., S. Nishi and S. Chiba (2007) "Temperature-related diversity of shell colour in the intertidal gastropod *Batillaria*." *Journal of Molluscan Studies* **73**: 235-240.

Morris, R. H., D. P. Abbott and E. C. Haderlie (1980) *Intertidal Invertebrates of California*. Stanford University Press, Stanford, 690 pp.

Muller, C. H. (1966) "The role of chemical inhibition (allelopathy) in vegetational composition." *Bulletin of the Torrey Botanical Club* **93**(5): 332-351.

Muñoz, J. L. P., G. R. Finke, P. A. Camus and F. Bozinovic (2005) "Thermoregulatory behavior, heat gain, and thermal tolerance in the periwinkle *Echinolittorina peruviana* in central Chile." *Comparative Biochemistry and Physiology* **142**: 92-98.

Newell, G. E. (1958) "The behaviour of *Littorina littorea* (L.) under natural conditions and its relation to position on the shore." *Journal of the Marine Biological Association of the United Kingdom* **37**: 229-239.

Newell, G. E. (1964) "Physiological aspects of the ecology of intertidal molluscs." *Physiology of Mollusca*. K. M. Wilbur and C. M. Yonge (eds.) Academic Press, New York, USA, **1:** 59-81.

Newell, R. C. (1969) "Effect of fluctuations in temperature on the metabolism of intertidal invertebrates." *American Zoologist* **9**: 293-307.

Newell, R. C. (1973) "Factors affecting the respiration of intertidal invertebrates." *American Zoologist* **13**: 513-528.

Newell, R. C. (1976) "Adaptations to intertidal life." *Adaptation to Environment: Essays on the Physiology of Marine Animals*. R. C. Newell (ed.) Butterworths, London, UK**:** 1-82.

Newell, R. C. and B. L. Bayne (1973) "A review on temperature and metabolic acclimation in intertidal marine invertebrates." *Netherlands Journal of Sea Research* **7**: 421-433.

Newell, R. C. and V. I. Pye (1970a) "The influence of thermal acclimation on the relation between oxygen consumption and temperature in *Littorina littorea* (L.) and *Mytilus edulis* L." *Comparative Biochemistry and Physiology* **34**: 385-397.

Newell, R. C. and V. I. Pye (1970b) "Seasonal changes in the effect of temperature on the oxygen consumption of the winkle *Littorina littorea* (L.) and the mussel *Mytilus edulis* L." *Comparative Biochemistry and Physiology* **34**: 367-383.

Newell, R. C. and V. I. Pye (1971) "Variations in the relationship between oxygen consumption, body size and summated tissue metabolism in the winkle *Littorina littorea*." *Journal of the Marine Biological Association of the United Kingdom* **51**: 315-338.

Nobel, P. S. (1999) *Physicochemical and Environmental Plant Physiology*. Academic Press, New York, USA, 635 pp.

O'Connor, M. P. and J. R. Spotila (1992) "Consider a spherical lizard: animals, models, and approximations." *American Zoologist* **32**: 179-193.

Okamura, B. and J. C. Partridge (1999) "Suspension feeding adaptations to extreme flow environments in a marine bryozoan." *Biological Bulletin* **196**: 205-215.

Orr, P. R. (1955) "Heat Death. I. Time-temperature relationships in marine animals." *Physiological Zoology* **28**: 290-294.

Orton, J. H. (1933) "Some limiting factors in the environment of the common limpet, *P. vulgata*." *Nature* **131**: 693-694.

Osovitz, C. J. and G. E. Hofmann (2005) "Thermal history-dependent expression of the *hsp70* gene in purple sea urchins: Biogeographic patterns and the effect of temperature acclimation." *Journal of Experimental Marine Biology and Ecology* **327**: 134-143.

Paine, R. T. (1966) "Food web complexity and species diversity." *The American Naturalist* **100**(910): 65-75.

Paine, R. T. (1974) "Intertidal community structure - experimental studies on relationship between a dominant competitor and its principal predator." *Oecologia* **15**: 93-120.

Parry, D. A. (1951) "Factors determining the temperature of terrestrial arthropods in sunlight." *Journal of Experimental Biology* **28**: 445-462.

Pombo, O. A. and A. Escofet (1996) "Effect of exploitation on the limpet *Lottia gigantea*: A field study in Baja California (Mexico) and California (U.S.A.)." *Pacific Science* **50**(4): 393-403.

Porter, W. P. and D. M. Gates (1969) "Thermodynamic equilibria of animals with environment." *Ecological Monographs* **39**(3): 228-244.

Porter, W. P., J. W. Mitchell, W. A. Beckman and C. B. DeWitt (1973) "Behavioral implications of mechanistic ecology: thermal and behavioral modeling of desert ecototherms and their microenvironment." *Oecologia* **13**: 1-54.

Porter, W. P., J. L. Sabo, C. R. Tracy, O. J. Reichman and N. Ramankutty (2002) "Physiology on a landscape scale: plant-animal interactions." *Integrative and Comparative Biology* **42**: 431-453.

Pullen, J. and M. LaBarbera (1991) "Modes of feeding in aggregations of barnacles and the shape of aggregations." *Biological Bulletin* **181**: 442-452.

Pye, V. I. and R. C. Newell (1973) "Factors affecting thermal compensation in the oxidative metabolism of the winkle *Littorina littorea*." *Netherlands Journal of Sea Research* **7**: 411-420.

Raffaelli, D. G. and R. N. Hughes (1978) "The effects of crevice size and availability on populations of *Littorina rudis* and *Littorina neritoides*." *Journal of Animal Ecology* **47**: 71-83.

Ramsay, J. A. (1935) "Methods of measuring the evaporation of water from animals." *Journal of Experimental Biology* **12**(4): 355-372.

Randall, D. J., W. Burggren and K. French (1997) *Eckert Animal Physiology: Mechanism and Adaptations, 4th edition*. W. H. Freeman and Company, New York, USA, 728 pp.

Rasband, W. S. (1997-2007) ImageJ. U. S. National Institutes of Health, Bethesda, Maryland, USA

Reid, D. G. (1987) "Natural selection for apostasy and crypsis acting on the shell color polymorphism of a mangrove snail, *Littoraria filosa* (Sowerby) Gastropoda: Littorinidae)." *Biological Journal of the Linnean Society* **30**(1): 1-24.

Reid, D. G. (1989) "The comparative morphology, phylogeny and evolution of the gastropod family Littorinidae." *Philosophical Transactions of the Royal Society of London, Series B.* **324**: 1-110.

Reid, D. G. (1996) *Systematics and Evolution of Littorina*. The Dorset Press, Dorchester, UK, 463 pp.

Reid, D. G. (2002) "Morphological review and phylogenetic analysis of *Nodilittorina* (Gastropoda: Littorinidae)." *Journal of Molluscan Studies* **68**: 259-281.

Reimchen, T. E. (1979) "Substratum heterogeneity, crypsis, and colour polymorphism in an intertidal snail (*Littorina mariae*)." *Canadian Journal of Zoology* **57**: 1070-1085.

Reimchen, T. E. (1989) "Shell colour ontogeny and tubeworm mimicry in a marine gastropod *Littorina mariae*." *Biological Journal of the Linnean Society* **36**: 97-109.

Roberts, D. A., G. E. Hofmann and G. N. Somero (1997) "Heat-shock protein expression in *Mytilus californianus*: acclimatization (seasonal and tidal-height comparisons) and acclimation effects." *Biological Bulletin* **192**(2): 309-320.

Roberts, D. J. and R. N. Hughes (1980) "Growth and reproductive rates of *Littorina rudis* from three contrasted shores in North Wales, UK." *Marine Biology* **58**: 47-54.

Rochette, R. and L. M. Dill (2000) "Mortality, behavior and the effects of predators on the intertidal distribution of littorinid gastropods." *Journal of Experimental Marine Biology and Ecology* **253**(2): 165-191.

Rosewater, J. (1978) "A case of double primary homonymy in eastern Pacific Littorinidae." *The Nautilus* **92**(3): 123-125.

Sanders, B. M., C. Hope, V. M. Pascoe and L. S. Martin (1991) "Characterization of the stress protein response in two species of *Collisella* limpets with different temperature tolerances." *Physiological Zoology* **64**(6): 1471-1489.

Sanderson, S. L. and R. Wassersug (1993) "Convergent and alternative designs for vertebrate suspension feeding." *The Skull*. J. Hanken and B. K. Hall (eds.) University of Chicago Press, Chicago, USA, **3:** 37-112

Sanford, E., D. Bermudez, M. D. Bertness and S. D. Gaines (1994) "Flow, food supply and acorn barnacle population dynamics." *Marine Ecology Progress Series* **104**: 49-62.

Sanford, E. and B. A. Menge (2001) "Spatial and temporal variation in barnacle growth in a coastal upwelling system." *Marine Ecology Progress Series* **209**: 143-157.

Sax, D. F. and J. H. Brown (2000) "The paradox of invasion." *Global Ecology and Biogeography* **9**: 363-371.

Schmidt-Nielsen, K., C. R. Taylor and A. Shkolnik (1971) "Desert snails: problems of heat, water and food." *Journal of Experimental Biology* **55**: 385-398.

Segal, E. (1956) "Microgeographic variation as thermal acclimation in an intertidal mollusc." *Biological Bulletin* **111**(1): 129-152.

Segal, E. and P. A. Dehnel (1962) "Osmotic behavior in an intertidal limpet, *Acmaea limatula*." *Biological Bulletin* **122**(3): 417-430.

Segal, E., K. P. Rao and T. W. James (1953) "Rate of activity as a function of intertidal height within populations of some littoral molluscs." *Nature* **172**: 1108-1109.

Sergievsky, S. O. (1992) "A review of ecophysiological studies of the colour polymorphism of *Littorina obtusata* (L.) and *L. saxatilis* (Olivi) in the White Sea." *Proceedings of the Third International Symposium on Littorinid biology*. J. Grahame, P. J. Mill and D. G. Reid (eds.) The Malacological Society of London, London**:** 235-245.

Shotwell, J. A. (1950) "The vertical zonation of *Acmaea*, the limpet." *Ecology* **31**(4): 647-649.

Smith, A. M. (1992) "Alternation between attachment mechanisms by limpets in the field." *Journal of Experimental Marine Biology and Ecology* **160**: 205-220.

Smith, A. M. and M. C. Morin (2002) "Biochemical differences between trail mucus and adhesive mucus from marsh periwinkle snails." *Biological Bulletin* **203**(3): 338-346.

Smith, D. C. (2001) "Effects of temperature and desiccation on tissue uric acid dynamics in *Littorina saxatilis* (Olivi)." *Journal of Shellfish Research* **20**(1): 485-488.

Smith, J. E. and G. E. Newell (1955) "The dynamics of the zonation of the common periwinkles (*Littorina littorea* (L.)) on a stony beach." *Journal of Animal Ecology* **24**(1): 35-56.

Sokolova, I. M. and V. J. Berger (2000) "Physiological variation related to shell colour polymorphism in White Sea *Littorina saxatilis*." *Journal of Experimental Marine Biology and Ecology* **245**(1): 1-23.

Sokolova, I. M., A. I. Granovitch, V. J. Berger and K. Johannesson (2000) "Intraspecific physiological variability of the gastropod *Littorina saxatilis* related to the vertical shore gradient in the White and North Seas." *Marine Biology* **137**(2): 297-308.

Sokolova, I. M. and H.-O. Pörtner (2003) "Metabolic plasticity and critical temperatures for aerobic scope in a eurythermal marine invertebrate (*Littorina saxatilis*, Gastropoda: Littorinidae) from different latitudes." *Journal of Experimental Biology* **206**: 195-207.

Sokolova, I. M. and H. O. Pörtner (2001) "Physiological adaptations to high intertidal life involve improved water conservation abilities and metabolic rate depression in *Littorina saxatilis*." *Marine Ecology Progress Series* **224**: 171-186.

Somero, G. N. (2002) "Thermal physiology and vertical zonation of intertidal animals: Optima, limits, and costs of living." *Integrative and Comparative Biology* **42**: 780-789.

Southward, A. J. (1958) "The zonation of plants and animals on rocky sea shores." *Biological Reviews* **33**: 137-177.

Stenseng, E., C. E. Braby and G. N. Somero (2005) "Evolutionary and acclimation-induced variation in the thermal limits of heart function in congeneric marine snails (Genus *Tegula*): implications for vertical zonation." *Biological Bulletin* **208**: 138-144.

Stillman, J. H. and G. N. Somero (2000) "A comparative analysis of the upper thermal tolerance limits of eastern Pacific porcelain crabs, genus *Petrolithses*: Influences of latitude, vertical zonation, acclimation, and phylogeny." *Physiological and Biochemical Zoology* **73**(2): 200-208.

Stimson, J. (1970) "Territorial behavior of the owl limpet *Lottia gigantea*." *Ecology* **51**(1): 113-118.

Stimson, J. (1973) "The role of the territory in the ecology of the intertidal limpet *Lottia gigantea*." *Ecology* **54**(5): 1020-1030.

Stirling, H. P. (1982) "The upper temperature tolerance of prosobranch gastropods of rocky shores at Hong Kong and Dar ES Salaam, Tanzania." *Journal of Experimental Marine Biology and Ecology* **63**(2): 133-144.

Struhsaker, J. W. (1968) "Selection mechanisms associated with intraspecific shell variation in *Littorina picta* (Prosobranchia: Mesogastropoda)." *Evolution* **22**: 459-480.

Suchanek, T. H. (1978) "The ecology of *Mytilus edulis* L. in exposed rocky intertidal communities." *Journal of Experimental Marine Biology and Ecology* **31**: 105-120.

Sutherland, J. P. (1970) "Dynamics of high and low populations of the limpet, *Acmaea scabra* (Gould)." *Ecological Monographs* **40**(2): 169-188.

Tansley, A. G. and R. S. Adamson (1925) "Studies of the vegetation of the English chalk: III. The chalk grasslands of Hampshire-Sussex border." *The Journal of Ecology* **13**(2): 177-223.

Tomanek, L. (2001) "The heat-shock response and patterns of vertical zonation in intertidal *Tegula* congeners." *Integrative and Comparative Biology* **42**: 797-807.

Tomanek, L. (2002) "The heat-shock response: Its variation, regulation, and ecological importance in intertidal gastropods (genus *Tegula*)." *Integrative and Comparative Biology* **42**: 797-807.

Tomanek, L. and E. Sanford (2003) "Heat-shock protein 70 (Hsp 70) as a biochemical stress indicator: an experimental field test in two congeneric intertidal gastropods (Genus: *Tegula*)." *Biological Bulletin* **205**: 276-284.

Tomanek, L. and G. N. Somero (1999) "Evolutionary and acclimation-induced variation in the heat-shock responses of congeneric marine snails (Genus *Tegula*) from different thermal habitats: implications for limits of thermotolerance and biogeography." *Journal of Experimental Biology* **202**: 2925-2936.

Tomanek, L. and G. N. Somero (2000) "Time course and magnitude of synthesis of heat-shock proteins in congeneric marine snails (Genus *Tegula*) from different tidal heights." *Physiological and Biochemical Zoology* **73**(2): 249-256.

Tracy, C. R., F. H. van Berkum, J. S. Tsuji, R. D. Stevenson, J. A. Nelson, B. M. Barnes and R. B. Huey (1984) "Errors resulting from linear approximations in energy balance equations." *Journal of Thermal Biology* **9**(4): 261-264.

Trager, G. C., D. Coughlin, A. Genin, Y. Achituv and A. Gangopadhyay (1992) "Foraging to the rhythm of ocean waves: porcelain crabs and barnacles

synchronize feeding motions with flow oscillations." *Journal of Experimental Marine Biology and Ecology* **164**: 73-86.

Trager, G. C., J. S. Hwang and J. R. Strickler (1990) "Barnacle suspension feeding in variable flow." *Marine Biology* **105**: 117-127.

Trussell, G. C. (2000) "Predator-induced plasticity and morphological trade-offs in latitudinally separated populations of *Littorina obtusata*." *Evolutionary Ecology Research* **2**: 803-822.

Trussell, G. C. (2002) "Evidence of countergradient variation in the growth of an intertidal snail in response to water velocity." *Marine Ecology Progress Series* **243**: 123-131.

Trussell, G. C. and M. O. Nicklin (2002) "Cue sensitivity, inducible defense, and trade-offs in a marine snail." *Ecology* **83**(6): 1635-1647.

Tsuchiya, M. (1983) "Mass mortality in a population of the mussel *Mytilus edulis* L. caused by high temperature on rocky shores." *Journal of Experimental Marine Biology and Ecology* **66**: 101-111.

Underwood, A. J. (1978) "A refutation of critical tidal levels as determinants of the structure of intertidal communities on British shores." *Journal of Experimental Marine Biology and Ecology* **33**: 261-276.

Underwood, A. J. (1980) "The effects of grazing by gastropods and physical factors on the upper limits of distribution of intertidal macroalgae." *Oecologia* **46**(2): 201-213.

Vermeij, G. J. (1971) "Temperature relationships of some tropical Pacific intertidal gastropods." *Marine Biology* **10**: 308-314.

Vermeij, G. J. (1972) "Intraspecific shore level size gradients in intertidal mollusks." *Ecology* **53**(4): 693-700.

Vermeij, G. J. (1973) "Morphological patterns in high-intertidal gastropods: adaptive strategies and their limitations." *Marine Biology* **20**(4): 319-346.

Vermeij, G. J. (1982) "Phenotypic evolution in a poorly dispersing snail after arrival of a predator." *Nature* **299**: 349-350.

Vogel, S. (1994) *Life in Moving Fluids*. Princeton University Press, Princeton, USA, 467 pp.

von Dassow, M. (2005) "Flow and conduit formation in the external fluid-transport system of a suspension feeder." *Journal of Experimental Biology* **208**: 2931-2938.

Wada, S. and A. Ito (2000) "Preliminary observation on "tip-lip" attachment in the periwinkle *Nodilittorina radiata*." *Bulletin of Marine Sciences and Fisheries Kochi University* **20**: 15-24.

Wallace, L. R. (1972) "Some factors affecting vertical distribution and resistance to desiccation in the limpet, *Acmaea testudinalis* (Müller)." *Biological Bulletin* **142**: 186-193.

Walsberg, G. E. (1992) "Quantifying radiative heat gain in animals." *American Zoologist* **32**: 217-224.

Watt, W. B. (1968) "Adaptive significance of pigment polymorphisms in *Colias* butterflies. I. Variation of melanin pigment in relation to thermoregulation." *Evolution* **22**: 437-458.

Whiles, M. R. and J. B. Wallace (1995) "Macroinvertebrate production in a headwater stream during recovery from anthropogenic disturbance and hydrologic extremes." *Canadian Journal of Fishery and Aquatic Science* **52**: 2402-2415.

Williams, G. A., M. De Pirro, K. M. Leun and D. Morritt (2005) "Physiological responses of heat stress on a tropical shore: the benefits of mushrooming behaviour in the limpet *Cellana grata*." *Marine Ecology Progress Series* **292**: 213-224.

Williams, G. A. and D. Morritt (1995) "Habitat partitioning and thermal tolerance in a tropical limpet, *Cellana grata*." *Marine Ecology Progress Series* **124**: 89-103.

Williams, S. T. and D. G. Reid (2004) "Speciation and diversity on tropical rocky shores: a global phylogeny of snails of the genus *Echinolittorina*." *Evolution* **58**(10): 2227-2251.

Williams, S. T., D. G. Reid and D. T. J. Littlewood (2003) "A molecular phylogeny of the Littorininae (Gastropoda: Littorinidae): unequal evolutionary rates, morphological parallelism, and biogeography of the Southern Ocean." *Molecular Phylogenetics and Evolution* **28**: 60-86.

Willmer, P. G. and D. M. Unwin (1981) "Field analyses of insect heat budgets: reflectance, size and heating rates." *Oecologia* **50**: 250-255.

Wilson, D. P. (1929) "A habit of the common periwinkle (*Littorina littorea* Linn)." *Nature* **124**(3125): 443.

Wolcott, T. G. (1973) "Physiological ecology and intertidal zonation in limpets (*Acmaea*) - critical look at limiting factors." *Biological Bulletin* **145**(2): 389-422.

Xavier, B. M., G. M. Branch and E. Wieters (2007) "Abundance, growth and recruitment of *Mytilus galloprovincialis* on the west coast of South Africa in relation to upwelling." *Marine Ecology Progress Series* **346**: 189-201.

Zacherl, D., S. D. Gaines and S. I. Lonhart (2003) "The limits to biogeographical distributions: insights from the northward range extension of the marine snail, *Kelletia kelletii* (Forbes, 1852)." *Journal of Biogeography* **30**: 913-924.

Zhang, Y. (2006) "Balancing food availability and hydrodynamic constraint: phenotypic plasticity and growth in *Simulium noelleri* blackfly larvae." *Oecologia* **147**: 39-46.